University of Alberta

Signal Transduction Mechanisms Underlying the Cilioexcitatory Action of Serotonin in Identified Ciliary Cells from *Helisoma trivolvis* Embryos

by

Shandra Anne Doran ©

A thesis submitted to the Faculty of Graduate Studies and Research in partial fulfillment of the requirements for the degree of Doctor of Philosophy

in

Physiology and Cell Biology
Department of Biological Sciences

Edmonton, Alberta
Spring 2005

Library and
Archives Canada

Published Heritage
Branch

395 Wellington Street
Ottawa ON K1A 0N4
Canada

Bibliothèque et
Archives Canada

Direction du
Patrimoine de l'édition

395, rue Wellington
Ottawa ON K1A 0N4
Canada

0-494-08226-7

Your file Votre référence
ISBN:
Our file Notre reference
ISBN:

NOTICE:
The author has granted a non-exclusive license allowing Library and Archives Canada to reproduce, publish, archive, preserve, conserve, communicate to the public by telecommunication or on the Internet, loan, distribute and sell theses worldwide, for commercial or non-commercial purposes, in microform, paper, electronic and/or any other formats.

The author retains copyright ownership and moral rights in this thesis. Neither the thesis nor substantial extracts from it may be printed or otherwise reproduced without the author's permission.

AVIS:
L'auteur a accordé une licence non exclusive permettant à la Bibliothèque et Archives Canada de reproduire, publier, archiver, sauvegarder, conserver, transmettre au public par télécommunication ou par l'Internet, prêter, distribuer et vendre des thèses partout dans le monde, à des fins commerciales ou autres, sur support microforme, papier, électronique et/ou autres formats.

L'auteur conserve la propriété du droit d'auteur et des droits moraux qui protège cette thèse. Ni la thèse ni des extraits substantiels de celle-ci ne doivent être imprimés ou autrement reproduits sans son autorisation.

In compliance with the Canadian Privacy Act some supporting forms may have been removed from this thesis.

While these forms may be included in the document page count, their removal does not represent any loss of content from the thesis.

Conformément à la loi canadienne sur la protection de la vie privée, quelques formulaires secondaires ont été enlevés de cette thèse.

Bien que ces formulaires aient inclus dans la pagination, il n'y aura aucun contenu manquant.

Canada

"To laugh often and much, to win the respect of intelligent people and the affection of children; to earn the appreciation of honest critics and endure the betrayal of false friends; to appreciate beauty, to find the best in others; to leave the world a bit better, whether by a healthy child, a garden patch or a redeemed social condition; to know even one life has breathed easier because you have lived. This is to have succeeded."

-Ralph Waldo Emerson

This thesis is dedicated to my left Achilles tendon,
for giving me the “break” I needed.

ABSTRACT

Early in development, embryos of the pond snail, *Helisoma trivolvis*, express superficial ciliary cells that are responsible for generating embryo rotation within the egg capsule. The neurotransmitter 5-hydroxytryptamine (5-HT) regulates ciliary activity in numerous systems, including *Helisoma*. The *Helisoma* model system is well-suited to an examination of the neural control of ciliary activity as well as the signal transduction pathways and potential "cross-talk" between pathways. The main objectives of this thesis are to characterize the three populations of superficial ciliary cells and to further examine the roles of Ca^{2+}, from intracellular and extracellular sources, and protein kinase C (PKC) in ciliary motility and 5-HT-induced cilioexcitation in *Helisoma* embryos.

A microdissection procedure was developed to culture identified ciliary cells as well as a technique to load *Helisoma* ciliary cells with Ca^{2+}-sensitive dyes. To test the hypothesis that the three ciliary subpopulations expressed on the surface of the embryo are distinct, each ciliary cell type was cultured and examined morphologically and physiologically using electron microscopy, immunohistochemistry, high-speed digital videomicroscopy and Ca^{2+} imaging. To further elucidate the signal transduction that underlies the cilioexcitatory response to 5-HT, pedal ciliary cells were cultured and the ciliary beat frequency and intracellular Ca^{2+} concentration ($[Ca^{2+}]_i$) were monitored in response to pharmacological perturbations of the Ca^{2+} and PKC signaling pathways.

The results showed that pedal and dorsolateral ciliary cells share structural and physiological characteristics, whereas the scattered single ciliary cells were structurally and physiologically distinct. Only the pedal and dorsolateral ciliary cells displayed cilioexcitatory responses to 5-HT. The phospholipase C-PKC pathway played a partial role in signal transduction, acting either in parallel to, or as a facilitator of, an additional signal transduction pathway. In contrast, Ca^{2+} released from an intracellular store was an essential step in the initial ciliary response and the influx of extracellular Ca^{2+} was required for the maintenance of the ciliary response. Finally, a novel caffeine-sensitive release mechanism, and possibly the mitochondria, were identified as regulatory elements in the intracellular Ca^{2+} store component of the response.

The experiments presented in this thesis further delineate the signal transduction pathways that underlie the cilioexcitatory response to 5-HT within a well-characterized embryonic neural circuit.

ACKNOWLEDGEMENTS

With all my being, I wish to thank my supervisor Jeff Goldberg for his guidance, his patience, his support, his wisdom, his humor and his love. Jiggy, you have assumed many titles throughout the years of our interaction and not the least of which is that of my friend-- you are my friend, always have been and always will be. Thank you for all that you have taught me about science, philosophy, truth, balance and life.

I must also extend a most heartfelt appreciation to my supervisory committee: John Chang and Declan Ali. John, you are brilliant, quirky and have one of the largest hearts of anyone I know. Please do not ever change. Declan, you have always been able to surprise me with that wonderful sense of humor that sits just below the surface of your fantastic intellect. All the best.

Thank you to everyone that was involved in the examination processes. To my external examiner Dennis Willows, thank you for coming to Edmonton in the middle of December and for all your input in the defense. To the "internal-external" examiners that joined for the exams, Bill Colmers, Christina Benishin and Mike Belosevic, thank you for the "terror and torture" but actually for making the process enjoyable. And to Paul Wong for chairing the candidacy exam and to Dick Peter for chairing the defense, thank you for being there to look out for my best interests.

Throughout my time in Biological Sciences I have had the very good fortune to interact with numerous wonderful people whose support and good humor enabled the completion of this thesis. I am truly blessed because I know that many of the friendships that I have made along the way I will carry forward. Naturally, I must acknowledge the graduate students with whom I have worked, laughed, drank and cried. These include: Annapurni "P" Narayanan, Jim Johnson, Aubrey Uretsky, Warren Yunker, Brian Weiss, Shihuan Kuang, Geoff "Moses" Boddy, Suraj Unniappan, Tara Klassen, Stefan Little, Kevin Friesen, Shawn Parries, Alex Eaves, Kee-Chan Ahn, Wan-Peng Sun, Grant Sawisky, Liz Orr, Martin Tresguerres and Todd Cole. You have all touched my life in

wonderful and unique ways. To the post doctoral fellows that I met along the way: Calvin Wong, Jane Fraser, Scott Kelly and Fabian Canosa, thank you for your friendship and for providing me with the hope that the end could actually be reached. I must also extend my appreciation to other profs and colleagues in Bio Sci for your support along the way: Greg Goss, Norm Stacey, Bill Samuel, Ruben Kaufman, Yuka Asai, Cagla Eskicioglu, Dawn Kieller and Rakesh Bhatnagar. A special thanks to my "bio sci mom" Maggie Haag for ALL that you have done for me. I cannot express how much I have appreciated it. Thanks to James Maclagan for all your help, support and abuse over the years and Ron Koss for technical assistance, helpful discussions and encouragement. For administrative help and general all around kindness, I want to acknowledge the assistance of Chesceri Mason, Gwen Jewett and Michelle Green. I must also acknowledge the Department of Biological Sciences for a Teaching Assistantship that supported me financially through this degree, as well as the Faculty of Graduate Studies and Research for an Andrew Stewart Memorial Graduate Research Prize and the Province of Alberta for a Graduate Fellowship. Further, this research would not have been possible without a Natural Sciences and Engineering Research Council of Canada operating grant to Jeff Goldberg.

I genuinely believe that with the backing of good friends and family absolutely anything is possible. There is no measure for how much I value my friends and can not put into words my appreciation for their support and affection. In addition to my aforementioned friends in Biological Sciences, others that are very close to my heart include: Mirka Pribylova, Melanie Leitch, Laurie Eisler, Mercy Tetteh-Wayoe, Sharon Milne, Bill Donahue, Solomon Ssenyange, Kyle Marcotte, Francois Parent and Darin MacDonald. Finally, to my family, I appreciate your love and encouragement. You certainly keep my life interesting.

Thank you to all mentioned here and to many others. The beauty with which you live your lives inspires me.

TABLE OF CONTENTS

INTRODUCTION. 1

1 Ciliary Structure and Activity. 2

- 1.1 Ciliary Structure. 3
    - The Axoneme. 3
    - The Central Pair Microtubules. 4
    - Dynein. 5
    - The Outer Dynein Arms. 7
    - The Inner Dynein Arms. 8
    - The Radial Spokes. 10
    - Nexin Links and Other Axonemal Structures. 12
- 1.2 Ciliary Activity. 13
    - The Microtubule Sliding Model. 13
    - The Switch Point Hypothesis. 14
    - The Production of Ciliary Bending. 15
    - Metachronism. 16
    - Modeling Ciliary/Flagellar Activity. 17

2 Extracellular Control of Ciliary Cells. 18

- 2.1 Chemical control of ciliary cells. 19
- 2.2 Mechanical control of ciliary cells. 24
- 2.3 Thermal and electrical control of ciliary cells. 25

3 Signal Transduction within Ciliary Cells. 27

- 3.1 Role of Ca^{2+}. 27
    - Ca^{2+} as a regulator of ciliary activity. 32
- 3.2 Role of cAMP-PKA. 36
    - cAMP as a regulator of ciliary activity. 37
- 3.3 Role of PKC. 40
    - PKC as a regulator of ciliary activity. 41
- 3.4 Role of NO-cGMP-PKG. 42
    - NO-cGMP-PKC as regulators of ciliary activity. 44

3.5 Role of other signaling pathways identified in ciliary cells. 45

4 Ciliary Cells in *Helisoma trivolvis* Embryos. 48

5 Objectives. 50

5.1 To characterize the three ciliary subpopulations expressed on the surface of the embryo. 50

5.2 To examine the roles of Ca^{2+} and PKC and their potential interactions during 5-HT-induced cilio-excitation in pedal ciliary cells. 51

5.3 To examine the involvement of intracellular Ca^{2+} stores in the ciliary response to 5-HT in pedal ciliary cells. 51

MATERIALS AND METHODS. 60

1 Animals. 60

2 Chemicals and Solutions. 60

2.1 Characterization of subpopulations of ciliary cells expressed on the surface of *Helisoma* embryos. 61

2.2 Roles of Ca^{2+} and PKC in the excitatory response to serotonin in pedal ciliary cells. 61

2.3 The involvement of intracellular Ca^{2+} stores in the excitatory response to 5-HT in pedal ciliary cells. 62

3 Mixed Population Ciliary Cell Culture. 62

4 Cell Culture of Identified Ciliary Cell Populations. 63

5 Electron Microscopy. 63

6 Ciliary Beat Frequency Analysis. 64

7 Ratiometric Ca^{2+} Imaging and Ca^{2+} Calibration. 65

7.1 Characterization of subpopulations of ciliary cells expressed on the surface of *Helisoma* embryos. 65

7.2 Roles of Ca^{2+} and PKC in the excitatory response to serotonin in pedal ciliary cells and the involvement of intracellular Ca^{2+} stores in the excitatory response to 5-HT in pedal ciliary cells. 67

8 Immunohistochemistry. 67

9 Preparation of antibodies to 5-HT1_{hel} and 5-HT7_{hel}. 68

10 Data Analysis . . . 68

RESULTS . . . 73

1 Characterization of subpopulations of ciliary cells expressed on the surface of *Helisoma* embryos . . . 73
  - 1.1 Anatomical characterization of ciliary cell subtypes *in vivo* . . . 73
  - 1.2 Examination of unidentified ciliary cells *in vitro* . . . 74
  - 1.3 Examination of physiological responses of identified ciliary cells *in vitro* . . . 75
  - 1.4 Differences in immunohistological staining for 5-HT and 5-HT receptors in the different subpopulations . . . 77

2 Roles of Ca^{2+} and PKC in the excitatory response to serotonin in pedal ciliary cells . . . 94
  - 2.1 Necessity for a change in $[Ca^{2+}]_i$ in 5-HT-stimulated ciliary beating. 94
  - 2.2 Involvement of PLC signaling in 5-HT-stimulated ciliary beating . . . 95
  - 2.3 Effect of 5-HT and DAG analogs on $[Ca^{2+}]_i$ in pedal ciliary cells . . . 95
  - 2.4 Effect of removing extracellular Ca^{2+} prior to DAG analog and 5-HT stimulation of pedal ciliary cells . . . 96
  - 2.5 Effect of PKC inhibitors on 5-HT stimulation of pedal ciliary cells . . . 97

3 The involvement of intracellular Ca^{2+} stores in the excitatory response to 5-HT in pedal ciliary cells . . . 109
  - 3.1 Mitochondrial involvement in Ca^{2+} regulation during 5-HT stimulation of pedal ciliary cells . . . 109
  - 3.2 Effect of thapsigargin-sensitive intracellular stores and IP_3 receptor pathway in the ciliary response to 5-HT . . . 110
  - 3.3 Involvement of caffeine-sensitive stores in ciliary activity . . . 112
  - 3.4 Involvement of ryanodine-sensitive stores . . . 113

DISCUSSION . . . 130

1 Identified populations of *Helisoma* ciliary cells . . . 130
  - 1.1 Mixed populations of *Helisoma* ciliary cells in culture . . . 131

  1.2 Innervated *Helisoma* ciilary cells. 132
  1.3 Non-innervated *Helisoma* ciliary cells. 136
2 Involvement of PKC and Ca^{2+} in ciliary activity in *Helisoma* ciliary cells. . . . 138
  2.1 The relative roles of intracellular Ca^{2+} release and Ca^{2+} influx. . . . 139
  2.2 Involvement of PKC in 5-HT-induced cilio-excitation. 142
3 Involvement of intracellular Ca^{2+} stores in ciliary activity of *Helisoma* ciliary cells. 145
  3.1 Role of mitochondrial-sequestered Ca^{2+} in the ciliary activity of pedal ciliary cells. 146
  3.2 Lack of involvement of conventional ER Ca^{2+} stores in the ciliary activity of pedal ciliary cells. 150
  3.3 Unique caffeine-sensitive store identified in the ciliary response to 5-HT in pedal ciliary cells. 153
  3.4 Interplay between ER and mitochondria in the regulation of intracellular Ca^{2+}. 155
4 Regulation of embryonic ciliary cells from *Helisoma trivolvis*. 156
5 Ciliary regulation at the level of the axoneme. 159
6 Future directions. 161

ENDNOTES. 169

REFERENCES. 170

APPENDIX. 207

LIST OF FIGURES

Figure 1 Schematic of the effective and recovery stroke of ciliary beating. 53

Figure 2 Schematic of the ciliary axoneme 55

Figure 3 Structure of the dynein heavy chain and organization of dynein motor complex 56

Figure 4 Model of the mechanochemical cycle of dynein arm-microtubule interactions 58

Figure 5 Schematic showing how a bend is produced from sliding microtubules. 59

Figure 6 Isolation of identified ciliary cells from *Helisoma trivolvis* embryos. 70

Figure 7 Microinjection of fura dextran into a cultured *Helisoma* ciliary cell. 71

Figure 8 DIC micrograph of pedal ciliary cell loaded with fura dextran. 72

Figure 9 SEM and TEM micrographs of the three ciliary subtypes in a stage E-28 embryo. 81

Figure 10 Effect of 5-HT and ionomycin on the intracellular Ca^{2+} concentration in unidentified ciliary cells in culture 82

Figure 11 Effect of 5-HT and ionomycin on CBF in pedal, dorsolateral and scattered single ciliary cells 83

Figure 12 Effect of 5-HT and ionomycin on intracellular Ca^{2+} concentration in pedal ciliary cells. 84

Figure 13 Effect of 5-HT and ionomycin on intracellular Ca^{2+} concentration in dorsolateral ciliary cells. 85

Figure 14 Effect of 5-HT and ionomycin on intracellular Ca^{2+} concentration in scattered single ciliary cells. 86

Figure 15 5-HT immunoreactivity in isolated tissue containing pedal ciliary cells. 87

Figure 16 5-HT immunoreactivity in isolated tissue containing dorsolateral ciliary cells. 88

Figure 17 5-HT immunoreactivity in isolated tissue containing scattered single ciliary cells. 89

Figure 18 5-HT1$_{hel}$ receptor immunoreactivity in identified *Helisoma* ciliary cells. 91

Figure 19 5-HT7$_{hel}$ receptor immunoreactivity in identified *Helisoma* ciliary cells. 93

Figure 20 Effect of BAPTA on the CBF response to 5-HT. 99

Figure 21 Effect of a PLC inhibitor on the CBF response to 5-HT. 100

Figure 22 The effect of PLC inhibitor U-73122 on 5-HT-induced changes in $[Ca^{2+}]_i$. 101

Figure 23 Effect of 5-HT and ionomycin on the intracellular Ca^{2+} concentration. 102

Figure 24 Effect of DAG analogs and ionomycin on the intracellular Ca^{2+} concentration. 103

Figure 25 Effect of removing extracellular Ca^{2+} on CBF and $[Ca^{2+}]_i$ responses to DOG. 104

Figure 26 Effect of removing extracellular Ca^{2+} on CBF and $[Ca^{2+}]_i$ responses to 5-HT. 105

Figure 27 Effect of PKC inhibitors on the CBF response to 5-HT. 106

Figure 28 Effect of PKC inhibitors on the $[Ca^{2+}]_i$ response to 5-HT. 108

Figure 29 Effect of carbonyl cyanide *m*-chlorophenylhydrazone (CCCP) on stimulated ciliary beating 116

Figure 30 Effect of ruthenium compounds on stimulated ciliary beating. 118

Figure 31 Effect of thapsigargin on ciliary beating in pedal cilia. 120

Figure 32 Effect of thapsigargin on intracellular Ca^{2+}. 121

Figure 33 Effect of xestospongin C on stimulated cliary beating. 122

Figure 34 Effect of caffeine and 5-HT on ciliary beating. 123

Figure 35 The effect of altering cyclic nucleotide signaling on ciliary beating. 125

Figure 36 Effect of caffeine pretreatment on 5-HT-stimulated ciliary beating. 126
Figure 37 Effect of stimulatory dose of ryanodine on ciliary beating. 127
Figure 38 Effect of ryanodine receptor inhibition on stimulated ciliary beating. 128
Figure 39 Effect of ryanodine pretreatment on caffeine-stimulated ciliary beating. 129
Figure 40 Signal transduction underlying basal and 5-HT-stimulated ciliary beating in *Helisoma* pedal ciliary cells. 166
Figure 41 Molecular complexity of the ciliary axoneme. 168

ABBREVIATIONS

5-HT	5-hydroxytryptamine; serotonin
$[Ca^{2+}]_i$	intracellular Ca^{2+} concentration
AA	arachidonic acid
AC	adenylyl cyclase
ADP	adenosine diphosphate
ATP	adenosine triphosphate
BAPTA	2-bis-(2-Aminophenoxy)-ethane-N,N,N,N'-tetraacetic acid
cADPR	cyclic adenosine 5'-diphosphoribose
CaM	calmodullin
CaMKII	calmodulin dependent kinase II
cAMP	3',5'-cyclic adenosine monophosphate
CBF	ciliary beat frequency
CCCP	carbonyl cyanide *m*-chlorophenylhydrazone
cGMP	3',5'-cyclic guanosine monophosphate
CICR	calcium-induced calcium release
DA	dopamine
DAG	diacylglycerol
DIC	Nomarski differential interference contrast microscopy
DMSO	dimethyl sulfoxide
DOG	1,2-Dioctanoyl-*sn*-glycerol
EGTA	ethyleneglycol-bis(2-aminoethylether)-N,N,N',N'-tetraacetic acid
ENC1	embryonic neuron C1
ER	endoplasmic reticulum
GC	guanylyl cyclase
GTP	guanosine triphosphate
HS	*Helisoma* saline
IONO	ionomycin
IP_3	inositol 1,4,5-trisphosphate
KLH	Keyhole Limpet hemocyanin

NAADP	nicotinic acid adenine dinucleotide phosphate
NADPH	nicotinamide adenine dinucleotide phosphate
NO	nitric oxide
NOS	nitric oxide synthase
OAG	1-Oleoyl-2-acetyl-*sn*-glycerol
PBS	phosphate buffered saline
PDE	phosphodiesterase
PKA	cAMP-dependent protein kinase
PKC	protein kinase C
PKG	cGMP-dependent protein kinase
PLA_2	phospholipase A_2
PLC	phospholipase C
PP	protein phosphatase
PRK	PKC-related kinase
PS	phosphatidylserine
PTP	permeability transition pore
RACK	receptors for activated C-kinase
RaM	rapid uptake mode
RGS2	regulator of G-protein signaling protein 2
RICK	receptors for inactive C-kinase
ROS	reactive oxygen species
Ru360	$(\mu)[(HCO_2)(NH_3)_4Ru]_2Cl_3$
SEM	scanning electron microscopy
SERCA	sarcoplasmic/endoplasmic reticulum Ca^{2+} ATPases
SSCC	scattered single ciliary cell
TEM	transmission election microscopy

INTRODUCTION

The beautiful rhythmic, and often synchronous pattern of ciliary beating has captured the attention of scientists for over 300 years. Since the earliest description of ciliary activity by Antony Van Leeuwenhoek in 1675 (Satir, 1995), these unique organelles have continued to fascinate and challenge biologists. Cilia are hair-like, cellular extensions that function to generate fluid currents over the cell surface (reviewed in Satir and Sleigh, 1990). This current flow is important in a number of biological activities, including: unicellular movement (Chia et al., 1984), filter feeding (Murakami and Machemer, 1982), particle clearance in host-defense (Salathe and Bookman, 1995) and the determination of left-right asymmetry (Essner et al., 2002). Aspects of the ultrastructure of these organelles and the characteristic pattern in which they beat appear highly conserved amidst the wide array of organisms in which cilia are found. However, many questions continue to be intensely studied in regards to the extracellular cues that regulate ciliary beating, the signal transduction cascades involved in mediating ciliary activity, as well as the molecular components within the ciliary structure that translate intracellular signals into mechanical beating.

Early in development, embryos of the fresh water pond snail, *Helisoma trivolvis* (Mollusca, Gastropoda, Pulmonata, Basommatophora, Planorbidae), express ciliary cells on the surface that are responsible for generating embryo rotation within the egg capsule (Diefenbach *et al.*, 1991; Koss *et al.*, 2003). The neurotransmitter 5-hydroxytryptamine (5-HT; serotonin) has been shown to regulate ciliary activity in numerous systems, including *Helisoma* (Diefenbach *et al.*, 1991; Kuang and Goldberg, 2002). Experiments performed on mass dissociated ciliary cells have revealed that 5-HT-stimulated cilio-excitation relies on numerous intracellular signaling pathways, including: changes in intracellular Ca^{2+} concentration ($[Ca^{2+}]_i$), protein kinase C (PKC) and nitric oxide (NO) (Christopher *et al.*, 1996; 1999; Cole *et al.*, 2002; Doran *et al.*, 2003). The main objectives of this thesis are to characterize the populations of ciliary cells expressed on the surface of the embryo and to further examine the roles of Ca^{2+}, from intracellular and extracellular sources, and PKC in ciliary motility and 5-HT-induced cilio-excitation within *Helisoma* embryos. It is hypothesized that 5-HT activates multiple signal transduction pathways that act in concert with one another to mediate an increase in the rate of ciliary beating.

1 Ciliary Structure and Activity

Motile cilia are found in plants, unicellular protozoans, and most groups of animal species, with the notable exception of some nematodes and arthropods (Rivera, 1962). When an organism bears a single cilium, it is termed a flagellum, whereas the term cilium is used when the organelles occur in larger numbers. The structure and mechanisms of movement of eukaryotic flagella and cilia are very similar and often considered identical. This is in contrast with prokaryotic flagella that are an extracellular appendage of the cell. They display a very different protein composition and mechanism of movement as compared to cilia (Witman, 1990), and will not be discussed further. Additionally, single nonmotile cilia are being identified on many cell types in both invertebrates and vertebrate species. The function of this cilium, referred to as the primary cilium, has remained the subject of much speculation. Given the ubiquity of the primary cilium and the complement of specific receptors on this "antenna" to the extracellular environment, it has been postulated that it functions as a sensory organelle (Pazour and Witman, 2003). Although fascinating, primary cilia also will not be discussed further.

Cilia beat in an asymmetrical manner with an effective stroke, resulting from a progressive bend at the base of the cilium that causes the cilium to move rapidly through the medium, followed by a recovery stroke, where the bend is propagated along the ciliary shaft until the cilium returns to the original position. This pattern results in fluid movement parallel to the surface of the cell in the direction of the effective stroke (Figure 1). This activity is brought about through the interaction of some of the >250 polypeptides that comprise the ciliary axoneme, the microtubular array that provides the structural support and machinery necessary for ciliary motility (Luck, 1984; Witman, 1990). Although numerous organisms are examined in the study of cilia and flagella, the green algae *Chlamydomonas reinhardtii* has been invaluable in elucidating ciliary structure and activity. *Chlamydomonas* possess two large flagella that propel the organism through an aqueous environment. The successful application of numerous molecular genetic approaches, including the ability to generate viable mutant strains, has yielded a wealth of information about ciliary structure and activity from this model system.

1.1 Ciliary Structure

The Axoneme

The axonemal arrangement of microtubules within motile cilia is highly conserved in a typical 9x2+2 longitudinal arrangement, referring to two central singlet microtubules surrounded by nine outer doublets of microtubules, all enclosed by a specialized extension of the cell membrane. The other structures that compose the axoneme include outer and inner dynein arms, radial spokes, and nexin links (Figure 2). These structures will be discussed in more detail subsequently. Axonemal microtubules, similar to cytoplasmic microtubules, are composed of α- and β-tubulin heterodimers that form protofilaments, accounting for seventy percent of the protein mass within the axoneme (Dutcher, 1995). The conjoined outer doublets consist of a circular A tubule that contains 13 protofilaments, and a B tubule containing 10 or 11 protofilaments (depending on the species) that shares part of the wall of the A tubule; this common wall is thought to be composed of the intermediate-filament-like protein tektin (Satir and Sleigh, 1990). The $\alpha\beta$-tubulin dimers within the protofilaments coil with a periodicity of 8 nm, which is thought to provide a basis for the positioning of microtubule associated structures (Witman, 1990).

The axoneme is assembled above the basal body, a cytoplasmic structure that is characterized by a ring of nine triplet microtubules and serves as the organizational center of the axoneme. The outer doublets are assembled directly above the basal body and remain connected to the microtubules of the basal body, as the A and B tubules of the outer doublets are contiguous with the A and B microtubules of the basal body triplets (Dutcher, 1995; Witman 1990). Similar to cytoplasmic microtubules, the axonemal doublets are polarized, with the fast polymerizing end most distal to the basal body. Axonemal doublets are acetylated during assembly, which in addition to enabling interactions with other axonemal proteins, is thought to provide stability (Witman, 1990; Satir and Sleigh, 1990). The central pair microtubules appear to rely on the basal body for correct placement during assembly, but are not continuous with basal body microtubules (Dutcher, 1995). The central pair originates in the transition zone, which is a specialized region between the base of the axoneme and the distal end of the basal body (Witman, 1990). Within the transition zone, invaginations of the cell membrane appear to interact with the axoneme, forming a transmembrane complex that is termed the ciliary necklace. Interestingly, breakage of the ciliary shaft during deciliation occurs within the transition zone above the ciliary necklace. As studied in *Chlamydomonas reinhardtii*, this process is Ca^{2+} dependent and most likely involves centrin, a Ca^{2+}-binding protein found in the transition zone (Sanders and Salisbury, 1989).

The Central Pair Microtubules

The central pair microtubules, similar to cytoplasmic microtubules, are less rigid than the highly supported outer doublets, and associate with as many as 23 nontubulin polypeptides (Dutcher, 1984). The central pair is the only structure within the axoneme that displays an obvious asymmetry, which may be important in the differential regulation of other axonemal structures (Wargo and Smith, 2003). The two microtubules, referred to as C1 and C2, can be distinguished by different subsets of associated polypeptides. In C1, the associated polypeptides form two long projections (1a and 1b) and two short projections (1c and 1d), whereas C2 has three short projections (2a, 2b and 2c; Dutcher, 1995; Wargo and Smith, 2003). The projections repeat longitudinally every 16 nm, with one of the microtubules also having barbs that repeat every 32 nm (Witman, 1990). These projections from the central pair microtubules have been referred to as the central sheath, because they appeared in early electron micrographs as filaments wrapping around the microtubules (Witman, 1990).

Early electron micrograph studies of ciliary beating in *Paramecium* revealed that the central pair rotates with respect to the nine outer doublets during each beat of the cilium (Omoto and Kung, 1979). The phenomenon of central pair rotation has been demonstrated directly in the marine alga *Micromonas pusilla*, where the central pair extends beyond the 9 + 2 region (Omoto and Witman, 1981), and in demembranated *Chlamydomonas* and sea urchin sperm (Omoto *et al.*, 1999). It is believed that the central pair microtubules regulate the circumferential and longitudinal shear forces of the sliding microtubules to produce effective bending of the axoneme (discussed below). Furthermore, it has been shown that the central pair microtubules are involved in a Ca^{2+}-dependent decrease in the velocity of microtubule sliding in sea urchin sperm flagella, a process thought to involve the Ca^{2+}-binding protein calmodulin (CaM; Bannai *et al.*, 2000). Finally, the central pair microtubules, along with the radial spokes, participate in a signal transduction pathway involving casein kinase 1 and protein phosphatase 1 that regulates the activity of the inner dynein arms (Smith, 2002a).

Dynein

Inner and outer dynein arms extend from each A tubule of the outer doublet toward the B tubule of the adjacent doublet (Figure 2). Dyneins are 1-2 MDa, multi-component, molecular motor proteins that generate force toward the minus end of microtubules (Figure 3; reviewed in King, 2000). First discovered in axonemes over thirty years ago, dynein is responsible for generating the force necessary to drive ciliary beating. The dynein motor complex is composed of one or more dynein heavy chains, and several intermediate and light chains. Given the precise control required to regulate axonemal bending and oscillation, not to mention the various roles that cytoplasmic dynein plays in other parts of the cell, it is not surprising that the composition of each dynein motor appears to be specific to a particular function. At least 16 different dynein heavy chains have been identified in *Chlamydomonas*, with 14 thought to function within the flagellum (King, 2000).

The inner and outer axonemal dynein arms (discussed below) are functionally distinct, likely a result of differences in their heavy chain isoforms and how they combine into hetero-dimers or –trimers at the N terminal regions (Asai and Brokaw, 1993). The N-terminal or stem of the dynein complex forms a stable association with the A tubule, the "cargo" to be transported. Intermediate chain/light chain complexes also interact with the dynein heavy chain to form a trimeric docking complex that facilitates A microtubule binding (Figure 3; King 2003). The intermediate chain/light chain complex is also believed to be required for the localization of the dynein complex to its appropriate site within the axoneme (King, 2003).

The adenosine triphosphate (ATP)ase of the dynein motor resides in the globular head of the C-terminal domain of the heavy chain, which has six copies of the ancient AAA^+ ATP-binding module (Figure 3). The catalytic γ-phosphate-binding site, or dynein P-loop that engages in nucleotide binding and ATP hydrolysis, is located near the middle of the dynein heavy chain amino acid sequence within the first AAA^+ domain and is identical in all heavy chain sequences identified to date (Gibbons, 1995; Asai and Brokaw, 1993; King, 2003). Interestingly, the heavy chain sequence possesses three additional copies of the consensus P-loop motif for nucleotide binding that are evenly spaced through the middle of the sequence (Saraste *et al.*, 1990). The functional significance of these sites had been the subject of much speculation, but a recent *in vitro* motility study by Kikushima *et al.* (2004) has suggested that a process of adenosine diphosphate (ADP) binding to multiple sites on the inner arm dynein regulates microtubular movement. The domain that binds dynein to the microtubules of the adjacent B tubule is believed to reside in an anti-parallel arranged coiled-coil segment at the tip of a stalk emanating from the C-terminal head (Figure 3; Asai and Brokaw, 1993; King, 2000).

The Outer Dynein Arms

The outer dynein arms attach to the A tubule with a periodicity of 24 nm (Figure 2B) and are believed to be necessary for the majority of the power generation during beating and the control of beat frequency (Asai and Brokaw, 1993; Taylor *et al.*, 1999). Studies examining a loss of outer dynein arms, either through high salt extraction or mutation, have revealed that the axoneme remains mobile, but the velocity is significantly reduced (Gibbons and Gibbons, 1973; Brokaw, 1999; Kamiya, 1995). The number of heavy chains in the outer dynein arms can vary between species; in *Chlamydomonas*, the outer arm contains three dynein heavy chains, known as α, β and γ (King, 2003), whereas sea urchin sperm flagella contain two (α and β) heavy chains (Asai and Brokaw, 1993). The heavy chains exhibit distinct enzymatic and motor properties and also interact with at least ten additional polypeptides. This includes the aforementioned intermediate chain/light chain complex, direct interaction between the individual heavy chains and at least one light chain that directly regulates heavy chain activity (King, 2003).

Distinct regulatory inputs appear to affect dynein heavy chain activity. In *Chlamydomonas* flagella, the N-terminal of the α and β heavy chains interact with thioredoxin family polypeptides that contain redox-active sites, implicating redox-reactions in the regulation of axonemal motors (Patel-King *et al.*, 1996). Further, DC3, a subunit of the outer dynein arm-docking complex in *Chlamydomonas*, has also been determined to be redox- sensitive, in addition to being a Ca^{2+} binding protein (Casey *et al.*, 2003). The γ heavy chain interacts with at least two distinct classes of light chain proteins, LC1 and LC4. LC1, belonging to the leucine-rich repeat family of proteins, binds at or near the ATP hydrolytic site of the γ heavy chain and is believed to regulate ATPase activity. In contrast, LC4 contains an EF hand domain, indicating a likely role for Ca^{2+} in regulating the activity of the outer dynein arm (King. 2003). Similarly, Ca^{2+} binding to a component of the dynein complex is necessary for β heavy chain interaction with microtubules in the presence of ATP (Sakato and King, 2003). Finally, phosphorylation also appears to play an important role in dynein regulation as 3',5'-cyclic adenosine monophosphate (cAMP)-dependent phosphorylation of p29, a regulatory light chain associated with the outer dynein arm, controls ciliary beat frequency in *Paramecium* (Satir *et al.*, 1993). Interestingly, the phosphorylation of p29 was shown to be sensitive to the level of Ca^{2+} (Hamasaki *et al.*, 1989). Thus, it appears that redox states, protein composition of accessory polypeptides, Ca^{2+} and phosphorylation states are involved in the regulatory control of outer dynein arm activity.

The Inner Dynein Arms

The inner dynein arms, like the outer dynein arms, are attached to the A tubule of the outer doublets and extend towards the B tubule of the adjacent doublets. They are believed to be responsible for generating the specific changes in ciliary shape during the ciliary beat cycle (Taylor *et al.*, 1999). *Chlamydomonas* mutants lacking all or components of the inner arm are generally immobile, whereas mutants lacking only the outer arms can still generate movement, albeit at a much slower rate.

Mutants of *Chlamydomonas* have been invaluable in assessing the structure and function of the inner dynein arms (see Kamiya, 1995 for review of *Chlamydomonas* mutants). Inner dynein arms have greater structural complexity than outer arms, resulting in the emergence of a number of different models (one model is shown in Figure 2B). Much of the current evidence has suggested that each longitudinal 96 nm segment of the doublet microtubules contains 3 different inner dynein arm complexes, the IDA1, IDA2 and IDA3. IDA1, referred to as a triad, is associated with the first radial spoke within a 96 nm repeat and has three globular heads. Each of the other two complexes has two globular heads and are thus referred to as dyads (summarized in Witman, 1990). An alternative model suggests that there are two morphologically different rows of inner dynein arms within a 96 nm longitudinal segment (Muto *et al.*, 1991). In an effort to resolve these different possibilities, which are believed to result from interpreting a three-dimensional structure from two-dimensional micrographs, Taylor and colleagues (1999) used a computer modeling approach to propose that within the 96 nm repeat, there are three different inner dynein arm complexes, each containing four inner dynein arms, three dyads and one-single-headed arm. Undoubtedly, further refinements will be made to the proposed structure of inner dynein arms.

Eleven inner arm dynein heavy chain genes have been identified through sequence homology and expression studies, with eight inner arm dynein heavy chains having been isolated from *Chlamydomonas* flagellar extracts (reviewed in Porter and Sale, 2000). Each inner dynein arm is thought to be composed of several heavy chains complexed with several intermediate and light chains. At least seven distinct inner dynein arm isoforms have been identified: one two-headed form and six single-headed isoforms, with a complex arrangement of these isoforms within 96 nm repeats and throughout the length of the entire axoneme (Porter and Sale, 2000). Given that the individual dyneins are believed to function differently, the specific location within the 96 nm repeat and along the axoneme may be very important in enabling precise control of the waveform during beating.

The complexity of the inner arms and difficulty in resolving their structure result in a situation where less is known about the molecular regulation of the inner dynein arms, as compared to the outer dynein arms. The dynein regulatory complex, composed of seven tightly bound axonemal polypeptides, is believed to mediate the attachment of appropriate dynein isoforms to specific positions on the A tubule (Piperno *et al.*, 1994). The dynein regulatory complex is located in close proximity to radial spoke 2 (within a 96 nm repeat) and an inner dynein arm. The dynein regulatory complex is also thought to be involved in transmitting signals from the radial spokes to the inner dynein arms to regulate activity (Gardner *et al.*, 1994). When radial spoke regulation was removed in *Chlamydomonas* mutants, the activity of the inner dynein arms was directly affected by an interaction that involved cAMP-dependent protein kinase (PKA) and protein phosphatase 1 (Habermacher and Sale, 1995). Certain dynein heavy chains of the inner arm have also been demonstrated to interact with centrin, a light chain Ca^{2+} binding protein, suggesting a role for Ca^{2+} in inner arm regulation (LeDizet and Piperno, 1995). *Chlamydomonas* mutant experiments in which the assembly or activity of the IDA1 complex was disrupted suggested that the first inner dynein arm complex, within the 96 nm repeat, plays the most important role in the control of ciliary and flagellar beating (reviewed in Porter and Sale, 2000). There are at least two known subunits of IDA 1 that are thought to be involved in regulating its activity. The first is Tctex1, a light chain that has been shown to interact with protein kinases. The second is IC138, another light chain whose phosphorylation state has been correlated to microtubule sliding velocities (Porter and Sale, 2000). Further, casein kinase 1 has been located on the outer doublets within *Chlamydomonas* axonemes, and is likely responsible for IC138 phosphorylation; activity of this kinase inhibits I1 dynein driven microtubule sliding (Porter and Sale, 2000).

The Radial Spokes

Groups of two or three radial spokes (depending on the species) extend from the A tubule of each doublet toward the center of the axoneme, repeating at an interval of 96 nm (Figure 2; Witman, 1990). The radial spoke, consisting of a thin stalk and a bulbous head, is located in close proximity to the inner dynein arms, enabling an interaction between the two structures. In *Chlamydomonas* the radial spoke is composed of at least 22 polypeptides, with at least 5 localized in the head (for review see Luck, 1984).

Identification of radial spoke composition is assisting in identifying how these structures regulate activity. Radial spoke protein 3 participates in both the assembly of radial spokes (Diener *et al.*, 1993) and in regulating ciliary activity by anchoring PKA close to the inner dynein arms (Gaillard *et al.*, 2001). In addition to PKA, Ca^{2+} has also been identified as an important regulatory signal in ciliary and flagellar activity, often thought to act through CaM. In the first localization of CaM to an axonemal structure using biochemical techniques, it was found within the radial spoke (Yang *et al.*, 2001). This specific protein was later identified as radial spoke protein 2, which also contains a GAF domain, a ubiquitous segment in signal transduction proteins that binds molecules such as 3',5'-cyclic guanosine monophosphate (cGMP; Yang *et al.*, 2004). Functionally, the localization of CaM to radial spoke protein 2 is supported by findings that Ca^{2+} inhibits dynein activity through a mechanism involving the radial spokes, as well as the central pair microtubules (Nakano *et al.*, 2002). CaM-dependent kinase II (CaMKII), in addition to CaM, has also been implicated in the regulation of Ca^{2+} signals by the central pair/radial spoke complex (Smith, 2002b). Finally, radial spoke protein 2, as well as 4 other spoke proteins, have been identified as target phosphorylation sites *in vivo* (Piperno *et al.*, 1981), again supporting the conclusion that this structure plays an important role in regulating axonemal activity. Further characterization of radial spoke composition should continue to yield information about its regulatory role.

A combination of structural and genetic evidence has indicated that the radial spokes and central pair microtubules interact as key regulators of dynein arm activity (reviewed in Smith and Lefebvre, 1997). One model suggests that the projections from the central pair function like a "distributer" to provide local signals to the radial spokes that selectively activate or inactivate specific dynein arms (Omoto *et al.*, 1999). In support of this model, *Chlamydomonas* mutants lacking the central pair/radial spoke structures are paralyzed under physiological conditions. The central pair/radial spoke complex is believed to regulate the rate of dynein-driven microtubule sliding, and thus control the size and shape of the bend in the cilium. A study by Smith and Sale (1992) suggests that there is a constitutive control system that inhibits dynein activity in the absence of signals from the central pair/radial spoke complex. It is thought that cAMP-dependent phosphorylation inhibits dynein activity, whereas radial spokes act to override the endogenous protein kinase(s). Consistent with this hypothesis, the radial spokes have been shown to activate inner dynein arms through the dephosphorylation of a critical dynein component, a process mediated by axonemal type-1 phosphatase (Habermacher and Sale, 1996). Additional support comes from bypass suppressor mutant experiments on paralyzed central pair/radial spoke mutants, whereby pharmacological induction of phosphatase activity partially restored ciliary motility (Huang *et al.*, 1982).

A second function attributed to the central pair/radial spoke complex is to coordinate inner and outer arm activity at physiological levels of ATP (Porter and Sale, 2000). High levels of ATP inhibit the outer arms by binding to an outer arm dynein heavy chain; however, the central pair/radial spoke complex may override this inhibition through activation of the inner arms (Omoto *et al.*, 1996). Recently, radial spoke protein 23 (or p61), identified as a component of the radial stalk, was shown to contain a novel nucleoside diphosphate kinase domain, in addition to two classes of IQ motifs that bind CaM (Patel-King *et al.*, 2004). It may be that nucleotides in addition to ATP play a role in the signal transduction events mediated by the radial spokes.

Nexin Links and Other Axonemal Structures

Nexin links are highly elastic thin fibers that connect the A tubule of one outer doublet to the B tubule of an adjacent doublet at intervals of 96 nm (Figure 2). They are thought to be responsible for limiting microtubule sliding within a certain range in the intact axoneme (Warner, 1976; Minoura *et al.*, 1999). However, there is also evidence to suggest that nexin undergoes attachment-detachment cycles in connecting the outer doublets, given that the elastic properties of nexin are reduced *in vivo* (Bozkurt and Woolley, 1993). The nexin links exhibit oscillatory behavior and step-wise jumping when microtubule sliding is mechanically constrained. During microtubule sliding, transverse forces are created within the interdoublet gap and it is proposed that the nexin links transfer these forces into regulatory signals for the dynein regulatory complex through rapid expansion and slow relaxation. The resulting signals are proposed to control local ATPase activity of the dynein arms (Woolley, 1997; Cibert, 2001).

There are several axonemal structures in addition to those already discussed, only some of which may be general characteristics of ciliary and flagellar axonemes. The outer pairs of doublets that lie on the plane of beat are connected by a highly reinforced bridge. Similarly, a central pair bridge connects the two central tubules (Witman, 1990). In *Chlamydomonas* and other green algae, structures projecting into the lumen of specific B tubules that lie in the plane of the beat and are thought to control the flagellar waveform (Witman, 1990). Finally, there are bridges that link the cell membrane to microtubules along the length of the entire axoneme, including the base and the distal tip of each cilium (reviewed in Dentler, 1990). These membrane connections may serve to anchor the microtubules, bind proteins and other structures to the membrane, and function in the transport of material up and down the axoneme. The close proximity of the membrane with the microtubules may also be important in ciliary regulation, as Ca^{2+} influx occurs throughout the entire cilium, as revealed by Ca^{2+} imaging studies in the ciliate *Didinium nasutum* (Iwadate and Suzaki, 2004).

1.2 Ciliary Activity

The Microtubule Sliding Model

It is well accepted that ciliary and flagellar motility results from a dynein-driven sliding of specific microtubules along their adjacent doublets. The sliding microtubule model, roughly analogous to the sliding filament mechanism for muscle contraction, was inferred from the predicted sliding geometry of sea urchin axonemes during ciliary bends (Brokaw, 1965), examination of electron micrographs of *Paramecium* ciliary tips (Satir, 1968) and the observed sliding during flagellar disintegration (Summers and Gibbons, 1971). Direct observation of microtubule sliding in actively bending demembranated sea urchin spermatozoa flagella was accomplished using gold beads as position markers (Brokaw, 1989). Electron micrographs of partially trypsin-digested axonemes revealed that the addition of ATP induced the A tubule of one outer doublet to push an adjacent doublet in a base to tip direction, resulting in microtubule sliding and disintegration of the axoneme (Sale and Satir, 1977). Together, these observations prompted a model of the mechanochemical cycle of ciliary beating (Figure 4; Satir *et al.*, 1981). This model holds that in an inactive state, or rigor, the dynein arm which is permanently attached to the A tubule stretches across the interdoublet gap to attach to a specific binding site on the B tubule of the adjacent doublet. The binding of ATP to dynein, but not hydrolysis, causes the dynein arm to shorten and release from the B tubule. The dynein arm then extends 40° basally and reattaches to a more proximal site on the B tubule of the adjacent doublet, in a process that is driven by ATP hydrolysis and the release of ADP and P_i. Subsequent to reattachment, the dynein arm returns to rigor position, causing distal sliding of the adjacent doublet. When the dynein arms are not active, the doublets return to their original position through a passive process.

The Switch Point Hypothesis

The Switch Point Hypothesis was developed to account for the fact that a single cycle of ciliary beating consists of an effective stroke followed by a recovery stroke, even though the microtubule sliding caused by dynein arms occurs exclusively in a proximal-distal direction (Satir and Matsuoka, 1989). This model states that there is asynchrony in dynein arm activity, with one half of the axoneme in an active cycling state during the effective stroke, followed by activation of the other half during the recovery stroke. It is believed that there are at least two different axonemal switches, one to control the on/off state of one set of doublets and another to control the on/off state of the other set of doublets. The central pair/radial spoke complex is thought to coordinate the switching events with doublets 1-4 interacting with one of the central pair microtubules and doublets 6-9 interacting with the other central microtubule (Satir and Sleigh, 1990).

A dynamic analysis of the propagation velocity and shape of the ciliary bend during a beat cycle has suggested that there may be nine separate activation events, rather than the two proposed in the original Switch-Point Hypothesis. In this case, separate activation of the individual doublets might facilitate a timed progression of activation along the length of the axoneme to control the frequency of beating, as well as the phase relationship in the activation of doublets around the circumference of the axoneme to regulate the shape of the bend (Satir and Sleigh, 1990). In support of this possibility, electron micrograph analysis of *Chlamydomonas* wildtype and mutant axonemes has revealed that the C1 central microtubule is oriented toward the position of actively-sliding microtubules, and that levels of Ca^{2+} may control central pair orientation (Wargo and Smith, 2003). These findings were confirmed using a microtubule sliding assay, where subsets of microtubules were activated in a Ca^{2+}-dependent manner following ATP introduction (Wargo *et al.*, 2004).

The Production of Ciliary Bending

Once microtubule sliding had been well-established as a central process in ciliary beating, it was important to explain how the movement of these non-elastic elements produces the characteristic bending that is observed in ciliary and flagellar activity. The transformation of microtubule sliding into bending lies in the internal resistance within the axoneme. The basal body is a fixed point where the outer doublets are permanently linked together, a prerequisite for the generation of curvature (Figure 5). However, if there were only a single linkage point, microtubule sliding would only give rise to back and forth oscillations at this junction between the basal body and the axoneme. To enable the conversion of microtubule sliding into propagated bending along the axoneme, the force created by sliding, or sliding shear, must be restricted by a structural component that lies normal to this force and imposes a local resistance to enable a bend to develop (Cosson, 1992). Thus, a bend is formed and propagated by the continuous opening of links located on the leading edge of the bend occurring simultaneously with the closing of links on the trailing edge of the bend. Although the central pair/radial spoke complex does play a role in regulating bend formation, it is not believed to be the structure that forms the resistive links. *Chlamydomonas* mutants lacking the central pair/radial spoke complex can still display bending behavior, albeit with altered properties (Huang *et al.*, 1982). In contrast, the nexin links are the most likely candidates thought to impose localized attachments and detachments that facilitate bending.

Implication of the nexin links as the key resistive structures in bend formation comes from experiments where mild trypsin digestion disrupts the nexin links causing impairment to bend formation (King and Witman, 1988). Further, studies have revealed that nexin links do detach from adjacent doublets and undergo a mechanical cycle of rapid extension, slow relaxation and stand-by in the connection between the outer doublets (Cibert, 2001). However, it should be noted that trypsin treatment also disrupts the dynein heavy chains, so the dynein arms themselves could impose a restriction to sliding when in the tightly binding rigor formation. Furthermore, different dynein subunits or molecules may function in rigor formation and force generation, with these structures being tightly regulated temporally or spatially along the axoneme (Cosson, 1992). Indeed, since uniform and simultaneous activity of the dynein arms would prevent the propagation of a bend along the length of the axoneme, there must be local control to generate active sliding in a temporally controlled manner. Altogether, the formation of bending requires precise control of numerous components of the axoneme, including a feedback loop monitoring physical parameters such as the curvature of the outer doublets, distance between the outer doublets, shear displacement, changes in velocity of microtubule sliding and bend formation (Witman, 1990).

Metachronism

Metachronal coordination between cilia occurs when cilia beat with a phase difference between adjacent rows, allowing the ciliary tips to form a moving wave pattern. Metachronal waves may appear in different forms depending on the direction of wave propagation; symplectic metachronism is the situation where the wave propagates in the direction of the effective stroke, antiplectic metachronism occurs when the wave is opposite to the effective stroke and diapletic metachronism results when the metachronal wave is perpendicular to the effective stroke (reviewed in Sleigh, 1966). Examination of cilia in *Paramecium* revealed that the type of metachronism may change in response to changes in the environment, with membrane potential and Ca^{2+}

levels regulating both the metachronism and the direction of the effective and recovery stroke (Machemer, 1972). It has also been speculated that metachronism results from hydrodynamic influences (Gheber and Priel, 1989). Although the reason for metachronal waves is incompletely understood, evidence is starting to suggest that metachronism reduces the energy expenditure required for beating. It has been shown that the mechanical work done during the effective stroke is five times that of the recovery stroke, and that there is energetic efficiency when cilia beat metachronally (Gueron and Levit-Gurevich, 1999).

Modeling Ciliary/Flagellar Activity

Possibly the earliest study to postulate a model for ciliary and flagellar motion is that of Gray and Hancock (1955). This examination of sea urchin spermatozoa propulsion sought to simplify some of the physical properties of ciliary and flagella motion through highly viscous and incompressible surroundings. Since that time, extensive study has been directed towards modeling ciliary/flagellar activity.

Certain general considerations are held in modeling ciliary activity. First, cilia operate in a low Reynolds number (an estimate of the ratio of the inertial forces to the viscous forces acting on the system) environment where inertia is negligible. Second, for optimal function the effective stroke takes advantage of high viscous resistance to generate thrust. Finally, the slow tangential recovery stroke returns the cilia to the ready position by minimizing viscous resistance (Gueron and Levit-Gurevich, 1999; Holwill *et al.*, 1995). Furthermore, there are numerous other factors incorporated in models of ciliary/flagellar motility, including the internal forces generated within the axoneme, the hydrodynamic influence of the viscous aqueous environment and ciliary interactions. Modeling has yielded information about ciliary action during filter feeding, shown through flow simulations (Silvester, 1988), and revealed how axonemal bends are propagated (Cosson, 1992). The first computer models enabled a 3-dimensional representation of the axoneme that was empowered with the appropriate axonemal composition to facilitate analysis and prediction of how structures move and change during bending (Gueron and Liron, 1993; Holwill and Satir, 1994).

Intense study in the area of computer modeling resulted in the development of the Geometric Clutch Hypothesis, an interesting model put forward to suggest a unified mechanism underlying ciliary and flagellar beating. This hypothesis states that transverse forces develop across the axoneme in the plane of the beat, having maximal effect on doublets 2-4 on one side of the axoneme and doublets 7-9 on the other side. This transverse force brings these doublets into close proximity, allowing dynein bridges to form and then terminate when transverse forces cause the doublets to separate. Thus, it is these transverse forces that regulate dynein activity (Lindemann, 1994; Lindemann and Kanous, 1995). This model is able to produce ciliary and flagellar waveforms, but is limited by a cursory account of the underlying hydrodynamics. Continued work has developed models which couple the internal force generation of molecular motors through the passive and elastic structures of the axoneme with the external fluid dynamics (Dillon and Fauci, 2000; Gueron and Levit-Gurevich, 2001).

2 Extracellular Control of Ciliary Cells

Cilia possess an inherent capability to generate motility, whereby a precise, yet incompletely understood interaction between the numerous diverse axonemal structures results in ciliary beating. However, cilia are responsive to several extracellular signals that regulate multiple aspects of ciliary beating, including frequency, direction, waveform and activity state. This responsiveness to the external environment is an important feature and may explain why many sensory structures have developed with cilia as a central component. The external cues that motile cilia respond to include chemical, mechanical, thermal and electrical signals. These external signals are coupled to ciliary activity through a variety of intracellular signaling cascades (discussed in the next section). While protozoan, invertebrate and vertebrate examples will be discussed, it is interesting to note that much of the research investigating the physiological regulation of cilia by external stimuli has been performed on invertebrate models.

2.1 Chemical control of ciliary cells

In examining the factors thought to regulate ciliary activity, most of the attention has focused on chemical regulators, with the neurotransmitter 5-HT probably being the most recognized agent that alters ciliary beating. In the late 1950's and early 1960's, it was revealed that 5-HT released from the branchial nerve had a cilio-excitatory affect on gill cilia of the bivalve *Mytilus edulis* (Aiello, 1957). 5-HT was also identified as the endogenous regulator of the prototrochal and velar cilia in nudibranch embryos (Koshtoyants *et al.*, 1961). Since that time, 5-HT has been identified as the predominant cilio-excitatory agent in both intact epithelial tissue and isolated cells in both invertebrates and vertebrates.

Numerous examples of serotonergic neuronal control of cilia are found among the molluscs, including: 5-HT released from the branchial nerve controls lateral gill cilia in *Mytilus edulis* (Paparo and Murphy, 1975a; 1975b), 5-HT released from the paired pedal ganglion neurons Pd 21 in *Tritonia diomedea* regulates the ciliated foot epithelium (Audesirk *et al.*, 1979), paired pedal A-cluster neurons regulate foot cilia in *Lymnaea stagnalis* (Syed and Winlow, 1989), serotonergic neurons innervate the ciliated velum of *Aplysia californica* (Marois and Carew, 1997) and 5-HT released from the paired ENC1 neurons regulates ciliary activity in *Helisoma trivolvis* embryos (Kuang and Goldberg, 2001). A cilio-inhibitory role for 5-HT has been demonstrated in the ciliated epithelium of the esophagus of *Tritonia diomedea* (Pavlova *et al.*, 1999). This result is interesting because it demonstrates that there are different regulatory roles for 5-HT on ciliated epithelium within the same animal. In embryos of the gastropod *Physa elliptica*, 5-HT caused an increase in the rate of cilia-driven rotation, and interestingly, so do a number of putative serotonin reuptake inhibitors (Uhler *et al.*, 2000). However, the endogenous presence of 5-HT was not demonstrated.

Similarly, ciliary beat frequency (CBF) was increased with exogenous application of 5-HT to the sea urchin larvae *Pseudocentrotus depressus* and *Hemicentrotus pulcherrimus* (Mogami *et al.*, 1992; Wada *et al.*, 1997), although once again endogenous presence of the neurotransmitter remains to be shown. A unique role for 5-HT, as well as catecholamines, has been revealed in the regeneration of cilia in the ciliated protozoan *Tetrahymena thermophila* (Castrodad *et al.*, 1988). 5-HT has also been shown to have a cilio-excitatory effect on the ciliated epithelium of frog palantine mucosa (Maruyama *et al.*, 1984). Interestingly, in this system 5-HT synthesis was detected within epithelial cells, suggesting possible regulatory action within the tissue. Exogenous 5-HT application caused an increase in ciliary activity in rat brain slices and isolated ependymal cells (Nguyen *et al.*, 2001).

Dopamine (DA) is another commonly identified cilio-regulatory agent, however, unlike 5-HT it is often associated with decreased ciliary beating. In some cases where neural innervation of cilia has been demonstrated, 5-HT and DA act antagonistically to exert tight control on ciliary activity, as seen in the brachial nerve innervation of lateral gill cilia in *Mytilus edulis* (Paparo and Murphy, 1975a; Catapane, 1983). High-affinity DA receptors in the palp and gill tissue of *Mytilus californianus* further suggest that DA plays a role in these ciliated tissues (Smith 1982). The transient apical catecholaminergic (TAC) neurons in embryonic *Lymnaea stagnalis*, identified as the homologues to ENC1s in *Helisoma*, were shown to regulate ciliary activity through long projections that branched extensively under the ciliated apical plate (Voronezhskaya *et al.*, 1999). Additionally, the short, cilia-bearing projections of the neurons that penetrate the epithelium of *Lymnaea* embryos are homologs to the dendritic knob of ENC1s. Dopamine has also been identified to stimulate ciliary activity of cells on the pedal epithelium of the marine mollusc *Tritonia diomedea* (Woodward *et al.*, 2002). Cilio-inhibition by DA, as mediated by DA-containing cells within the ciliated epithelium, has been demonstrated in frog palatine mucosa (Maruyama *et al.*, 1983). Cilio-reversal by DA was demonstrated in the pluteus larvae of the sea urchin *Pseudocentrotus depressus* (Mogaml *et al.*, 1992), whereas another study revealed DA-induced decreases in the CBF in *Pseudocentrotus depressus* and *Hemicentrotus pulcherrimus* (Wada *et al.*, 1997). The endogenous presence of DA was not demonstrated within the sea urchin larvae, limiting conclusions about the physiological role of DA within this system.

A third neurotransmitter known to regulate ciliary activity in a variety of systems is noradrenalin. In the polychaete *Spirobranchus giganteus*, larval ciliary cells are stimulated in the presence of adrenergic receptor agonists. Further, ciliary responses are blocked in the presence of adrenergic receptor antagonists, suggesting an endogeneous adrenergic regulatory pathway (Marsden and Hassessian, 1986). In frog palatine mucosa, sympathetic release of noradrenaline was shown to have a cilio-inhibitory effect at concentrations less than 10^{-7} M, and a cilio-excitatory effect at higher concentrations (Maruyama, 1984). The presence of β-adrenergic receptors has been demonstrated in rabbit tracheal epithelial cells (Lansley *et al.*, 1992) and canine bronchial epithelium (Tamaoki *et al.*, 1993), suggesting that an adrenergic pathway controlling ciliary activity may be important in mammals. Various α- and β- adrenergic agonists cause a cilio-excitatory effect when exogenously applied to the sea urchin larvae *Psammechinus miliaris*; however, endogenous expression was not demonstrated (Soliman, 1983). In addition to the well-characterized involvement of 5-HT and DA in the *Mytilus edulis* system, exogenous application of noradrenalin caused a cilio-inhibitory effect on the veliger larvae of this organism (Beiras and Widdows, 1995). Noradrenalin may serve an important cilio-regulatory role in the larval stage organism given that the neurotransmitter is also an active inducer of metamorphosis (Pires *et al.*, 1997; Kimura *et al.*, 2003).

An additional neurotransmitter commonly identified to regulate cilia is acetylcholine. Ciliary activity in pedal epithelial cells from *Tritonia* is inhibited by acetylcholine, with the presence of this neurotransmitter localized to neurites located near the ciliary basal surface (Woodward *et al.*, 2002). Similarly, ciliary arrest in the ascidians *Chelyosoma productum* and *Ciona intestinalis* has been demonstrated to result from a cholinergic pathway (Arkett, 1987; Arkett *et al.*, 1989). In contrast, acetylcholine causes increased ciliary beating in frog palate epithelium (Aiello *et al.*, 1991). Direct cholinergic synaptic contacts between intraepithelial nerve endings and ciliated cells have been demonstrated (Chu and Kennedy, 1994). Similarly, an extensive network of autonomic nerve fibers innervating airway epithelium have been identified in other vertebrate systems. Accordingly, acetylcholine cilio-excitation has been demonstrated in ovine ciliated airway epithelium (Salathe *et al.*, 1997) and human respiratory epithelium (Yang *et al.*, 1996).

Another chemical regulator of ciliary activity is extracellular ATP. The binding of extracellular ATP to purinergic receptors is recognized to stimulate a number of biological activities including neuronal excitation, contraction and secretion (Burnstock, 1976). Extracellular ATP was first linked to cilio-excitation in the ciliated epithelium of frog palate over fifty years ago (Varhous and Deyup, 1953). Since that time, ATP has been recognized as one of the most potent activators of ciliary beating, particularly in mammalian systems. However, the physiological relevance of extracellular ATP is not well understood. Despite this, the examination of ATP effects on ciliary activity has been particularly useful in determining intracellular signaling events thought to underlie ciliary beating (see next section). ATP application has been demonstrated to enhance ciliary beating in frog palate and esophagus epithelium (Weiss *et al.*, 1992; Tarasiuk *et al.*, 1995) and rabbit airway epithelium (Korngreen and Priel, 1996). ATP application to ovine and human airway epithelial cells has been important in examining species differences in the signaling cascades thought to underlie the ciliary response to ATP (Nlend *et al.*, 2002; Lieb *et al.*, 2002).

There is also evidence that ATP-related compounds are able to cause enhancement of CBF. In hamster oviductal epithelium, the binding of ATP and adenosine to separate receptors on ciliated cells suggests that there may be functional cross-talk between multiple signal transduction pathways (Morales *et al.*, 2000). Similarly, differential effects of ATP and UTP on the profile of cilia-excitation suggest that there is an interplay between the type and state of the nucleotides and the purinoceptors activated (Morse *et al.*, 2001). A cilio-inhibitory role for ATP has been identified in ependymal cells from rat brain, whereby 5-HT plays an antagonistic cilio-excitatory role (Nguyen *et al.*, 2001).

Additional compounds that have been shown to exert an effect on ciliary activity include various neuropeptides and hormones. Certain neurons in the pedal ganglion of the nudibranch *Tritonia diomedea* synthesize three novel peptides, termed Tpeps. When applied to isolated cells from the pedal epithelium, Tpeps produce an increase in CBF (Willows *et al.*, 1997). Immunolabelling reveals the presence of Tpeps in specific cells in the brain, foot and ciliated epithelium in not only *Tritonia diomedea*, but the gastropod *Lymnaea stagnalis* as well, suggesting a general cilio-regulatory role for these neuropeptides in molluscs. The neuropeptide substance P caused an increase in ciliary beating in frog palate, both through direct stimulation of the ciliary cells, and indirectly through stimulation of acetylcholine release (Aiello *et al.*, 1991). The inhibitory neuromodulator neuropeptide Y, seen to colocalize with noradrenalin in sympathetic neurons, was postulated to regulate ciliary cells. In human tracheal and bronchial ciliated cells, exogenous application of neuropeptide Y does cause a decrease in CBF (Wong *et al.*, 1998). However, it remains to be determined if this effect is physiologically relevant. In rabbit trachea, the hormone arginine vasopressin caused an increase in CBF with a peak and plateau profile (Tamaoki *et al.*, 1998). Similarly, prostaglandin E_2 stimulated ciliary activity in rabbit oviduct (Verdugo, 1980).

Finally, ethanol was hypothesized to decrease ciliary activity given that chronic alcoholism can impair lung function. Interestingly, low to moderate ethanol concentrations have been demonstrated to increase ciliary activity. In ovine tracheal epithelium, ethanol concentrations of 0.01- 0.1% increased ciliary activity, with a reduction in ciliary activity occurring at concentrations higher than 2% (Maurer and Liebman, 1988). In bovine bronchial epithelial cells ethanol concentrations of 10 mM caused a rapid stimulation of ciliary activity and it was only at concentrations higher than 1000 mM that a decrease in CBF was observed (Sisson, 1995).

2.2 Mechanical control of ciliary cells

In addition to responding to numerous chemical agents, mechanical activation of cilia has been demonstrated in numerous systems. The mechanism by which cilia are mechanically stimulated is not completely understood, but in many systems changes in ciliary activity have been linked to Ca^{2+} influx. In *Paramecium*, physical contact on the anterior surface of the organism, such as a collision during locomotion, results in a reversal of ciliary beating coupled to an increase in CBF (Naitoh and Eckert, 1969). It is thought that this response results from membrane depolarization and Ca^{2+} influx through voltage-gated Ca^{2+} channels. Macrocilia in the ctenophore *Beroe* occur in dense bands on the inner margin of the lip, with a single macrocilium consisting of approximately 2500 ciliary axonemes cross-linked to one another and contained within a common membrane. During feeding, active beating of the macrocilia enable the lips to spread over prey. Activation of ciliary beating is believed to result from physical contact of the prey with the macrocilia. Experimentally, repetitive mechanical stimulation was demonstrated to result in widespread activation of macrocilia (Tamm, 1988). Mechanical stimulation is thought to excite the pharyngeal nerve net and result in a depolarization event that opens voltage-gated Ca^{2+} channels. Interestingly, in lateral gill ciliary cells of *Mytilus edulis*, mechanical stimulation has been shown to generate a Ca^{2+}-dependent depolarizing receptor potential that produces local arrest of ciliary activity (Murakami and Machemer, 1982). However, when lateral gill ciliary cells have been arrested by a rapid introduction of Ca^{2+}, either through application of ionophore or DA, a mechanical stimulation initiates a recovery in ciliary activity (Strommel, 1986).

Mechanical stimulation of ciliary cells has also been demonstrated in vertebrate systems. In the ciliated epithelium of the oviduct of the salamander *Necturus maculosus*, mechanical stimulation causes a transient membrane depolarization and increase in CBF that varies with the intensity of the stimulus (Murakami and Eckert, 1972). Once again, this response was dependent on a Ca^{2+} influx. Similarly, cultured ciliary cells from rabbit tracheal mucosa exhibit a mechanically stimulated increase in CBF that is dependent on extracellular Ca^{2+} (Sanderson and Dirksen, 1986). This response was transmitted to adjacent cells in all directions, suggesting possible electrical coupling of the ciliary cells. The mechanical stimulation of ciliated respiratory epithelium plays a crucial role in host defense of most vertebrate species, as ciliary beating serves to clear debris from respiratory passages. It is evident that in many systems, physical contact with ciliary cells results in an important functional change in ciliary activity.

2.3 Thermal and electrical control of ciliary cells

Many biological activities show a dependence on temperature, and ciliary beating is no different. Generally, an increase in temperature produces an increase in CBF until a maximum temperature is reached, beyond which activity is impaired. Early work by Gray in frontal gill cilia from *Mytilus edulis* gill cilia agrees with this generalization (reviewed in Rivera, 1962). Further work in *Mytilus* revealed that changes in temperature alter the beating rhythmicity of lateral gill cilia (Stefano *et al.*, 1977). Interestingly, in epithelial tissue cultures from frog palate, ATP-induced increases in CBF were found to be temperature insensitive in the temperature range of 15-25°C (Ovadyahu *et al.*, 1988). Similarly, a study in human nasal epithelium found that while a linear relationship exists between increased temperature and increased ciliary beating in the temperature range of 19-32°C, there is no effect of temperature on CBF between 32-40°C, the normal functioning temperature range for this tissue (Green *et al.*, 1995). In rabbit tracheal epithelial cells, basal CBF tripled when the temperature was increased from 20-23°C to 37°C. Further work revealed that cells at 37°C exhibited a larger increase in CBF following mechanical stimulation, but the amplitude of the change in $[Ca^{2+}]_i$ was significantly reduced at this temperature (Lansley and Sanderson, 1999). Work in human nasal epithelium examining ciliary beating at reduced temperatures (< 10°C) has revealed that PKC and CaMKII may be involved in the temperature regulation of CBF (Mwimbi *et al.*, 2003). These signaling pathways may be important in regulating how the cilia in hibernating animals remain beating in thermal conditions that normally reduce ciliary activity.

Although not yet shown to be physiological, electric currents have also been demonstrated to alter ciliary activity. The most striking example is the galvanotaxis of *Paramecium*. When a current was passed through the medium in which a *Paramecium* was swimming, the CBF of the cilia facing the anode increased, whereas the cilia facing the cathode reversed direction. This resulted in a reorientation of the organism with the anterior end pointing towards the cathode and forward swimming in that direction (reviewed in Eckert, 1972). In contrast, in the presence of an electric current, the ciliated protozoan *Opalina* reorients and swims toward the anode (reviewed in Naitoh and Eckert, 1974). Again, the cellular basis for this behavior has been explained by localized changes in membrane potential. Work done in both the *Paramecium* and *Opalina* systems has revealed that depolarization and hyperpolarization of the cell membrane both result in an increase in CBF, whereby depolarization also produces a shift in the plane of the effective stroke (Eckert, 1972). This depolarization-induced ciliary reversal is dependent on increases in intracellular Ca^{2+}.

There is some limited research to indicate that photic stimulation can also alter ciliary activity. In gill cilia of *Mytilus*, photoactivation of two neuronal chromoproteins (red-hemoprotein and yellow-carotenoprotein) altered ciliary activity in a manner that was dependent on intact innervation of the ciliary cells (Paparo and Murphy, 1978). Photosensitive behavior is also exhibited by *Paramecium bursaria*, as these organisms will accumulate in lighted areas. It is believed that photosensors are found on both somatic and ciliary structures, as even deciliated cells exhibited some capacity to respond to light. Indeed, this result was further supported by the immunodetection of a rhodopsin-like protein on ciliary and somatic membranes (Nakaoka *et al.*, 1991). Thus, ciliary cells exhibit the ability to detect and respond to a vast array of extracellular stimuli.

3 Signal Transduction within Ciliary Cells

Numerous studies of demembranated cilia and flagella have revealed that the intrinsic program for beating resides within the axoneme, as demonstrated by the fact that ATP-reactivation is sufficient to restore dynein coordination of normal beating in the absence of other signaling mechanisms. However, it is becoming more apparent that numerous adaptive mechanisms modify axonemal activity in response to stimuli. Much of the study of ciliary cells in the past three decades has focused on determining these signal transduction pathways that regulate ciliary activity, with a focus on vertebrate systems. Yet, despite the highly conserved ciliary ultrastructure, there does not appear to be a unified underlying regulatory mechanism for altering activity. Rather, there is huge diversity among the systems examined. The predominant signal transduction pathways identified to control ciliary activity are changes in $[Ca^{2+}]_i$, cAMP-PKA, PKC, and NO acting through cGMP and cGMP-dependent protein kinase (PKG).

3.1 Role of Ca^{2+}

Although different signaling pathways have been identified to modulate ciliary motility, usually in a species-specific fashion, Ca^{2+} is recognized to be a universal participant in all systems examined. This ubiquitous signaling molecule controls a staggering array of biological activities including fertilization, gene transcription, muscle contraction, exocytosis and cell death (Berridge *et al.*, 2000). Cellular activity is modified through controlled changes in $[Ca^{2+}]_i$, with these signals exerting different effects through the spatial and temporal nature of the Ca^{2+} event. Resting cytosolic levels of Ca^{2+} are in the low nanomolar range, while the concentration in the extracellular environment is three orders of magnitude higher, in the low millimolar range (Clapman, 1995). The level of intracellular Ca^{2+} is maintained through efficient buffering by protein components of the cytosol, energy-dependent processes of uptake into various intracellular organelles, and active extrusion across the plasma membrane through Ca^{2+} ATPases and Na^{+}/Ca^{2+} exchange. The strict maintenance of resting $[Ca^{2+}]_i$ in the intracellular environment is necessary to ensure that different biological processes are not prematurely initiated, and to allow rapid responses to Ca^{2+} signals. Changes in Ca^{2+} may occur as localized microscopic changes, such as in microdomains around the mouth of a channel, or large-scale global changes, which can be propagated across the entire cell and even between cells (Bootman *et al.*, 2001). These signals may also be temporally coded, as changes in Ca^{2+} are seen to occur in microseconds, as in the case of Ca^{2+}sparks in arterial smooth muscle, or over the course of hours, such as in the Ca^{2+} transients that control cell division (Berridge *et al*, 1998). Further, it is thought that Ca^{2+} oscillations are also relevant signals, with the frequency and amplitude of these signals providing regulatory instructions.

To facilitate control over multiple Ca^{2+}-mediated cell processes, not only are the signals coded spatially and temporally, but also there are multiple sources of Ca^{2+} with unique release and uptake properties that may act independently or cooperatively to generate Ca^{2+} signals. These sources can be broadly classified into two categories: Ca^{2+} entry across the plasma membrane and Ca^{2+} release from intracellular stores. The unequal distribution of Ca^{2+} across the plasma membrane and the negative membrane potential creates a substantial driving force for Ca^{2+} entry that the cell harnesses to generate rapid and specific signals. Plasma membrane Ca^{2+} channels are activated by numerous stimuli, including membrane depolarization, extracellular ligands, intracellular ligands, stretch and intracellular Ca^{2+} dynamics (Berridge *et al.*, 2000). Each of these activators of Ca^{2+} channels have been identified to play a role in facilitating Ca^{2+} entry into ciliary cells in a species-specific manner. Voltage-dependent Ca^{2+} channels have received considerable attention and are probably the best understood means of Ca^{2+} influx. Members of this broad family of channels are characterized by their activation through changes in membrane potential and their pharmacological and physiological profiles (Kits and Mansvelder, 1996; Tsien and Tsien, 1990). Even before these channels had been originally identified, their existence had been hypothesized in *Paramecium*, where changes in ciliary beating resulted from changes in membrane potential or $[Ca^{2+}]_i$. It was believed that these two conditions were linked and that membrane depolarization caused a change in Ca^{2+} conductance (Eckert, 1972). Indeed Eckert had been correct in this initial postulation, as the existence of voltage-dependent channels was confirmed in *Paramecium* a few years later (Brehm and Eckert, 1978). Ligand-gated channels may also be important for Ca^{2+} entry into ciliary cells. Acetylcholine, ATP and 5-HT have all been shown to stimulate ligand-gated Ca^{2+} channels (Burnashev, 1998). As these neurotransmitters also modulate ciliary motility, ligand-gated Ca^{2+} channels may be important in the signal transduction of these responses.

Release of Ca^{2+} from intracellular stores is an intricate process including multiple organelles and distinct mechanisms for Ca^{2+} release and uptake. The intracellular messengers thought to stimulate Ca^{2+} release from stores include inositol 1,4,5-trisphosphate (IP_3), cyclic adenosine 5'-diphosphoribose (cADPR), NO, reactive oxygen species (ROS), nicotinic acid adenine dinucleotide phosphate (NAADP), diacylglycerol (DAG), arachidonic acid (AA), sphingosine, sphingosine-1-phosphate and Ca^{2+} itself (Bootman *et al.*, 2002). The endoplasmic reticulum (ER) plays a central role in intracellular signaling and is the most commonly identified organelle to participate in sequestration and release of Ca^{2+}. Pumps on the ER membrane (sarcoplasmic/endoplasmic reticulum Ca^{2+} ATPases; SERCA) actively move Ca^{2+} into the ER where Ca^{2+}-binding proteins, such as calsequestrin and calreticulin, facilitate the storage of high levels of Ca^{2+}. To stimulate release, the ER is sensitive to some of the aforementioned messengers, including Ca^{2+}. Ca^{2+} can initiate a positive feedback process known as calcium-induced calcium release (CICR), whereby Ca^{2+} entry events at the plasma membrane or other intracellular Ca^{2+} release events are coupled to release at the ER. This mechanism is involved in initiating regenerative Ca^{2+} signals and global Ca^{2+} changes (Berridge, 2002).

The IP_3 and ryanodine receptors are the major Ca^{2+} release channels on the ER. IP_3, generated by phospholipase C (PLC)-mediated cleavage of the membrane phosphsolipid phosphatidylinositol 4,5-bisphosphate, acts on three sub-types of IP_3 receptors that appear to differ in their ATP and Ca^{2+} sensitivity (Johnson and Chang, 2000). It was believed that IP_3 binding to its receptors was obligatory for release through these channels; however, recent evidence suggests that Ca^{2+} release through IP_3 channels may be differentially regulated. For example, a group of Ca^{2+}-binding proteins that belong to the neuronal calcium sensors subfamily can bind and activate IP_3 receptors, independent of IP_3 (Yang *et al.*, 2002). Ryanodine receptors, believed to be functionally distinct from IP_3-sensitive channels, have three known isoforms (Johnson and Chang, 2000). One of the endogenous signals identified to activate ryanodine receptors is the novel second messenger cADPR, which can be generated by the enzymes ADP-ribosyl cyclase and CD38 (Pozzan *et al.*, 1994). More recently, NAADP has been identified to activate an ER store that is insensitive to IP_3 and cADPR (Genazzani and Galione, 1997), thus implicating a third type of Ca^{2+} release channel on the ER with a unique pharmacological profile. Additionally, the sphingomyelinase signaling pathway has been putatively identified to play a role in initiating ER Ca^{2+} signaling; however, its precise role and mechanism of action require further clarification (Berridge, 2002).

Mitochondria are organelles that also accumulate Ca^{2+} within their inner membrane and participate in the physiological regulation of Ca^{2+} signals. Ca^{2+} is sequestered into mitochondria through two mechanisms that have not yet been identified at the molecular level: a uniporter that utilizes the electrochemical proton gradient and a rapid uptake mode (RaM; Ganitkevich, 2003; Jacobson and Duchen, 2004). The uniporter, a high capacity/low affinity transport system that is activated by high extramitochondrial levels of Ca^{2+}, may be very important in shaping the spatial and temporal characteristics of Ca^{2+} signals (Duchen, 1999; Rizzuto *et al.*, 2000). In contrast, RaM is a more efficient mechanism of Ca^{2+} uptake characterized by a transient time course of activation (Rizzuto *et al.*, 2000). The fact that both the uniporter and the RaM are activated by ATP and guanosine triphosphate (GTP) and inhibited by ruthenium red raises the possibility that both mechanisms act on the same pore in different conformations (Jacobson and Duchen, 2004).

Ca^{2+} is released from mitochondria through three different pathways: Na^+-independent Ca^{2+} efflux, Na^+-dependent Ca^{2+} efflux and activation of the permeability transition pore (PTP; Rizzuto *et al.*, 2000). Na^+-independent Ca^{2+} efflux is most likely coupled to H^+ entry with a stoichiometry of >2 H^+ to 1 Ca^{2+} (Ganitkevich, 2003). The dominant Ca^{2+} efflux pathway appears to be through a 3 Na^+/1 Ca^{2+} exchange that is driven by the transmitochondrial membrane potential (Ganitkevich, 2003). The PTP is a non-selective channel located on the inner membrane that exhibits low and high conductance states (Rizzuto *et al.*, 2000). The involvement of the PTP in Ca^{2+} cycling is poorly understood, but activation of the high conductance state is associated with a collapse of the mitochondrial membrane potential and release of mitochondrial factors that trigger apotosis (Ganitkevich, 2003).

To facilitate rapid regulation of cytosolic Ca^{2+} signals, mitochondria lie in close proximity to sites of Ca^{2+} release and entry. The mitochondria and ER form a highly connected dynamic network to assist each other in the shaping of Ca^{2+} signals (Berridge, 2002). The interplay between these organelles is also important in homeostasis of the cell, as Ca^{2+} fluxes between the ER and mitochondria are associated with the generation of stress signals and onset of apoptosis (Berridge, 2002). Additionally, other organelles have been identified to participate in Ca^{2+} signaling, including the Golgi, secretory granules and the nucleus (Johnson and Chang, 2000). However, less is known about the Ca^{2+} uptake and release mechanisms from these organelles. Thus, intracellular organelles form an elaborate network for the uptake and release of Ca^{2+}.

To elicit biological activity, Ca^{2+} binds to a vast array of Ca^{2+}-regulated enzymes and structural proteins. The most commonly identified structural motifs that bind Ca^{2+} are the EF hand domain and C2-domain. The EF hand consists of an N-terminal helix (the E helix) and a C-terminal helix (the F helix) that are connected by a coordinating loop that interacts with Ca^{2+} ions (Chin and Means, 2000). Proteins with EF hand domains exhibit two types of responses to Ca^{2+}: the first functions to buffer or transport Ca^{2+} by binding without a change in structural conformation, the second undergoes a conformational change upon binding and functions as a Ca^{2+} sensor to integrate Ca^{2+} signals into cellular responses (Chin and Means, 2000). C2-domains consist of approximately 130 amino acid residues folded into two four stranded β-sheets, with Ca^{2+} binding occurring at the top three loops (Rizo and Sudhof, 1998). The C2-domains are most commonly found in proteins that target the plasma membrane and involved in signal transduction or membrane trafficking.

To exert a biological effect, Ca^{2+} binds directly to a target protein or Ca^{2+} acts through an intermediary messenger that couples Ca^{2+} to biochemical and cellular changes. These effector proteins, many of which possess either or both of the Ca^{2+}-binding domains discussed, include, among many others: CaM, calpain, neuronal calcium sensor proteins, PKC, adenylyl cyclase (AC), phospholipase A_2 (PLA_2), phospholipase C (PLC) and nitric oxide synthase (NOS).

CaM is the most intensively studied Ca^{2+}-sensing protein. This ubiquitous enzyme of the EF hand family, comprising at least 0.1% of the protein content of the cell, undergoes cellular redistribution in response to Ca^{2+} signals and a conformational change upon Ca^{2+} binding (Chin and Means, 2000). CaM regulates, through either activation or inhibition, AC, phosphodiesterase (PDE), protein kinases, protein phoshatases, plasma membrane ion channels and pumps, as well as intracellular Ca^{2+} release channels (Chin and Means, 2000). CaM, with its far reaching and diverse effects, is only one of a myriad of Ca^{2+}-regulated effector proteins. When these additional proteins are considered along with the diverse Ca^{2+} signals that can be established within the cell, it becomes apparent that Ca^{2+} can enable intricate and elaborate control over a vast array of biological activities.

Ca^{2+} as a regulator of ciliary activity

Ca^{2+} is recognized as the most important second messenger that participates in the regulation of ciliary beating. One of the best characterized ciliary responses to Ca^{2+} is ciliary reversal in *Paramecium*. Mechanical stimulation on the anterior part of the cell stimulates a graded regenerative membrane depolarization that activates voltage-dependent Ca^{2+} channels (reviewed in Preston and Saimi, 1990; Tamm, 1994). The influx of Ca^{2+} acts at the level of the axoneme to trigger reversed beating. Ca^{2+}-triggered ciliary reversal has also been demonstrated in other ciliates (reviewed in Plattner and Klauke, 2001), as well as in the ciliary comb plate of ctenophores (Nakamura and Tamm, 1985). Photolysis of caged Ca^{2+} in *Paramecium* and the ciliate *Didinium nasutum* indicate that the Ca^{2+}-sensitive region for ciliary reversal is located throughout the cilium (Iwadate, 2003; Iwadate and Suzaki, 2004). Similarly, in larvae of the ctenophore *Mnemiopsis leidyi*, Ca^{2+} imaging with the indicator Ca Green dextran revealed that Ca^{2+} entry occurs throughout the cilium, indicating an even distribution of voltage-dependent Ca^{2+} channels (Tamm and Terasaki, 1994). As suggested by work from *Paramecium*, it is thought that the regulation of ciliary reversal is mediated by the interaction of Ca^{2+} with CaM within the cilium (Nakaoka *et al.*, 1984). *Paramecium* also exhibits a hyperpolarization-induced increase in CBF. Hyperpolarizing the membrane in the absence of a K^+ currents, revealed an inward Ca^{2+} current that consisted of two components. The secondary sustained Ca^{2+} current was linked to an increase in CBF. As deciliation did not impair this current, it was concluded that it must pass through the somatic membrane rather than the ciliary membrane (Nakaoka and Iwatsuki, 1992).

Numerous invertebrate ciliary systems have been demonstrated to involve Ca^{2+} in the regulation of ciliary beating. The initiation of ciliary beating of the macrocilia on the lips of the ctenophore *Beroe* is a component of the feeding behavior of the animal. In this system, mechanical stimulation evokes a membrane depolarization, activation of voltage-dependent Ca^{2+} channels, and influx of Ca^{2+} that, in concert with CaM, activates ciliary beating (Tamm 1988). Similarly, the cilia-driven swimming of the trochophore larva of the polychaete

Spirobranchus giganteus is dependent on Ca^{2+} influx and CaM (Marsden and Hassessian, 1986). Interestingly, the various populations of gill cilia of *Mytilus edulis* appear to be differentially regulated by Ca^{2+}. Increases in $[Ca^{2+}]_i$ in the lateral gill that occur in response to DA release from the branchial nerve cause ciliary arrest (Paparo and Murphy, 1975a; 1975b). Given that this Ca^{2+}-dependent ciliary arrest was blocked by the addition of the CaM antagonist trifluoperazine, it was concluded that Ca^{2+}-CaM interactions underlie the ciliary arrest response (Reed and Satir, 1980). In contrast, in the abfrontal ciliary cells of the *Mytilus* gill, mechanical stimulation caused Ca^{2+}-dependent generator and regenerative potentials that enhance ciliary activity (Strommel, 1984a). Again, application of CaM inhibitors abolished the Ca^{2+}-triggered increase in ciliary beating, indicating that CaM is also necessary in mediating this response (Strommel, 1984b).

The involvement of Ca^{2+} in ciliary activity has been thoroughly examined in vertebrate systems. Ca^{2+} has been found to be associated with cilio-excitation in almost all systems examined; this includes the oviduct of the salamander *Necturus maculosus*, where mechanical stimulation produced a membrane depolarization that resulted in Ca^{2+} influx and an increase in CBF (Murakami and Eckert, 1972), and human respiratory epithelium, where Ca^{2+} ionophore-stimulated CBF increases were dependent on CaM (Di Benedetto *et al.*, 1991). In rabbit tracheal epithelial ciliary cells, simultaneous measurement of beat frequency and $[Ca^{2+}]_i$ suggest that low to moderate changes in Ca^{2+} concentrations at the base of the axoneme regulate ciliary activity (Lansley and Sanderson, 1999). Further, it is not the absolute $[Ca^{2+}]_i$ that directly regulates the rate of CBF, but rather it is changes in $[Ca^{2+}]_i$ that alter CBF (Evans and Sanderson, 1999). Similar results have been found in cultured sheep tracheal epithelial cells, where monitoring changes in $[Ca^{2+}]_i$ and CBF in the same ciliary cell demonstrated that Ca^{2+} is a key intracellular regulator of ciliary activity (Salathe and Bookman, 1995). Further work in ovine tracheal epithelium suggests that the Ca^{2+}-induced change in CBF occurs too rapidly for phosphorylation reactions involving CaM or protein kinases and phosphatases.

Rather, it was proposed that Ca^{2+} binds directly to an axonemal Ca^{2+}-binding element (Salathe and Bookman, 1999). Conversely, examination of the ciliary cells from the esophagus and palate of the frog *Rana ridibunda* revealed that Ca^{2+} is an intermediate signal transduction element (Zagoory *et al.*, 2002). Acetylcholine stimulation produces a time-dependent increase in the second messengers cGMP and cAMP in a Ca^{2+}-CaM dependent manner. Similarly, in rabbit tracheal epithelial cells, increases of Ca^{2+} alone or Ca^{2+}-CaM do not alter the CBF. Rather, cyclic nucleotides are required to produce a modest increase in ciliary beating, an effect that is augmented by the addition of Ca^{2+} (Ma *et al.*, 2002). Thus, it appears that the Ca^{2+} regulation of ciliary beating is an intricate process that may be unique to the species examined.

The process of ciliary regulation by Ca^{2+} is further complicated when Ca^{2+} release from intracellular stores is considered. Ca^{2+} release through ryanodine receptors on the ER has been proposed to stimulate increased ciliary beating in pedal epithelial cells from *Tritonia* (Woodward and Willows, 2003). In this system it is hypothesized that a neurotransmitter-triggered reduction of a Cl^- current results in a cascade of membrane depolarization, activation of voltage-gated Ca^{2+} channels, Ca^{2+} influx and stimulation of CICR through ryanodine receptors on the ER. In frog esophageal and palate epithelia, inhibitors of voltage-dependent Ca^{2+} channels have no effect on ATP-induced increases in CBF, whereas quinidine, a calcium-dependent K^+ channels blocker, inhibits the effects of ATP (Weiss *et al.*, 1992). From these results, it was hypothesized that ATP-receptor activation stimulates a signaling cascade that mobilizes intracellular Ca^{2+}, which in turn activates calcium-dependent K^+ channels to cause a change in membrane potential. Further work on frog esophageal cells suggests that acetylcholine stimulation causes release of Ca^{2+} from intracellular stores (Zagoory *et al.*, 2001). Inhibition of PLC with U-73122 and depletion of thapsigargin-sensitive stores abolished the acetylcholine stimulation of CBF, whereas Ca^{2+} channel blockers had no effect. Furthermore, CaM inhibition attenuated the acetylcholine-induced increase in $[Ca^{2+}]_i$ and abolished the increase in CBF, suggesting that intracellular Ca^{2+} release is necessary for CBF enhancement, but does not lead directly to it. Similar conclusions were drawn from experiments on sheep tracheal epithelial cells (Salathe *et al.*,1997), however, an additional role for mitochondrial Ca^{2+} stores was revealed in that system (Salathe *et al.*, 2001).

Hormonal stimulation of rabbit ciliary cells has also been demonstrated to rely on Ca^{2+} release from intracellular stores. The prostaglandin E_2 stimulation of CBF in rabbit oviduct requires Ca^{2+} release from intracellular stores, as demonstrated by Ca^{2+} depletion experiments (Verdugo, 1980). Likewise, arginine vasopressin-stimulated increases in CBF and $[Ca^{2+}]_i$ were abolished by thapsigargin pretreatments (Tamaoki *et al.*, 1998). To complicate matters further, purinergic stimulation of rabbit airway epithelia involves multiple Ca^{2+} sources. It was hypothesized that the initial increase in CBF results from a rapid release of Ca^{2+} from thapsigargin-insensitive stores adjacent to the cilia, followed by a release from thapsigargin-sensitive stores located within the cell cytoplasm. In contrast, the sustained component of the CBF response results from Ca^{2+} influx through non-voltage dependent Ca^{2+} channels (Korngreen and Priel, 1996). Additionally, purinergic and mechanical stimulation of CBF and $[Ca^{2+}]_i$ in rabbit tracheal epithelial cells involves the production of the second messenger IP_3 to trigger intracellular Ca^{2+} release and the propagation of ciliary stimulation intercellularly via IP_3 and Ca^{2+} diffusion through gap junctions (Hansen *et al.*, 1995).

3.2 Role of cAMP-PKA

Possibly the most important second messenger molecule in the regulation of ciliary activity, next to Ca^{2+}, is the cyclic nucleotide cAMP. This signaling molecule, the first to be termed a second messenger, is produced from ATP by the enzyme AC in response to a variety of cellular signals, most commonly through the activation of a G-protein coupled receptor (Kopperud *et al.*, 2003). The term AC actually refers to a broad family of enzymes. The multi-domain protein class III AC is responsible for the generation of cAMP, which is involved in signaling in a vast array of organisms (Linder and Schultz, 2003). AC exhibits highly complex membrane topologies with conserved duplicated catalytic domains (reviewed in Cooper, 2003). The structural diversity of this enzyme, along with its susceptibility to regulation by a broad range of mechanisms, enables a high degree of specificity in cAMP signal transduction. The degradation of cAMP is regulated by the PDE family of enzymes that hydrolyze cyclic nucleotides. Like AC, activation of a G-protein coupled receptor may regulate PDE activity.

cAMP microdomains have been identified within cells and are shaped by the subcellular localization of enzymes and cAMP targets (Tasken and Aandahl, 2003). The most widely identified target of cAMP is PKA. In an inactive state, PKA consists of two catalytic subunits bound to a regulatory subunit dimer. Upon cooperative binding of two cAMP molecules to the A and B sites in each of the regulatory subunits, the tetramer dissociates into one dimer of regulatory subunits with four bound cAMP, and two active catalytic subunits that can phosphorylate serine and threonine residues on target proteins (Tasken and Aandahl, 2004). One example of PKA action, amidst the multitude of cellular activities that PKA is engaged in, is the regulation Ca^{2+} release from intracellular stores through the phosphorylation of IP_3 receptors (reviewed in Bugrim, 1999). PKA is found in most cells and exists as two isozymes: PKAI, which is soluble and is active cytoplasmically, and PKAII, which is particulate and confined to subcellular structures and compartments (Tasken and Aandahl, 2004). This subcellular localization is controlled by a class of proteins called A-kinase anchor proteins that tether inactive PKA, via the regulatory domain, to specific sites (reviewed in Tasken and Aandahl, 2004). In addition to PKA activation, cAMP acts on other cellular targets, including: cyclic nucleotide-gated ion channels and guanine nucleotide exchange factors that regulate Ras-related proteins (Dremier *et al.*, 2003; Springett *et al.*, 2004).

cAMP as a regulator of ciliary activity

Although not as widespread in its cilio-regulatory role as Ca^{2+}, cAMP, in some cases acting through PKA, has been implicated in the ciliary control of numerous systems, including protozoans. Pharmacological manipulations of cAMP and PKA revealed that this signaling pathway is involved in the osmosis-controlled ciliary motility in the trematode *Schistosoma mansoni miracidia* (Matsuyama *et al.*, 2004). As previously mentioned, a membrane hyperpolarization in *Paramecium* is associated with an increase in the rate of forward swimming through increased ciliary beating. This membrane hyperpolarization has been linked to increases in the formation of cAMP (Schultz *et al.*, 1984), whereby the hyperpolarization activates a K^+ efflux that directly regulates AC activity (Schultz *et al.*, 1992). Further work on *Paramecium* demonstrates that PKA phosphorylates ciliary target proteins *in vitro* (Bonini and Nelson, 1990). Specifically, a 29 kDa polypeptide that copurifies with 22S dynein was phosphorylated in a cAMP- and Ca^{2+}-dependent manner. cAMP-mediated phosphorylation of this identified peptide significantly increased the velocity of *in vitro* microtubule sliding, suggesting a possible role for this 29 kDa polypeptide as a regulatory dynein light chain (Hamasaki *et al.*, 1991). The 29 kDa polypeptide is also located in 12S dynein, where it is similarly phosphorylated in a cAMP-dependent manner (Walczak and Nelson, 1993). An ortholog of this regulatory dynein light chain has also been identified in *Tetrahymena*. This polypeptide, termed p34, exhibits cAMP-dependent phosphorylation that generates a 70% increase in the velocity of microtubule sliding *in vitro* (Christensen *et al.*, 2001). Finally, PKA has also been identified to be involved in flagellar activity in *Chlamydomonas*. It is believed that the central pair/radial spoke complex functions to override the inhibitory action of PKA phosphorylation of inner arm dynein targets; one such target is IC138 (Porter and Sale, 2000). Studies have also located at least two A-kinase anchor proteins within the axoneme, one associated with C2 of the central pair microtubules and the other with the radial spoke (Porter and Sale, 2000).

Likewise in invertebrate species, stimulation of cAMP is associated with increases in the rate of ciliary beating. In sea urchin larvae cAMP was shown to be the mediator of monoaminergic cilioexcitation (Soliman, 1984). Similarly in the lateral gill cilia of *Mytilus edulis*, cAMP, rather than Ca^{2+}, was identified as the predominant signal transduction element regulating ciliary activity (Murakami, 1983), particularly in 5-HT cilio-excitation (Murakami, 1987). In isolated permeabilized cilia from the lateral gill, polypeptides that are similar in molecular weight to dynein light chains undergo cAMP-dependent protein phosphorylation (Stommel and Stephens, 1985). Given that 5-HT activates AC in gill cilia and sperm flagella from both *Mytilus edulis* and the surf clam *Spisula solidissima*, a comparative study examined potential dynein targets for cAMP action. Interestingly, cAMP-dependent, Ca^{2+}-independent phosphorylation was evident on specific dynein light chains in cilia, but only on dynein heavy chains in flagella (Stephens and Prior, 1992). However, microtubule translocation was not examined, so conclusions from these results may be limited.

The involvement of cAMP in modulating ciliary activity in vertebrate systems has also been examined. In rabbit tracheal epithelial cells, application of 8-bromo cAMP caused a dose-dependent increase in CBF, with similar results being obtained with other cAMP analogues. PDE inhibition or AC activation also produced an increase in CBF, suggesting cAMP involvement in mucociliary transport function (Tamaoki *et al.*, 1989). Similarly, studies in hamster oviductal epithelium implicate cAMP in adenosine-induced cilio-excitation (Morales *et al.*, 2000). In bovine bronchial epithelial cells, increases in cAMP and PKA, as well as cGMP and PKG, were correlated to stimulated ciliary activity (Wyatt *et al.*, 1998). In ovine tracheal mucosa, protein extraction from isolated axonemes revealed that a protein with a molecular weight of 26 kDa was the only protein to be phosphorylated in a cAMP-dependent manner; this phosphorylation was Ca^{2+} independent and could be blocked by PKA inhibition (Salathe *et al.*, 1993a).

Multiple roles for PKA in the enhancement of CBF have been identified in frog esophagus. Simultaneous monitoring of $[Ca^{2+}]_i$ and CBF revealed that application of dibutyryl cAMP or AC activation through forskolin caused a large, transient increase in $[Ca^{2+}]_i$ that was independent of extracellular Ca^{2+}, as well as an increase in CBF with a peak and plateau profile. The presumed Ca^{2+} release from stores was abolished by thapsigargin and the PLC inhibitor U-73122; however, application of forskolin in the presence of these inhibitors still produced the elevated plateau component of the CBF response. Furthermore, in the presence of the PKA inhibitor H-89, the Ca^{2+} and CBF responses were lost (Braiman *et al.*, 1998). Taken together these results suggest that PKA induces Ca^{2+} release from intracellular stores to initiate a rapid change in CBF, as well as an enhancement in CBF that is not dependent on a change in Ca^{2+}. Finally, the stimulation of human ciliary cells has also been shown to involve the cAMP-PKA signaling pathway (Lieb *et al.*, 2002). However, results of this study indicate that cAMP and PKA are not the only signal transduction elements involved in purinergic stimulation. Rather, like most other ciliary systems examined, there is an interplay between regulating pathways. Further, in human ciliary axonemes, PKA phosphorylates a 23 kDa axonemal protein and associates with a novel 28 kDa A-kinase anchor protein, termed AKAP28, found in airway cilia (Kultgen *et al.*, 2002). This anchor protein may play a role in specific modulation of ciliary activity through the localization of PKA to certain sites within the axoneme.

3.3 Role of PKC

A third signaling pathway implicated in ciliary regulation is PKC, one of the first protein kinases identified. PKC is a serine/threonine specific kinase that represents a large gene family of isoenzymes that differ in the mode of activation, structure and expression profiles in different tissues (reviewed in Hug and Sarre, 1993). Twelve distinct members of the PKC family have been identified in mammalian cells, with several non-mammalian isoforms also known (Mellor and Parker, 1998). The mammalian isoforms have been grouped into smaller sub-families on the basis of sequence homology in the regulatory domain of the enzyme (Csukai and Mochly-Rosen, 1999). The most studied group is the conventional PKCs which comprise the α, βI, βII and γ subtypes. These isozymes are characterized by a dependence on phosphatidylserine (PS) and the second messengers Ca^{2+} and diacylglycerol (DAG), as well as activation by phorbol myristyl acetate, a tumor promoting phorbol ester drug. DAG is generated following G-protein coupled receptor activation of PLC, which cleaves the polar head from inositol phospholipids (Rebecchi and Pentyala, 2000). PLC hydrolyzes the lipid phosphatidylinositol 4,5-bisphosphate into two intracellular signaling products, IP_3 and DAG. It should be noted that DAG and phorbol esters have other intracellular targets in addition to PKC (Brose and Rosenmund, 2002). The novel PKCs consist of the ε, η, δ and θ iosforms and are similar to conventional PKCs, but are Ca^{2+}-insensitive. The atypical PKCs consist of ι and ζ isoforms and like novel PKCs, are Ca^{2+}-insensitive. However, the atypical PKCs do not respond to phorbol esters or DAG (for review of PKC isoform subfamilies, see Mellor and Parker, 1998 or Hug and Sarre, 1993). Activation of the atypical isoforms also relies on lipid signaling, possibly ceramide or phosphatidylinositol 3,4,5-triphosphate (Csukai and Mochly-Rosen, 1999; Ruvolo, 2003). Finally, an additional grouping of enzymes has recently been added, the PKC-related kinases (PRKs), that presently remain less-well characterized (Mellor and Parker, 1998).

The protein sequence of the various PKC isoforms reveals that there are conserved and variable regions within the enzyme structure. For the most part, the catalytic domain is highly conserved, with the variable, isoform-unique sequences lying within the regulatory domain (Mellor and Parker, 1998; Csukai and Mochly-Rosen, 1999). Similar to other signaling proteins, the localization of PKC appears to be important in establishing specificity of signaling. Individual isozymes have been identified to target specific intracellular sites following activation, partly due to the involvement of receptors for activated C-kinase proteins (RACKs; Csukai and Mochly-Rosen, 1999). Receptors for inactive C-kinase (RICKs) have also been proposed to target PKC to different subcellular locations, whereby site-specific phosphorylation is mediated by movement from RICK to RACK (Sim and Scott, 1999). PS has also been suggested to play a role in targeting PKC to specific cellular sites (Sim and Scott, 1999).

PKC as a regulator of ciliary activity

The diversity of this enzyme family and specific targeting to subcelluar locations enables PKC to mediate a vast array of cellular functions, from proliferation to apoptosis (Dempsey *et al.*, 2000). Within ciliary cells, PKC appears to have a somewhat controversial role in regulating ciliary activity. With the exception of *Helisoma* ciliary cells, most studies examining the involvement of PKC in ciliary activity have focused on vertebrate systems. In rabbit tracheal and sheep epithelium, phorbol ester activation of PKC causes a reduction in the CBF (Kobayashi *et al.*, 1988; Salathe *et al.*, 1993b). In sheep epithelium, PKC phosphorylates a 37 kDa polypeptide (Salathe *et al.*, 1993b). Furthermore, application of PKC inhibitors in human tracheal and bronchial ciliary cells demonstrated that neuropeptide Y-induced cilio-inhibition involved a member of the novel PKC family, independent of PKA (Wong *et al.*, 1998; Mwimbi *et al.*, 2002). In contrast, in frog esophagus, PKC activation produces an enhancement in ciliary beating and an increase in $[Ca^{2+}]_i$ via influx through voltage-independent Ca^{2+} channels (Levin *et al.*, 1997). The results of this study implicated PKC signaling in the ciliary response to purinergic stimulation. Thus, it appears that PKC's role in regulating ciliary activity is species specific.

3.4 Role of NO-cGMP-PKG

Like cAMP, cGMP is a cyclic nucleotide second messenger that participates in a plethora of biological activities. cGMP is produced from GTP by the family of enzymes called guanylyl cyclases (GCs). GCs are related to class III AC as they exhibit some amino acid sequence homology in the catalytic region (Krumenacker *et al.*, 2004). For several of the GCs, it has been demonstrated that GTP-specificity results from two amino acid substitutions within the regulatory domain of the protein. The lysine-aspartate pair in AC defines ATP as the substrate, whereas in GC these amino acids are replaced with glutamate-cysteine (Linder and Schultz, 2003). There are two types of GC: particulate and soluble. Particulate guanylyl cyclases (pGCs), which exist as homodimers at the plasma membrane and may be an integral part of membrane receptors, are often activated by ligand binding to an extracellular N-terminus (Krumenacker *et al.*, 2004). Soluble guanylyl cyclases (sGCs) are heme-containing, cytosolic heterodimeric enzymes composed of α and β subunits (Krumenacker *et al.*, 2004). sGC has received considerable attention because the presence of a prosthetic heme group enables the enzyme to be activated by NO (Friebe and Koesling, 2003).

NO is a membrane-permeable, uncharged free radical gaseous compound that plays a diverse role in cell signaling. NO is produced by the enzyme NOS, which catalyzes the conversion of L-arginine to L-citrulline through two consecutive oxidations and a variety of cofactors (Hanafy *et al.*, 2001). Three isoforms of NOS, each derived from a distinct gene product, have been identified. Neuronal NOS (NOS I) is found in high levels in neuronal tissue as well as some non-neuronal tissue. It is activated by CaM in the presence of high levels of Ca^{2+} and is thought to produce NO that functions as a neurotransmitter (Krumenacker *et al.*, 2004). Inducible NOS (NOS II) is a Ca^{2+}-independent isoform found in macrophages, hepatocytes and smooth muscle cells among others. It is not present in resting cells, but is expressed in an active form in response to lipopolysaccharide and cytokine stimulation, often as a cytotoxic response (Krumenacker *et al.*, 2004). Finally, endothelial NOS (NOS III) was originally discovered to produce endothelium-derived relaxing factor, later identified as NO. Similar to neuronal NOS, it is activated by intracellular Ca^{2+} and CaM binding (Krumenacker *et al.*, 2004). NOSI and NOSIII are also referred to as constitutive NOS enzymes. In broad terms, NO is considered to have two main actions: cGMP-independent effects, which are mediated through reactive nitrogen species, and cGMP effects, which follow from NO activation of sGC (Krumenacker *et al.*, 2004).

cGMP has four recognized targets that mediate its activity: PKG, cyclic-nucleotide-gated channels, PKA and PDE (Hanafy *et al.*, 2001). PKG is a serine/threonine protein kinase that is activated by cGMP binding and exists in two forms, PKGI and PKGII (Hanafy *et al.*, 2001). Although considerably less is known about PKG than other protein kinases, it exerts through phosphorylation the following actions: IP_3 receptor inhibition, activation of phospholambin in SERCAs, inhibition of thromboxane in platelets, activation of myosin-binding subunit of myosin light chain phosphatase and activation of cAMP response element binding protein (reviewed in Hanafy *et al.*, 2001). Similar to cAMP, cGMP activates cyclic nucleotide-gated ion channels. This is of particular importance in the sensory transduction mechanisms of photoreceptors and other sensory receptors. The similarity of the cyclic nucleotide-binding domains of PKG and PKA enables cross-talk between cAMP and cGMP pathways. Finally, cGMP is central to activation of some members of the PDE family of enzymes. This family consists of five characterized groups: Ca^{2+}/CaM-dependent, cGMP-stimulated, cGMP-inhibited, cAMP-specific and cGMP-specific (Hanafy *et al.*, 2001).

NO-cGMP-PKC as regulators of ciliary activity

Within ciliary cells the involvement of NO, cGMP and PKG in regulating ciliary activity has been examined in a variety of systems. In *Paramecium*, a novel PKG was discovered to be enriched within the cilia (Miglietta and Nelson, 1988). The structure of this kinase and some of its functional characteristics, including the ability to use both GTP and ATP as a phosphate donor, suggest that it may represent a monomer precursor to the dimeric vertebrate enzyme. cGMP was demonstrated to induce forward swimming in detergent-permeabilized *Paramecium*, more effectively than cAMP. Furthermore, the addition of cGMP or its analogs was able to prevent Ca^{2+} from inducing backward swimming (Bonini and Nelson, 1988). Unlike cAMP, cGMP alters the helical pattern of paramecium swimming, suggesting that cGMP initiates a change in ciliary beat direction. The results of this study indicate that both cAMP and cGMP act as second messengers in regulating ciliary activity, albeit in different capacities. Accordingly, PKG phosphorylates an axonemal target distinct from the protein targets of PKA (Ann and Nelson, 1995).

NO, cGMP and PKG have also been examined in the ciliary regulation of a variety of vertebrate systems. Collectively, these studies revealed that this signaling pathway may have a rather elaborate and controversial role in ciliary activity. In bovine bronchial epithelial cells, NOS inhibitors decrease the ciliary response to various stimuli. This effect is reversed with the addition of the NOS substrate L-arginine or NO donors, suggesting that an NO-dependent pathway participates in cilio-excitation (Jain *et al.*, 1993). Additional work in bovine cells implicated PKG, as well as PKA, in cilio-excitation (Wyatt *et al.*, 1998). Similarly, an interconnection of Ca^{2+}, PKA and PKG signaling pathways has been demonstrated in acetylcholine-stimulated ciliary cells from the frog esophagus and palate (Zagoory *et al.*, 2002). This is consistent with studies of rabbit tracheal epithelial cells, where PKG stimulates ciliary beating in a Ca^{2+}-dependent fashion (Uzlaner and Priel, 1999). However, other work in rabbit trachea suggested that cGMP, acting through PKG, can induce an increase in ciliary beating in a Ca^{2+}-independent fashion, in addition to a Ca^{2+}-dependent manner (Zhang and Sanderson, 2003). Studies of rat tracheal epithelial cells have also implicated the NO-cGMP-PKG pathway in cilio-excitation (Li *et al.*, 2000) and endothelial NOS as the enzyme believed to be responsible for endogenous NO production (Zhan *et al.*, 2003). Furthermore, in cultured human adenoid explants, the activation of two different signal transduction pathways was able to alter ciliary beating: adrenergic stimulation was mediated by cAMP, whereas muscarinic activation involved prostaglandins, NO and cGMP (Yang *et al.*, 1996). Conversely, NO-cGMP does not participate in acetylcholine-induced cilio-excitation in ovine tracheal epithelial cells, despite the finding that these cells contain NOS, as shown through nicotinamide adenine dinucleotide phosphate (NADPH)-diaphorase staining (Salathe *et al.*, 2000). Thus, it appears that NO, cGMP and PKG, similar to PKC, play variable roles in the regulation of ciliary cells depending on the system examined.

3.5 Role of other signaling pathways identified in ciliary cells

Additional signaling elements that participate in regulating ciliary activity include protein phosphatases (PPs), AA metabolites, other kinases and G-protein signaling protein 2 (RGS2). Protein phosphorylation is a crucial component of cellular signaling, as exemplified by the fact that 2-3% of the eukaryotic genome codes for protein kinases (Hubbard and Cohen, 1993). However, equally important is the reversal of this process by PPs. Eukaryotic PPs are functionally and structurally diverse, and are coded by three distinct gene families (Barford, 1996). The PPP and PPM families are responsible for the dephosphorylation of phosphoserine and phosphothreonine residues, whereas the PTPs (protein tyrosine phosphatase) dephosphorylate phosphotyrosine. Three abundant members of the PPP family, PP1, PP2A and PP2B (calcineurin), and one member of the PPM family, PP2C, have been implicated in ciliary control. Using *Chlamydomonas* mutants, it was determined that PP1 located within the radial spokes regulates inner dynein arm activity through the dephosphorylation of a dynein component. It is likely that cAMP mediates phosphorylation of this same compound, resulting in an inhibition of axonemal motility (Habermarcher and Sale, 1996). Further, in *Chlamydomonas* axonemes, PP2A is anchored on the outer doublets at the base of the I1 complex and is believed to dephosphorylate IC138 to modulate inner dynein arm activity (Porter and Sale, 2000). Similarly, PP2C dephosphorylates a 29- and/or 65- kDa protein within the axoneme of *Paramecium caudatum* to terminate cAMP activity (Noguchi *et al.*, 2003). While immunogold labeling indicated that PP2B is also associated with cilia in *Paramecium*, the functional role of this PP remains to be determined (Momayezi *et al.*, 2000). Continued study of the involvement of PPs may further reveal how these enzymes are essential to the intricate regulation of ciliary activity.

Considering that mucous transport by ciliary cells within the respiratory tract of vertebrates is essential to host defense, it is not surprising that chemical substances involved in immune responses affect ciliary activity. Hydrolysis of phospholipids by the enzyme PLA_2 generates AA, which is then metabolized by either cyclooxygenase or lipoxygenase to generate a variety of products (Akiba and Sato, 2004). In chicken tracheal epithelium, application of leuoktriene C_4, an AA metabolite, caused a Ca^{2+}-dependent decrease in the rate of ciliary beating (Weisman *et al.*, 1990). In contrast, an analog of thromboxane A_2, another AA metabolite, caused an increase in ciliary beating in rabbit tracheal epithelial cells (Chiyotani *et al.*, 1992). This stimulatory effect was blocked by AA metabolite inhibitors, as well as Ca^{2+} and PKC inhibitors, suggesting an interplay between these signaling pathways. As mentioned previously, muscarinic receptor stimulation in human adenoid cells causes an increase in CBF through the production of prostaglandins, products of the cyclooxygenase AA pathway (Yang *et al.*, 1996). Taken together, these findings suggest that AA metabolites may play an important role in the regulation of ciliary activity in airway epithelium.

In addition to the kinases already mentioned, there are three additional enzymes found within the axoneme that affect ciliary activity. Using *Chlamydomonas* mutants lacking either the central apparatus or the C1 central microtubule, it was demonstrated in a microtubule sliding assay that the central apparatus regulates dynein activity through PP2A and casein kinase 1, rather than PKA (Smith, 2002a). Similarly, cloning of the outer dynein arm genes from *Chlamydomonas* revealed the presence of a previously unidentified adenylate kinase isoform. Adenylate kinase activity was significantly reduced in mutants lacking subunits of the outer arm or outer dynein arm-docking complex, suggesting that adenylate kinase is anchored in close proximity to the outer dynein arm (Wirschell *et al.*, 2004). A novel nucleoside diphosphate kinase has been localized to the radial spoke within *Chlamydomonas* flagellum (Patel-King *et al.*, 2004). The activity of this kinase suggests that nucleotides other than ATP may be involved, in a Ca^{2+}-dependent manner, in the regulation of axonemal motility. Additionally, the involvement of RGS2 in purinergic signaling was demonstrated in human and ovine airway epithelial cells (Nlend *et al.*, 2002). Overexpression of RGS2 inhibited the CBF and $[Ca^{2+}]_i$ responses to ATP, whereas the use of antisense oligonucleotides to reduce RGS2 levels enhanced the CBF and $[Ca^{2+}]_i$ responses to ATP. Thus, it is evident that the intracellular signaling responsible for regulating ciliary motility is intricate and highly diverse. Continued research is revealing that numerous signal transduction pathways are involved and most likely interact to modulate activity in any given system.

4 Ciliary Cells in *Helisoma trivolvis* Embryos

The direct-developing embryos of the gastropod mollusc *Helisoma trivolvis* present an opportunity to study neuro-ciliary interactions during development. Three subpopulations of ciliary cells are expressed on the surface of the embryo early in the development of *Helisoma trivolvis*: paired dorsolateral ciliary bands, a single pedal band and numerous scattered single ciliary cells (SSCCs; originally called isolated tufts of cilia; Diefenbach *et al.*, 1991; Kuang and Goldberg, 2001; Koss *et al.*, 2003). The coordinated beating of the dorsolateral and pedal cilia are responsible for generating the earliest embryo behavior: rotation within the egg capsule (Diefenbach *et al.*, 1991). This rotation is composed of a slow basal rate of rotation interrupted by transient periods of accelerated ciliary beating, termed surges (Diefenbach *et al.*, 1991). The onset of this behavior coincides with the appearance of the first pair of serotonergic neurons to develop within the animal, called embryonic neurons C1 (ENC1s; Goldberg and Kater, 1989; Diefenbach *et al.*, 1991). Prior to the development of the central nervous system in *Helisoma*, these sensory-motor neurons innervate the most medial cell of each dorsolateral band and the pedal band of ciliary cells (Diefenbach *et al.*, 1991; Goldberg, 1998; Kuang and Goldberg, 2001; Koss *et al.*, 2003). The ENC1-ciliary neural circuits generate cilia-driven rotational movements within the egg capsule in response to egg capsule oxygen content (Kuang et al., 2002). Exposure to hypoxia triggers an adaptive behavior where the release of 5-HT from ENC1s onto ciliary cells causes the embryos to increase their rate of rotation within the egg capsule to stir intracapsular fluid and facilitate oxygen diffusion into the egg capsule (Kuang *et al.*, 2003).

Not surprisingly, studies examining unidentified *Helisoma* ciliary cells in culture have revealed that cilio-excitation involves changes in $[Ca^{2+}]_i$ (Christopher *et al.*, 1996). Using time-lapse videomicroscopy to measure CBF, it was determined that pharmacologically increasing $[Ca^{2+}]_i$, using the Ca^{2+} ionophore A23187, KCl and thapsigargin, stimulates ciliary beating and that the excitatory response to 5-HT involves Ca^{2+} influx through verapamil and nifedipine sensitive

Ca^{2+} channels (Christopher *et al.*, 1996). Interestingly, this study further revealed that the cilio-excitatory action of 5-HT does not appear to involve the cAMP signaling pathway, as elevating intracellular cAMP did not mimic the 5-HT-induced increase in CBF. Rather, a unique isoform of PKC that is DAG-dependent and phorbol ester-insensitive appears to mediate the cilio-excitatory effect of 5-HT in a manner that is dependent on extracellular Ca^{2+} (Christopher *et al.*, 1999). Whereas the PKC inhibitors bisindolylmaleimide and calphostin C caused a significant, yet incomplete inhibition of the cilio-excitatory effect of 5-HT (Christopher *et al.*, 1999), application of the CaM inhibitor calmidazloium fully inhibited 5-HT-induced ciliary stimulation, suggesting that CaM plays an integral role within the cilium (Doran *et al.*, 2004). The inability of *Helisoma* embryos to adequately uptake membrane-permeable forms of Ca^{2+} indicators has limited the examination of role of Ca^{2+} and other signal transduction agents involved 5-HT cilio-excitation (Christopher, 1997).

Within whole embryos, NADPH diaphorase staining suggested the presence of NOS in the dorsolateral ciliary cells and ENC1's sensory apparatus at stage E25, with additional expression in the pedal ciliary cells and ENC1's soma and descending neurite at later stages (stage E35-E40; Cole et al., 2002). Additionally, pharmacological manipulations of NO content altered embryo behavior. Whereas the application of NO donors increased the rate of embryo rotation, NOS inhibitors decreased the rate of embryo rotation (Cole et al., 2002). Furthermore, the behavioral data suggested that NO had effects on both ENC1 and ciliary cells. Taken together, these results indicate that embryonic ciliary cells were sites of NO activity. Studies on mass-dissociated cultured ciliary cells revealed that endogenous NO constitutively stimulates ciliary beating, given the finding that the application of the NOS inhibitor 7-Nitroindazole significantly reduced the rate of basal ciliary beating (Doran *et al.*, 2003). Additionally, the cilioexcitatory effects of 5-HT depend on an NO, sGC and cGMP pathway, yet application of 5-HT does not reliably produce an increase in NO that is detectable with the fluorescent indicator DAF-2 (Doran *et al.*, 2003). As with numerous other systems examined for the signal transduction thought to underlie ciliary activity, the 5-HT-induced ciliary stimulation in *Helisoma trivolvis* embryos appears to involve multiple signaling pathways.

5 Objectives

The ENC1-ciliary cell neural circuit in *Helisoma* embryos represents an excellent model for the integrated study of the control of ciliary beating. Cell and tissue culture preparations are well suited for the examination of the signal transduction pathways that underlie the ciliary response to 5-HT. Furthermore, complementary experiments on intact embryos enable an investigation of the involvement of ciliary activity in the behavior and development of the whole animal. The overall objective of this thesis is to further elucidate the signal transduction pathways and possible interactions that underlie 5-HT-induced cilio-excitation in *Helisoma* embryos. To this end, a technique to load *Helisoma* ciliary cells with Ca^{2+} indicators was developed, as well as a microdissection procedure to facilitate the culturing of identified ciliary cells. The specific objectives of this thesis are as follows:

5.1 To characterize the three ciliary subpopulations expressed on the surface of the embryo

The occurrence of 5-HT non-responsive cells in experiments on mass-dissociated cell cultures prompted the hypothesis that sub-populations of ciliary cells may be differentially regulated (Christopher, 1997). Furthermore, examination of ciliary activity of the various ciliary cell types in the whole embryo indicated that while perturbation of ENC1 alters ciliary activity in the pedal and dorsolateral ciliary cells, it does not affect the SSCCs (Kuang and Goldberg, 2002). To explore these population differences in greater detail, the pedal, dorsolateral and SSCCs were isolated and cultured to facilitate an examination of morphological and physiological differences. Each of the three subtypes was examined using scanning and transmission electron microscopy. As well, tissue explants containing identified ciliary cells were immunohistologically treated with antibodies against 5-HT and two 5-HT receptors cloned from *Helisoma*. Finally, the CBF response to 5-HT of each of the populations was determined using high-speed digital videomicroscopy, and changes in $[Ca^{2+}]_i$ were imaged in ciliary cells microinjected with fura dextran.

5.2 To examine the roles of Ca^{2+} and PKC and their potential interactions during 5-HT-induced cilio-excitation in pedal ciliary cells

The signal transduction studies to date on unidentified ciliary cells have implicated Ca^{2+} influx, CaM, PKC, cGMP and NO, but not cAMP, in the cilio-excitatory response to serotonin. However, little is known about how these various signal transduction elements interact to produce the response. In this section, the goal was to test the hypothesis that Ca^{2+} and PKC pathways interact to mediate the cilio-excitatory response to 5-HT, and to determine the nature of this interaction. For ease of study, only pedal ciliary cells were cultured and CBF and $[Ca^{2+}]_i$ were monitored in response to 5-HT stimulation and in response to pharmacological manipulations of the Ca^{2+}, PLC and PKC pathways.

5.3 To examine the involvement of intracellular Ca^{2+} stores in the ciliary response to 5-HT in pedal ciliary cells

Given the ubiquity with which Ca^{2+} is recognized to regulate ciliary activity, it is surprising that so little attention has been directed to the examination of how intracellular sources of Ca^{2+} participate in regulating ciliary activity. Findings from the examination of the previous objective reveal that changes in $[Ca^{2+}]_i$ are necessary for the cilio-excitatory response to 5-HT in *Helisoma* ciliary cells and the source of this Ca^{2+} in the initial response is from intracellular stores. The goal of this objective was to test the hypothesis that source(s) of intracellular Ca^{2+} are necessary for the ciliary response to 5-HT. Using cultured pedal ciliary cells, the CBF response was determined following treatments that altered Ca^{2+} release from or uptake into various intracellular sources of Ca^{2+} including the IP_3 receptors, ryanodine receptors and SERCA pumps on the ER, as well as perturbing mitochondrial Ca^{2+} cycling.

The *Helisoma* model system facilitates an examination of the neural control of ciliary activity as well as the signal transduction pathways and potential "cross-talk" between pathways. Together, the experiments presented in this thesis further delineate the signal transduction pathways that underlie the cilio-excitatory response to 5-HT within a well-characterized embryonic neural circuit.

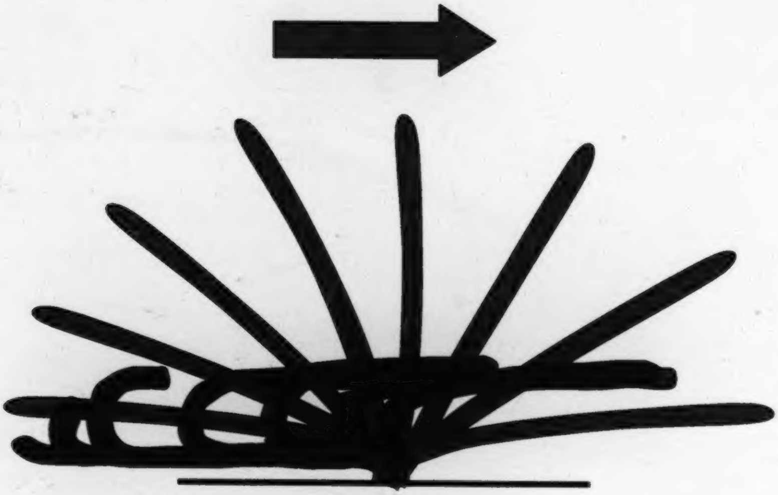

Figure 1. The asymmetric pattern of ciliary beating. The effective stroke (light green), resulting from a large bend at the base of the cilium, causes fluid movement parallel to the surface of the cell in the direction of the arrow. The recovery stroke (dark green) consists of a propagation of the bend along the shaft of the cilium that returns the cilium to the original position.

Figure 2. Organization of the ciliary axoneme. A. Cross section through a eukaryotic cilium reveals a highly conserved 9 + 2 microtubular arrangement, with 9 outer doublets surrounding a central pair of microtubules. Accessory structures are indicated. Adapted from Sakato and King, 2004. B. Longitudinal profile of the axoneme showing the position of the dynein arms and the radial spokes within a 96 nm segment.

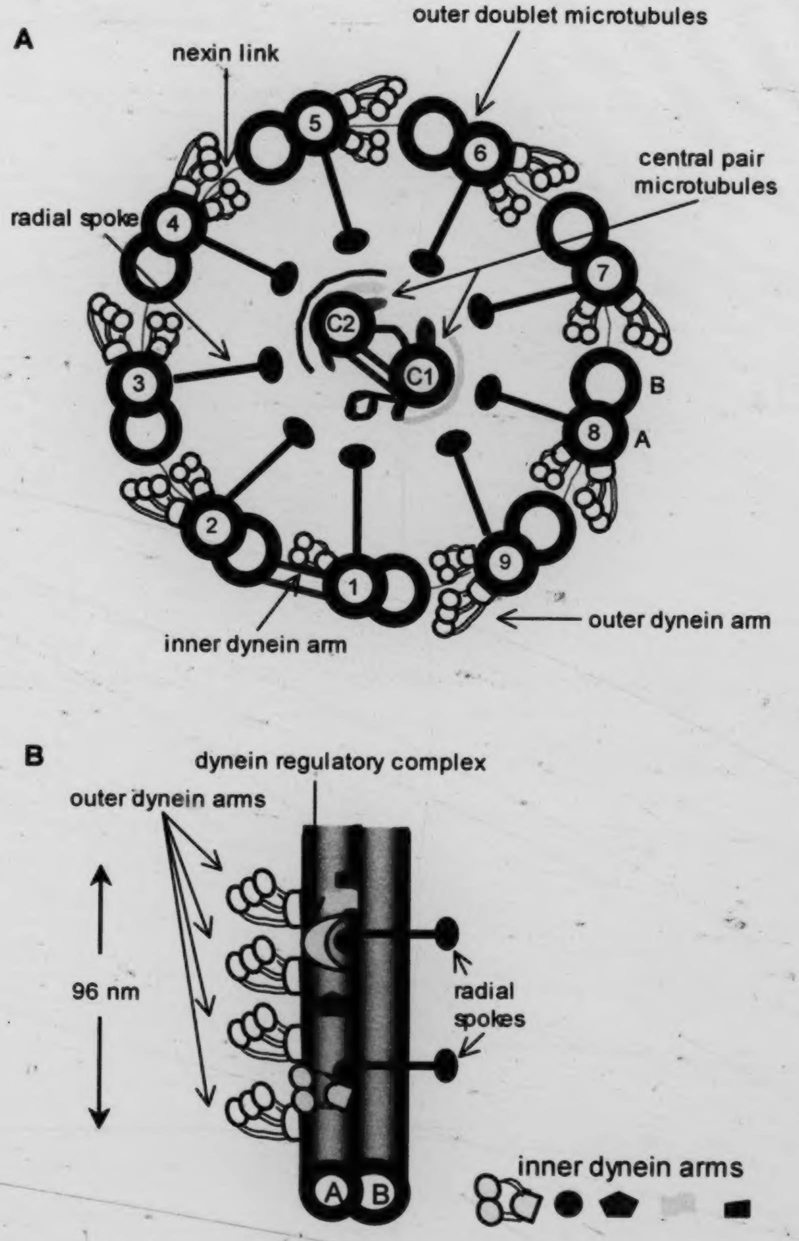
A
outer doublet microtubules
nexin link
central pair microtubules
radial spoke
C1
C2
1
2
3
4
5
6
7
8
9
B
A
inner dynein arm
outer dynein arm
B
dynein regulatory complex
outer dynein arms
96 nm
radial spokes
A
B
inner dynein arms

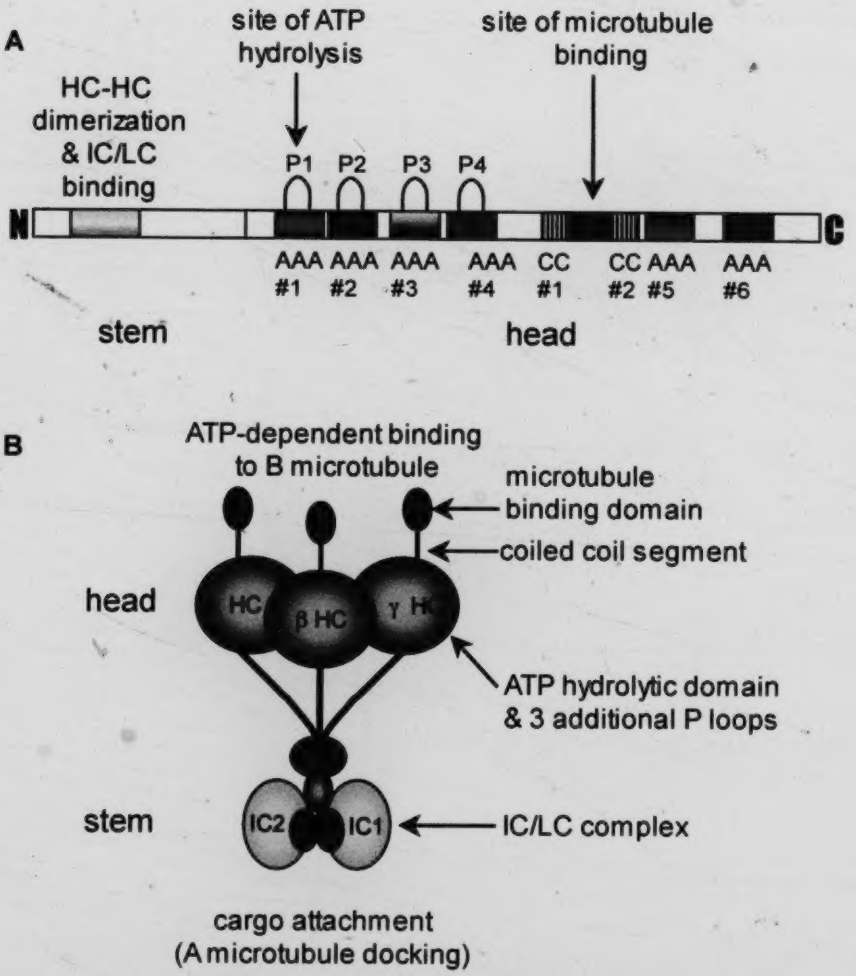
A
site of ATP hydrolysis
site of microtubule binding
HC-HC dimerization & IC/LC binding
P1
P2
P3
P4
N
C
AAA #1
AAA #2
AAA #3
AAA #4
CC #1
CC #2
AAA #5
AAA #6
stem
head
B
ATP-dependent binding to B microtubule
microtubule binding domain
coiled coil segment
head
HC
β HC
γ HC
ATP hydrolytic domain & 3 additional P loops
stem
IC2
IC1
IC/LC complex
cargo attachment (A microtubule docking)

Figure 3. Structure of the dynein heavy chain and organization of the dynein motor complex. A Map of the dynein heavy chain showing the location of various functional and structural domains. B Model of a generalized dynein outer arm illustrating the location of various components. Abbreviations: HC- heavy chain, IC- intermediate chain, LC- light chain, CC- coiled coil. Adapted from King, 2000 and Sakato and King, 2004.

Figure 4. Model of the mechanochemical cycle of dynein arm-microtubule interactions. A. Dynein arm (pink cross bridge) in rigor state. B. In the presence of ATP, the dynein arm releases from the N+1 doublet. C. Dynein arm swings 40° basally in conjunction with ATP hydrolysis. D. Dynein arm reattaches to a more basal location on the N+1 doublet as ADP and Pi are released. E. The dynein arm returns to rigor position, causing the N+1 doublet to slide distal relative to the N doublet. Adapted from Satir *et al.*, 1981.

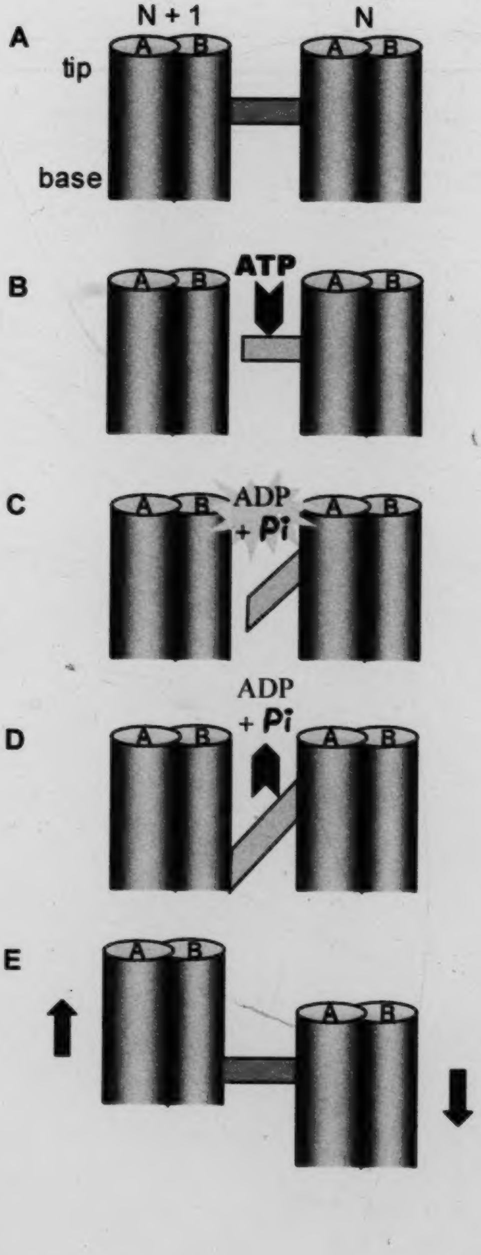
A
N + 1
N
A
B
A
B
tip
base
B
ATP
C
ADP
+ Pi
D
ADP
+ Pi
E

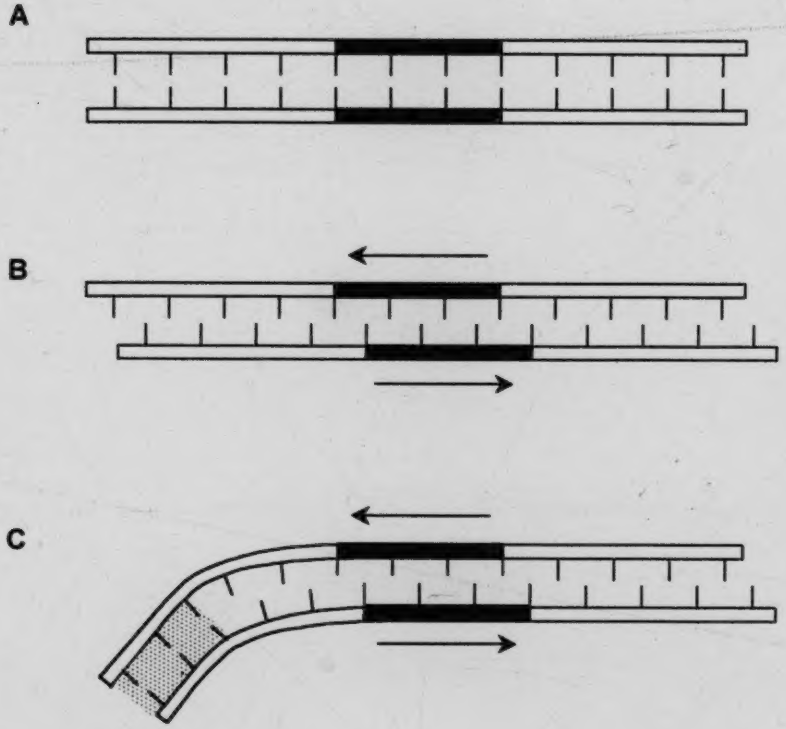

Figure 5. Schematic showing how the sliding of two flexible structures, such as microtubules, can result in the formation of bending. A. Two microtubules prior to sliding. B. When shearing force is generated in the blackened section this produces microtubule sliding in the direction indicated by the arrows. C. An area of internal resistance (shaded section) converts the force of sliding into bending in the area between the resistance and the generation of the shearing force. Adapted from Witman, 1990.

MATERIALS AND METHODS

1 Animals

Helisoma trivolvis embryos were collected from a laboratory-reared albino colony raised at the University of Alberta. Snails were housed in flow-through glass aquaria containing an oyster shell substratum and de-chlorinated water (~25°C). They were maintained on a 12 hr – 12 hr light-dark cycle and fed Romaine lettuce and trout pellets (NU-WAY, United Feeds, Calgary, Canada). Egg masses were collected using a razor blade, as previously described, from large plastic petri plates placed in the aquaria (Diefenbach *et al.*, 1991). After collection, egg masses were maintained at room temperature in artificial pond water (APW; 0.025% Instant Ocean, Aquarium Systems, Mentor, Ohio) in a 150 mm petri dish. Embryos between stages E20 and E35 were used in this study, which represents 20-35% of intracapsular development (Diefenbach *et al.*, 1998; Goldberg, 1995).

2 Chemicals and Solutions

Embryonic cells were cultured in *Helisoma* defined medium (HDM: 50% Liebovitz-15 (Gibco, Burlington, ON), 40.0 mM NaCl, 1.7 mM KCl, 4.1 mM $CaCl_2$, 1.5 mM $MgCl_2$, 5.0 mM Hepes, 50 μg mL^{-1} gentamicin, 0.015% L-glutamine (Sigma, St. Louis, MO); pH 7.3-7.35). 5-HT (5-hydroxytryptamine creatine sulphate complex; Sigma) was dissolved in filtered distilled water and diluted to the working concentration in *Helisoma* saline (HS: 51.3 mM NaCl, 1.7 mM KCl, 4.1 mM $CaCl_2$, 1.5 mM $MgCl_2$, 5.0 mM Hepes; pH 7.33-7.35). 5-HT was prepared the day of use.

The specific chemicals and solutions used in each of the three main experimental studies are outlined below.

2.1 Characterization of subpopulations of ciliary cells expressed on the surface of *Helisoma* embryos

All imaging and CBF experiments were performed in HS. Fura dextran potassium salt (fura; 10 000 MW; Molecular Probes, Eugene, OR) was dissolved in filtered distilled water to a concentration of 2 mM. The Ca^{2+} ionophore ionomycin (ionomycin free acid; Calbiochem, La Jolla, CA) was dissolved in dimethyl sulfoxide (DMSO; Sigma) and then diluted to working concentration in HS so that the DMSO level did not exceed 0.1%.

2.2 Roles of Ca^{2+} and PKC in the excitatory response to serotonin in pedal ciliary cells

In all imaging and CBF experiments, cell cultures were perfused with HS unless otherwise stated. For 0 Ca^{2+} experiments, saline was prepared by replacing Ca^{2+} with Mg^{2+} and adding 1.0 mM ethyleneglycol-bis(2-aminoethylether)-N,N,N',N'-tetraacetic acid (EGTA; Sigma). For Ca^{2+} imaging, fura-2 pentapotassium salt (Molecular Probes) was dissolved in filtered distilled H_2O to a concentration of 2 mM. 1,2-*bis*(*o*-Aminophenoxy)ethane-N,N,N',N'-tetraacetic Acid tetrapotassium salt (BAPTA; Molecular Probes) was dissolved in filtered distilled H_2O and mixed with fura-2 pentapotassium salt (Molecular Probes) for a BAPTA concentration of 50 mM and a fura-2 concentration of 1 mM. The fura-2 was included in the pipette solution as a fluorescent marker to confirm that the microinjection was successful. The PLC inhibitor U-73122 and its less active analog U-73343 (Calbiochem) were dissolved in chloroform (Sigma), dried under nitrogen, dissolved in DMSO prior to use and then diluted to working concentration in HS so that the DMSO level did not exceed 0.1%. The DAG analogs 1-Oleoyl-2-acetyl-*sn*-glycerol (OAG; Calbiochem) and 1,2-Dioctanoyl-*sn*-glycerol (DOG; Calbiochem), the PKC inhibitors bisindolylmaleimide (Calbiochem) and calphostin C (Calbiochem) and the Ca^{2+} ionophore ionomycin (ionomycin free acid; Calbiochem) were dissolved in DMSO and then diluted to working concentration in HS so that the DMSO level did not exceed 0.1%. Given that Calphostin C is light activated, a fiber optic light source was used to illuminate the perfusion syringe containing Calphostin C prior to perfusion.

2.3 The involvement of intracellular Ca^{2+} stores in the excitatory response to 5-HT in pedal ciliary cells.

CBF experiments were performed in HS. Thapsigargin (Calbiochem) and LY83583 were dissolved in 100% ethanol and diluted to working concentration in HS so that the EtOH content did not exceed 0.1%. Caffeine (Sigma) was dissolved in HS to its working concentration on and the day of use. Carbonyl cyanide *m*-chlorophenylhydrazone (CCCP; Calbiochem), ruthenium red (Calbiochem), xestospongin C (Sigma), dantrolene (Calbiochem), high purity ryanodine (99.5%; Calbiochem), forskolin (Sigma) and 3-isobutyl-1-methylxanthine (IBMX; Sigma) were dissolved in DMSO and diluted to the working concentrations in HS so that the DMSO content did not exceed 0.1%. $(\mu)[(HCO_2)(NH_3)_4Ru]_2Cl_3$ (RU 360; Calbiochem) was reconstituted in deoxygenated H_2O and diluted in HS immediately prior to use, as this compound is unstable in aqueous environments.

3 Mixed Population Ciliary Cell Culture

Embryonic ciliated cells were cultured as previously described (Christopher et al., 1996, 1999). Briefly, egg masses were disinfected with 35% ethanol and the embryos were removed using a 30 gauge needle to pierce the egg capsule and gently aspirated from the egg capsule using a pasteur pipette. Isolated embryos were treated with 0.2% trypsin (Sigma) for 30 min and then mass dissociated by repeatedly passing them through a 63 µm nylon mesh (Small Parts Inc., Miami, FL). The resulting cell suspension was plated on poly-L-lysine coated (hydrobromide, MW 4000-15000, 1 µg mL^{-1}, Sigma) culture dishes (Falcon 3001) for ciliary beat experiments and on poly-L-lysine coated glass bottom dishes for imaging experiments and immunohistochemistry. The cultures were maintained in the dark at room temperature (20-22 °C) for 18-24 hours to enable cells to adhere to the substrate.

4 Cell Culture of Identified Ciliary Cell Populations

Egg masses were incubated in antibiotic-containing HS (150 µg mL^{-1} gentamicin sulfate; Sigma) for 15 min prior to removal of embryos. Embryos were removed by gently tearing the egg capsule and freeing the embryos with a stream of HS ejected from a Pasteur pipette. After removal from the egg capsule, embryos were immersed in HS and examined with Normarski differential interference contrast (DIC) optics on an inverted compound microscope (Nikon, Diaphot) for identification of the pedal, dorsolateral and scattered single ciliary cell groups. An identified cluster of ciliary cells (Figure 6) was gently sucked into the 30 µm tip of a glass micropipette (World Precision Instruments, Sarasota, FL) using a micrometer syringe (Gilmont Instruments, Barrington, IL) and the remainder of the embryo was surgically detached with a 30 gauge needle (Becton-Dickinson, Mississauga, ON). The tissue explants containing identified ciliary cells were then expelled onto poly-L-lysine-coated glass-bottom culture dishes containing HDM. The culture dishes were maintained in the dark at room temperature (20-22 °C) for 18-24 hours to enable the explants to adhere to the substrate.

5 Electron Microscopy

For scanning electron microscopy (SEM), isolated embryos were transferred to glass vials and fixed for 30-60 min in 2% OsO4 in 0.01 M phosphate-buffered saline (PBS), pH 7.5. Specimens were then rinsed 2 x 10-min in PBS and dehydrated in an ascending ethanol series of 30%, 50%, 70% and 100%. After three changes of 100% ethanol, the ethanol was replaced by isoamyl acetate in 30% increments until saturation. Subsequently, specimens were dried via CO_2 critical point drying, sputter-coated with gold-paladium and viewed with a Cambridge Stereocan S250 scanning electron microscope.

For transmission electron microscopy (TEM), embryos were fixed for 1 h in 2.5% glutaraldehyde in 0.01 M phosphate buffer (PBS; pH 7.5), followed by a 1 h post-fixation in 2% OsO_4 in 1.25% sodium bicarbonate (pH 7.2, Wood and Luft, 1965). They were then dehydrated through an ethanol series and directly embedded in Spurrs (Ted Pella Inc., Redding, CA). After a polymerization period of 48 h, silver-gold sections were cut, collected on copper grids and stained with uranyl acetate and Reynold's lead citrate for 20 min and 5 min, respectively. TEM sections were then observed with a FEI transmission electron microscope (Morgagni model; Hillsboro, OR).

6 Ciliary Beat Frequency Analysis

For the quantification of ciliary beating in identified ciliary populations, ciliary cells were viewed on an inverted microscope (Zeiss Axiovert 135; Zeiss, ON, Canada) with differential interference contrast optics and a 100 X objective. Ciliary beating was recorded using either a high-speed digital videocamera (Vitana) linked to a Macintosh Powerbook containing Pixelink software (generously provided by Improvision, Inc., Guelph, Ont., Canada) or a Retiga Ex digital CCD camera (Q-Imaging, Burnaby, BC, Canada) linked to a Pentium 4 PC computer containing Northern Eclipse software (Empix Imaging Inc., Mississauga, ON). With both cameras, videos were collected at greater than 50 frames per second for 1 sec segments, once per minute over the course of the experiment. Off-line analysis was performed on a Macintosh G4 computer using the public domain NIH Image program (written by Wayne Rasband at the U.S. National Institutes of Health and available from the Internet by anonymous FTP from zippy.nimh.nih.gov) and Particle Analysis (a user-contributed macro written by C.J.H. Wong at the University of Alberta). The displacement of the cilia from an initial position was calculated in both X and Y coordinates. The CBF was then determined by performing an autocorrelation on the resulting displacement waveform. The CBF for each time point was the result of an average of three measurements made in approximately the same location on the cell over the course of the experiment. In the experiments examining the ciliary beating of the individual ciliary cell types, a few experiments were performed at a higher temporal resolution to determine if there were undetected changes in CBF in response to drug treatments. Given that the CBF experiments with a collection rate of once every 15 seconds revealed no additional events, the data is presented with the collection rate at once every minute.

7 Ratiometric Ca^{2+} Imaging and Ca^{2+} Calibration

The Ca^{2+} imaging procedures used in the comparative study of ciliary subpopulations were different than those used in subsequent experiments.

7.1 Characterization of subpopulations of ciliary cells expressed on the surface of *Helisoma* embryos

Fura dextran (Molecular Probes) was dissolved in filtered distilled water to a concentration of 2 mM. Fura dextran was utilized instead of the free acid form of the indicator because it is considered to be less toxic to the cell and more resistant to subcellular compartmentalization (Tombal *et al.*, 1999). The dye was backloaded into custom-pulled sharp micropipettes (1.0 mm glass with filament; World Precision Instruments Inc., Sarasota, FL). An Eppendorf Femtojet Rapid injection system mounted on an inverted Nikon Eclipse microscope was used to microinject cultured ciliated cells under 1000 X DIC optics (Figure 7). Microinjection pipettes were inserted into cells for less than 2 seconds, during which time dye was injected with an injection pressure of 650-750 hPa. Loaded ciliated cells were imaged with a 100 X oil-immersion objective (1.3 N.A. Fluor) on an inverted microscope (Zeiss, Axiovert 135) with excitation at 340 nm and 380 nm from an Hg-Xe arc lamp (Hamamatsu, Hamamatsu, Japan; Figure 8). Emission fluorescence at 510 nm was collected using an intensified charge-coupled device (ICCD) video camera (Paultek Imaging, Grass Valley, CA).

Neutral density filters (Omega Optical, Brattleboro, VT) were used to ensure that fluorescent images were within the sensitivity range of the camera. Data were collected as 8-bit images using custom software kindly provided by Dr. S. Kater (University of Utah). Captured images were digitized through a QuickCapture frame grabber board (Data Translation, Mississauga, ON) and saved to a computer for off-line analysis (Macintosh Quadra 950). Vehicle or drug-containing solutions were perfused into the culture dish using a gravity-driven perfusion set-up at approximately 1 mL/min with a latency of 15 sec (Warner Instruments Corp., Holliston, MA). Images were analyzed for whole cell fluorescence intensity on a Macintosh G4 computer using the public domain NIH Image program and Ca^{2+}Ratiometrics (a user-contributed macro, written by C. J. H. Wong at the University of Alberta).

The 340/380 ratios, which provides a relative measure of cytoplasmic free calcium concentration, were converted to estimates of $[Ca^{2+}]_i$ using the equation $[Ca^{2+}]_i = K_d (R - R_{min})/(R_{max} - R) (F_o/F_s)$ (Grynkiewicz et al., 1985). The K_d was determined to be 0.586 μM using thin wall glass capillary tubes (20 nm in width; VitroCom Inc., Mt. Lks., NJ.) filled with one of eleven different Ca^{2+} buffer solutions (Ca^{2+} concentration ranged from 0 μM to 39 μM; Calcium calibration buffer kit with magnesium II, Molecular Probes) and 50 μM fura dextran. Fluorescence values acquired from the images taken with excitation at both 340 nm and 380 nm for all eleven Ca^{2+} buffer solutions were entered into a computer program available on the Molecular Probes website (www.probes.com/resources/calc/kd.html) to determine the value of K_d. This value for K_d is consistent with other *in vitro* estimates for fura dextran (Konishi and Watanabe, 1995; Tombal *et al.*, 1999). The values for R_{min}, R_{max}, F_o and F_s were determined *in situ* using ciliary cells loaded with fura dextran. Cells were permeabilized with 50 μM ionomycin in the presence of either Ca^{2+}-free HS with 1.0 mM ethylene glycol-bis (b-aminoethyl Ether) N, N, N, N- Tetraacetic acid (EGTA) for the determination of R_{min} and F_o or unaltered HS for the determination of R_{max} and F_s.

7.2 Roles of Ca^{2+}, PKC and intracellular Ca^{2+} stores in the excitatory response to serotonin in pedal ciliary cells

Fura-2 pentapotassium salt (Molecular Probes) was dissolved in filtered distilled water to a concentration of 2 mM and backloaded into custom pulled micropipettes (1.0 mm glass with filament; World Precision Instruments Inc.). Identified pedal ciliary cells were microinjected using an Eppendorf Femtojet Rapid Injection System (Brinkmann) mounted on an inverted Nikon Eclipse microscope as previously mentioned. Loaded ciliated cells were imaged with a 100 X oil-immersion objective (1.3 N.A. Fluor) on an inverted microscope (Zeiss, Axiovert 135) with excitation at 340 nm and 380 nm from an Hg-Xe arc lamp (Hamamatsu, Hamamatsu, Japan). Emission fluorescence at 510 nm was collected using a Retiga Ex digital CCD camera (Q-Imaging) linked to a Pentium 4 PC computer containing Northern Eclipse software (Empix Imaging Inc.). The Ca^{2+} imaging subprogram IonWaveN was used to capture and analyze images. Calcium imaging data was presented as the 340/380 ratio, which provides a relative measure of cytoplasmic free calcium concentration (Grynkiewicz *et al.*, 1985). Given that the measured ratios displayed little spatial variability (data not shown), the 340/380 ratio was determined from the average of two to three regions of interest over the cell. Vehicle or drug-containing solutions were perfused into the culture dish using gravity-driven perfusion at approximately 1 mL/min (Warner).

8 Immunohistochemistry

Identified populations of ciliary cells cultured on glass-bottom petri dishes were fixed in 4% paraformaldehyde in 0.01 M phosphate-buffered saline (PBS) at 4 °C for 1 hour. The cells were washed 3 x 10 min in PBS. This and subsequent steps were performed at room temperature with agitation at 80 rpm (American Rotator V) unless otherwise stated. Embryos were washed in PBS containing 3% horse serum (Sigma) and 0.3% Triton X-100 for 1 hour. This was followed by incubation in rabbit anti-5-HT (Sigma), anti-5-$HT1_{hel}$ or anti-5-$HT7_{hel}$ antiserum diluted 1:1000 in PBS containing 1% horse serum and 0.4% Triton X-100 for 12 hours at 4 °C. The cells were then washed 4 X 7 min with 0.4% Triton X-100 in PBS and then incubated for 1 hour with goat anti-rabbit immunoglobulin G conjugated to Alexa 488 (Molecular Probes, Eugene, OR) that was diluted in a solution of 1% horse serum and 0.3% Triton X-100 in PBS. This was followed by 4 X 5 min washes in 0.3% Triton X-100 in PBS and 2 X 10 min washes in PBS. The cells were examined in 80% glycerol in PBS. Control experiments were also performed where the primary antibody was excluded. Additional control experiments for the receptor antibody experiments were performed where the pre-immune serum from the same rabbit as the one used to generate the primary antibody was used in place of the primary antibody. Finally, given that the 5-HT receptor antiserum was generated using keyhole limpet hemocyanin (KLH) as a carrier, a preabsorption control was performed to account for non-specific KLH binding. The results of this protocol did not alter the immunostaining detected for either 5-$HT1_{hel}$ or 5-$HT7_{hel}$.

9 Preparation of antibodies to 5-$HT1_{hel}$ and 5-$HT7_{hel}$

Antibodies to the 5-HT receptors 5-$HT1_{hel}$ and 5-$HT7_{hel}$ cloned from *Helisoma* were raised against peptides derived from intracellular loop sequences that had a high antigenicity. Peptide 5-$HT1_{hel}$ (Residues 409-423, YSRTREKLELKRERK) and Peptide 5-$HT7_{hel}$ (Residues 246-261, YFKIWRVSSKIAKAEA) were prepared by Washington Biotechnology (Baltimore, MD). Peptides were synthesized, coupled to KLH, and used to immunize rabbits. Sera were collected when the antibody gave a positive reaction against the antigen at a titer of >100,000 in an Enzyme-Linked Immunosorbent Assay.

10 Data Analysis

Results are presented as mean ± standard error of the mean (S.E.M.) unless otherwise stated. Statistical significance was determined by a Student's *t* test or analysis of variance (ANOVA) followed by Fisher's protected least significant difference (PLSD) test.

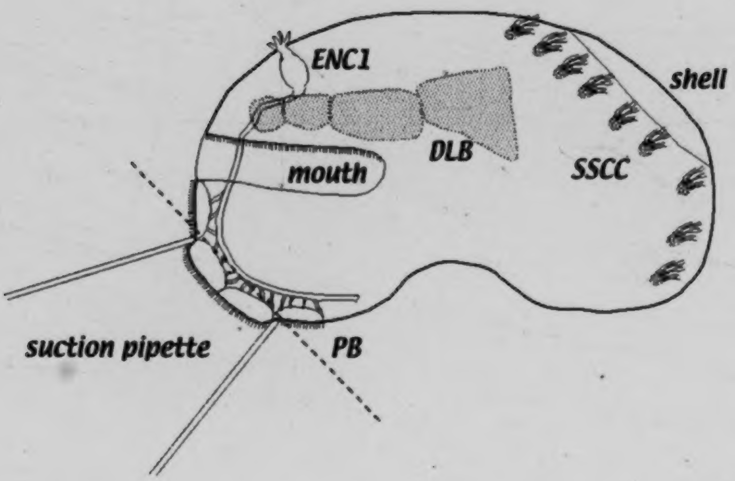

Figure 6. Isolation of identified ciliary cells from *Helisoma trivolvis* embryos. Schematic of a side view a stage E30 *Helisoma trivolvis* embryo reveals the location of the various cilliary cells and embryonic neuron C1 (ENC1). A suction pipette was used to remove identified pieces of tissue from the surface of the embryo. DLB- dorsolateral ciliary band, PB- pedal ciliary band, SSCC- scattered single ciliary cell.

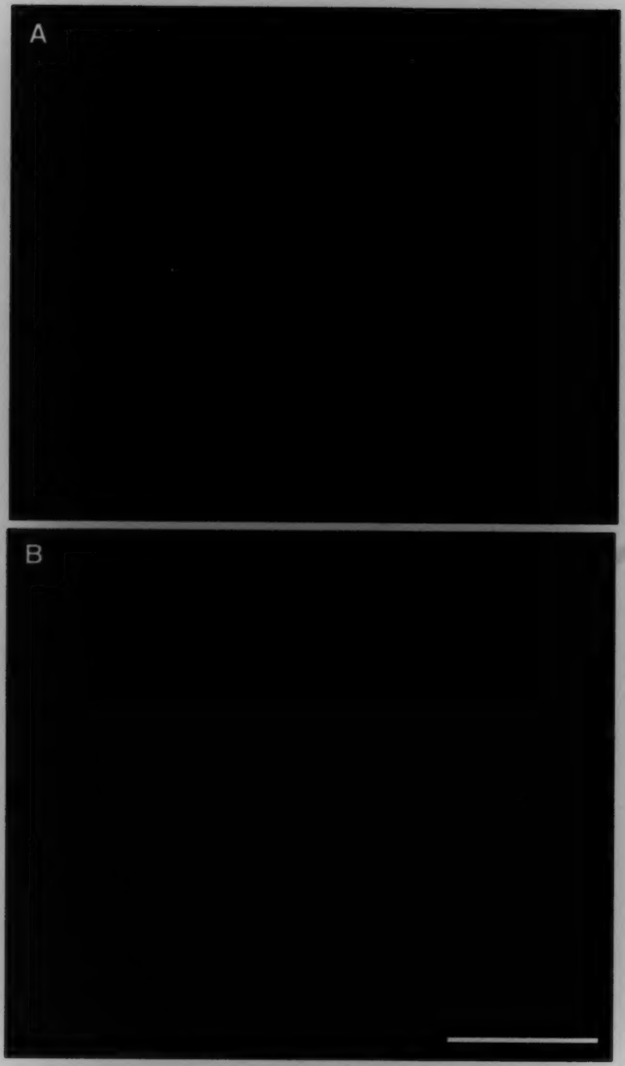

Figure 7. Microinjection of fura dextran into a cultured *Helisoma* ciliary cell. A. Fluorescence micrograph of micropipette loading with fura dextran and a ciliary cell prior to laoding. B. Fluorescence micrograph of the same ciliary cell during microinjection. Scale bar is 10 µm.

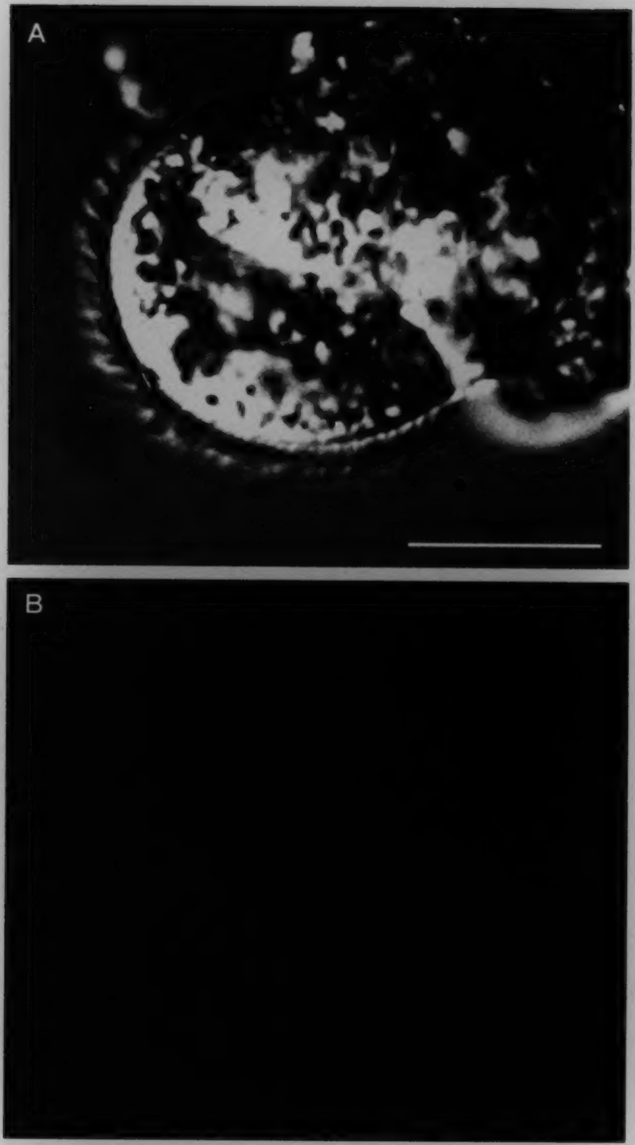

Figure 8. Pedal ciliary cell loaded with fura dextran. A DIC micrograph of a pedal ciliary cell within a cultured tissue explant. B. Corresponding fluorescence micrograph showing fura dextran fluoresence from the same cell. Scale bar is 10 μm.

RESULTS

1 Characterization of subpopulations of ciliary cells expressed on the surface of *Helisoma* embryos[1]

In this section, the morphology and physiology of some of the individual sub-populations of *Helisoma* ciliary cells are characterized. By developing a technique to culture identified ciliary cells, it was possible to study the pedal, dorsolateral and scattered single ciliary cells (SSCCs) individually. Given that previous attempts to image intracellular Ca^{2+} in these embryonic cells using membrane-permeable indicators were unsuccessful (Christopher, 1997), ciliary cells were microinjected with membrane impermeable fura dextran for calcium imaging experiments. These results suggest that the pedal and the dorsolateral ciliary populations share many physiological and anatomical characteristics, whereas the SSCCs represent a distinct ciliary subtype.

1.1 Anatomical characterization of ciliary cell subtypes *in vivo*[2]

Embryos were processed for scanning and transmission electron microscopy to compare the morphology and fine structure of pedal ciliary cells, dorsolateral ciliary cells and SSCCs. Figure 9A shows the location of ciliary populations in a stage E30 embryo. Pedal and dorsolateral ciliary cells occurred in distinct anterior ciliary bands, whereas the SSCCs were most prevalent in the posterior region of the embryo.

Structurally, pedal and dorsolateral ciliary cells appeared identical in profile and contents. Cilia were arranged in an organized fashion and ranged in number from 600 to 800 per cell (Figures 9B and C). In sectional profile, pedal and dorsolateral cells were long, thin, flattened cells with an elliptical nucleus containing a large nucleolus (Figures 9D; see Koss *et al.*, 2003). Microvilli surrounded the base of each cilium (Figures 9B and C). The cilia possessed a typical 9x2+2 arrangement of microtubules (data not shown) and a basal foot arose from one side of the basal body. A lengthy primary rootlet extended into the cell from the base of the cilium and an accessory rootlet arose from the opposite side of the basal body; both rootlets were striated (Figure 9D). Each ciliary cell contained many prominent mitochondria that were localized beneath the ciliary basal bodies (Figure 9D). Granular endoplasmic reticulum was abundant and tended to be concentrated toward the cell periphery. Pedal and dorsolateral ciliary cells consistently displayed extensive patches of cytoplasm that appeared to be devoid of organelles, except for some small electron translucent vesicles ranging in size from 0.03 to 0.06µm in diameter (Figure 9D). A previous study has revealed that these regions contain vesicles which display 5-HT immunoreactivity (Koss *et al.*, 2003).

In comparison to the cells of the pedal and dorsolateral ciliary bands, SSCCs differed in profile and content. Apically, only 35 to 50 cilia emerged from the cell surface. The SSCC cilia displayed a more random orientation and a greater length than the pedal or dorsolateral cilia (Figure 9E). Furthermore, SSCCs were smaller, had a wedge or cuboidal shape, and a centrally-located nucleus. The fine structure of individual cilia was similar to pedal and dorsolateral cilia, including a 9x2+2 arrangement of microtubules (Figure 9F inset). However, there were no accessory ciliary rootlets arising laterally from the basal body (Figure 9F). The cytoplasm of the scattered single ciliated cells contained less prominent mitochondria and an absence of electron-translucent regions. Finally, the SSCCs had no basal cellular extensions that were found on innervated pedal and dorsolateral ciliary cells as previously described (Koss *et al.*, 2003). Thus, the different morphology and fine structure of the SSCCs, in comparison to the pedal and dorsolateral ciliary cells, suggest that ciliary subtypes may exhibit different physiological profiles.

1.2 Examination of unidentified ciliary cells *in vitro*

The necessity of Ca^{2+} influx in cilio-excitation (Christopher et al., 1996) prompted the hypothesis that 5-HT, the primary cilio-excitatory neurotransmitter in *Helisoma* embryos, would induce a change in $[Ca^{2+}]_i$. Using fast microinjection, unidentified ciliary cells in culture were loaded with fura-2 dextran. Whereas the calcium ionophore ionomycin (10 μM) caused an increase in the 340/380 ratio in all cells examined, only 4 of 8 cells responded to 100 μM 5-HT with an increase in $[Ca^{2+}]_i$ (Figure 10). This finding prompted the hypothesis that one or more of the sub-populations of ciliary cells in mass dissociated cultures do not respond to 5-HT with a change in $[Ca^{2+}]_i$.

1.3 Examination of physiological responses of identified ciliary cells *in vitro*

Both the calcium imaging results described above and in previous *in vivo* measurements of CBF (Kuang and Goldberg, 2001) suggest that the different ciliary populations display distinct physiological properties. To test this, the effect of exogenous 5-HT on CBF in identified ciliary cells in culture was examined. In pedal ciliary cells, perfusion with 100 μM 5-HT produced a rapid, statistically significant increase in CBF (Figure 11A). The pedal ciliary cells roughly doubled the rate of ciliary beating within 1 minute of the start of 5-HT perfusion. This high CBF was maintained for 10 minutes, with only marginal desensitization (Figure 11A). A five minute washout with HS produced a partial recovery in CBF and a challenge with 10 μM ionomycin increased CBF to values similar to those induced by 100 μM 5-HT.

To ensure that microinjection with fura dextran did not alter the physiological responses of these cells, the ciliary response to serotonin and ionomycin was examined in pedal ciliary cells that had been loaded with fura dextran. These cells exhibited a nearly identical CBF response to serotonin and ionomycin as pedal ciliary cells that were not loaded with fura dextran (Figure 11B). Perfusion with 100 μM serotonin produced a rapid, statistically significant increase in CBF, followed by a partial recovery in response to HS washout. Perfusion of 10 μM ionomycin produced an increase in CBF to approximately the same amplitude as serotonin. The results of this experiment suggest that microinjection of fura dextran does not impair the cell's ability to respond to serotonin or ionomycin with changes in CBF.

A similar effect was observed in dorsolateral ciliary cells, as 100 μM 5-HT produced a rapid, statistically significant increase in the rate of ciliary beating within 1 minute of 5-HT perfusion (Figure 11C). These observations are consistent with *in vivo* results on the effect of 5-HT on dorsolateral and pedal ciliary cells (Kuang and Goldberg, 2001). Washout with HS produced a partial recovery in CBF over 5 minutes, and 10 μM ionomycin again produced an increase in CBF that was similar to the serotonin response. As with pedal cilia, ionomycin produced a change in the ciliary beat mechanics in dorsolateral cilia, and in one of the cells the ionophore treatment killed the cell (data not shown).

The SSCCs are small, cuboidal cells with longer cilia (Figure 9E) and different ciliary beat profiles than the pedal and dorsolateral ciliary cells. These cells exhibited higher basal rates of ciliary activity, an unstable ciliary beat profile, and no discernable response to 100 μM 5-HT (Figure 11D). Furthermore, 10 μM ionomycin did not appear to produce a change in CBF (Figure 11D). These data suggest that ciliary beating in SSCCs may be regulated differently than in pedal and dorsolateral ciliary cells.

To further examine the physiological differences in the subpopulations of *Helisoma* ciliary cells and determine why only a percentage of mass dissociated cells in culture respond to 5-HT with an increase in $[Ca^{2+}]_i$, intracellular Ca^{2+} was imaged in identified ciliary cells *in vitro*. When calibrated for $[Ca^{2+}]_i$, the baseline values for both pedal and dorsolateral ciliary cells was between 50 and 150 nM. In pedal ciliary cells, two different types of Ca^{2+} responses were evident during perfusion with 100 μM 5-HT. The first type of response was an initial peak followed by a sustained plateau in the 340/380 ratio (n = 4 cells, Figure 12A), with an average increase of approximately 350 nM, followed by a sustained rise in $[Ca^{2+}]_i$ of 150 nM above baseline. Alternatively, cells exhibited a gradual increase in the 340/380 ratio (n = 5 cells, Figure 12B), with the increase in $[Ca^{2+}]_i$ approximately 150 nM above baseline. In both cases, perfusion with 10 μM ionomycin produced a large increase in the 340/380 ratio (Figure 12A and B);

this increase in $[Ca^{2+}]_i$ was highly variable in amplitude, ranging from 300 nM to 1300 nM. A similar result was observed with the dorsolateral cells, as they either exhibited a rapid peak and plateau in the 340/380 ratio (n = 3 cells; Figure 13A) or a gradual rise in the 340/380 ratio over the 10 min perfusion with 5-HT (n = 6 cells; Figure 13B). The magnitude of these 5-HT responses was also similar to that observed in pedal ciliary cells. Both types of responses were followed by an ionomycin-induced increase in the 340/380 ratio (Figure 13); the magnitude of the ionomycin-induced increase in $[Ca^{2+}]_i$ ranged from 250 nM to 600 nM. In both pedal and dorsolateral cells, little or no recovery of $[Ca^{2+}]_i$ was observed after washout of 5-HT over the time frame examined. These data indicate that 5-HT does elicit an increase in $[Ca^{2+}]_i$ within pedal and dorsolateral ciliary cells, but with a slower time course than observed during the CBF measurements.

Consistent with the CBF results, intracellular calcium measurements revealed large differences between the SSCCs and the other ciliary subtypes. In four of nine SSCCs examined, the resting $[Ca^{2+}]_i$ was stable at approximately 100 nM, 5-HT perfusion did not stimulate a notable change in the 340/380 ratio, and 10 μM ionomycin produced a relatively small rise in the 340/380 ratio (Figure 14A). In contrast, five of nine SSCCs exhibited irregular spikes in the 340/380 ratio, both in HS and during 5-HT perfusion (Figure 14B). The timing, duration and amplitude of these events were highly variable, depending on the cell. In most of these cells, 10 μM ionomycin only produced a transient increase in the 340/380 ratio. These data reinforce the notion that the SSCCs display different physiological characteristics than the pedal and dorsolateral cells, including insensitivity to 5-HT.

1.4 Differences in immunohistological staining for 5-HT and 5-HT receptors in the different subpopulations[3]

To further characterize differences in the various ciliary cells in culture, tissue explants containing pedal, dorsolateral or SSCCs were processed for 5-HT immunoreactivity. It was hypothesized that tissue explants containing pedal ciliary cells would be immunopositive for 5-HT, given that ENC1s distal primary neurite branches extensively below the pedal ciliary cells (Koss *et al.*, 2003), and remains of these neurites were thought to persist in culture. As expected, the tissue explants pedal ciliary cells reliably demonstrated the presence of 5-HT immunoreactivity below their basal surfaces (Figure 15). Given that only the most medial of the four cells that comprise each of the dorsolateral bands is innervated by ENC1 (Koss *et al.*, 2003), it was hypothesized that immunoreactivity in tissue explants with dorsolateral cells would be more intermittent. Indeed, 5-HT immunoreactivity was more inconsistent in tissue explants containing dorsolateral ciliary cells (Figure 16). Finally, as 5-HT immunoreactivity has not been detected in the posterior of the embryo (Goldberg and Kater, 1989), it was hypothesized that tissue explants containing SSCCs cultured from the posterior of the embryo would be devoid of 5-HT immunoreactivity. Again, this prediction was confirmed with immunostaining (Figure 17). Interestingly, aspects of the developing shell were highly auto-fluorescent (Figure 17B).

Since some of the ciliary subtypes responded to 5-HT with changes in CBF and $[Ca^{2+}]_i$, immunohistochemistry was employed to determine if identified ciliary cells express the two 5-HT receptors whose genes were recently cloned from *Helisoma trivolvis*. Isolated ciliary tissues were exposed to antibodies raised against the cloned 5-HT receptors, 5-HT1_{hel} and 5-HT7_{hel} (Mapara et al., 2001). All pedal ciliary cells expressed 5-HT1_{hel} immunoreactivity strongly over the apical surface of the cells, with weaker immunoreactivity throughout the remainder of the cell (n = 15 cells; Figure 18A). A majority of dorsolateral ciliary cells also expressed 5-HT1_{hel} immunoreactivity, with 76% of cells (n = 25 cells) exhibiting strong surface expression and weaker distribution throughout the cell (Figure 18B). In the SSCCs, 0% of cells exhibited 5-HT1_{hel} immunoreactivity within the cell (n = 23 cells; Figure 18C1 and 18C2). However, neighbouring nonciliary epithelial cells were consistently immunoreactive (Figure 18C). Rabbit pre-immune serum, used in parallel controls to examine specificity of the antibody staining, did not exhibit any immunoreactivity (Figure 18D).

5-HT7$_{hel}$ immunoreactivity was more inconsistent than 5-HT1$_{hel}$ for pedal and dorsolateral ciliary cells. 5-HT7$_{hel}$ was expressed in only 40% of pedal cells examined (n = 25 cells; Figure 19A). In most of these cells, there was strong expression on the apical surface of the cell, with a small percentage displaying a punctate distribution on the basal surface (data not shown). Less than half of the pedal cells examined (40%) demonstrated 5-HT7$_{hel}$ expression (Figure 19B). Similarly, only 46% of dorsolateral ciliary cells expressed 5-HT7$_{hel}$ strongly on the apical surface and weakly throughout the remainder of the cell (n = 24 cells; Figure 19C), while the majority (54%) did not exhibit any 5-HT7$_{hel}$ expression (Figure 19D). Finally, there was no expression of 5-HT7$_{hel}$ within any of the SSCCs, but again there was expression in the surrounding epithelial cells (n = 22 cells; Figure 19E). Taken together, these data implicate the 5-HT1$_{hel}$ receptors, and possibly 5-HT7$_{hel}$ receptors, in the signal transduction pathway for serotonin induced cilioexcitation in both pedal and dorsolateral cells.

Figure 9. Whole mount scanning electron micrographs (SEM) and transmission electron micrgraphs (TEM) showing the overall external and internal anatomy of the three ciliary subtypes of a stage E-28 embryo. A. Left lateral view SEM showing the position of the scattered single ciliary cells (sc) relative to the dorsolateral ciliary bands (dl) and pedal ciliary band (p). The shell (sh) and mouth (mo) are also shown. Scale bar is 25 µm. B. SEM showing the configuration and density of cilia of a dorsolateral ciliary cell. Scale bar is 1 µm. C. SEM showing the configuration and density of cilia of a pedal ciliary cell. Scale bar is 1 µm. D. TEM of a dorsolateral ciliary cell showing numerous mitochondria (mi) and the nucleus (n). Electron translucent regions are designated by an arrow. The cilia (c) with basal body (bb), ciliary rootlet (cr) and accessory ciliary rootlet (acr) are also shown. Scale bar is 1 µm. E. SEM showing the configuration and density of cilia of one of the scattered single ciliated cells. Scale bar is 1 µm. F. TEM of a scattered single ciliated cell showing the cytoplasm. Note the cilia (c) with basal body (bb), ciliary rootlet (cr), less prominent mitochondria (mi) and the nucleus (n). Inset: Cross section through a cilium of showing the 9x2+2 doublets of microtubules. Scale bar is 0.5 µm.

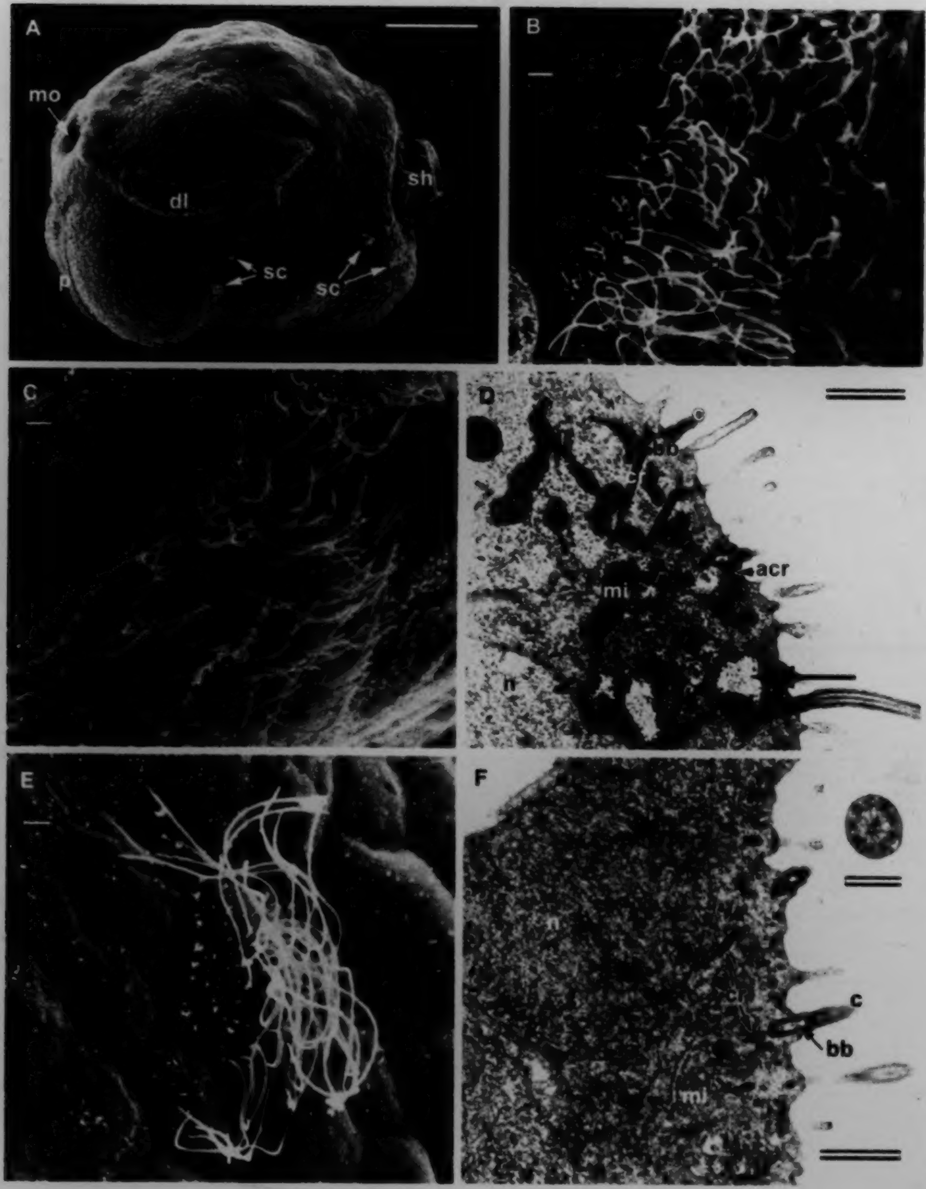
A
mo
dl
sh
p
sc
sc
B
C
D
c
bb
c
acr
mi
n
E
F
n
c
bb
mi

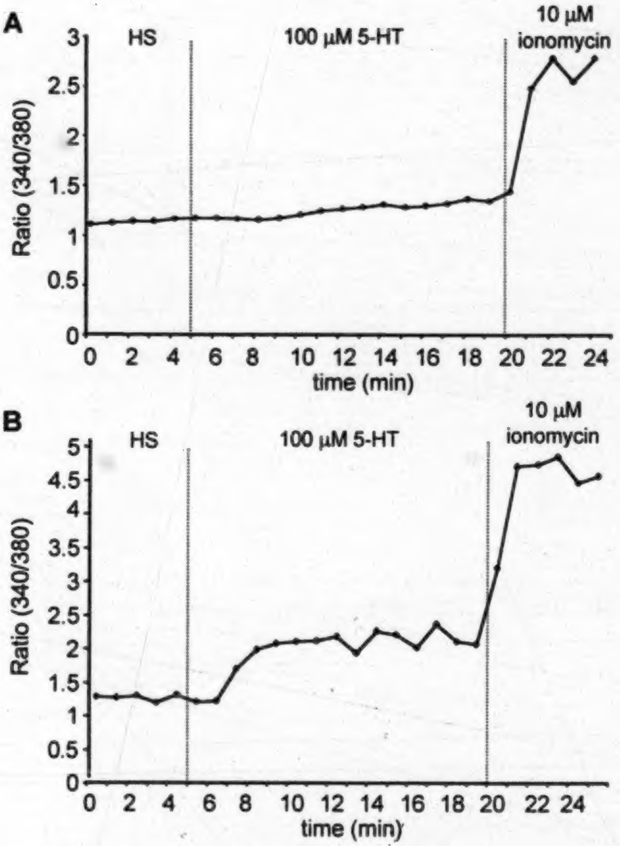

Figure 10. Effect of 5-HT and ionomycin on the intracellular Ca^{2+} concentration in unidentified ciliary cells in culture. Ciliary cells microinjected with fura-2 dextran were imaged at one minute intervals in the presence of saline (HS), 5-HT, or ionomycin. A. Representative trace of a ciliary cell that was not affected by a 15 min application of 100 μM 5-HT, but displayed a rapid rise in the 340/380 in response to 10 μM ionomycin. B. Representative trace of an unidentified ciliated cell responding to both 100 μM 5-HT application and 10 μM ionomycin with an increase in the 340/380 ratio. Dotted lines represent the time at which drug treatments were initiated.

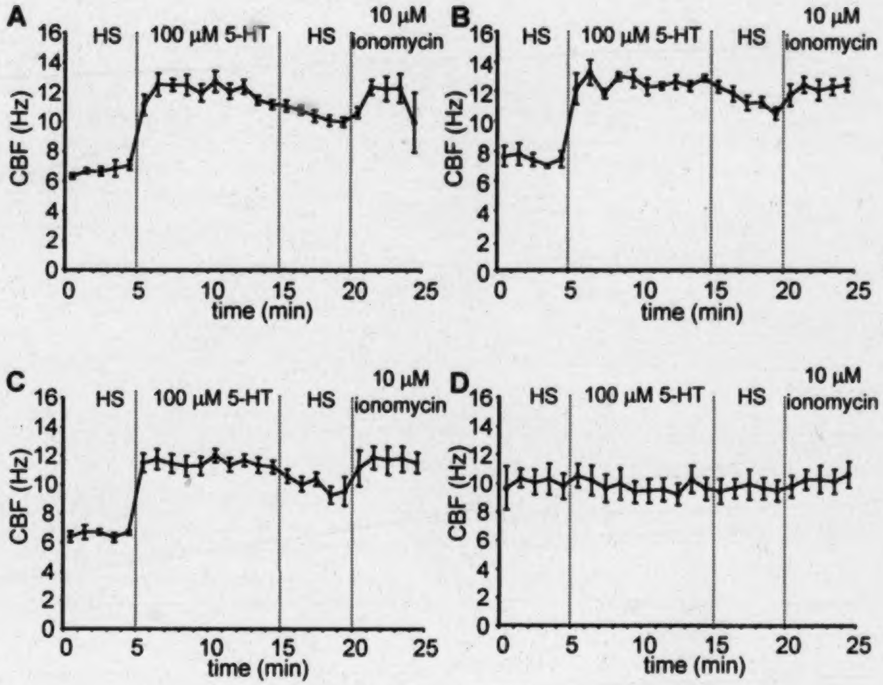

Figure 11. Effect of 5-HT and ionomycin on CBF in pedal, dorsolateral and scattered single ciliary cells. Perfusion with 100 µM 5-HT resulted in an approximate doubling in the rate of ciliary beating in pedal (A), fura dextran-loaded pedal (B) and dorsolateral (C) ciliary cells. This 5-HT stimulated increase in CBF was statistically significant in all cases. The CBF partially recovered when cells were perfused for 5 min with *Helisoma* saline (HS), whereas perfusion with 10 µM ionomycin further stimulated CBF in pedal (A), fura dextran-loaded pedal (B) and dorsolateral (C) ciliary cells. The scattered single ciliary cells did not display cilio-excitatory responses to 5-HT or ionomycin (D). Measurements were taken once every minute and n=6 cells for A,C and D and n=4 for B. Dotted lines represent the time when the specified treatments were initiated.

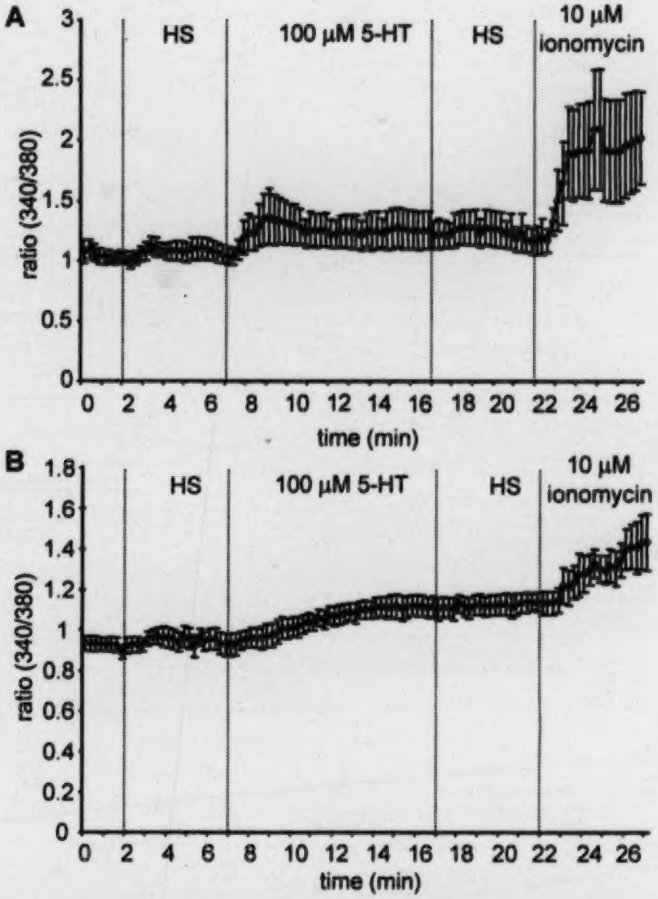

Figure 12. Effect of 5-HT and ionomycin on intracellular Ca^{2+} concentration in pedal ciliary cells. Pedal ciliary cells were microinjected with fura-2 dextran and imaged once every 15 sec. Application of 100 μM 5-HT generated two different $[Ca^{2+}]_i$ profiles, an early peak in the 340/380 ratio followed by a sustained plateau (A; n=4 cells) or a gradual rise in the 340/380 ratio over the course of drug application (B; n=5 cells). In both cases, the $[Ca^{2+}]_i$ did not recover within 5 minutes of exposure to *Helisoma* saline (HS), whereas 10 μM ionomycin stimulated a large increase in the 340/380 ratio. Dotted lines represent the time when the specified treatments were initiated.

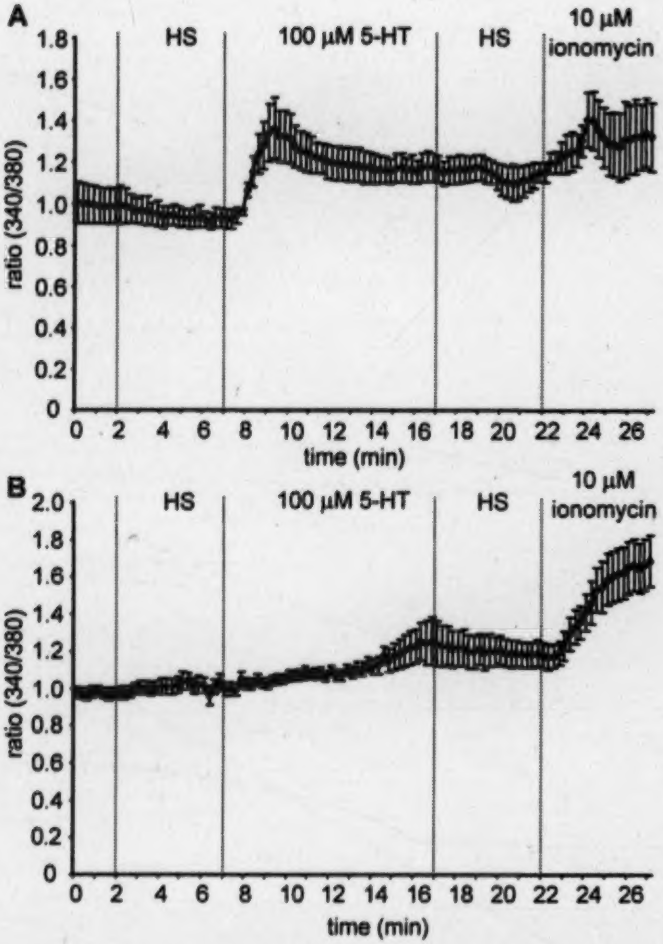

Figure 13. Effect of 5-HT and ionomycin on intracellular Ca^{2+} concentration in dorsolateral ciliary cells. Dorsolateral ciliary cells were microinjected with fura-2 dextran and imaged once every 15 sec. Application of 100 µM 5-HT generated two different types of changes in $[Ca^{2+}]_i$, an early peak followed by sustained plateau (A; n=3 cells) or a gradual rise in the 340/380 ratio over the course of 5-HT perfusion (B; n=6 cells). In all cells, regardless of the response, 10 µM ionomycin produced an increase in the 340/380 ratio. Dotted lines represent the time when the specified treatments were initiated.

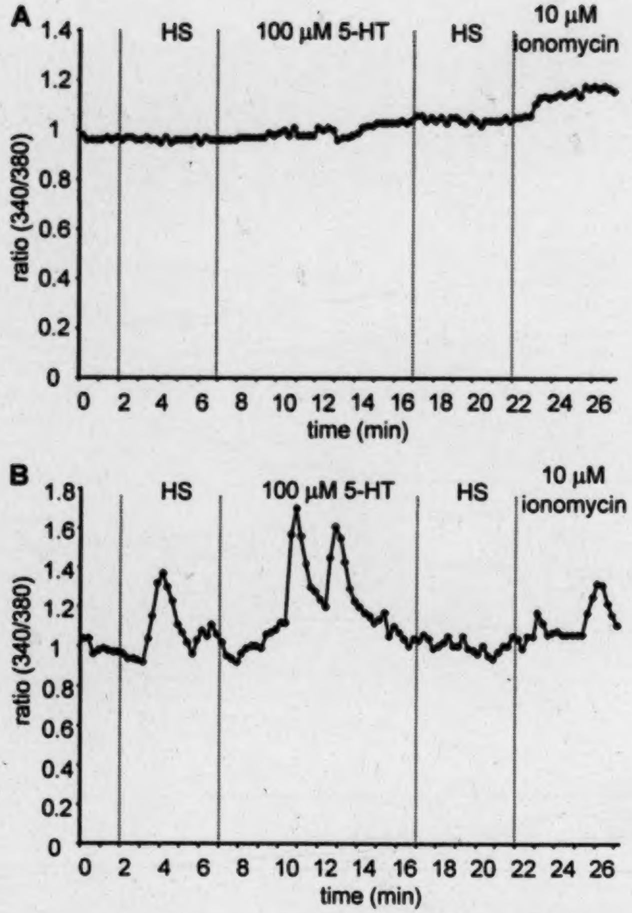

Figure 14. Effect of 5-HT and ionomycin on intracellular Ca^{2+} concentration in scattered single ciliary cells. Scattered single ciliary cells were microinjected with fura-2 dextran and imaged once every 15 sec. A) A representative trace of an SSCCI that did not respond to 100 μM 5-HT and exhibited only a weak increase in the 340/380 ratio in response to 10 μM ionomycin. B) A representative trace of an SSCC that displayed spikes in the 340/380 ratio. Dotted lines represent the time when the specified treatments were initiated.

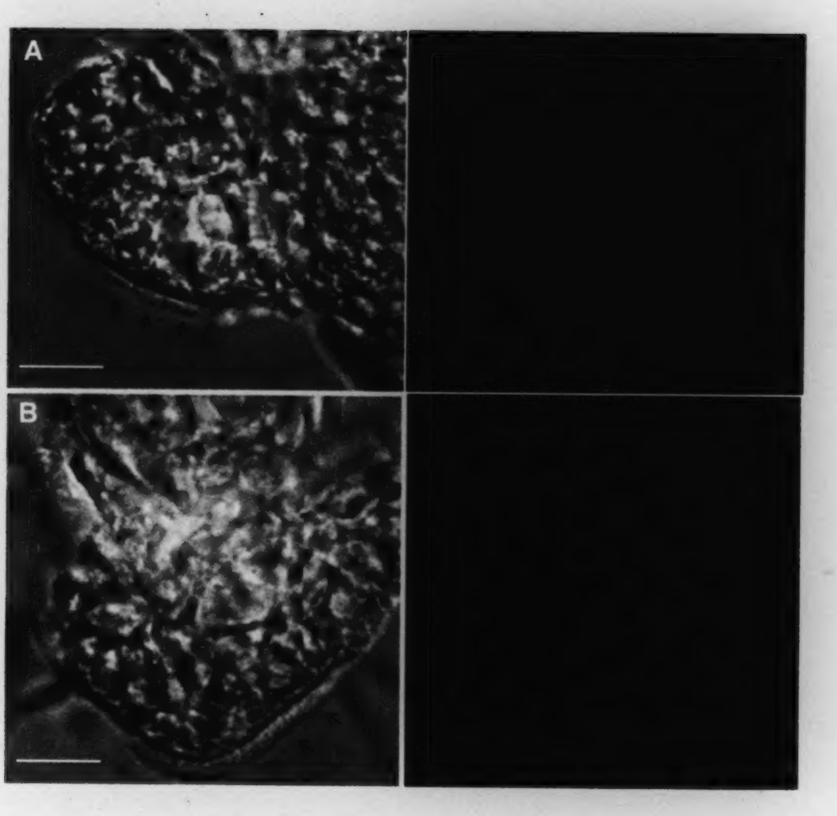

Figure 15. 5-HT immunoreactivity in an isolated tissue explant containing pedal ciliary cells. Nomarski differential interference contrast (DIC) images (left panels) and corresponding fluorescence micrographs (right panels) of tissue explants containing identified ciliary cells that were processed for 5-HT immunoreactivity. Arrows indicate the ciliated cell margin. A and B show different tissue explants. The scale bar is10 µm.

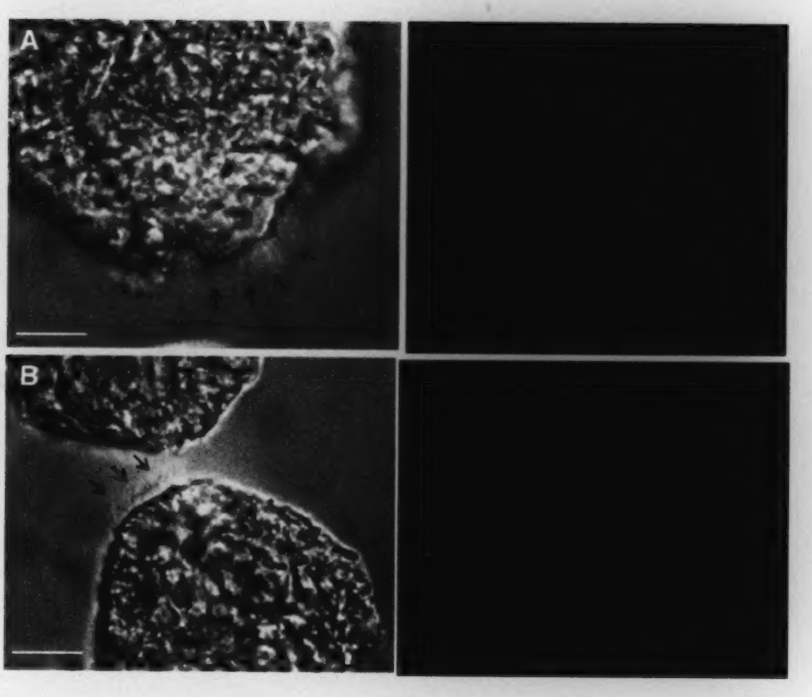

Figure 16. 5-HT immunoreactivity in isolated tissue containing dorsolateral ciliary cells. Nomarski differential interference contrast (DIC) images (left panels) and corresponding fluorescence micrographs (right panels) of tissue explants containing identified ciliary cells that were processed for 5-HT immunoreactivity. A. Immunopositive staining below a dorsolateral ciliary cell. B. Absence of immunoreactivity below a dorsolateral ciliary cell. Arrows indicate the cilated cells margin. The scale bar is 10 µm.

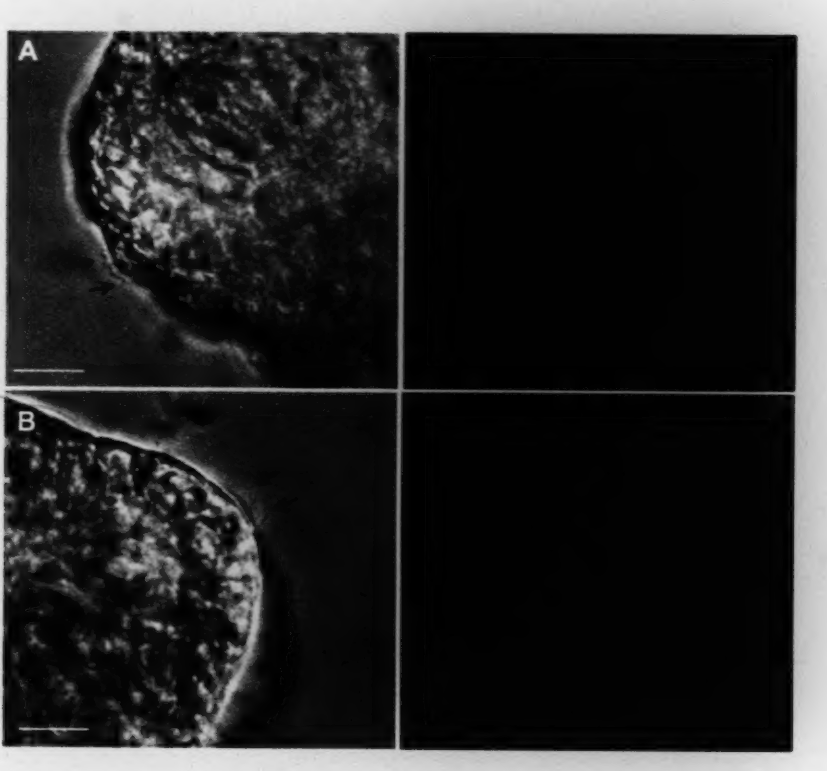

Figure 17. 5-HT immunoreactivity in isolated tissue containing scattered single ciliary cells. Nomarski differential interference contrast (DIC) images (left panels) and corresponding fluorescence micrographs (right panels) of tissue explants containing identified ciliary cells that were processed for 5-HT immunoreactivity. A and B demonstrate a lack of immunoreactivity below scattered single ciliary cells. Arrows indicate the ciliated cells margin. The scale bar is 10 μm.

Figure 18. 5-HT1_{hel} receptor immunoreactivity in identified *Helisoma* ciliary cells. Nomarski differential interference contrast (DIC) images (left panels) and corresponding fluorescence micrographs (right panels) of tissue explants containing identified ciliary cells that were processed for 5-HT1_{hel} immunoreactivity. Arrows indicate the apical surface of the ciliary cells. A) Immunopositive pedal ciliary cell. B) Immunoreactivity in multiple dorsolateral ciliary cells. C) Immunoreactivity restricted to the non-ciliary epithelial cells (asterisks) surrounding an unstained single ciliary cell. D) A control explant containing pedal ciliary cells was exposed to preimmune serum instead of primary antibody. The scale bar is10 µm.

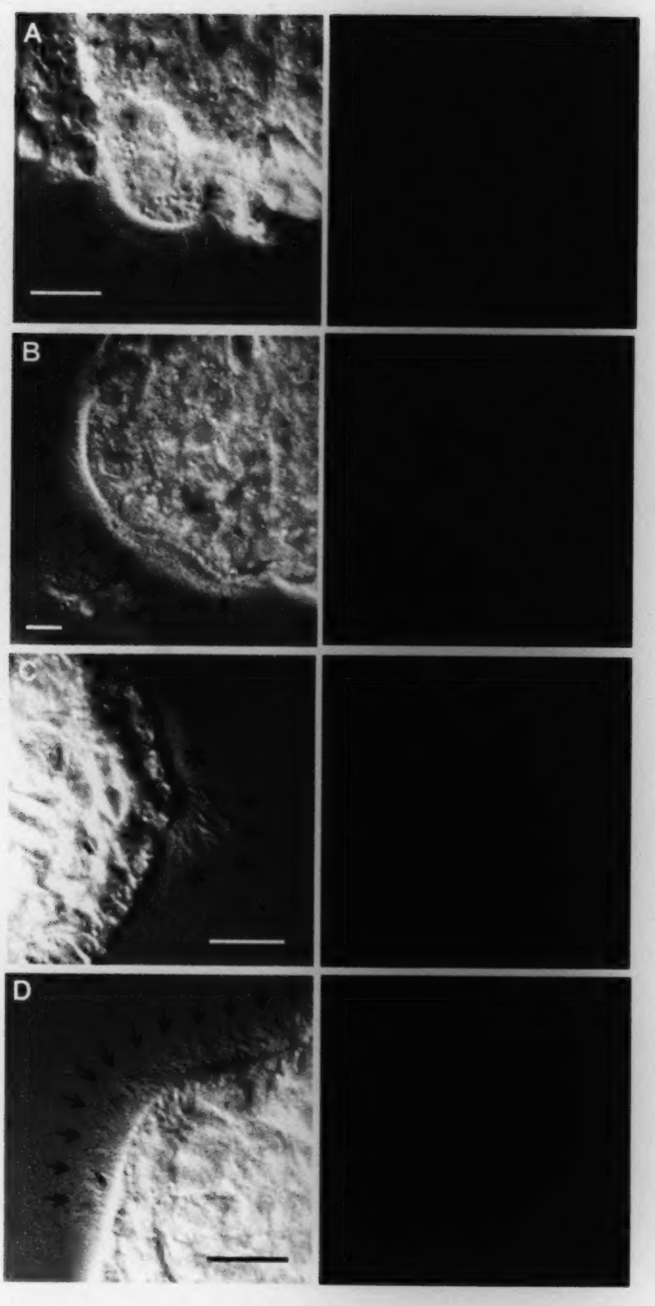
A
B
C
D

Figure 19. 5-HT7$_{\text{hel}}$ receptor immunoreactivity in identified *Helisoma* ciliary cells. DIC images (left panels) and corresponding fluorescence micrographs (right panels) of tissue explants containing identified ciliary cells that were processed for 5-HT7$_{\text{hel}}$ immunoreactivity. Arrows indicate the apical surface of the ciliary cells. A) Immunopositive pedal ciliary cells. B) Immunonegative pedal ciliary cells. C) Immunopositive dorsolateral ciliary cells. D) Immunonegative dorosolateral ciliary cells. E) As with 5-HT7$_{\text{hel}}$ immunoreactivity, 5-HT7$_{\text{hel}}$ immunoreactivity was restricted to non-ciliary epithelial cells (asterisks) surrounding the scattered single ciliary cell. Scale bar is 10 µm.

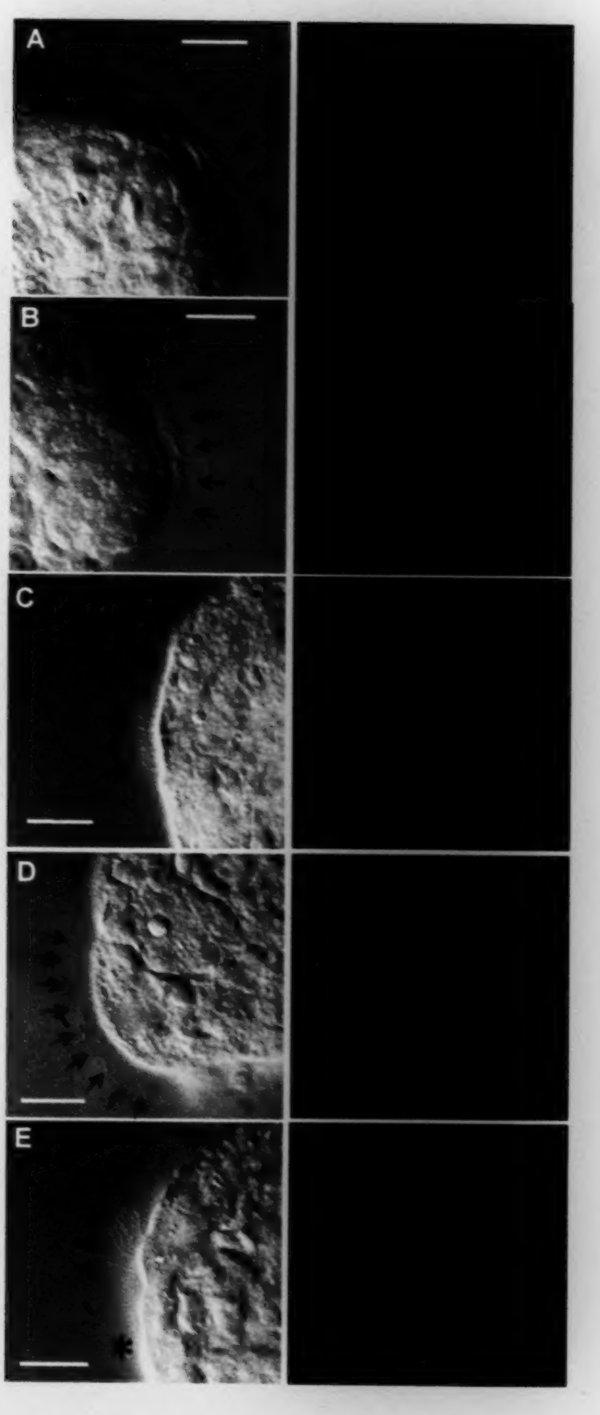
A
B
C
D
E

2 Roles of Ca^{2+} and PKC in the excitatory response to serotonin in pedal ciliary cells[4]

In this section, I examine the hypothesis that Ca^{2+} and PKC pathways interact to mediate the cilio-excitatory response to 5-HT. To examine the roles of the different signal transduction pathways and possible interactions, only pedal ciliary cells were used. Considering that all cells of the pedal ciliary band are innervated by ENC1, it was thought that the culturing of these cells might provide a more uniform population to examine the signal transduction mechanisms underlying the response to 5-HT.

In these experiments the Ca^{2+} indicator fura 2 pentapotassium salt replaced the fura dextran used in the previous section. The rationale for changing the Ca^{2+} indicator was to use an indicator with a lower K_d for Ca^{2+} to possibly increase the sensitivity for measurements of lower amplitude changes in $[Ca^{2+}]_i$. These experiments examined the necessity for increases in $[Ca^{2+}]_i$ and PLC signaling in 5-HT-induced cilio-excitation, as well as the involvement of Ca^{2+} influx. Further, DAG analogs and PKC inhibitors were employed to examine the PKC pathway.

2.1 Necessity for increase in $[Ca^{2+}]_i$ in 5-HT-stimulated ciliary beating

To confirm that increases in $[Ca^{2+}]_i$ are necessary for the ciliary response to 5-HT in *Helisoma*, the highly-selective, fast Ca^{2+} chelator BAPTA was used to buffer intracellular Ca^{2+}. Given that previous attempts to load embryonic *Helisoma* ciliary cells with membrane-permeable AM ester molecules have been unsuccessful (Christopher, 1997), BAPTA tetrapotassium salt was microinjected into cultured ciliary cells. Fura 2 was included in the injection pipette as a fluorescent indicator of injection success. Ciliary cells injected with BAPTA maintained a consistent basal CBF that was not significantly different from fura 2-injected controls ($p > 0.05$; Figure 20). Furthermore, ciliary cells microinjected with BAPTA did not exhibit any change in the rate of ciliary beating in response to 100 μM 5-HT (Figure 20). In contrast, ciliary cells microinjected with fura-2 alone exhibited a significant increase in the rate of ciliary beating in response to 5-HT ($p < 0.05$; Figure 20), consistent with the earlier findings that microinjected fura-2 does not alter the CBF response to 5-HT (Figure 11B). These results suggest that an increase in $[Ca^{2+}]_i$ is necessary for the cilio-excitatory response to 5-HT in *Helisoma* ciliary cells.

2.2 Involvement of PLC signaling in 5-HT-stimulated ciliary beating

Given that DAG analogs have been shown to produce a cilio-excitatory response, while PKC inhibitors partially inhibit 5-HT-induced stimulation (Christopher *et al.*, 1999), it was hypothesized that PLC participates in the CBF response to 5-HT. While 5-HT produced a significant increase in CBF ($p < 0.05$) in HS, the addition of the PLC inhibitor U-73122 (10 μM) ten minutes prior to 5-HT stimulation caused a significant reduction in the CBF response to 5-HT at all time points (Figure 21; $p < 0.05$). In contrast, in the presence of U-73433 (10 μM), a weakly active analog of U-73122, 5-HT caused a large increase in CBF that was similar to that caused by 5-HT alone ($p > 0.05$). In the absence of PLC inhibitor, 5-HT increased the CBF from 5.9 ± 0.3 Hz to 14.8 ± 0.8, whereas in the presence of the active PLC inhibitor, U-73122, 5-HT increased the CBF from 5.7 ± 0.5 Hz to 9.8 ± 0.8 Hz. This result suggests that activation of PLC is a signal transduction component in 5-HT-stimulated ciliary beating. Interestingly, in the presence of 10 μM U-73122, 100 μM 5-HT was still able to produce a change in $[Ca^{2+}]_i$ as revealed through Ca^{2+} imaging (Figure 22).

2.3 Effect of 5-HT and DAG analogs on $[Ca^{2+}]_i$ in pedal ciliary cells

Considering that changes in $[Ca^{2+}]_i$ are necessary for the ciliary response to 5-HT and that PLC activity can lead to changes in $[Ca^{2+}]_i$, we measured relative changes in $[Ca^{2+}]_i$ in response to 5-HT (Figure 23) and DAG analogs (Figure 24) in fura 2-injected cells. Consistent with earlier findings (Figure 12), 100 μM 5-HT elicited a Ca^{2+} response that fit one of two different profiles. 5-HT caused either a slow, gradual rise in $[Ca^{2+}]_i$ (n = 5 cells; Figure 23A), or a more rapid peak and plateau response in $[Ca^{2+}]_i$ (n = 6 cells; Figure 23B). With both responses, little recovery in $[Ca^{2+}]_i$ was observed during a five minute washout period, and perfusion with 10 μM ionomycin produced an increase in $[Ca^{2+}]_i$ that was highly variable in amplitude (Figure 23).

Application of the DAG analog OAG (100 μM) produced a slow, small amplitude increase in $[Ca^{2+}]_i$ (n = 7 cells; Figure 24A), whereas perfusion with 100 μM DOG, a different DAG analog, produced a marginally larger and more rapid increase in $[Ca^{2+}]_i$ (n = 6 cells; Figure 24B). In both cases, application of 10 μM ionomycin following washout of the DAG analog produced a large amplitude Ca^{2+} response (Figure 24). These findings suggest that PKC may play a role in the generation of the Ca^{2+} signal that develops following 5-HT stimulation.

2.4 Effect of removing extracellular Ca^{2+} prior to stimulation of pedal ciliary cells with a DAG analog or 5-HT

To further investigate the interaction between the PKC and Ca^{2+} pathways, we examined the effects of DOG following the removal of extracellular Ca^{2+}. In Ca^{2+}-containing HS, application of 100 μM DOG caused a transient significant increase in CBF from 6.3 ± 0.4 Hz to 9.9 ± 0.5 Hz (Figure 25A; $p < 0.05$). In contrast, when ciliary cells were placed in 0 Ca^{2+} HS two minutes prior to exposure to 100 μM DOG, there was no change in the rate of ciliary beating either before or during the DOG treatment (Figure 25A). Ca^{2+} imaging revealed that the DOG-induced rise in $[Ca^{2+}]_i$ that was observed when cells were bathed in normal HS (Figure 24B) was also completely abolished in 0 Ca^{2+} HS (Figure 25B). The $[Ca^{2+}]_i$ underwent a gradual decline in the presence of 0 Ca^{2+} HS, which rebounded when cells were returned to Ca^{2+}-containing HS. These findings suggest that DAG analogs, and subsequent PKC activation, cause an increase in $[Ca^{2+}]_i$ and a transient increase in CBF through the stimulation of a Ca^{2+} influx event.

To begin to relate the Ca^{2+} -dependent effects of PKC activation with the events underlying the ciliary response to 5-HT, 5-HT-induced changes in CBF and Ca^{2+} were examined when extracellular Ca^{2+} was removed. In Ca^{2+}-containing HS, 5-HT caused a significant increase in CBF that was maintained for the duration of the 5-HT treatment. Exposure of cells to 0 Ca^{2+} HS caused no change in the basal CBF. Surprisingly, when cells were treated with 5-HT after two minutes in 0 Ca^{2+} HS, they still displayed a robust response to 5-HT (Figure 26A). The initial component of this response was not significantly different from control cells exposed to 5-HT in normal HS ($p > 0.05$). However, after the first minute in 5-HT, the rate of ciliary beating decreased and remained at a partially elevated level that was significantly different from both control cells maintained in 0 Ca^{2+} and ciliary cells exposed to 5-HT in the presence of extracellular Ca^{2+} ($p < 0.05$). In contrast to these CBF results, the removal of extracellular Ca^{2+} completely abolished the increase in $[Ca^{2+}]_i$ that was observed during exposure to 5-HT (Figure 26B). As seen before, the $[Ca^{2+}]_i$ gradually declined in 0 Ca^{2+} HS and rebounded upon return to Ca^{2+}-containing HS. These data suggest that maintenance of 5-HT-stimulated ciliary beating and the observed Ca^{2+} response to 5-HT are dependent on extracellular Ca^{2+}, but the initial 5-HT-induced increase in CBF is not regulated by Ca^{2+} influx. Taken together with the previous results, these data also begin to demonstrate that PKC activation may have multiple effects, only some of which are involved in mediating the cilio-excitatory action of 5-HT.

2.5 Effect of PKC inhibitors on 5-HT stimulation of pedal ciliary cells

The differing ciliary responses to DAG analogs and 5-HT prompted further investigation of PKC's role during 5-HT stimulation of *Helisoma* ciliary cells. The effects of two PKC inhibitors on 5-HT-stimulated ciliary beating were tested. bisindolylmaleimide is a PKC inhibitor known to act at the catalytic domain, and calphostin C acts at the DAG binding site (Delmas *et al.*, 2004). Both concentrations of Bisindolylmaleimide, 10 and 100 nM, caused a reduction in the increase of CBF induced by 5-HT, with only 10 nM causing a significant inhibition (Figure 27A; $p < 0.05$). Similarly, 10 nM calphostin C caused a significant reduction in the increase of CBF induced by 5-HT (Figure 27B; $p < 0.05$). Since the PKC inhibitors only caused a partial reduction in the 5-HT-stimulated increase in CBF, these results suggest that PKC plays a major role in mediating the response to 5-HT, but is not the exclusive signal transduction pathway in the response.

To continue to examine the role of PKC in 5-HT stimulation of ciliary cells, the effect of PKC inhibitors on the 5-HT-induced changes in $[Ca^{2+}]_i$ were examined. PKC inhibitors were perfused ten minutes prior to the application of 100 μM 5-HT. Representative traces reveal that neither 10 nM calphostin C (Figure 28B) nor 10 nM and 100 nM of bisindolylmaleimide (Figure 28C and D) caused any inhibition in the 5-HT-induced change in $[Ca^{2+}]_i$ versus a control response (Figure 28A). The amplitude of the peak changes in $[Ca^{2+}]_i$ following 5-HT application in the presence of PKC inhibitors was not significantly different from control (Figure 28E). Interestingly, the PKC inhibitors reliably caused a small, transient increase in $[Ca^{2+}]_i$ within one minute of the onset inhibitor perfusion, although this was not significantly different from control (Figure 28E). These findings suggest that PKC is not involved in the regulation of plasma membrane Ca^{2+} channels that mediate the Ca^{2+} influx following 5-HT stimulation in *Helisoma* ciliary cells. Rather, PKC may phosphorylate an axonemal protein or some other target to participate in the signal transduction of the ciliary response to 5-HT.

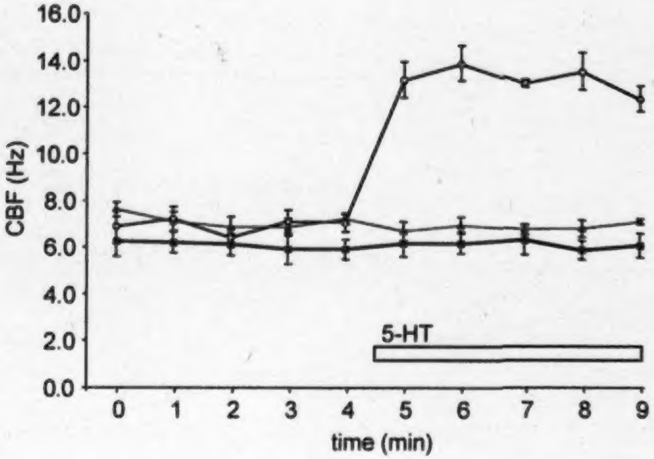

Figure 20. Effect of BAPTA on the CBF response to 5-HT. Ciliary cells, microinjected with 50 mM BAPTA salt mixed with 1mM fura-2, did not exhibit any change in CBF when exposed to 100 μM 5-HT (black squares; n=6 cells). Ciliary cells microinjected with fura-2 alone demonstrated a significant increase in CBF when exposed to 5-HT (open circles; $p < 0.05$ at all time points; n=4 cells). Control ciliary cells were injected with BAPTA and fura-2, but not exposed to 5-HT (open triangles; n=4 cells). The horizontal bar indicates the duration of treatment with 5-HT.

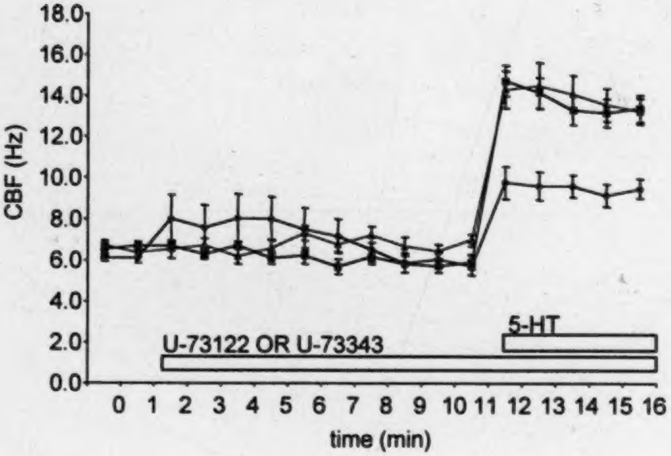

Figure 21. Effect of a PLC inhibitor on the CBF response to 5-HT. Ciliary cells exposed to 10 μM U-73122 for ten minutes prior to 100 μM 5-HT application demonstrated a significantly smaller CBF response to 5-HT (open diamonds; $p < 0.05$ at all time points; n= 6 cells) than control cells exposed to either 5-HT alone (HS; black squares; n= 6 cells) or U-73343 and 5-HT (gray triangles; n= 6 cells). The horizontal bars indicate the duration of treatment with the specififed drug.

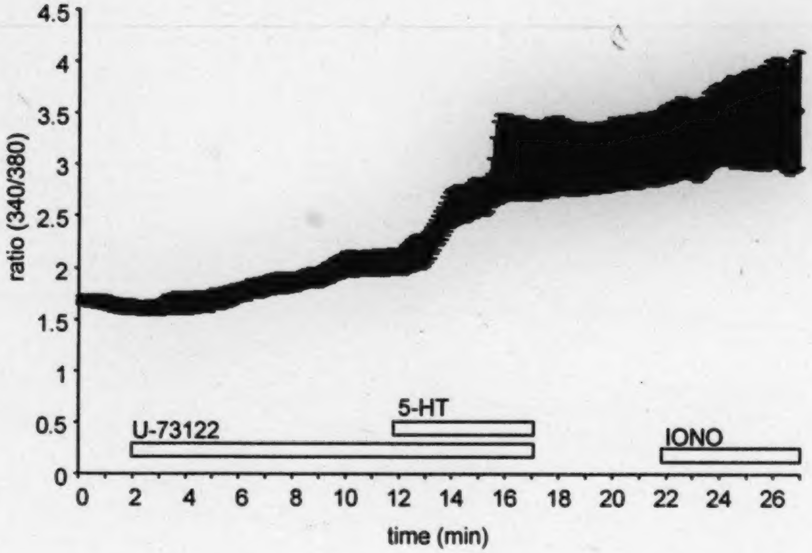

Figure 22. Effect of a PLC inhibitor on 5-HT-induced changes in $[Ca^{2+}]_i$. The 340/380 ratio of ciliary cells microinjected with fura-2 salt and was measured every five seconds in the presence of 10 μM U-73122, 100 μM 5-HT and 10 μM ionomycin (IONO; n=7 cells). The specific drugs were applied during the period indicated by horizontal bars; where no bar appears, the cells were perfused with *Helisoma* saline (HS).

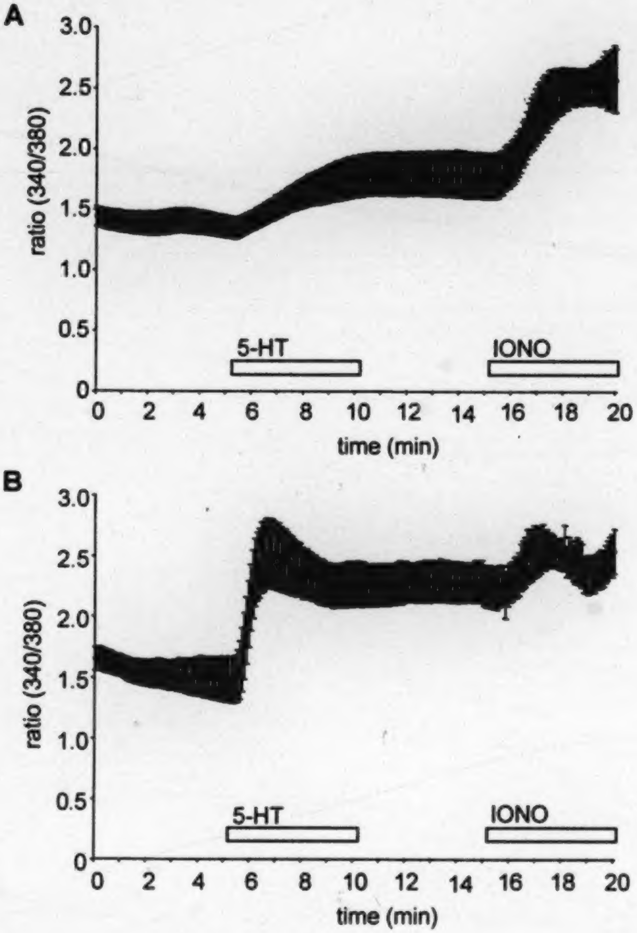

Figure 23. Effect of 5-HT and ionomycin on the intracellular Ca^{2+} concentration. Ciliary cells microinjected with fura-2 salt were imaged every five seconds in the presence of HS, 100 µM 5-HT, or 10 µM ionomycin (IONO). A. Averaged response demonstrating a gradual rise in the 340/380 ratio over the course of 5-HT application (n=5 cells). B. Averaged response showing an early peak in the 340/380 ratio followed by a sustained plateau (n=6 cells). The specific drugs were applied during the period indicated by horizontal bars; where no bar appears, the cells were perfused with *Helisoma* saline (HS).

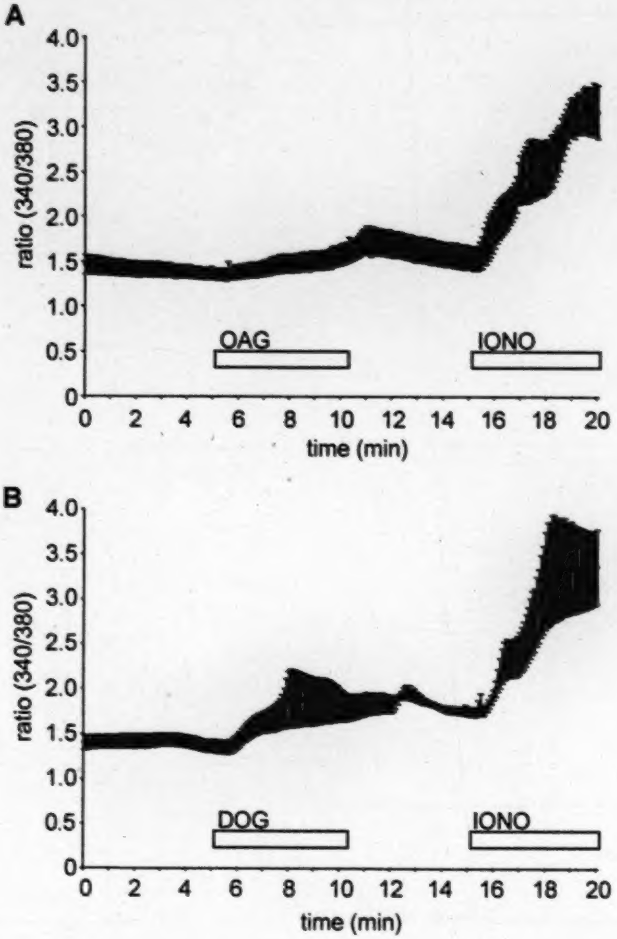

Figure 24. Effect of DAG analogs and ionomycin on the intracellular Ca^{2+} concentration. A. Change in the 340/380 ratio for cells exposed to 100 μM 1-Oleoyl-2-acetyl-*sn*-glycerol (OAG; n= 7 cells) and, following OAG washout, 10 μM ionomycin (IONO). B. Change in the 340/380 ratio for cells exposed to100 μM1,2-Dioctanoyl-*sn*-glycerol (DOG; n= 6 cells) and, following DOG washout, 10 μM ionomycin . The specific drugs were applied during the period indicated by the horizontal bars; where no bar appears the cells were perfused with *Helisoma* saline (HS).

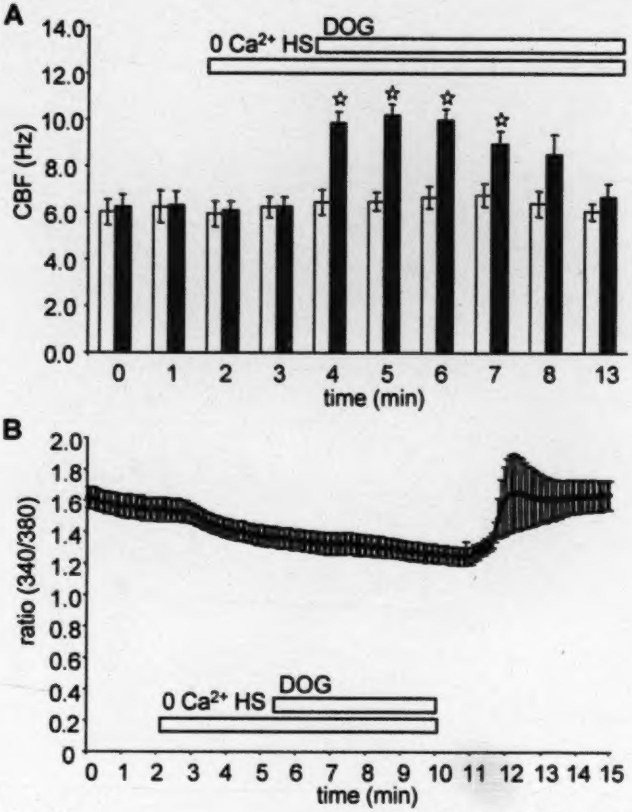

Figure 25. Effect of removing extracellular Ca^{2+} on CBF and $[Ca^{2+}]_i$ responses to DOG. A. Ciliary cells exposed to 0 Ca^{2+} *Helisoma saline* (HS) for two minutes prior to 100 μM 1,2-Dioctanoyl-*sn*-glycerol (DOG) application did not exhibit any change in CBF (white bars; n= 6 cells). Control cells bathed in regular HS showed a significant increase in CBF in response to DOG that lasted four minutes (grey bars; stars: $p < 0.05$; n= 5 cells). B. The average change in the 340/380 ratio in response to 100 μM DOG application when 0 Ca^{2+} HS was introduced three minutes prior (n= 6 cells). The specific treatments were applied during the period indicated by horizontal bars; where no bar appears, the cells were perfused with HS.

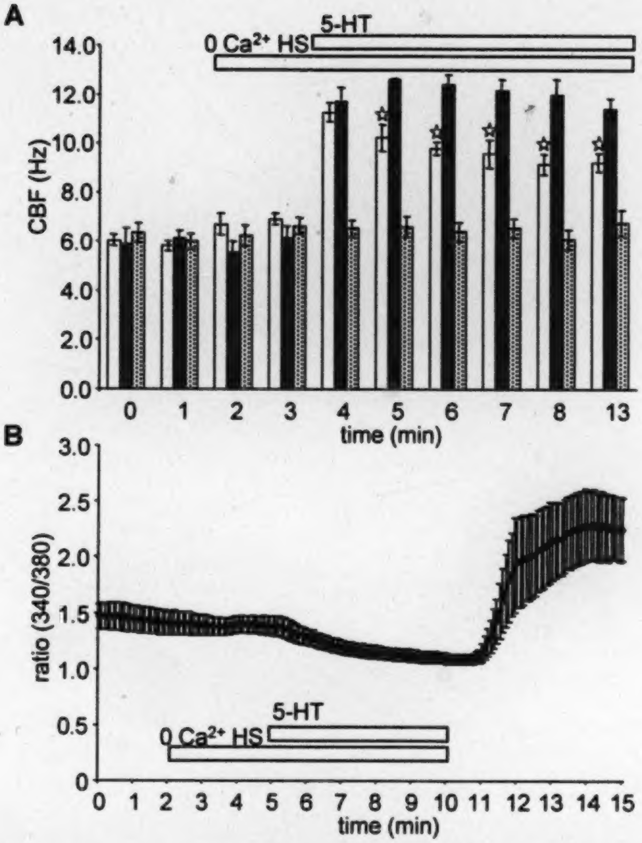

Figure 26. Effect of removing extracellular Ca^{2+} on CBF and $[Ca^{2+}]_i$ responses to 5-HT. A. Ciliary cells exposed to 0 Ca^{2+} *Helisoma saline* (HS) for two minutes prior to 100 μM 5-HT application demonstrated a significant increase in CBF that declined to an elevated plateau (white bars; $p < 0.05$; n= 5 cells). Ciliary cells bathed in HS prior to 100 μM 5-HT application demonstrated a significant increase in CBF that was maintained over the time points examined (grey bars; $p < 0.05$; n= 4 cells). Stars indicate a significance difference between ciliary cells exposed to 5-HT in the presence and absence of extracellular Ca^{2+}. Ciliary cells maintained in 0 Ca^{2+} HS over the time course examined demonstrated a constant basal CBF (dotted bars; n= 5 cells). B. The average change in the 340/380 ratio in response to 100 μM 5-HT when 0 Ca^{2+} HS was introduced three minutes prior (n= 6 cells). The specific treatments were applied during the period indicated by horizontal bars; where no bar appears, the cells were perfused with HS.

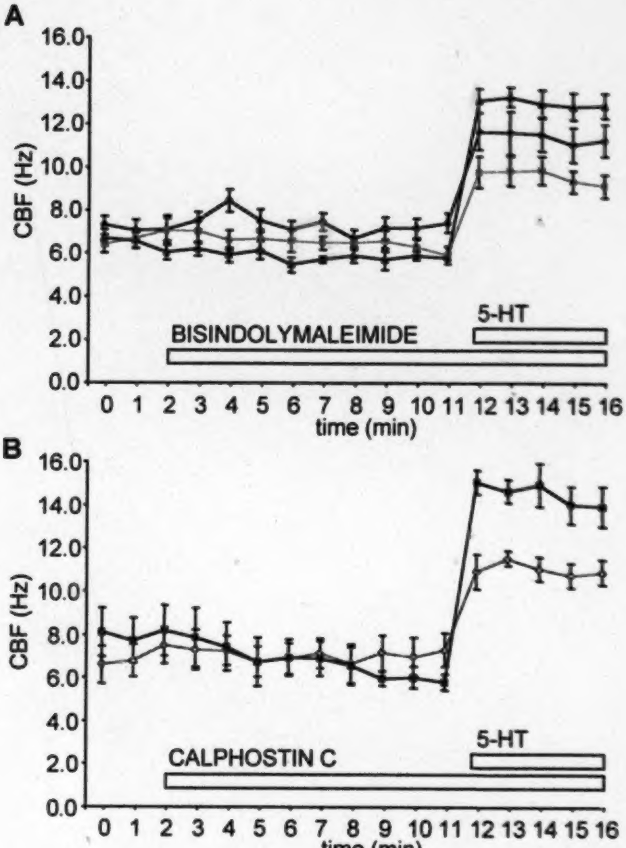

Figure 27. Effect of PKC inhibitors on the CBF response to 5-HT. A. CBF response to 10 nM (grey squares; n= 7 cells) and 100 nM (open diamonds; n= 7 cells) Bisindolylmaleimide application ten minutes prior to 5-HT (100 µM) stimulation. Only the 10 nM dose of Bisindolylmaleimide caused a significant reduction ($p < 0.05$ at all time points) versus non-inhibited controls (black triangles; n= 5 cells). B. 10 nM Calphostin C caused a significant inhibition in the 5-HT-stimulated increase in CBF (open grey diamonds; $p < 0.05$ at all time points; n= 5 cells) versus non-inhibited controls (black squares; n= 4 cells). Duration of drug application is indicated by horizontal bars.

Figure 28. Effect of PKC inhibitors on the $[Ca^{2+}]_i$ response to 5-HT. A. Representative trace showing the change in the 340/380 ratio in response to 100 µM 5-HT and 10 µM ionomycin (IONO). B. Representative trace showing the change in the 340/380 ratio in response to 100 µM 5-HT in the presence of 10 nM Calcphostin C (CAL C), followed by the response to 10 µM ionomycin. C. Representative trace showing the change in the 340/380 ratio in response to 100 µM 5-HT in the presence of 10 nM Bisindolylmaleimide (BIS), followed by the response to 10 µM ionomycin. D. Representative trace showing the change in the 340/380 ratio in response to 100 µM 5-HT in the presence of 100 nM Bisindolylmaleimide followed by the response to10 µM ionomycin. The specific treatments were applied during the period indicated by horizontal bars; where no bar appears, the cells were perfused with *Helisoma* saline (HS). Arrows in B, C, and D indicate the small transient increase in $[Ca^{2+}]_i$ that reliably occurred at onset of exposure to PKC inhibitor. E. The normalized changes in the 340/380 ratio for each of the four treatments at the start of inhibitor perfusion (4 min) and at the peak of the 5-HT response. In the presence of 10 nM Calphostin C (grey bars; n= 7 cells), 10 nM Bisindolylmaleimide (dotted bars; n= 7 cells) and 100 nM Bisindolylmaleimide (plaid bars; n= 7 cells), 5-HT caused increases in the 340/380 ratios that were not significantly different ($p > 0.05$) from the corresponding 5-HT response in the absence of inhibitor control (black bars; n= 6 cells).

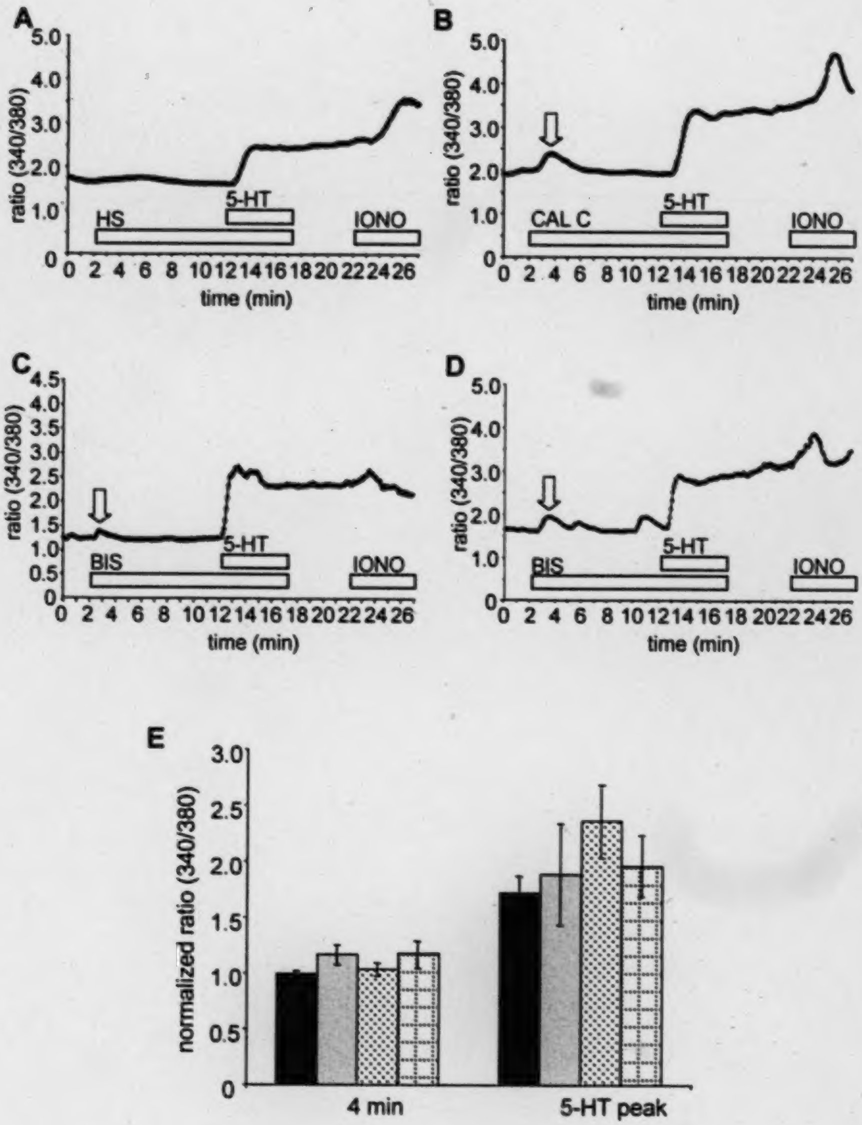
A
5.0
4.0
3.0
2.0
1.0
0
ratio (340/380)
HS
5-HT
IONO
0 2 4 6 8 10 12 14 16 18 20 22 24 26
time (min)
B
5.0
4.0
3.0
2.0
1.0
0
ratio (340/380)
CAL C
5-HT
IONO
0 2 4 6 8 10 12 14 16 18 20 22 24 26
time (min)
C
4.5
4.0
3.5
3.0
2.5
2.0
1.5
1.0
0.5
0
ratio (340/380)
BIS
5-HT
IONO
0 2 4 6 8 10 12 14 16 18 20 22 24 26
time (min)
D
5.0
4.0
3.0
2.0
1.0
0
ratio (340/380)
BIS
5-HT
IONO
0 2 4 6 8 10 12 14 16 18 20 22 24 26
time (min)
E
3.0
2.5
2.0
1.5
1.0
0.5
0
normalized ratio (340/380)
4 min
5-HT peak

3 The involvement of intracellular Ca^{2+} stores in the excitatory response to 5-HT in pedal ciliary cells[5]

After establishing that an increase in $[Ca^{2+}]_i$ is necessary for 5-HT stimulation of ciliary beating (Figure 20), and that 5-HT can alter CBF in the absence of extracellular Ca^{2+} (Figure 26A), it became apparent that sources of intracellular Ca^{2+} participate in the ciliary response to 5-HT. Using pharmacological manipulations on different intracellular Ca^{2+} stores, I examine the role of intracellular stores in 5-HT-stimulated ciliary beating of pedal ciliary cells. Considering the number and prominent location of mitochondria adjacent to ciliary structures within pedal ciliary cells (Figure 9), it was hypothesized that this organelle actively participates in Ca^{2+} homeostasis to regulate ciliary activity. Additionally, some of the functionally distinct stores of the ER were examined for their involvement in ciliary beating and the ciliary response to 5-HT.

3.1 Mitochondrial involvement in Ca^{2+} regulation during 5-HT stimulation of pedal ciliary cells

To begin to examine the possible involvement of mitochondria in 5-HT-stimulated ciliary beating, ciliary cells were pretreated with the protonophore CCCP before 5-HT stimulation. CCCP uncouples electron transport in the respiratory chain from H^+ pumping and thereby collapses the proton-motive force within the mitochondria, indirectly decreasing the activity of the mitochondrial Ca^{2+} uniporter (Rizzuto *et al.*, 2000; Ganitkevich, 2003). Whereas 100 μM 5-HT produced a robust increase in CBF in control cells, a ten minute pretreatment with 10 μM CCCP caused a significant reduction in the response to 5-HT (Figure 29A; $p < 0.05$). Interestingly, within the first minute of exposure to 10 μM CCCP, ciliary cells reliably exhibited a significant reduction in CBF versus the resting rate of ciliary beating (Figure 29; $p < 0.05$). The CBF usually returned to the resting level within the second minute of exposure to the drug. To determine if the loss of the ciliary response to 5-HT was due to a disruption of ATP production within the mitochondria rather than an effect on Ca^{2+}, the Ca^{2+} ionophore ionomycin was used to test whether the cells retained the ability to produce an elevation in CBF in the presence of CCCP. Under control conditions, application of 10 μM ionomycin produced a doubling in the rate of ciliary beating (Figure 29B). In the presence of 10 μM CCCP, 10 μM ionomycin still produced a significant increase in CBF ($p < 0.05$), although the amplitude of this response was attenuated (Figure 29B). These data suggest that mitochondrial regulation of Ca^{2+} may be involved in the ciliary response to 5-HT.

To further test for mitochondrial involvement, the ruthenium compounds ruthenium red and Ru360 were used to directly inhibit mitochondrial Ca^{2+} uptake through the Ca^{2+} uniporter. Both of these substances have been demonstrated to significantly reduce Ca^{2+} uptake into mitochondria (Zhou and Bers, 2002; Bruce *et al.*, 2004). Given that ruthenium red is known to have some nonspecific effects (Kargacin *et al.*, 1998), whereas the derivative Ru360 is a more specific inhibitor of mitochondrial uptake (Matlib *et al.*, 1998), both drugs were tested. A 30 minute pretreatment with 50 μM ruthenium red did not alter either basal ciliary beating or the response to 100 μM 5-HT, as compared with control cells maintained in HS (Figure 30A). Similarly, a 30 minute pretreatment with 10 μM Ru360 did not affect basal ciliary beating or the ciliary response to 100 μM 5-HT (Figure 30B). In contrast to the findings using CCCP, these results do not implicate Ca^{2+} regulation via the mitochondrial uniporter in the ciliary response to 5-HT. However, since the ruthenium compounds have difficulty permeating the plasma membrane in some systems (Jacobson and Duchen, 2004), further experiments are required to positively establish a role for mitochondria in the ciliary response to 5-HT.

3.2 Effect of thapsigargin-sensitive intracellular stores and the IP_3 receptor pathway in the ciliary response to 5-HT

The ER is the most recognized and best studied intracellular Ca^{2+} store. Therefore, to further define the role played by intracellular Ca^{2+} stores in ciliary activity, different stores of the ER were examined pharmacologically. As evidence suggests that thapsigargin alters Ca^{2+} sequestration through SERCA pumps in IP_3-sensitive stores (Thastrup *et al.*, 1990), results from experiments that pharmacologically manipulate the SERCA pump and the IP_3 receptor are presented together. Thapsigargin is a sesquiterpene lactone that inhibits all known isoforms of the SERCA pump and thereby produces an increase in cytosolic Ca^{2+} as the high concentration of Ca^{2+} within the ER leaks into the cytoplasm (Lytton *et al.*, 1991). In fact, a long duration pretreatment with thapsigargin is believed to deplete thapsigargin-sensitive Ca^{2+} stores.

Application of 1.0 μM thapsigargin produced a rapid, significant increase in the rate of ciliary beating in pedal ciliary cells that began to decline after four minutes in thapsigargin (Figure 31A; $p < 0.05$). The rate of ciliary beating returned to basal values at approximately 50 min (Figure 31A). A 30 min pretreatment with 1.0 μM thapsigargin prior to exposure to 100 μM 5-HT produced a ciliary response to 5-HT that was significantly higher than the CBF response of control cells (Figure 31B; $p < 0.05$). The CBF of control cells maintained in HS and then exposed to 5-HT for five minutes was 12.35 ± 0.34 Hz, whereas the CBF of cells exposed to thapsigargin prior to 5-HT application was 15.63 ± 0.55 Hz. In contrast to the 30 min pretreatment, thapsigargin treatment of cells for 60 min prior to 5-HT application caused no facilitation of the 5-HT response, nor did it diminish the 5-HT response (Figure 31C). The CBF of control cells maintained in HS and then exposed to 5-HT for five minutes was 12.53 ± 0.29 Hz and the CBF of cells pretreated with thapsigargin and exposed to 5-HT was 12.87 ± 0.28 Hz. To confirm that thapsigargin was indeed producing a change in intracellular $[Ca^{2+}]_i$, pedal cells loaded with fura-2 were imaged during a 60 min perfusion with 1.0 μM thapsigargin followed by a five minute application of 100 μM 5-HT. Thapsigargin produced a modest, sustained rise in the 340/380 ratio, whereas the application of 5-HT produced a large increase in the 340/380 ratio (Figure 32). Taken together, these data suggest that thapsigargin can induce an increase in $[Ca^{2+}]_i$ with an associated rise in CBF, but that the intracellular stores that mediate the ciliary response to 5-HT are thapsigargin-insensitive.

One of the most important signaling molecules that triggers Ca^{2+} release from stores on the ER is IP_3. Given the finding that the PLC signaling pathway is involved in the ciliary response to 5-HT (Figure 21), it was hypothesized that IP_3, one of the downstream products of PLC activity, is involved in triggering Ca^{2+} release in response to 5-HT. Ten minute pretreatment of 1.0 µM xestospongin C, a non-competitive inhibitor of IP_3-mediated Ca^{2+} release, did not affect basal CBF nor did it significantly alter the 5-HT-induced increase in CBF versus vehicle controls, with the exception of the 13 minute time point (Figure 33). This finding indicates that IP_3-mediated Ca^{2+} release does not participate in the signaling pathway underlying 5-HT-stimulated cilio-excitation.

3.3 Involvement of caffeine-sensitive stores in ciliary activity

Given the apparent lack of involvement of thapsigargin-sensitive stores and the related IP_3 receptor signaling pathway in the ciliary response to 5-HT, other ER Ca^{2+} stores were examined. In addition to having other cellular affects, caffeine is a stimulator of intracellular Ca^{2+} release most likely through the activation of ryanodine receptor channels (Sitsapesan *et al.*, 1995). Application of 10 mM caffeine produced an increase in CBF that was indistinguishable from that induced by 100 µM 5-HT (Figure 34).

To account for the reported action of caffeine as a PDE inhibitor (Camello *et al.*, 1996), the effect of altering cyclic nucleotide signaling was examined. In the presence of the PDE inhibitor IBMX (100 µM), the rate of ciliary beating increased from 6.34 ± 0.14 Hz to 11.49 ± 0.69 Hz within one minute, remained elevated for five minutes, and then began a gradual decline (Figure 35A). Previous work has suggested that this stimulatory effect of IBMX may result from increased levels of cGMP, as opposed to cAMP (Christopher *et al.*, 1996; Doran *et al.*, 2003). To confirm this, the adenylate cyclase activator forskolin was applied to pedal ciliary cells. Application of 10 µM forskolin did not alter the rate of ciliary beating over ten minutes (Figure 35B), suggesting that cAMP is not participating in the cilio-excitatory response. To determine if the stimulatory effect of caffeine was mediated by increased cGMP levels resulting from PDE inhibition, the effect of caffeine was examined in the presence of the sGC inhibitor LY83583. A ten minute pretreatment with 10 μM LY83583 did not alter basal ciliary beating, nor did it significantly change the initial CBF response to 10 mM caffeine (Figure 35C). Interestingly, the caffeine-stimulated increase in ciliary beating decayed more rapidly in the presence of LY 83583, as compared to control cells (Figure 35C). These data indicate that caffeine has a stimulatory effect on the rate of ciliary beating that does not appear to initially rely on the PDE inhibitory action of caffeine.

To determine whether a caffeine-sensitive store mediates the cilio-excitatory response to 5-HT, the same experimental design used with the thapsigargin depletion experiments was adopted. A 60 minute pretreatment with 10 mM caffeine was used to empty caffeine-sensitive stores prior to application of 5-HT. 10 mM caffeine stimulated a rapid increase in CBF that declined to basal levels after 60 min. Ciliary cells maintained in HS for 60 min demonstrated a significant increase in CBF from 6.50 ± 0.23 Hz to 13.44 ± 0.41 Hz in response to 100 μM 5-HT ($p < 0.05$). In contrast, the CBF of ciliary cells incubated in 10 mM caffeine for 60 min did not significantly respond to 100 μM 5-HT, as CBF increased from 7.05 ± 0.50 Hz to 8.06 ± 0.75 Hz (Figure 36). This result implicates a caffeine-sensitive store in the cilio-excitatory response to 5-HT.

3.4 Involvement of ryanodine-sensitive stores

Ryanodine-sensitive Ca^{2+} stores are thought to be functionally and spatially distinct from IP_3 stores and are a target of caffeine action (Pizzo *et al.*, 1997; Pozzan *et al.*, 1994). Given that the experiments described above implicated a caffeine-sensitive store in the cilio-excitatory response, activation and inhibition of ryanodine receptors were examined. Ryanodine is believed to produce dose-dependent differential responses on ryanodine receptors; at micromolar concentrations ryanodine blocks all three of the ryanodine receptor isoforms, whereas nanomolar concentrations of ryanodine activate the receptor by stabilizing it in a conductance state (Ehrlich *et al.*, 1994; Johnson and Chang, 2000). While 100 μM 5-HT produced a robust increase in CBF, application of 10 nM ryanodine, normally an activating dose, had no effect on CBF (Figure 37). To further examine the role of the ryanodine-sensitive stores in the response to 5-HT, both an inhibitory dose of ryanodine and the ryanodine receptor antagonist dantrolene were used. Ten minute application of 10 μM ryanodine did not alter the CBF response to 100 μM 5-HT, as compared with vehicle control cells (Figure 38A). Interestingly, this dose of ryanodine did produce a transient, non-significant rise in CBF during the first four minutes of drug application. A similar finding was seen when dantrolene was used to pretreat pedal ciliary cells. Ten minute pretreatment with 50 μM dantrolene did not alter the CBF response to 100 μM 5-HT observed in vehicle control cells; however, the dantrolene treatment did not stimulate the transient rise in CBF that occurred in response to 10 μM ryanodine (Figure 38B).

Finally to confirm that caffeine effects were independent of a ryanodine-sensitive store, the ability of ryanodine to inhibit the cilio-excitatory effect of caffeine was examined. The change in CBF stimulated by 10 mM caffeine in ciliary cells pretreated with 10 μM ryanodine was indistinguishable from the caffeine-induced increase in CBF in control cells maintained in HS (Figure 39). Once again, this dose of ryanodine did produce a transient, non-significant rise in the rate of basal ciliary beating over the first few minutes of drug application. Taken together these findings support that conclusion that the cilio-excitatory response to 5-HT is mediated by Ca^{2+} released from a caffeine-sensitive, ryanodine-insensitive intracellular Ca^{2+} store.

Figure 29. Effect of carbonyl cyanide *m*-chlorophenylhydrazone (CCCP) on stimulated ciliary beating. A. Pretreatment with CCCP (10 μM) significantly reduced the cilio-excitatory effect of 100 μM 5-HT (open squares, n = 6 cells; $p < 0.05$) as compared with control cells that were pretreated with DMSO (closed triangles, n = 5 cells). B. The Ca^{2+} ionophore, ionomycin (IONO; 10 μM), stimulated a significant increase in CBF when pretreated with DMSO (closed triangles, n = 4 cells; $p < 0.05$). Pretreatment with CCCP (10 μM) caused a partial reduction of the cilio-excitatory effect of 10 μM ionomycin, however ionomycin still produced a significant increase in CBF (open squares, n = 5 cells; $p < 0.05$). Duration of drug application is indicated by horizontal bars.

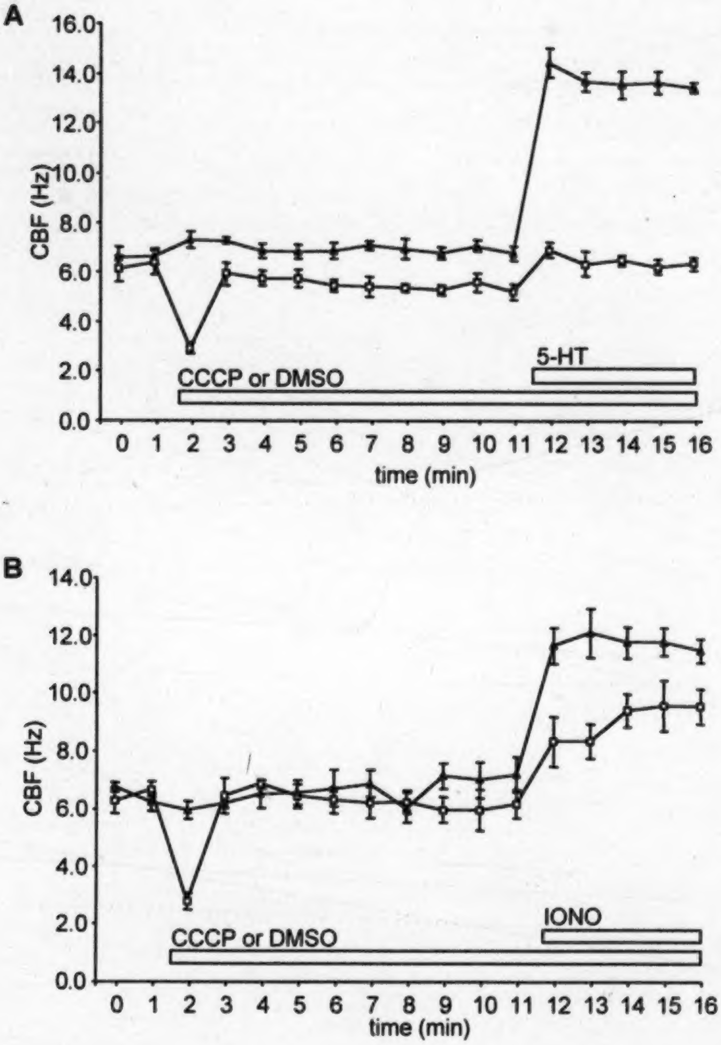
A
16.0
14.0
12.0
10.0
8.0
6.0
4.0
2.0
0.0
CBF (Hz)
5-HT
CCCP or DMSO
0 1 2 3 4 5 6 7 8 9 10 11 12 13 14 15 16
time (min)
B
14.0
12.0
10.0
8.0
6.0
4.0
2.0
0.0
CBF (Hz)
IONO
CCCP or DMSO
0 1 2 3 4 5 6 7 8 9 10 11 12 13 14 15 16
time (min)

Figure 30. Effect of ruthenium compounds on stimulated ciliary beating. A. 30 min pretreatment with 50 µM ruthenium red, which blocks transmembrane Ca^{2+} fluxes, did not cause a significant change in the CBF response to 100 µM 5-HT (light bars, n = 6 cells), as compared with control cells pretreated with HS (dark bars, n = 5 cells). B. Similarly, 30 min pretreatment with10 µM Ru360, which specifically blocks Ca^{2+}uptake into the mitochondria, did not significantly change the CBF response to 100 µM 5-HT (light bars, n = 7 cells) when compared with control cells within HS (dark bars, n = 5 cells). Duration of drug applications are indicated by horizontal bars.

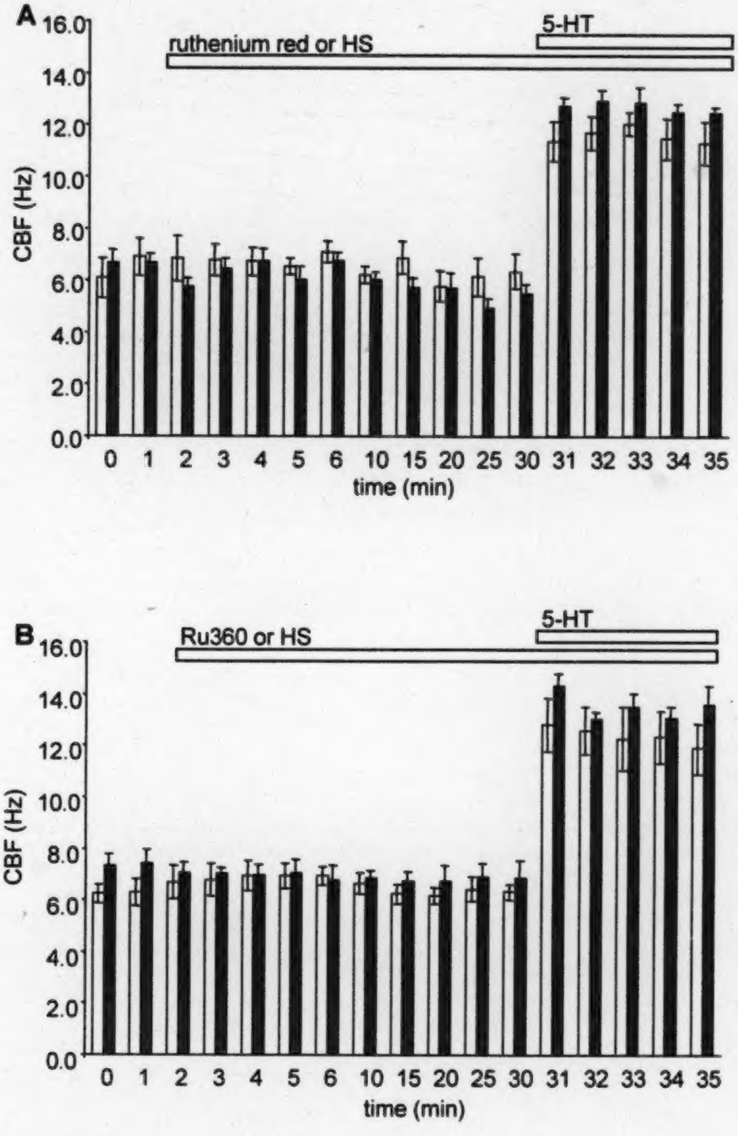
A
16.0
14.0
12.0
10.0
8.0
6.0
4.0
2.0
0.0
CBF (Hz)
ruthenium red or HS
5-HT
0 1 2 3 4 5 6 10 15 20 25 30 31 32 33 34 35
time (min)
B
16.0
14.0
12.0
10.0
8.0
6.0
4.0
2.0
0.0
CBF (Hz)
Ru360 or HS
5-HT
0 1 2 3 4 5 6 10 15 20 25 30 31 32 33 34 35
time (min)

Figure 31. Effect of thapsigargin on ciliary beating in pedal cilia. A. Application of 1.0 μM thapsigargin produced a significant peak and plateau increase in the rate of ciliary beating (n = 5 cells, $p < 0.05$), with the CBF remaining returning to basal at approximately 50 min. B. 30 min preincubation with 1.0 μM thapsigargin produced a significant increase in the ciliary beat response to 100 μM 5-HT(light bars, n= 5 cells; $p < 0.05$), as compared to control cells maintained in HS before treatment with 100 μM 5-HT (dark bars, n = 5 cells). C. 60 min pretreatment with 1.0 μM thapsigargin did not alter the ciliary beat response to 100 μM 5-HT (light bars, n = 5 cells), as compared to the response of control cells maintained in HS (dark bars, n = 5 cells). Duration of drug applications are indicated by horizontal bars.

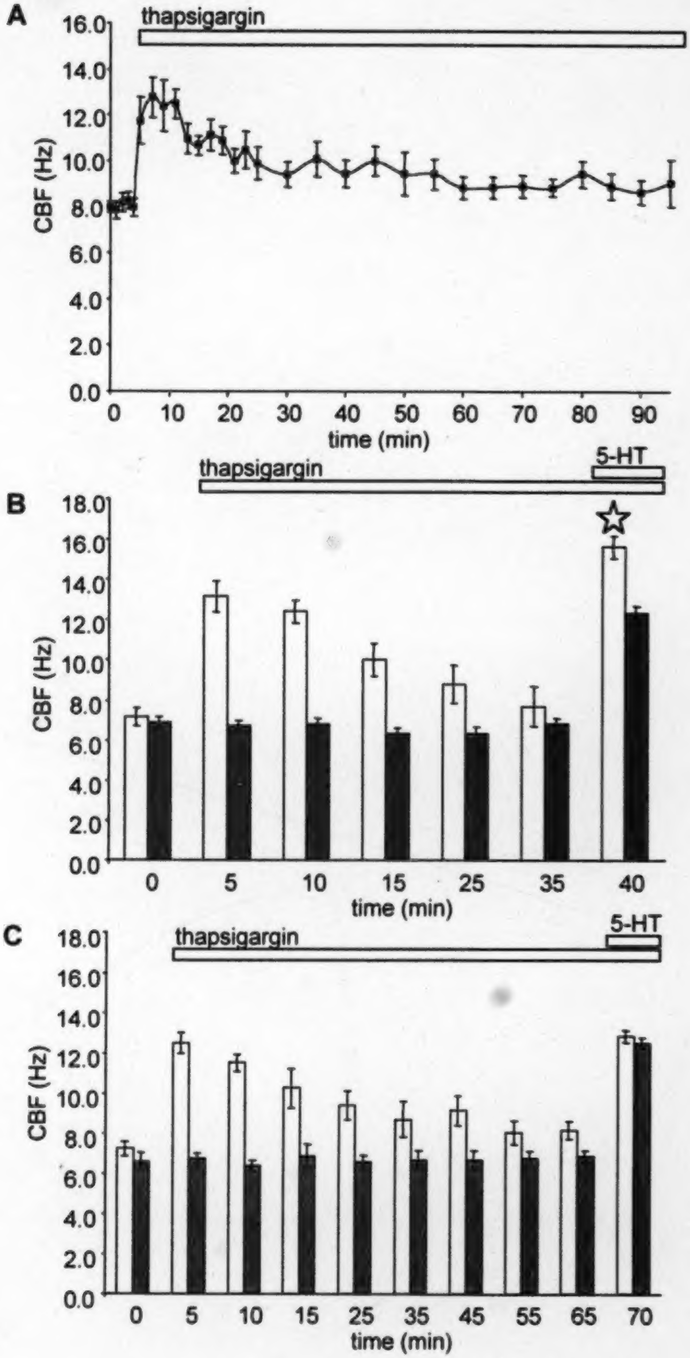
A
thapsigargin
CBF (Hz)
16.0
14.0
12.0
10.0
8.0
6.0
4.0
2.0
0.0
0
10
20
30
40
50
60
70
80
90
time (min)
B
thapsigargin
5-HT
☆
CBF (Hz)
18.0
16.0
14.0
12.0
10.0
8.0
6.0
4.0
2.0
0.0
0
5
10
15
25
35
40
time (min)
C
thapsigargin
5-HT
CBF (Hz)
18.0
16.0
14.0
12.0
10.0
8.0
6.0
4.0
2.0
0.0
0
5
10
15
25
35
45
55
65
70
time (min)

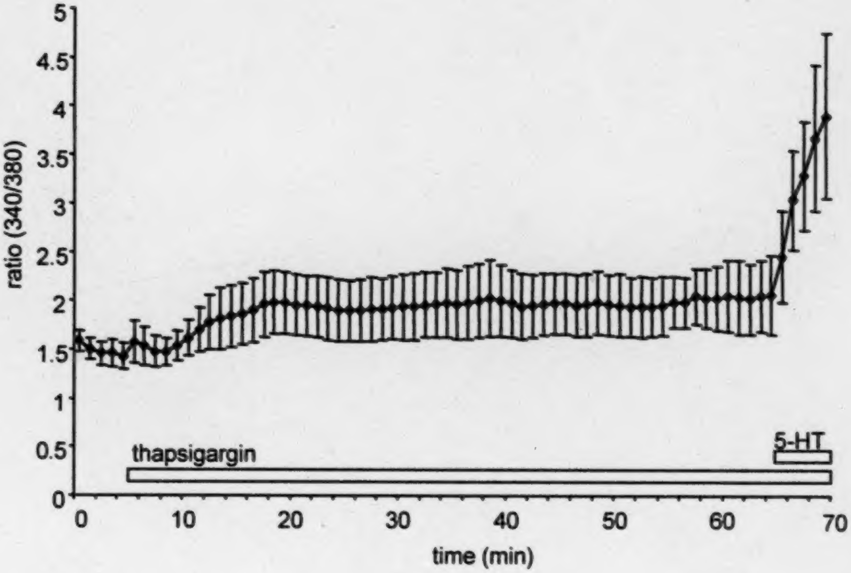

Figure 32. Effect of thapsigargin on intracellular Ca^{2+}. 60 min treatment with 1.0 μM thapsigargin caused a sustained increase in $[Ca^{2+}]_i$ that did not prevent 100 μM 5-HT from producing an additional increase in $[Ca^{2+}]_i$ (n = 5 cells). Duration of drug applications are indicated by horizontal bars.

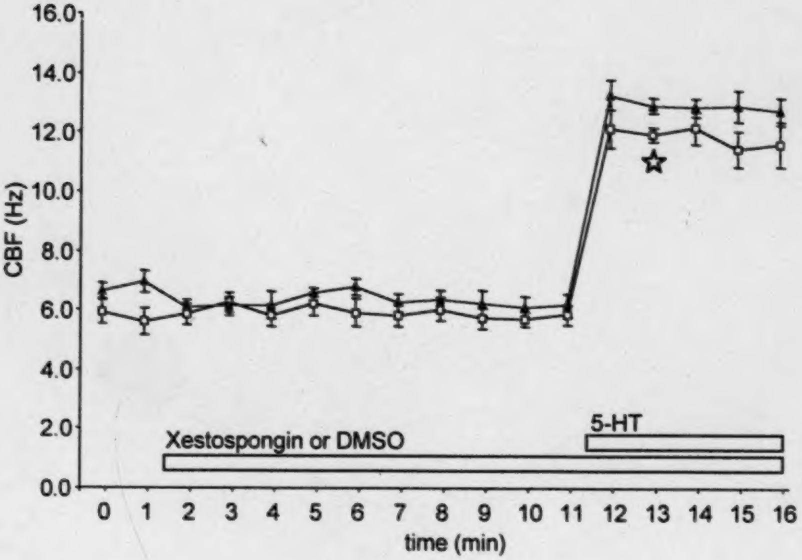

Figure 33. Effect of xestospongin C on stimulated cliary beating. Pretreatment with 1.0 µM xestospongin C, a membrane-permeable blocker of IP_3 mediated Ca^{2+} release, did not significantly affect the 5-HT-induced increase in CBF (open squares, n = 7 cells) versus control cells exposed to the vehicle DMSO (closed triangles, n = 5 cells), with the exception of the 13 minute time point. Star indicates significance versus the DMSO control at the same time point ($p < 0.05$). Duration of drug applications are indicated by horizontal bars.

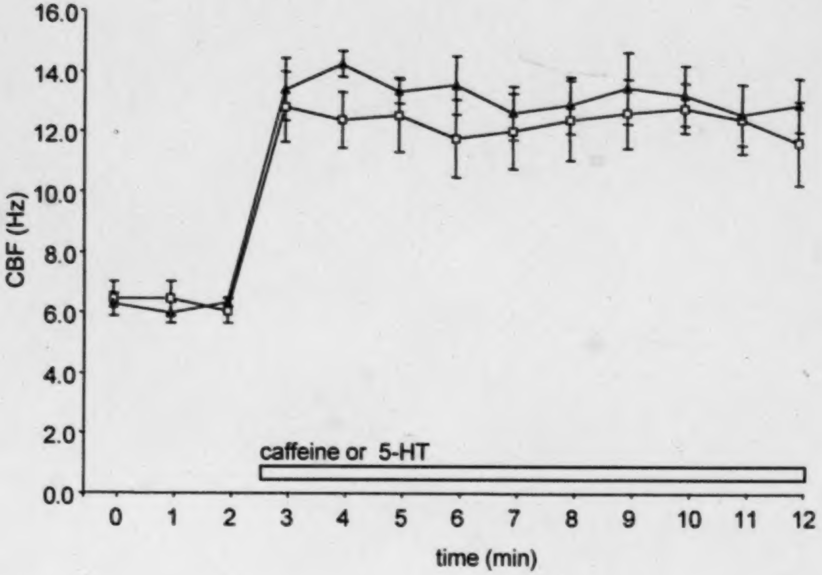

Figure 34. Effect of caffeine and 5-HT on ciliary beating. Treatment with 10 mM caffeine (open squares, n = 7 cells) caused a significant increase in CBF ($p < 0.05$) that did not differ significantly from the effect of 100 μM 5-HT (closed triangles, n = 5 cells). The duration of the specified drug is indicated by the horizontal bar.

Figure 35. The effect of altering cyclic nucleotide signaling on ciliary beating. A. Application of the phosphodiesterase inhibitor IBMX (100 µM) caused a significant increase in CBF (open squares, n = 6 cells, $p < 0.05$) versus control cells maintained in HS (closed triangles, n = 4 cells). B. Application of the adenylate cyclase activator, forskolin (10 µM) did not produce a change in the rate of ciliary beating (n = 5 cells). C. 10 min pretreatment with the soluble guanylate cyclase inhibitor LY83583 (10 µM) did not significantly change the CBF response to 10 mM caffeine (open square, n = 6 cells), versus control cells maintained in HS prior to caffeine (10 mM) application (closed triangles, n = 5 cells). Duration of drug applications are indicated by horizontal bars.

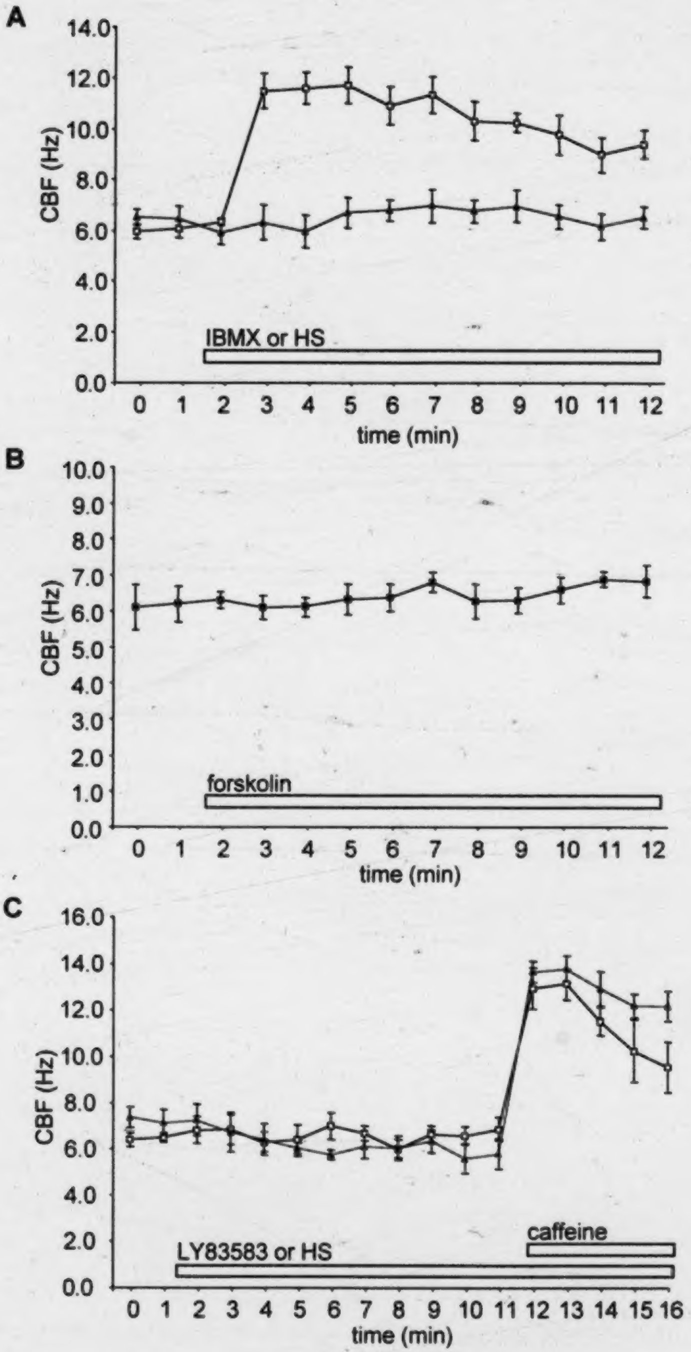
A
CBF (Hz)
14.0
12.0
10.0
8.0
6.0
4.0
2.0
0.0
IBMX or HS
0 1 2 3 4 5 6 7 8 9 10 11 12
time (min)
B
CBF (Hz)
10.0
9.0
8.0
7.0
6.0
5.0
4.0
3.0
2.0
1.0
0.0
forskolin
0 1 2 3 4 5 6 7 8 9 10 11 12
time (min)
C
CBF (Hz)
16.0
14.0
12.0
10.0
8.0
6.0
4.0
2.0
0.0
caffeine
LY83583 or HS
0 1 2 3 4 5 6 7 8 9 10 11 12 13 14 15 16
time (min)

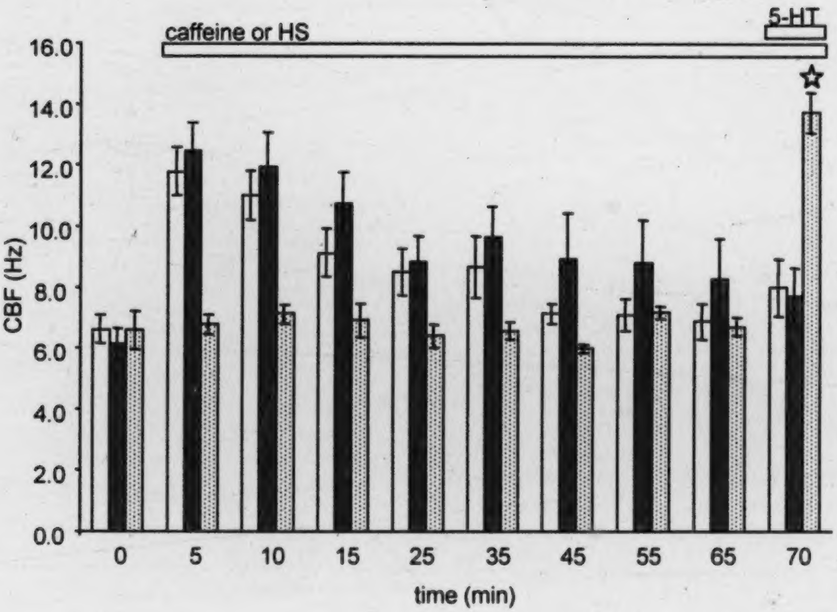

Figure 36. Effect of caffeine pretreatment on 5-HT-stimulated ciliary beating. 60 min exposure to 10 mM caffeine abolished the 100 μM 5-HT-induced increase in CBF (light bars; n = 6 cells), as compared with control cells maintained in HS for 60 min prior to 5-HT application (dotted bars; n = 5 cells). Exposure to caffeine alone caused an increase in CBF that returned to basal after 60 min (dark bars; n = 5 cells). Star indicates significance between the treatments at that time point ($p < 0.05$). Duration of drug applications are indicated by horizontal bars.

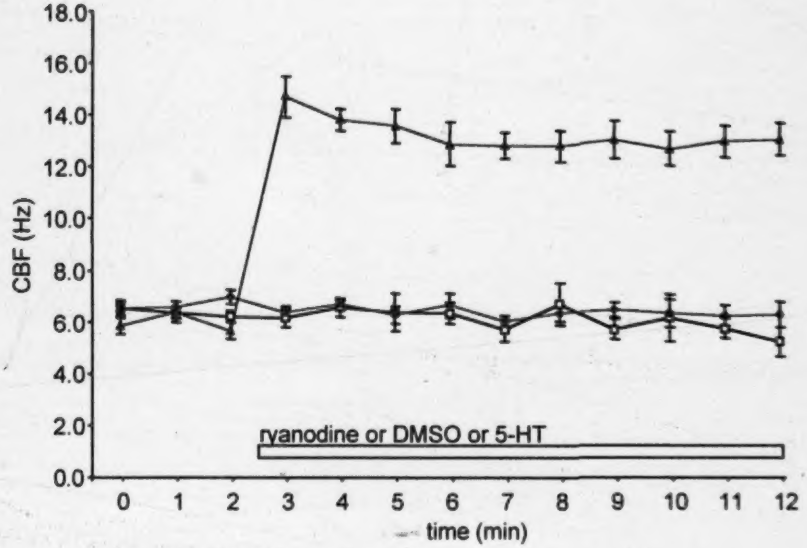

Figure 37. Effect of a stimulatory dose of ryanodine on ciliary beating. Treatment with 10 nM ryanodine, a dose thought to stimulate ryanodine receptors, did not stimulate a change in CBF (open squares, n = 5 cells), nor did the DMSO control (closed diamonds, n = 4 cells). In contrast, 100 µM 5-HT caused a significant increase in CBF (closed triangles, n = 4 cells; $p < 0.05$). Duration of the specified drug application is indicated by the horizontal bar.

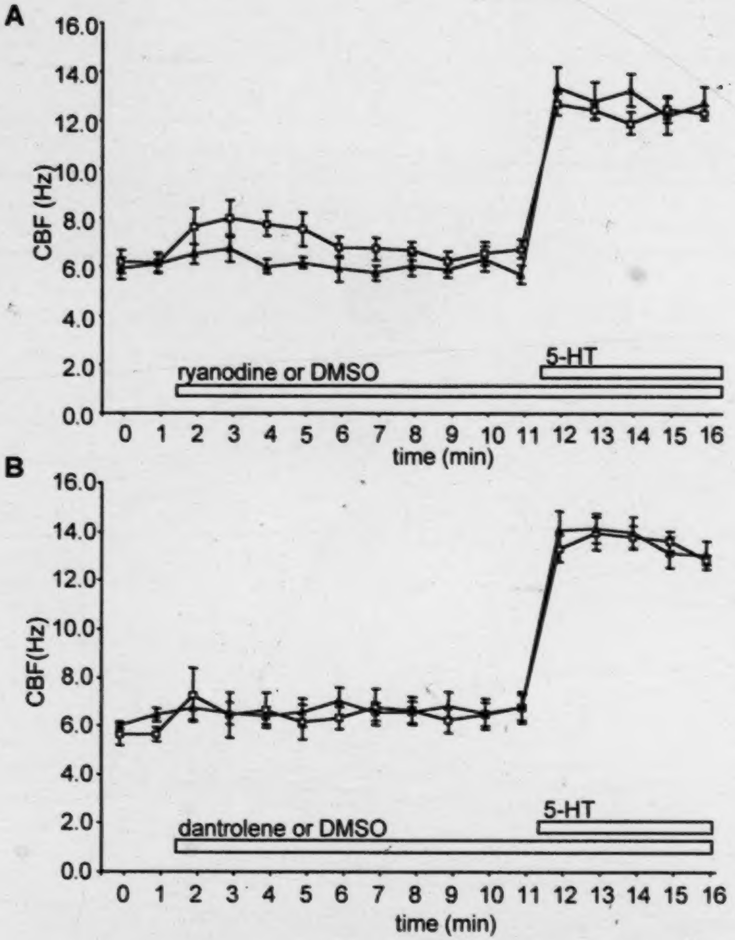

Figure 38. Effect of ryanodine receptor inhibition on stimulated ciliary beating. A. Pretreatment with 10 μM ryanodine, a dose believed to inhibit ryanodine channels, did not significantly affect the cilio-excitatory effect of 100 μM 5-HT (open squares, n = 7 cells), as compared with control cells pretreated with DMSO (closed triangles, n = 5 cells). B. Pretreatment with 50 μM dantrolene, a ryanodine receptor inhibitor, did not significantly affect the 5-HT-induced (100 μM) increase in CBF (open squares; n = 5 cells) as compared with cells treated with DMSO (closed triangles, n = 5 cells). Duration of drug applications are indicated by horizontal bars.

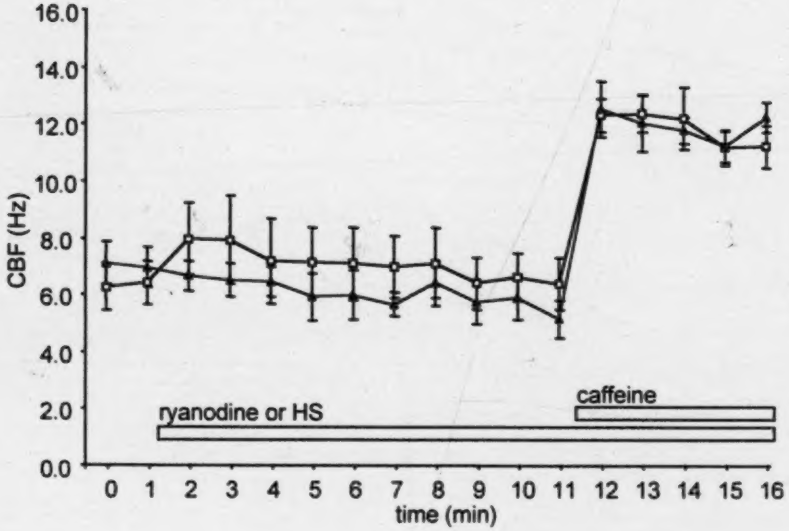

Figure 39. Effect of ryanodine pretreatment on caffeine-stimulated ciliary beating. 10 min pretreatment with 10 μM ryanodine did not significantly alter the 10 mM caffeine-induced increase in CBF (open squares, n = 6 cells), as compared with control cells maintained in HS prior (closed triangles, n = 5 cells). Duration of drug applications are indicated by horizontal bars.

DISCUSSION

Ciliary cells are a widespread cell type throughout the biological world. Cilia perform numerous biological functions in protozoans and metazoans alike. In needing to respond to a variety of extracellular cues, the intracellular regulation of ciliary activity appears to require the interaction of many different second messengers and signal transduction cascades. The ciliary cells expressed on the surface of embryos from the snail *Helisoma trivolvis* are highly amenable to study of ciliary regulation at the molecular, cellular and organismal levels. In this thesis, the pedal, dorsolateral and scattered single ciliary cells were characterized morphologically and physiologically. Then, the roles of PKC and Ca^{2+} as signal transduction elements in the cilio-excitatory response to 5-HT were examined in pedal ciliary cells.

1 Identified populations of *Helisoma* ciliary cells

Early in development, *Helisoma* embryos exhibit cilia-driven rotation within the egg capsule that is augmented by hypoxia (Diefenbach et al., 1991; Kuang et al., 2002). It is believed that embryo rotation facilitates mixing of intracapsular fluid to enhance oxygen diffusion into the egg capsule (Kuang et al., 2002; Hunter and Vogel, 1985). The surface of the embryo contains three known subpopulations of ciliary cells: pedal, dorsolateral and SSCCs. Furthermore, ciliary cells are also expressed on the roof of the mouth and further down the gut. The activity of the pedal and dorsolateral ciliary bands is stimulated by 5-HT release from ENC1s, a bilateral pair of sensory-motor neurons (Kuang and Goldberg, 2001). Previous studies on unidentified ciliary cells in culture demonstrated that Ca^{2+} influx and the activity of a unique PKC isoform are signal transduction elements in the cilio-excitatory response to 5-HT (Christopher et al., 1996; 1999). Results presented herein on unidentified ciliary cells in culture demonstrated that only some ciliary cells respond to 5-HT with an elevation in $[Ca^{2+}]$. These heterogeneous cellular responses, as well as structural differences between the subtypes, prompted the development of a new microdissection technique for harvesting and culturing surface ciliary cells of known subtype. Pedal, dorsolateral and SSCCs were removed from the surface of the embryo using a suction micropipette and plated in culture. Findings revealed that pedal and dorsolateral ciliary cells are similar in terms of CBF and cytoplasmic calcium responses to 5-HT, and the distribution of 5-HT receptor proteins. In contrast, the SSCCs neither responded to 5-HT in CBF and calcium imaging experiments, nor did they express 5-HT receptor proteins.

1.1 Mixed populations of *Helisoma* ciliary cells in culture

A wide variety of signal transduction elements have been shown to participate in regulating ciliary beating in the array of organisms examined. However, changes in $[Ca^{2+}]_i$ appear to be a possible universal mechanism in altering CBF. Ca^{2+} regulates ciliary activity in invertebrate systems such as ctenophore larvae (Tamm and Terasaki, 1994), *Paramecium* (Eckert, 1972) and *Mytilus edulis* (Murakami and Machemer, 1982) and in almost all vertebrate systems examined, including the salamander *Necturus maculosus* (Murakami and Eckert, 1971), frog esophagus (Levin et al., 1997), rabbit trachea (Lansley and Sanderson, 1999) and human respiratory epithelium (Di Benedetto et al., 1991). It appears that Ca^{2+} is either required to bind to a Ca^{2+}-binding protein at the level of the cilium or is necessary in the activation of other signal transduction cascades that result in phosphorylation of a target protein within the cilium. Although it has been previously demonstrated that extracellular Ca^{2+} is necessary in stimulated ciliary beating in *Helisoma* ciliary cells (Christopher et al., 1996; 1999), direct imaging of intracellular Ca^{2+} had not been previously performed because embryonic *Helisoma* cells do not readily accept or retain the acetoxymethyl ester indicators (Christopher, 1997). Here, embryonic tissue was loaded using pressure microinjection of fura-2 dextran. An interesting finding from these initial Ca^{2+} imaging experiments on unidentified ciliary cells was that half of those cells examined did not exhibit an increase in Ca^{2+} in response to 5-

HT (Figure 10). Previous experiments on unidentified ciliary cells in culture revealed that a smaller percentage of cells did not exhibit an increase in CBF in response to 5-HT (Christopher et al., 1996). This finding, as well as results from CBF experiments *in vivo* (Kuang and Goldberg, 2001), suggest that the observed variations in the CBF and Ca^{2+} responses from cells in culture may be the result of population differences within the mass dissociated cells in culture. This conclusion was further supported by the electron microscopy analysis of ciliary populations. Thus, in some ciliary subtypes, 5-HT may stimulate ciliary beating without producing a rise in intracellular Ca^{2+}, whereas other subtypes may show no response at all.

The Ca^{2+}-binding protein CaM has been shown in both invertebrates (Nakaoka et al., 1984) and vertebrates (Di Benedetto et al., 1991) to participate in mediating cilio-excitation. Likewise in *Helisoma* ciliary cells, CaM appears to be a necessary component in the cilio-excitatory response to 5-HT, as the Ca^{2+}/CaM dependent enzyme inhibitor calmidazolium inhibited this response in unidentified ciliary cells (Doran *et al.*, 2004). As application of the inhibitor alone had no effect on basal CBF, it appears that CaM is recruited in the 5-HT response but does not contribute to basal ciliary beating. This is consistent with experiments on tracheal ciliary cells from rabbit that suggested that basal ciliary activity is independent of $[Ca^{2+}]_i$ (Ma *et al.*, 2002). This profile of CaM activity may also provide clues about the NOS isoform thought to be expressed in embryonic cilia (Cole et al., 2002). Since NO has been demonstrated to have a constitutive cilio-excitatory action in *Helisoma* ciliary cells (Doran et al, 2003), the ineffectiveness of calmidazolium on basal ciliary beating suggests that embryonic ciliary cells contain a Ca^{2+}/calmodulin-independent isoform of NOS. Whether this isoform is a unique member of the inducible (i) NOS family, or is a novel isoform, remains to be determined.

1.2 Innervated *Helisoma* ciliary cells

The pedal and dorsolateral ciliary bands on the *Helisoma* embryo are innervated by the serotonergic ENC1s (Kuang and Goldberg, 2001; Koss et al., 2003). These postsynaptic ciliary cells exhibit the typical structure of cells containing motile cilia (Figure 9; Sleigh, 1962). This includes a 9x2+2 microtubule arrangement and an extensive primary and accessory rootlet structure in close proximity to numerous mitochondria. These cells also have regions of electron translucent cytoplasm that contain 5-HT-immunoreactive vesicles, thought to be the products of endocytotic 5-HT uptake by postsynaptic ciliary cells (Koss *et al.*, 2003). Taken together, this morphological data supports the conclusion that the pedal and dorsolateral ciliary cells have the necessary machinery to exhibit physiological responses to a chemical regulator.

The development of the cell isolation techniques described in this thesis permitted the study of the effects of 5-HT on identified ciliary cells in culture. Both pedal and dorsolateral cilia respond to 5-HT perfusion with a significant increase in CBF, which reaches to a maximum within 45 sec (Figure 11). Thus, there appears to be a functional 5-HT receptor on the surface of both these cell types. Prompted by previous evidence that extracellular Ca^{2+} is required for the 5-HT-stimulated increases in CBF and the fact that ionomycin was able to increase the rate of ciliary beating, imaging of intracellular Ca^{2+} in response to exogenous 5-HT was performed. Both pedal and dorsolateral cells exhibited two different types of Ca^{2+} responses to 5-HT (Figures 12 and 13). Whereas the CBF consistently increased rapidly following 5-HT application, imaging experiments revealed that detectable changes in Ca^{2+} lagged behind the changes in CBF, regardless of which type of Ca^{2+} response occurred. The peak and plateau response is suggestive of the profile seen in other ciliary cells, where there is an initial release from intracellular Ca^{2+} stores followed by a sustained Ca^{2+} influx (Salathe et al., 1997; Korngreen and Priel, 1994). In contrast, the slower rising change in $[Ca^{2+}]_i$ is less typical. All of these results are consistent with an early rise in calcium occurring in a restricted cellular compartment, possibly immediately below the cilia (Lansley and Sanderson, 1999), that is not detectable in whole-cell analysis. Through diffusion and Ca^{2+} buffering mechanisms, the localized early signal may be transformed into the delayed peak and plateau signal or slow-rising signal that we observed in whole cell measurements. An alternative, albeit less likely explanation, is that the initial ciliary response to 5-HT is not dependent on a rise in $[Ca^{2+}]_i$. However, the ability of injected BAPTA to completely prevent the CBF response to 5-HT strongly argues against this interpretation.

An interesting finding from these experiments is the slow decay of both the CBF and $[Ca^{2+}]_i$ following washout of the 5-HT. In contrast to these experimentally-induced responses, the ciliary responses to endogenously-released 5-HT in intact embryos are transient, producing periodic increases in the embryo rotation (Kuang and Goldberg, 2001; Cole *et al.*, 2002; Diefenbach *et al.*, 1991). Thus, maintained exposure to elevated concentrations of 5-HT causes long-term changes in ciliary activity, the function of which is not fully understood. Similar maintained increases in CBF were observed after prolonged laser-stimulation of ENC1 in intact embryos (Kuang and Goldberg, 2001). Furthermore, repeated exposure of embryos to environmental hypoxia caused a facilitation of the embryonic rotation response, a form of plasticity that is likely related to the slow response decay observed herein (Kuang *et al.*, 2002). Perhaps the slowly rising Ca^{2+} signal observed in this study functions primarily to produce a maintained state of elevated CBF, rather than mediating the initial increases in CBF observed during transient exposure to 5-HT.

As anticipated, the tissue explants containing pedal ciliary cells retained 5-HT immunoreactivity after one day in culture (Figure 15). This result assists in verifying that pedal ciliary cells were isolated and cultured. The presence of remains of ENC1 neurite may explain why pedal ciliary cells in tissue explants were seen to exhibit periodic, albeit somewhat rare, surges in the rate of ciliary beating, consistent with behavior exhibited by the whole embryo (Doran, unpublished observations). Cultured explants containing dorsolateral ciliary cells exhibited more intermittent expression of 5-HT immunoreactivity (Figure 16). This result was not surprising, given that only one of the four cells comprising each dorsolateral ciliary band is innervated by ENC1 (Koss *et al.*, 2003).

Consistent with the fact that no 5-HT immunoreactivity has been detected in the posterior aspect of the whole embryo, tissue explants containing SSCCs were devoid of 5-HT immunoreactivity (Figure 17).

The pedal and dorsolateral ciliary cells showed similar immunoreactivity to the antibodies raised against the recently cloned *Helisoma* 5-HT receptors (Figures 18 and 19). The 5-HT1$_{hel}$ protein was strongly expressed on the apical surface, with weaker expression throughout the other regions of the cells. The surface expression may indicate the presence of 5-HT in the intracapsular fluid that may contribute to the tonic rotation displayed by the embryos. Pulsatile release of 5-HT from ENC1 is believed to be responsible for the generation of periodic surges in rotation that are superimposed upon a slow basal rate of spinning (Kuang and Goldberg, 2001; Diefenbach et al., 1991). Thus, either a different 5-HT receptor, or a lower concentration of the same receptor is expressed on the basal surface of the pedal and dorsolateral ciliary cells to mediate ENC1-ciliary cell communication.

In contrast to the consistent ciliary cell expression of the 5-HT1$_{hel}$ receptor, the 5-HT7$_{hel}$ protein was expressed in only a minority of pedal and dorsolateral cells. There was either strong, specific expression that resembled the 5-HT1$_{hel}$ pattern or no expression at all. This inconsistent expression, together with significant differences in the molecular structure between the 5-HT1$_{hel}$ and 5-HT7$_{hel}$ genes (Mapara et al., 2001) suggest that the 5-HT7$_{hel}$ receptors play a different role than the 5-HT1$_{hel}$ receptors. Furthermore, the appearance of the 5-HT7$_{hel}$ immunoreactivity in only some cells may suggest that this protein only begins to be expressed around stage E25, with a more complete expression pattern occurring at later stages. In order to fully investigate this hypothesis, more studies are required to examine embryos at different stages of embryonic and postembryonic development.

Interestingly, the amino acid sequence of the two 5-HT receptors cloned from *Helisoma* place one in the 5-HT1 family of receptors, typically linked to the G protein G$_{i/o}$ that causes inhibition of cAMP, and the other in the 5-HT7 family of receptor that is linked to G$_s$ and stimulation of cAMP. At present there is no indication that a cAMP pathway participates in the regulation of *Helisoma* ciliary cells, and it may be that while these invertebrate receptor sequences are similar to known mammalian receptors, the actual intracellular effectors to which these receptors are coupled may be different.

1.3 Non-innervated *Helisoma* ciliary cells

In stage E25 *Helisoma* embryos, at least three groups of ciliary cells are not directly innervated by ENC1 or other identified neurons, the lateral cells of the dorsolateral bands, the SSCCs and the ciliary cells lining the gut. Since the gut cells are not accessible to the microdissection techniques introduced in this study, their physiological characteristics remain unclear. The dorsolateral ciliary bands each contain four cells, with only the most medial one in each band receiving innervation (Koss et al., 2003). Despite this arrangement, the dorsolateral band cells appear to display similar 5-HT receptor immunoreactivity and responsiveness to 5-HT. Thus, paracrine actions of 5-HT and electrical or chemical signals passing through gap junctions (Koss et al., 2003) may well contribute to the ENC1-induced stimulation of these non-innervated cells (Kuang and Goldberg, 2001).

Kuang and Goldberg (2001) identified the SSCCs as a third subtype of ciliary cells expressed on the surface of the embryo during development. These non-innervated cells have a different morphology from either the pedal or dorsolateral ciliary cells and do not respond to 5-HT *in vivo*. While the SSCCs do exhibit the 9x2+2 microtubular arrangement indicative of motile cilia (Sleigh, 1962), these cells differ from the pedal and dorsolateral cilia in their less organized ciliary arrangement, a simpler rootlet structure, less prominent mitochondria, and the absence of electron translucent regions (Figure 9). The SSCCs are not innervated by ENC1 and do not show any anatomical evidence of neurite-ciliary cell apposition sites. These morphological differences support the findings that the SSCCs are physiologically distinct from the pedal and dorsolateral ciliary cells. Results presented in this thesis confirmed that 5-HT does not stimulate a change in CBF in these cells *in vitro* (Figure 11D). Thus, it is likely that these SSCCs, the ciliary cells lining the dorsal surface of the mouth and the uncharacterized gut ciliary cells contributed to the populations of non-responsive cells observed in mass-dissociated cultures (Christopher et al., 1996).

The SSCCs were observed to exhibit two states of activity, a quiescent phase with slow ciliary beating and abbreviated ciliary beat strokes, and an active beating phase with very rapid ciliary beating and full ciliary beat strokes (data not shown). Neither the pedal nor the dorsolateral ciliary cells exhibited either of these states under resting conditions. The mechanics of the ciliary beating in the SSCCs was also different from that exhibited by the other two populations; the SSCCs beat in a flagellar fashion whereas the other two subtypes exhibited more typical ciliary wave-like beating. This observation is consistent with the finding that the SSCCs exhibited longer cilia with a different rootlet structure. The Ca^{2+} profiles in these cells also support the idea of two different states of activity, with some cells demonstrating a relatively flat baseline with no response to 5-HT, and other cells showing an unstable baseline and intermittent calcium spikes, both in the presence and absence of 5-HT (Figure 14). It may be that the fluctuations in $[Ca^{2+}]_i$ are responsible for maintaining the high rate of ciliary beating demonstrated by these cells. Oscillations in $[Ca^{2+}]_i$ have been shown to regulate the CBF in rabbit airway epithelium (Evans and Sanderson, 1999) and ovine tracheal epithelial cells (Salathe and Bookman, 1995). Simultaneous CBF and Ca^{2+} imaging experiments need to be performed to determine if the type of Ca^{2+} activity correlates to the ciliary beat state of the cell. In some SSCCs examined, ionomycin perfusion produced a small amplitude change in intracellular Ca^{2+} that was often transient. This response to calcium ionophore further suggests that the SSCCs regulate intracellular Ca^{2+} through different mechanisms than the pedal and dorsolateral ciliary cells.

The absence of CBF and Ca^{2+} responses to 5-HT, and the lack of immunoreactivity to 5-HT, 5-HT1_{hel} and 5-HT7_{hel} suggests that the SSCCs may be responsive to a non-neuronal cue. One possibility is that these cells are activated by mechanical stimuli. This is suggested by the finding that the start of saline perfusion triggered some SSCCs to switch from the quiescent to active phase of ciliary beating, a result not observed in the other ciliary cell types. A possible role for mechanosensitive ciliary cells in the *Helisoma* embryo would be to keep the surface of the animal free of debris during development. This may be especially important on the posterior aspect of the embryo to ensure that particulate matter does not interfere with the deposition of shell matrix. Mechanical stimulation of the cell membrane has been identified to regulate ciliary activity in *Paramecium* and the lateral gill cilia of *Mytilus edulis* (Eckert, 1972; Murakami and Takahashi, 1975; Murakami and Machemer, 1982). In these systems, mechanical stimuli generates a change in membrane potential that leads to alterations in ion conductances, specifically enabling Ca^{2+} entry, which in turn modifies ciliary activity. Alternatively, the SSCCs may be immature at the embryonic stages examined in this study, differentiating at later stages under the influence of posterior embryonic neurons, such as those described by Croll and Voronezhskaya (1996) in other gastropod species. Although similar dopamine- and FMRFamide-containing neurons have yet to be found in stage E25 *Helisoma* embryos (Goldberg, 1995), further studies are necessary to determine whether the SSCCs eventually become innervated in *Helisoma* embryos.

2 Involvement of PKC and Ca^{2+} in ciliary activity in *Helisoma* ciliary cells

The ENC1-ciliary cell neural circuit in embryos from *Helisoma trivolvis* is conducive to the study of neural control of ciliary beating and the underlying signal transduction mechanisms (Christopher *et al.*, 1996; 1999; Kuang *et al.*, 2002; Kuang and Goldberg, 2001). 5-HT is released by ENC1 in response to hypoxia and causes an increase in CBF that involves Ca^{2+}, PKC and NO (Christopher *et al.*, 1996; 1999; Doran *et al.*, 2003; Kuang *et al.*, 2002; this thesis). In the present study, experiments examining the roles for Ca^{2+} and PKC in the ciliary response to 5-HT demonstrated that changes in $[Ca^{2+}]_i$ are necessary for 5-HT-induced cilio-excitation, whereby Ca^{2+} release from intracellular stores mediates the initial ciliary response to 5-HT while Ca^{2+} influx is necessary for maintenance of the ciliary response. Inhibitors of PLC and PKC revealed that the PKC signaling pathway participates only partially in mediating the CBF response to 5-HT, possibly playing a facilitatory role or acting in parallel to a second pathway. Further, while PKC activation through DAG analogs produces an increase in $[Ca^{2+}]_i$, the PKC pathway does not mediate the 5-HT-stimulated changes in $[Ca^{2+}]_i$.

2.1 The relative roles of intracellular Ca^{2+} release and Ca^{2+} influx

As mentioned previously, a change in $[Ca^{2+}]_i$ appears to be a universal component in the regulation of stimulated ciliary beating in invertebrate and vertebrate systems alike (Tamm and Terasaki, 1994; Murakami and Machemer, 1982; Eckert, 1972; Lansley and Sanderson, 1999; Salathe and Bookman, 1995; Di Benedetto *et al.*, 1991). In the presence of the fast, Ca^{2+} selective chelator BAPTA, *Helisoma* ciliary cells fail to respond to 5-HT, indicating that this system also requires an increase in $[Ca^{2+}]_i$ for ciliary excitation (Figure 20). Ca^{2+} imaging performed in this thesis indicated that 5-HT induces an increase in $[Ca^{2+}]_i$. However, this signal develops with a greater latency and slower time course than the 5-HT-stimulated increase in CBF. This finding is supported by work done on rabbit trachea that revealed that the Ca^{2+} ionophore ionomycin induces a marked increase in CBF before a change in $[Ca^{2+}]_i$ is detected (Korngreen and Priel, 1994). It was suggested that the increase in CBF occurs when the $[Ca^{2+}]_i$ beneath the ciliary membrane rises to a critical level, albeit below the detection limit of the imaging system. As the $[Ca^{2+}]_i$ continues to rise above the threshold for detection, a visible Ca^{2+} signal emerges. Interestingly, this delayed Ca^{2+} signal within *Helisoma* ciliary cells also consistently developed in the center of the cell, then giving rise to a global change in Ca^{2+}, as opposed to a more spatially restricted signal along the ciliated periphery of the cell (data not shown). This pattern may result from an effective Ca^{2+}-buffering system concentrated below the ciliated membrane that limits the amplitude of the local rise in $[Ca^{2+}]_i$. More detailed Ca^{2+} imaging studies examining the spatial distribution of Ca^{2+} during 5-HT stimulation need to be performed.

As observed in experiments using both fura dextran and fura 2 salt, two different Ca^{2+} profiles that result from 5-HT stimulation is an interesting finding in *Helisoma* ciliary cells. The slow rise in Ca^{2+} is less typical of the type of Ca^{2+} signals observed in other ciliary cells (Korngreen and Priel, 1994; Salathe and Bookman, 1995; Evans and Sanderson, 1999). It may be that changes in $[Ca^{2+}]_i$ directly related to the regulation of CBF occur in a spatially restricted component of the cell and go undetected. In this case, the slowly developing rise in Ca^{2+} maybe due to activation of capacitative entry calcium channels that facilitate refilling of intracellular Ca^{2+} stores (Berridge, 1995). More characteristic of Ca^{2+} signaling in ciliary cells is the participation of both intracellular stores release and Ca^{2+} influx. The peak and plateau response, seen in this thesis is suggestive of the pattern of rapid release from intracellular stores followed by Ca^{2+} entry through plasma membrane Ca^{2+} channels that has been observed in other systems (Korngreen and Priel, 1994; Salathe *et al.*, 1997).

The results from experiments performed in the absence of extracellular Ca^{2+} support the model of Ca^{2+} release from stores followed by Ca^{2+} influx through membrane channels. The initial CBF response to 5-HT in 0 Ca^{2+} saline did not differ from control cells in Ca^{2+}-containing saline (Figure 26). In contrast, the rate of ciliary beating declined to an intermediate level in the absence of extracellular Ca^{2+}, but remained high in the presence of extracellular Ca^{2+}, suggesting that Ca^{2+} influx is required for the maintenance of 5-HT cilio-excitation. Interestingly, the measurements of $[Ca^{2+}]_i$ revealed a complete abolishment of the increase in $[Ca^{2+}]_i$ following 5-HT application in the absence of extracellular Ca^{2+}. Once again, it may be possible that the initial Ca^{2+} event, presumably a release from intracellular stores, is highly localized to the ciliated periphery of the cell or even within the intraciliary region. Specialized cellular domains that facilitate localized signaling have been identified to exist within cells (Paradiso *et al.*, 1995). This idea of restricted areas of signaling is important in specifying which cellular processes get activated with the proper timing, while preventing large-scale global rises in $[Ca^{2+}]_i$ that can be cytotoxic.

A model for the maintenance of steep cytosolic Ca^{2+} gradients suggests that there is dynamic integration between plasma membrane channels and intracellular stores to cause active Ca^{2+} redistribution (Braiman and Priel, 2001; Braiman *et al.*, 2000). This model, developed in a variety of vertebrate ciliary cells, accounts for the sustained high $[Ca^{2+}]_i$ along the ciliated periphery of the cell. Ultrastructural analysis of *Helisoma* ciliary cells revealed that there is extensive endoplasmic reticulum, as well as numerous mitochondria located in close proximity with ciliary basal bodies (Figure 9). Mitochondria have been identified to play a significant role in regulating Ca^{2+} dynamics within the cell (Pozzan *et al.*, 1994); the high density of mitochondria in *Helisoma* ciliary cells may signify that this organelle actively participates in Ca^{2+} uptake and release (Pozzan *et al.*, 1994). Research from ovine tracheal epithelium supports this possibility, as mitochondria were shown to participate in Ca^{2+} regulation following acetylcholine stimulation of ciliary cells (Salathe and Bookman, 1995). Thus, the cellular architecture in *Helisoma* ciliary cells suggests that there may be an integrated system for the regulation of cytosolic Ca^{2+} concentration and prompted an investigation into the involvement of intracellular Ca^{2+} stores.

As observed in the fura dextran Ca^{2+} imaging experiments of the pedal and dorsolateral ciliary cells in the first section of results, the Ca^{2+} signal was very slow to decline following washout of the 5-HT. The fact that the 5-HT-induced Ca^{2+} signal is dependent on extracellular influx and appears necessary for maintained cilio-excitation supports the aforementioned hypothesis that the slowly rising Ca^{2+} signal functions primarily in a secondary stage of elevated CBF, possibly required in the refilling of intracellular Ca^{2+} stores. *In vivo*, 5-HT release from ENC1 is postulated to occur in a pulsatile fashion, which gives rise to transient, periodic increases in the embryo rotation (Cole *et al.*, 2002; Diefenbach *et al.*, 1991; Kuang and Goldberg, 2001). Thus, maintained exposure to elevated concentrations of 5-HT may alter how the cell regulates

$[Ca^{2+}]_i$ as additional buffering mechanisms are engaged or disengaged during the five-minute exposure.

The finding that the initial 5-HT-induced increase in CBF is retained when ciliary cells are placed in 0 Ca^{2+} *Helisoma* saline is in contrast to earlier work on *Helisoma* ciliary cells. In the previous study, exposure to 0 Ca^{2+} saline for greater than ten minutes caused a complete abolishment of 5-HT stimulation of CBF (Christopher *et al.*, 1996), whereas in the present study, exposure to 0 Ca^{2+} for two minutes prior to neurotransmitter application had no effect on the initial response. These differing results may further support the idea that Ca^{2+} release from intracellular stores mediates the initial CBF response to 5-HT. The change in ion concentration gradient across the membrane and presence of EGTA in the extracellular environment could create a sufficient outward driving force to cause the rapid depletion of the active intracellular Ca^{2+} store in a period as short as ten minutes. The imaging experiments revealed that basal $[Ca^{2+}]_i$ begins to decrease after only a few minutes in 0 Ca^{2+} saline. Interestingly, exposure to 0 Ca^{2+} did not affect that rate of basal ciliary beating over a period of greater than ten minutes, despite the associated decline in $[Ca^{2+}]_i$. This result is consistent with experiments on rabbit tracheal ciliary cells, suggesting that basal ciliary activity is independent of $[Ca^{2+}]_i$ in diverse systems (Ma *et al.*, 2002).

2.2 Involvement of PKC in 5-HT-induced cilio-excitation

Previous work on *Helisoma* ciliary cells revealed that DAG analogs, but not phorbol esters, could induce transient increases in CBF, that DAG stimulation requires extracellular Ca^{2+} and that PKC inhibitors partially inhibit the CBF response to 5-HT (Christopher *et al.*, 1999). These findings prompted further exploration of the involvement of PKC in 5-HT cilio-excitation and the potential interaction between PKC and Ca^{2+}. Most commonly, PKC signaling is initiated when PLC_{β}, stimulated following G-protein coupled receptor activation, liberates IP_3 and DAG (Delmas *et al.*, 2004). IP_3 triggers release of Ca^{2+} from the endoplasmic reticulum and DAG activates PKC. In this section, the focus was on the PKC signaling pathway, as the involvement of Ca^{2+} release from intracellular stores in *Helisoma* ciliary cells was examined subsequently. Upstream inhibition of the PKC signaling pathway with the PLC inhibitor, U-73122, produced a significant, but partial decrease in the CBF response to 5-HT (Figure 21). Similarly, the PKC inhibitors bisindolylmaleimide and calphostin C only produced a partial inhibition of 5-HT-stimulated ciliary beating (Figure 27). Together, these results suggest that PKC is not the only signal transduction element involved in mediating the cilioexcitatory response to serotonin. PKC may act by facilitating the activity of an additional pathway that plays a more direct role in relaying stimulation from the 5-HT receptor to the ciliary machinery. Alternatively, PKC may act in parallel with an additional pathway, each providing a partial component of the full response. Previous experiments on *Helisoma* ciliary cells suggest that a possible candidate for this additional signal transduction pathway is GC-cGMP-PKG (Doran *et al.*, 2003), which has been implicated in numerous ciliary systems (Zhang and Sanderson, 2003; Uzlaner and Priel, 1999; Wyatt *et al.*, 1998; Bonini and Nelson, 1990).

In efforts to further clarify how PKC may be involved in 5-HT cilio-excitation, the effect of PKC inhibitors on the 5-HT-stimulated changes in $[Ca^{2+}]_i$ was examined (Figure 28). A model developed from studies done in frog tracheal epithelium suggests that PKC participates in sustained CBF enhancement through the phosphorylation of non-voltage operated Ca^{2+} channels (Levin *et al.*, 1997). Consideration of this model, taken together with results presented in this thesis indicating that the 5-HT-stimulated increase in $[Ca^{2+}]_i$ was dependent on extracellular Ca^{2+} and necessary for sustained cilio-excitation, prompted the hypothesis that PKC may participate in Ca^{2+} regulation through the phosphorylation of membrane ion channels. Surprisingly, bisindolylmaleimide and calphostin C did not inhibit the 5-HT-stimulated increase in $[Ca^{2+}]_i$ despite their effect on the CBF response. Similarly, in imaging experiments with the PLC inhibitor U-73122, the drug did not appear to inhibit the 5-HT-induced changes in $[Ca^{2+}]_i$ (Figure 22). These results lead to the conclusion that in *Helisoma* ciliary cells, the main role for PKC is not phosphorylation of Ca^{2+}

channels on the plasma membrane. Rather, it appears that PKC acts on some other target. Since PKC has been demonstrated to regulate CaM in *Paramecium* (Hinrichsen and Blackshear, 1993), taken together with the established role for CaM in *Helisoma* ciliary cells (Doran *et al.*, 2003), CaM is a possible candidate as a target of PKC activity. Alternatively, PKC has also been demonstrated to phosphorylate the ciliary membrane protein p37 in ovine tracheal epithelium and cause a decrease in ciliary beating (Salathe *et al.*, 1993). Given the tremendous diversity in signaling pathways identified in the various ciliary systems examined, it is entirely plausible that in *Helisoma*, PKC could phosphorylate an axonemal protein to stimulate or facilitate an increase in CBF.

DAG analogs cause an increase in CBF, but this response is transient and of a lower amplitude than the 5-HT-induced cilio-excitation. This is not surprising, as PKC is only one of several signal transduction elements that are triggered when 5-HT binds to membrane receptors. It may be that, in addition to phosphorylation of a target axonemal protein, DAG-stimulated PKC acts to regulate plasma membrane Ca^{2+} channels to cause an increase in $[Ca^{2+}]_i$, followed by cilio-excitation. However, this PKC pathway appears to be linked to a cellular response other than 5-HT-induced cilio-excitation. This scenario explains why stimulation of ciliary beating by DAG analogs required extracellular Ca^{2+} whereas 5-HT, acting through additional pathways, still induced an increase in CBF in the absence of extracellular Ca^{2+} (Figure 25). It is interesting to examine the Ca^{2+} responses to ionomycin following application of DAG analogs. Following 5-HT stimulation of ciliary cells, ionomycin produced variable responses; often these responses were transient, indicating that some cells were able to buffer the ionophore-induced changes in $[Ca^{2+}]_i$. In contrast, following the application of both OAG and DOG, ionomycin tended to cause large amplitude changes in $[Ca^{2+}]_i$ that continued to increase over the course of ionophore application. Given that 5-HT initiates a broader cascade of signal transduction events than DAG analogs, it may be that some of these signal transduction elements function in the homeostatic regulation of $[Ca^{2+}]_i$ following ionophore-induced Ca^{2+} influx.

Taken together, the data presented in this section of the thesis suggest that increases in $[Ca^{2+}]_i$ are necessary for 5-HT stimulation of ciliary beating and that these changes in $[Ca^{2+}]_i$ are the result of an integration between Ca^{2+} release from stores and influx through ion channels. It seems likely that dynamic changes in $[Ca^{2+}]_i$ may be occurring in a spatially restricted region along the ciliated periphery of the cell. Further, it appears that while PLC signaling, and more specifically PKC activation, contributes to the 5-HT-induced increase in CBF, PKC does not appear to regulate Ca^{2+} entry into the cell during the 5-HT response. Rather, it may play a role in regulating the activity of a structural or signal transduction protein that is centrally involved in mediating the ciliary response to serotonin.

3 Involvement of intracellular Ca^{2+} stores in 5-HT-induced cilio-excitation

Intracellular Ca^{2+} signals are generated through a complex interplay of not only the timing and amplitude of the Ca^{2+} event, but the source of the signaling ion as well. Given that changes in $[Ca^{2+}]_i$ have been identified as a universal regulator in ciliary activity, it is surprising that more attention has not been directed at examining the source of Ca^{2+}. The confirmation that a change in $[Ca^{2+}]_i$ was necessary for the ciliary response to 5-HT (Figure 20) and the finding that 5-HT initiated an increase in CBF in the absence of extracellular Ca^{2+} (Figure 26) indicated that one or multiple sources of intracellular Ca^{2+} participate in 5-HT-induced cilio-excitation. To investigate this hypothesis, pharmacological agents manipulating distinct Ca^{2+} stores in the mitochondria and the ER were employed. The results suggest that the increase in CBF in response to 5-HT may involve Ca^{2+} release from a mitochondrial store, but not thapsigargin-sensitive stores on the ER nor the related the IP_3-signaling pathway. Interestingly, 5-HT-induced cilio-excitation also utilizes a unique caffeine-sensitive Ca^{2+} store, one that does not appear to function through the ryanodine receptor pathway which is commonly implicated in caffeine responses.

3.1 Role of mitochondrial-sequestered Ca^{2+} in the ciliary activity of pedal ciliary cells

Physiological Ca^{2+} signals may affect mitochondrial function, both by stimulating key metabolic enzymes and, under some conditions, by promoting apoptosis. It is thought that the increased $[Ca^{2+}]_i$ associated with increased cellular metabolic activity may be coupled to increased aerobic metabolism via Ca^{2+} uptake into mitochondria (Ganitkevich, 2003; Parekh, 2003a). If Ca^{2+} levels within the mitochondrial matrix reach sufficiently high levels, the permeability transition pore would be activated to initiate signals associated with cell death. Mitochondria, in turn, may affect both Ca^{2+} release from the ER and capacitative Ca^{2+} entry across the plasma membrane, thereby shaping the intracellular Ca^{2+} signal. Interactions between mitochondria and the ER are dependent on the spatial localization of mitochondria within the cell. Considering this and the energy demands of beating cilia, it is not surprising that TEM analysis of pedal ciliary cells revealed numerous, prominent mitochondria in direct proximity to both the ER and ciliary basal structures (Figure 9). To investigate the physiological involvement of mitochondria in the signal transduction underlying stimulated ciliary beating, the uncoupler CCCP and the mitochondrial uniporter inhibitors ruthenium red and Ru360 were used. Application of CCCP caused a large transient decrease in the rate of basal ciliary beating, dramatically reduced the 5-HT-stimulated increase in CBF, and weakly attenuated the ciliary response to the Ca^{2+} ionophore ionomycin (Figure 29). In contrast, ruthenium red or Ru360 did not alter the cilio-excitatory response to 5-HT (Figure 30).

The conflicting nature of these data, combined with possible non-specific effects and difficulty in handling these pharmacological agents complicates the interpretation of these results. Uncoupling agents, such as CCCP, disrupt the proton gradient and thereby depolarize the mitochondrial membrane potential to eliminate the driving force for Ca^{2+} into the mitochondria. Given that most mitochondrial functions harness this membrane potential, it is difficult to dissect out effects due to the disruption of Ca^{2+} regulation versus changes in mitochondrial and cellular ATP (reviewed in Jacobson and Duchen, 2004).

Further non-specific effects of protonophores include plasma membrane hyperpolarization due to increased H^+ permeability, activation of H^+- and Na^+-dependent plasma membrane currents and cytoplasmic acidification (reviewed in Ganitkevich, 2003). Membrane hyperpolarization has been identified in the regulation of ciliary activity through alterations in chloride currents in murine respiratory cells and cells of the pedal epithelium of *Tritonia diomedea* (Tarran *et al.*, 2000; Woodward and Willows, 2003). Similarly, changes in intracellular pH have recently been shown to alter ciliary activity in human airway ciliary cells (Sutto *et al.*, 2004). Although acidification of ciliary cells using butyrate did not alter the rate of basal ciliary beating in *Helisoma* ciliary cells (Kuang, 2002), it remains unknown how membrane excitability affects ciliary activity in *Helisoma* ciliary cells. Thus, it is evident that conclusions from experiments with CCCP are problematic

In efforts to examine whether the loss of the ciliary response to 5-HT was due to cellular depletion of ATP rather than Ca^{2+} disruption, CCCP pretreatment was paired with ionomycin stimulation (Figure 29). The fact that pedal ciliary cells still exhibited cilio-excitation in response to ionomycin, albeit attenuated, suggests that ATP depletion was not solely responsible for the loss of the ciliary response to 5-HT. In the face of other metabolic challenges, these embryonic ciliary cells have exhibited a high capacity to maintain ciliary activity, further suggesting that the effect of CCCP on ciliary beating is due to a mitochondrial effect other than disruption of ATP production. For example, whole embryos placed under hypoxic conditions, which should impair aerobic metabolism, exhibit accelerated ciliary beating that persists over the course of many hours. This suggests that these cells exhibit tremendous energy reserves (Kuang *et al.*, 2003). Furthermore, tissue explants containing ciliary cells can maintain the 5-HT-stimulated high rates of ciliary beating for hours without supplementing the saline (Doran, unpublished observations). Finally, the mitochondrial disrupter rotenone does not alter the rate of basal ciliary beating (Kuang, 2002). Therefore, the finding that CCCP fully inhibits 5-HT cilio-excitation, together with the high energy reserves demonstrated by these several examples, strongly implicate a role for mitochondrial control of $[Ca^{2+}]_i$ in cilio-excitation.

Ruthenium red is a non-competitive inhibitor widely used to block Ca^{2+} uptake into the mitochondria via inhibition of the mitochondrial uniporter (Rizzuto *et al.*, 2000). Although this action would more directly link mitochondrial Ca^{2+} regulation with the ciliary response, ruthenium red also exhibits effects on other cellular activities including inhibition of Ca^{2+} release channels on the sarcoplasmic or endoplasmic reticulum, as well as inhibition of plasma membrane Ca^{2+} channels (Kargacin *et al.*, 1998; reviewed in Ganitkevich, 2003). Additionally, there is controversy over the membrane permeability of this hexavalent cation (Jacobson and Duchen, 2004). A direct time-dependent rate of ruthenium red uptake into mammalian cardiac myocytes was demonstrated; a 30 min incubation with 50 μM ruthenium red allowed sufficient accumulation of the inhibitor to disrupt Ca^{2+} uptake into the mitochondria (Zhou and Bers, 2002). Similar incubation protocols with ruthenium red have been used successfully with mouse parotid acinar cells and canine and rat myocytes (Bruce *et al.*, 2004; Kargacin *et al.*, 1998; Griffiths, 2000). In contrast, work performed on crayfish neuromuscular junction suggests that given the questionable membrane permeability, microinjection may be a better procedure for achieving sufficient intracellular levels of the drug (Tang and Zucker, 1997). The plasma membrane of ciliary cells surround a dense concentration of ciliary axonemes, basal bodies and ciliary rootlet structures. This arrangement may provide a difficult barrier for drugs that are marginally cell-permeable. Furthermore, embryonic ciliary cells from *Helisoma* do not readily retain acetoxymethyl ester compounds (Christopher, 1997; Doran, unpublished observations). It is unknown if these compounds cannot cross the plasma membrane or if the ciliary cells do not possess the appropriate esterases to cleave and trap these compounds. Thus, the negative result obtained with ruthenium red may stem from insufficient cellular loading, rather than a lack of mitochondrial involvement. It may be necessary to microinject ruthenium red into *Helisoma* ciliary cells to ensure successful loading of this compound into ciliary cells.

Unlike ruthenium red, Ru360 inhibits the mitochondrial uniporter with less non-specific cellular effects. However, Ru360 is highly unstable in aqueous environments, becoming rapidly inactivated through oxidization, making the compound difficult to work with (Jacobson and Duchen, 2004). Despite these concerns, Ru360 has been demonstrated to be taken up by cells and specifically block the mitochondrial uniporter (Zhou and Bers, 2002; Bruce *et al.*, 2004; Matlib *et al.*, 1998). Once again, the negative result obtained with Ru360 is questionable given the unstable nature of this compound. Although it could be anticipated that inhibition of the uniporter could initiate a release of Ca^{2+} which would stimulate ciliary beating, ruthenium red and Ru360 did not alter basal ciliary beating, again raising the possibility that these drugs were not properly tested.

Additionally, mitochondria can be seen to function as fixed buffers that effectively partition the cell into discrete Ca^{2+} compartments. This has been effectively demonstrated in pancreatic acinar cells, where mitochondria function to limit Ca^{2+} oscillations to the apical pore of this polarized epithelium (Park *et al.*, 2001). These mobile organelles may be positioned near sites of Ca^{2+} release and influx not only to facilitate inter-organelle communication and shape Ca^{2+} signals, but also to restrict the spread of Ca^{2+} signals. This may explain why Ca^{2+} signals were not detected along the ciliated periphery of the *Helisoma* ciliary cells. The mitochondria may function to spatially restrict increases in Ca^{2+} to the ciliary machinery. To examine this possibility it is necessary to image stimulated ciliary cells with greater spatial resolution and sensitivity.

A Ca^{2+} store that can be rapidly depleted was implicated in stimulated ciliary beating in *Helisoma* ciliary cells (Figure 26), as a ten minute incubation in 0 Ca^{2+} saline can abolish the 5-HT-stimulated cilio-excitation (Christopher *et al.*, 1996). Thus, the mitochondria may be necessary to any or all of the following: 1) engage the appropriate intracellular Ca^{2+} store in the ciliary response to 5-HT, 2) shape the resulting Ca^{2+} signal through uptake of released Ca^{2+} or 3) facilitate the refilling of this Ca^{2+} store. As an extension of this idea, the attenuated response to ionomycin following CCCP application may be the result of a disruption of a critical intracellular store. The ionophore-induced increase in ciliary beating may result from an interaction between Ca^{2+} influx and the activation of CICR from intracellular stores to stimulate an increase in ciliary beating. In the absence of a store component, ciliary beating is increased but not to the same degree as with intact intracellular machinery. Further work needs to be done to examine this possibility in light of the negative results obtained with ruthenium red and Ru360 and the stated concerns with the use of these drugs.

3.2 Involvement of conventional ER Ca^{2+} stores in the ciliary activity of pedal ciliary cells

The most commonly identified release mechanisms on intracellular Ca^{2+} stores of the ER are IP_3 receptor channels and ryanodine receptor channels. The involvement of these mechanisms in the cilio-excitatory response to 5-HT in *Helisoma* ciliary cells was examined and interestingly, they did not appear to be necessary for the response to 5-HT. Activity of SERCAs are commonly associated with the refilling of IP_3-mediated Ca^{2+} stores, although IP_3 stimulated, thapsigargin-insensitive Ca^{2+} pools have been identified (Pizzo *et al.*, 1997). Thapsigargin is a plant-derived sesquiterpene lactone that specifically blocks all members of the endoplasmic and sarcoplasmic reticulum Ca^{2+} pump family (Lytton *et al.*, 1991). Through inhibition of the uptake pathway, the intracellular store can be effectively emptied and rendered unavailable. Application of thapsigargin produced an increase in CBF in pedal ciliary cells, presumably through the leak of Ca^{2+} from the ER (Figure 31). A thapsigargin-sensitive Ca^{2+} store has been implicated in vasopressin-stimulated ciliary beating in rabbit tracheal epithelium and acetylcholine-stimulated ciliary beating in ovine tracheal epithelium (Tamaoki *et al.*, 1998; Salathe and Bookman, 1995). In *Helisoma* pedal ciliary cells, the 60 min pretreatment with thapsigargin, thought to be sufficient time to deplete the store, did not alter the 5-HT-stimulated increase in CBF, suggesting that a thapsigargin-sensitive store is not involved (Figure 31C). This is consistent with ATP-stimulated ciliary beating in rabbit tracheal cells, where the initial response is dependent on Ca^{2+} release from a thapsigargin-insensitive Ca^{2+} store adjacent to the cilia (Korngreen and Priel, 1996).

Interestingly, a 30 min pretreatment with thapsigargin produced a facilitation of the CBF response to 5-HT (Figure 31B). It seems likely that this enhanced response resulted from elevated levels of cytosolic Ca^{2+} stemming from leak from the ER and the inhibition of Ca^{2+} reuptake into the ER. After 60 min, although Ca^{2+} imaging revealed that the 340/380 ratio remained elevated above basal (Figure 32), the cell may have been able to reestablish basal levels of cytosolic Ca^{2+} in the vicinity of the cilia and reset its ability to buffer changes in Ca^{2+}, thereby enabling an increase in CBF that was no different from controls (Figure 32). Such a scenario has been suggested for other ciliated epithelial cells, where active Ca^{2+} redistribution would allow stable localized regions of tightly regulated Ca^{2+} near the plasma membrane (Braiman and Priel, 2001).

IP_3, a breakdown product of the phosphoinositide cascade, is the endogenous agonist of a highly studied family of Ca^{2+} release channels on the ER. Prompted by results suggesting that the PLC signaling pathway played a role in *Helisoma* ciliary cells (Figure 21), the possible involvement of IP_3-mediated intracellular Ca^{2+} release in 5-HT-stimulated ciliary beating was examined with the IP_3 channel inhibitor xestospongin C. Derived from an Australian marine sponge, xestospongin compounds are membrane-permeable IP_3 receptor blockers that do not interact with the IP_3 effector site and are highly selective over ryanodine receptors (Gafni *et al.*, 1997). The presence of xestospongin C did not interfere with the ciliary response to 5-HT, indicating that IP_3-mediated Ca^{2+} release from stores is not involved (Figure 33). Although initially surprising given the ubiquity with which IP_3 mediates Ca^{2+} release intracellularly, including in rabbit airway ciliated epithelial cells (Hansen *et al.*, 1995) and invertebrate neurons (Chameau *et al.*, 2001; Jin and Hawkins, 2003), this result may further supports the conclusion that the downstream effector of PLC activation, PKC, plays a subsidiary role in mediating 5-HT cilio-excitation as opposed to being a signal transduction element directly involved in the pathway. Given that inhibiting PKC or PLC only partially inhibits the CBF response to 5-HT and does not appear to alter the Ca^{2+} response, it has been proposed that PKC acts to modify ciliary beating possibly through the regulation of CaM or phosphorylation of an intraciliary protein (see Discussion 2.2: Involvement of PKC in the 5-HT-induced cilio-excitation).

In addition to IP_3 receptors, the ER also possesses a related but distinct family of Ca^{2+} channels called ryanodine receptors, so named because the plant alkaloid ryanodine strongly binds the receptors. Ryanodine receptors were first identified to be responsible for the release of Ca^{2+} in skeletal and cardiac muscle (Bennett *et al.*, 1996), and have since been identified in several excitable and nonexcitable cell types in mammals (Bennett *et al.*, 1996), as well as in neurons of the invertebrate *Aplysia californica* (Chameau *et al.*, 2001; Jin and Hawkins, 2003). Nanomolar concentrations of ryanodine are believed to activate ryanodine receptor channels, whereas micromolar concentrations are thought to specifically inhibit the channel (Ehrlich *et al.*, 1994). In *Helisoma* ciliary cells, the stimulatory dose of ryanodine did not alter the rate of ciliary beating, suggesting that this channel may not be involved in releasing Ca^{2+} in the vicinity of the cilia (Figure 37). Further, pretreatment with either the inhibitory dose of ryanodine or the ryanodine receptor inhibitor dantrolene did not produce any change in the CBF response to 5-HT in comparison with control cells, suggesting that ryanodine receptor-mediated Ca^{2+} release is not involved in 5-HT-stimulated ciliary beating (Figure 38). Likewise, ryanodine receptors are not involved in the intercellular propagation of mechanically stimulated Ca^{2+} waves in rabbit ciliated airway epithelial cells (Hansen *et al.*, 1995). However, there is only limited research on the role of ryanodine receptors, or indeed other intracellular Ca^{2+} release mechanisms, in ciliary beating. Interestingly, the micromolar dose of ryanodine stimulated a slight, transient rise in the rate of ciliary beating in the first few minutes following drug application. It may be that the initial introduction of ryanodine stimulated a transient release of Ca^{2+} that produced an increase in CBF. To examine this possibility, a ryanodine dose response experiment should be to performed along with Ca^{2+} imaging. It is possible the ryanodine concentrations needed to stimulate and inhibit ryanodine receptors may be right-shifted in *Helisoma* from those known for other systems.

3.3 Involvement of a unique caffeine-sensitive store in the ciliary response to 5-HT in pedal ciliary cells

Commonly used to probe ryanodine receptor activity, caffeine is a xanthine drug that stimulates intracellular Ca^{2+} release. In addition, it has other intracellular activities, such as inhibition of PDE and activation of plasma membrane channels. Application of caffeine produced an increase in CBF that was indistinguishable from the effect of 5-HT, presumably through a release of intracellular Ca^{2+} (Figure 34). To determine whether the effects of caffeine involved intracellular Ca^{2+} release or PDE inhibition, the PDE inhibitor IBMX was applied to ciliary cells. Although it caused a significant increase in CBF, the response was smaller than that produced by caffeine or 5-HT, and began to decline within 10 min (Figure 35A). Furthermore, forskolin, an activator of AC, did not alter basal ciliary beating (Figure 35B), corroborating the previous finding that cAMP does not regulate *Helisoma* ciliary activity (Christopher *et al.*, 1996). Taken together, these data suggest that the effects of PDE inhibition may not involve intracellular cAMP.

Alternatively, it is more probable that if caffeine were acting as a PDE inhibitor, it would alter intracellular levels of cGMP, given that NO has been shown to be constitutively active in *Helisoma* ciliary cells and involved in 5-HT-stimulated cilio-excitation (Doran *et al.*, 2003). In the presence of the soluble GC inhibitor LY83583, caffeine stimulated an increase in CBF that was no different from control cells (Figure 35C). Interestingly, the caffeine-stimulated increase in CBF in the presence of LY83583 decreased more rapidly than in control cells. It appears that a release of Ca^{2+} from intracellular stores is able to cause the initial increase in CBF, but that activity of cGMP is necessary for sustained ciliary beating. Indeed a complex interplay of signal transduction elements occurs in the regulation of ciliary beating in numerous systems.

One of the most significant results of this study is that a long pretreatment with caffeine abolished 5-HT-stimulated cilio-excitation (Figure 36). Thus, a caffeine-sensitive store is involved in stimulated ciliary activity in *Helisoma* ciliary cells. As mentioned, caffeine is often used as an agonist for ryanodine receptors. However, ryanodine receptor inhibition with ryanodine and dantrolene did not alter the ciliary response to 5-HT. Furthermore, pretreatment with an inhibitory dose of ryanodine did not inhibit the stimulatory effect of caffeine (Figure 39). Together, these results suggest that the stimulatory effects of caffeine and 5-HT are not acting through Ca^{2+} release via ryanodine receptor channels. Although there is some indication that caffeine may alter release through IP_3-mediated channels in canine cerebellum (Bezprozvanny *et al.*, 1994), the results of the xestospongin C and the thapsigargin experiments argue against this possibility. Rather, the essential intracellular Ca^{2+} store underlying the ciliary response in pedal ciliary cells most likely resembles the one described in leech P neurons. These cells possess a caffeine-sensitive intracellular Ca^{2+} store that is ryanodine-insensitive and independent of activity of intracellular Ca^{2+} pumps, as thapsigargin, cyclopiazonic acid and 2,5-di-(*t*-butyl)-1,4-hydroquinone had no effect on caffeine-induced Ca^{2+} increases (Schoppe *et al.*, 1997). Perhaps a Ca^{2+} store with these characteristics is more common in invertebrate systems. In goldfish pituitary cells, pituitary adenylate cyclase-activating polypeptide stimulation of growth hormone and gonadotropin hormone secretion also relies on intracellular Ca^{2+} release from a store with a similar pharmacological profile (Sawisky, 2004). In this system, hormone secretion involves the PLC signaling pathway, but not IP_3 receptor-mediated Ca^{2+} release. In addition there is limited or no involvement of mitochondrial Ca^{2+} stores, whereas release occurs from a unique caffeine-sensitive intracellular Ca^{2+} store.

Since caffeine is produced in plants, the endogenous signal transduction element that normally activates the caffeine-sensitive Ca^{2+} release channel during the ciliary response remains unknown. One possibility is that NAADP, a potent activator of Ca^{2+} release that was first identified in sea urchin eggs (Chini *et al.*, 1995), is the endogenous Ca^{2+} mobilizing agent. It was demonstrated that

L-type Ca^{2+} channels blockers inhibit NAADP-induced Ca^{2+} release (Genazzani *et al.*, 1997). This result is interesting in light of the finding that L-type Ca^{2+} channel blockers inhibit the ciliary response to 5-HT in *Helisoma* ciliary cells (Christopher *et al.*, 1996), even though the initial change in $[Ca^{2+}]_i$ is dependent on a release from intracellular Ca^{2+} stores. Further study is required to test this hypothesis.

3.4 Interplay between ER and mitochondria in the regulation of intracellular Ca^{2+}

The close apposition of the mitochondria with the ER, the cell membrane and basal ciliary structures is suggestive of a mitochondrial function beyond supplying the ATP required for ciliary beating. A dynamic interplay between the ER and mitochondria has been demonstrated and is believed to shape intracellular Ca^{2+} signals (reviewed in Ganitkevich, 2003; Hajnoczky *et al.*, 2000). The Ca^{2+} source, be it IP_3-evoked release, capacitative Ca^{2+} entry or leakage from the ER, has been demonstrated to alter the relationship between $[Ca^{2+}]_i$ and intramitochondrial Ca^{2+} (Collins *et al.*, 2001). Furthermore, specific interactions between mitochondria and endoplasmic reticulum are suggested by studies using green fluorescent protein-based Ca^{2+} sensors that can target the mitochondria (Filippin *et al.*, 2003). The mitochondria are also important in preventing Ca^{2+} depletion of regions of closely associated ER (Arnaudeau *et al.*, 2001) and exhibit functional heterogeneity within cells (Collins *et al.*, 2002).

This close association between the ER and mitochondria may explain why the initial introduction of CCCP caused a rapid, transient reduction in the rate of ciliary beating. The rapidity of this response and its subsequent recovery cannot be explained by a disruption in ATP production or supply. Rather, it may be that some other signal from the mitochondria, or signals between the ER and the mitochondria, may regulate basal ciliary beating. When this regulatory mechanism is disrupted another redundant control mechanism may enable basal ciliary beating. The interplay between the mitochondria and the ER may be even more important in stimulated ciliary beating. The disruption of the mitochondria with CCCP dramatically reduced 5-HT-induced cilio-excitation, possibly by altering the Ca^{2+} availability from a necessary intracellular store. Ca^{2+} uptake into mitochondria has been previously implicated in ovine ciliated airway epithelial cells. In these cells, acetylcholine induces both a transient increase in Ca^{2+} as well as a latent reduction in cytosolic Ca^{2+}. In the presence of the mitochondrial uncouplers CCCP and FCCP, the acetylcholine-stimulated reduction of cytosolic Ca^{2+} was abolished, suggesting a role for mitochondria in Ca^{2+} uptake (Salathe *et al.*, 2001).

It seems most probable that the global Ca^{2+} signal detected in *Helisoma* ciliary cells following 5-HT stimulation is the result of Ca^{2+} influx triggered to refill intracellular Ca^{2+} stores. The delay with which these signals develop following the application of 5-HT is suggestive of the triggering of store-operated channels on the plasma membrane (Parekh, 2003b). It may be that Ca^{2+} influx through Ca^{2+} release-activated Ca^{2+} channels is necessary for sustained stimulated ciliary beating, as has been suggested in rat brain ependymal ciliary cells (Nguyen *et al.*, 2001). Store-operated Ca^{2+} channels with similar biophysical characteristics as mammalian Ca^{2+} release-activated Ca^{2+} channels have been detected in the invertebrate *Drosophila* (Yeromin *et al.*, 2004). Also, the extended duration of these imaged Ca^{2+} signals may be indicative of the need to refill a store that was rapidly depleted upon prolonged exposure to 5-HT.

Although this study has highlighted the necessity of intracellular Ca^{2+} release in the cilio-excitation numerous questions remain. Further study is required to fully understand how intracellular Ca^{2+} stores participate in the cilio-excitatory response to 5-HT in pedal cells from *Helisoma* embryos.

4 Regulation of embryonic ciliary cells from *Helisoma trivolvis*

Through the integration of the findings presented in this thesis with previous studies, it is possible to generate a model of the signal transduction underlying 5-HT cilio-excitation in *Helisoma* embryos (Figure 40).

To recapitulate, three subpopulations of ciliary cells are expressed on the surface of the organism between stages E15-E30, the stages of embryogenesis examined in this investigation. The coordinated beating of two of these populations, the pedal and the dorsolateral ciliary cells, produces the first embryonic behavior: embryo rotation within the egg capsule (Diefenbach *et al.*, 1991). The pedal band of cilia and the most medial cell of the four comprising each dorsolateral band are innervated by ENC1s, a pair of serotonergic sensorimotor neurons that respond to levels of environmental oxygen (Koss *et al.*, 2003, Kuang *et al.*, 2002). 5-HT release from ENC1 stimulates ciliary activity in the pedal and dorsolateral ciliary cells, but does not alter activity in the third population of ciliary cells, the SSCCs (Kuang and Goldberg, 2001). Additionally, NADPH diaphorase staining on whole embryos revealed the presence of NOS in the chemosensory dendritic structure of ENC1 and the dorsolateral ciliary cells at stage E 25, and slightly later in development in the pedal ciliary cells and soma, apical dendrite and descending neurite of ENC1 (Cole *et al.*, 2002). Furthermore, results from experiments with NO donors and NOS inhibitors confirmed a role of for NO in regulating embryonic rotation by acting both on ENC1 and postsynaptic ciliary cells (Cole *et al.*, 2002).

Earlier studies on mass dissociated ciliary cells revealed that 5-HT-stimulated ciliary beating involves Ca^{2+} influx through L-type Ca^{2+} channels (Christopher *et al.*, 1996). This is further supported by the fact that application of KCl stimulated ciliary beating, although this result was complicated by a bi-phasic dose response to KCl, whereby higher doses inhibited the CBF (Christopher *et al.*, 1996). Interestingly, 5-HT-induced cilio-excitation does not appear to involve a cAMP pathway, but does involve a unique isoform of PKC (Christopher *et al.*, 1999). In unidentified cultured ciliary cells, NO working through sGC and cGMP was demonstrated to participate in the regulation of basal ciliary beating and 5-HT-stimulated cilio-excitation (Doran *et al.*, 2003); whether PKG is subsequently activated remains to be determined. In addition, CaM was shown to be necessary in the ciliary response to 5-HT (Doran *et al.*, 2004). As CaM has been identified to bind and interact directly with proteins within the axoneme in other systems, this is likely the site of CaM activity herein.

Consideration of these previous findings, taken together with evidence presented in this thesis, suggests the following conclusions about ciliary regulation in *Helisoma* ciliary cells. The SSCCs represent a distinct population of ciliary cells that have no discernable innervation at the stages of development examined in this study. Accordingly, these cells do not possess 5-HT receptors and do not respond to exogenous 5-HT application. It was suggested that these cells are mechanically stimulated and function to keep the surface of the developing embryo free of debris during shell development. The pedal and dorsolateral ciliary cells are innervated by ENC1 and do respond to exogenous 5-HT with a rapid increase in CBF and a delayed increase in $[Ca^{2+}]_i$. When tissue explants containing these two types of ciliary cells are cultured, they retain some indication of this innervation and express 5-HT receptors.

The present studies on pedal ciliary cells demonstrated that an increase in $[Ca^{2+}]_i$ is necessary for 5-HT cilio-excitation. This Ca^{2+} may be acting on many different targets, including CaM, axonemal proteins and other signal transduction elements. The initial CBF response to 5-HT involves an increase in $[Ca^{2+}]_i$ that results from Ca^{2+} release from caffeine-sensitive intracellular Ca^{2+} stores that can be rapidly depleted by exposure to caffeine or the removal of extracellular Ca^{2+}. This release of intracellular Ca^{2+} was not mediated by ryanodine receptor channels, nor did it arise from a thapsigargin-sensitive intracellular Ca^{2+} pool. Despite the fact that PLC signaling is involved in the ciliary response to 5-HT, IP_3 receptor Ca^{2+} channels were also not involved.

Numerous and prominent mitochondria within the vicinity of the ciliated periphery of the cell not only fulfill the energy requirements of beating cilia, but may participate in Ca^{2+} regulation. Although the results with the mitochondrial uniporter inhibitors were negative, the experiments with the mitochondrial uncoupler suggest that mitochondria are involved in shaping the Ca^{2+} signal necessary for the ciliary response to 5-HT. It is probable that the ER and mitochondria interact to enable the development of localized Ca^{2+} signals within a spatially restricted area below the cilia. Interestingly, Ca^{2+} influx is required for maintained stimulated ciliary beating, possibly to act on intraciliary targets or to refill intracellular Ca^{2+} stores. This sustained phase of stimulated ciliary beating also requires sGC activity.

The global Ca^{2+} signals detected in the imaging experiments presented in this thesis are suggestive of Ca^{2+} influx through Ca^{2+} channels activated to refill intracellular Ca^{2+} stores. It remains to be determined if these channels are responding to an intracellular signal generated by depleting stores or if these channels respond to some other signal such as a change in membrane potential or phosphorylation. A protein kinase implicated in the cilio-excitatory response to 5-HT but not believed to act in the phosphorylation of Ca^{2+} channels is PKC. PKC appears to play a role in modulating some part of the intracellular cascade that is triggered in response to 5-HT or may phosphorylate an intraciliary target. Alternatively, PKC may act in concert with other signal transduction agents to produce increased ciliary beating.

5 Ciliary regulation at the level of the axoneme

Despite the fact that the general design of the axoneme, including its >250 polypeptides, appears to be conserved throughout evolution (Figure 41A), the pattern of ciliary beating and the regulation of activity appear to be highly divergent among the systems examined. Studies on ciliary cells have focused on the structure of the axoneme, the generation and mechanics of ciliary beating, the extracellular regulators of activity and the intracellular signal transduction cascades that are initiated in response to extracellular agonists. However, as there has been little effort to link these various questions together, how signal transduction cascade act upon axonemal machinery to produce ciliary responses remains a mystery. The identification of more than 80 axonemal phosphoproteins, together with the direct localization of various kinases and phosphatases within the axoneme (Figure 41B) is a first step in solving this problem. Yet, the aforementioned species-specific differences in regulatory pathways suggest that these differences may extend to the level of the axoneme, thereby making it difficult to generalize about the identity and location of the enzymes responsible for regulating the activity of axonemal proteins. This difficulty may be compounded by the fact that much of the work done to identify intraciliary regulation of activity has been performed on one system, *Chlamydomonas* flagella.

With these considerations in mind, it is possible to speculate on some of the possible locations where the signaling cascades identified in this thesis may converge within the *Helisoma* axoneme. A recent study using porcine airway epithelium has indicated that ATP and ionomycin produce a change in the phosphorylation profile of a serine residue of seven intraciliary polypeptides, with three serine residues phosphorylated and four residues dephosphorylated (Gertsberg *et al.*, 2004). This finding has interesting implications for the *Helisoma* system because the change in phosphorylation profile is dependent on an active NO pathway. However, the specific axonemal location of the indicated serine residues remains to be determined. The finding that ionomycin can induce changes in phosphorylation also indicates that one of the targets for Ca^{2+} may be activation of the NO pathway. Similarly, the specific location within the axoneme of the PKC phosphorylated polypeptide p37 in sheep tracheal epithelium remains unknown (Salathe *et al.*, 1993). Yet, the general localization of this polypeptide within the axoneme indicates that PKC acts on axonemal targets.

Finally, numerous intraciliary targets for binding Ca^{2+} have been identified in *Chlamydomonas* flagella. Radial spoke protein 2 is a CaM binding protein that localizes CaM to the radial stalk in a Ca^{2+}-dependent manner (Yang *et al.*, 2004). Additionally, p61 (also termed RSP23) localized to the *Chlamydomonas* radial spoke has two classes of CaM binding sites, in addition to a novel nucleoside diphosphate kinase (Patel-King *et al.*, 2004). Given that the radial spoke has been proposed to control the size and shape of the bend (Porter and Sale, 2000), this finding suggests that Ca^{2+} and CaM, both of which are necessary for stimulated ciliary beating in *Helisoma* embryos, are some of the signals responsible for regulating this activity. Further, Ca^{2+}, CaM and CaMKII have been identified to regulate flagellar motility in *Chlamydomonas* in a manner that relies on an intact C1 central microtubule, in addition to the radial spokes (Smith, 2002). The smallest subunit of the outer dynein arm-docking complex, DC3, is a Ca^{2+}-binding protein, suggesting the Ca^{2+} may regulate the assembly and activity of the outer dynein arms (Casey *et al.*, 2003). Furthermore, Ca^{2+} binds directly to a component of the dynein complex that regulates ATP-dependent interactions between the β heavy chains and adjacent microtubules (Sakato and King, 2003). Ca^{2+} also acts upon the inner dynein arms, as three of the dynein heavy chains identified within a subset of the single-headed inner arms are associated with a 19 kDa light chain that is known as the Ca^{2+}-binding protein centrin (LeDizet and Piperno, 1995). It remains to be determined if these findings can be more broadly generalized to systems other than *Chlamydomonas*.

Additionally, numerous protein phosphatases are crucial to the regulation of ciliary activity. These enzymes have been localized to structures within in the axoneme, anchored in such a way as to enable the rapid dephosphorylation of specific targets. Although the participation of protein phosphatases remains to be examined within the *Helisoma* system, it seems most probable that these signaling agents are intimately involved in regulating ciliary beating and are localized within the ciliary axoneme.

6 Future directions

As mentioned, the ENC1-ciliary cell neural circuit in *Helisoma* embryos is an excellent model for studying different aspects of ciliary regulation. Not only are there distinguishable ciliary subpopulations on the surface of the embryo, but the endogenous extracellular regulator of the pedal and dorsolateral cells is known. Further, the activity of individual ciliary cells can be studied and correlated with the cilia-driven behavior of the whole organism. The current study sought to further elucidate aspects of ciliary regulation within this system, with the aim of increasing the understanding of ciliary cells in general.

Considering the breadth of this goal, it is not surprising that numerous questions remain.

The scattered single ciliary cells are the least understood of the ciliary cell populations expressed on the embryo surface. Anecdotal evidence suggests that these cells are responsive to mechanical disturbance, but it remains to be determined if these cells are truly mechanosensitive. Alternatively, it may be that these cells are immature at the stages looked at in this study, and may differentiate at later stages of development as further neuronal development leads to their innervation. It would be interesting to examine the extracellular regulation of the SSCCs, as well as the intracellular signal transduction pathways that regulate their activity.

Similarly, questions remain about the dorsolateral ciliary cells, as much of the current study focused on the pedal ciliary cells. It would be interesting to determine if the dorsolateral cells exhibit the same regulatory pathways as those identified in pedal ciliary cells. Also, given that only one of the four cells comprising each dorsolateral band is innervated by ENC1, it would be interesting to determine if all dorsolateral cells are regulated in a similar manner, or if there is heterogeneity in their regulatory pathways.

The ciliated epithelium of the mammalian respiratory tract is considered to be electrically non-excitable, whereas the unicellular ciliate *Paramecium* is responsive to electrical changes across the plasma membrane. It is unknown if *Helisoma* ciliary cells are electrically excitable. Pharmacological evidence suggests the presence of voltage-gated Ca^{2+} channels, as does the responsiveness to KCl. Electrophysiological studies may yield further insight into how *Helisoma* ciliary cells are regulated.

Ca^{2+} is the most ubiquitous second messenger identified in the regulation of ciliary activity. In *Helisoma* ciliary cells, an increase in $[Ca^{2+}]_i$, as mediated by a release from intracellular Ca^{2+} stores and Ca^{2+} influx, is required for 5-HT-induced cilio-excitation. However, the delayed global Ca^{2+} signals imaged in this study are not consistent with the rapid change in ciliary beating. It would be interesting to examine the development of Ca^{2+} signals in a more spatially restricted region along the ciliated periphery of the cell with the spatial resolution afforded by a confocal microscope. As Ca^{2+} influx is required for maintained cilio-excitation, identifying the signal to which Ca^{2+} channels respond, as well as the location of Ca^{2+} channels along the ciliated membrane, would assist in understanding the control of Ca^{2+} signaling within these cells. Further, many questions remain with regards to how intracellular Ca^{2+} stores shape the development of Ca^{2+} signals, such as: identification of the organelle that houses the caffeine-sensitive store; the endogenous release mechanism; and the involvement of mitochondrial stores in shaping the intracellular Ca^{2+} signals?

The NO signaling pathway has been implicated both in basal ciliary beating and during cilio-excitation. However, further study could address questions such as: the role of cGMP in the initiation of intracellular and intraciliary activity, the involvement of PKG, the Ca^{2+} dependency of the NOS isoform and how 5-HT binding to a receptor is coupled to NO activation?

It has been established that endogenous phosphatase activity within the ciliary ultrastructure is particularly important in regulating the intricate spatial and temporal control of ciliary proteins involved in ciliary beating. It would be interesting to examine how phosphatases are involved in the ciliary regulation of *Helisoma* ciliary cells.

Finally, it would be fascinating to begin to link the signal transduction pathways identified in this thesis to events within the *Helisoma* axoneme.

Cilia have fulfilled important biological roles throughout evolution. The effectiveness with which these organelles perform their function stems from their elegant design and explains why this structure has been conserved. Yet despite the ubiquity of this structure in the natural world, the regulation of ciliary activity continues to elude scientists. The aim of this study was to begin to characterize the populations of ciliary cells on the surface of *Helisoma* embryos and to further elucidate the underlying signal transduction in the cilio-excitatory response to the endogenous neurotransmitter 5-HT. Results of this study indicate that pedal and dorsolateral ciliary cells exhibit similar morphological and physiological profiles, while the SSCCs appear to be distinct. In examining the signal transduction pathways involved in the ciliary response to 5-HT in pedal ciliary cells, it was revealed that PKC may play a facilitatory role to the signal transduction cascade initiated by 5-HT or alternatively a parallel role to an additional signal transduction pathway, and that changes in $[Ca^{2+}]_i$, as mediated by both release of intracellular Ca^{2+} and Ca^{2+} influx, are critical to the response. These findings not only elaborate on the intracellular regulation of the ciliary activity within this well-characterized neural circuit in the *Helisoma* model system, but also support the growing body of knowledge about the intricate and complex regulation of this fascinating cell type that is found throughout the biological world.

Figure 40. Signal transduction underlying basal and 5-HT-stimulated ciliary beating in *Helisoma* pedal ciliary cells. NO, acting through sGC, cGMP and possibly PKG, is involved in regulating the rate of basal ciliary beating. Stimulated ciliary beating results from 5-HT binding to a membrane receptor; however, the downstream signaling cascade has not been fully elucidated. PKC participates in the ciliary response to 5-HT possibly through the phosphorylation of an intraciliary target protein or in concert with another signal transduction molecule. It has been speculated that the G-protein coupled 5-HT receptor may initiate cGMP signaling, and possibly PKG activation, to act on either intracellular Ca^{2+} stores or intraciliary targets. Stimulated ciliary beating does require an increase in $[Ca^{2+}]_i$ which acts through CaM. The source of Ca^{2+} for the initial response to 5-HT is a release from a caffeine-sensitive channel, and may involve some Ca^{2+} regulation by the mitochondria. Subsequent to Ca^{2+} release from an intracellular store, a Ca^{2+} influx is required for sustained stimulated ciliary beating. It is hypothesized that Ca^{2+} channels on the plasma membrane, necessary to refill intracellular Ca^2+ stores, are activated by a signal from the ER.

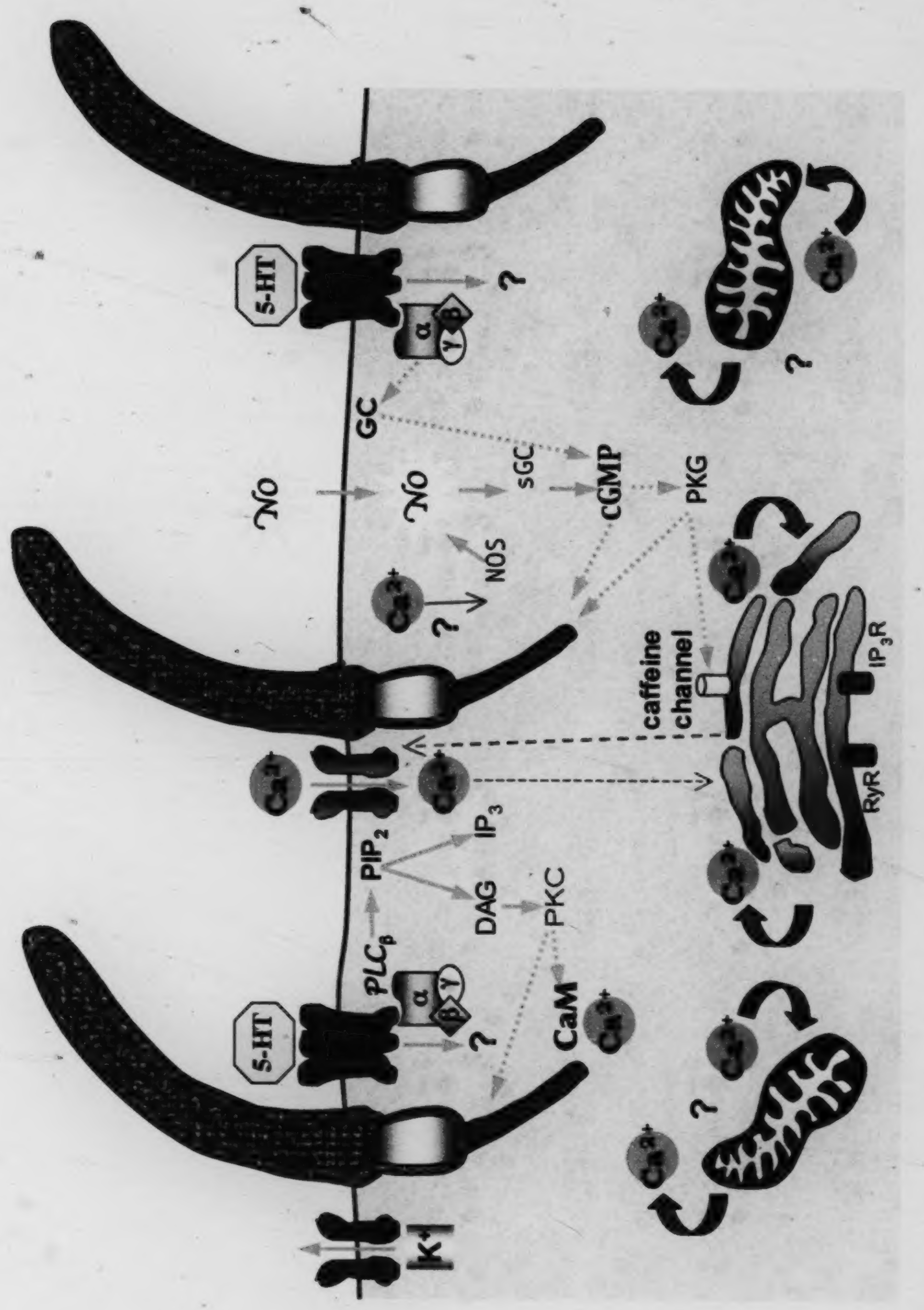
K+
5-HT
α
β
γ
PLCβ
PIP2
DAG
IP3
PKC
CaM
Ca2+
?
NO
NOS
sGC
GC
cGMP
PKG
caffeine channel
RyR
IP3R
5-HT
α
γ
β
?

Figure 41. Molecular complexity of the ciliary axoneme. A. Three dimensional schematic of the ciliary axoneme, including the central pair microtubules (purple), radial spokes (green), outer microtubule doublet (blue) and outer dynein arms (brown). The inner dynein arms (yellow) are only represented on the left proximal doublet (the outer dynein arms are absent in that location for clarity). B. Schematic cross section of a single outer outer microtubule doublet associated with the central pair microtubules. Putative kinases and phosphatases (green squares, red oval and pink and yellow triangles) are found in association with the outer dynein arms (ODA), inner dynein arms (IDA) radial spokes and central pair complex (C1 and C2). Adapted from Porter and Sale, 2000.

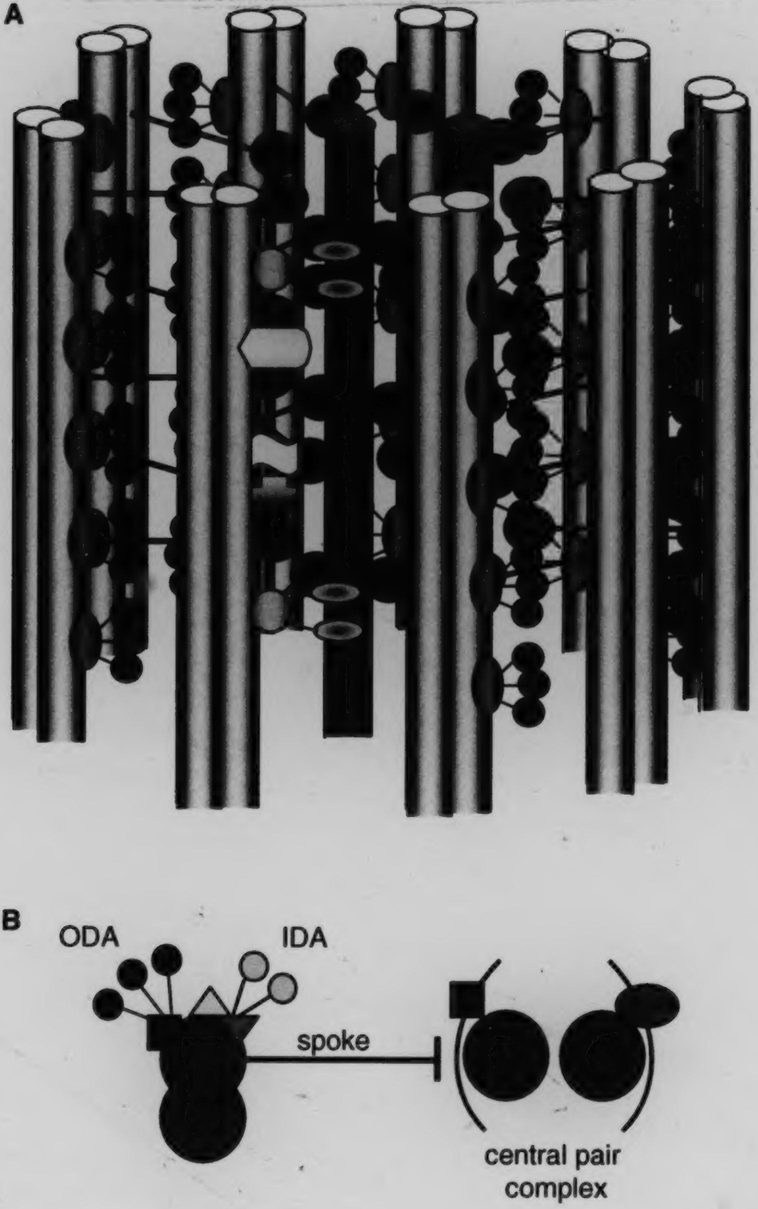
A
B
ODA
IDA
spoke
central pair complex

ENDNOTES

1 A version of this section of results has been published. Doran SA, Koss R, Tran CH, Christopher KJ, Gallin WJ and Goldberg JI. 2004. Effect of serotonin on ciliary beating and intracellular calcium concentration in identified populations of embryonic ciliary cells. J. Exp. Biol. 207: 1415-1429.

2 The technical assistance of Ron Koss for the scanning and transmission electron micrographs of cilia and ciliary cells is very greatly appreciated.

3 I wish to thank Shawn Parries for assistance with and helpful discussion about immunohistochemistry.

4 A version of this section of results has been submitted to the Canadian Journal of Physiology and Phramacology for review. Doran SA and Goldberg JI. Roles of calcium and protein kinase C in the excitatory response to serotonin in embryonic molluscan ciliary cells.

5 I wish to thank Jim Johnson for helpful discussion regarding intracellular Ca^{2+} stores pharmacology.

REFERENCES

Aiello EL. 1957. Influence of the branchial nerve and of 5-hydroxytryptamine on the ciliary activity of *Mytilus* gill. Biol. Bull. 113: 325.

Aiello E, Kennedy J and Hernandez C. 1991. Stimulation of frog ciliated cells in culture by acetylcholine and substance P. Comp. Biochem. Physiol. 99C: 497-506.

Akiba S and Sato T. 2004. Cellular function of calcium-independent phospholipase A_2. Biol. Pharm. Bull. 27: 1174-1178.

Ann KS and Nelson DL. 1995. Protein substrates for cGMP-dependent protein phosphorylation in cilia of wild-type and atlanta mutants of *Paramecium*. Cell Motil. Cytoskel. 30: 252-260.

Arkett SA. 1987. Ciliary arrest controlled by identified central neurons in a urochordate (Ascidiacea). J. Comp. Physiol. A 161: 837-847.

Arkett SA, Mackie GO and Singla CL. 1989. Neuronal organization of the acidian (Urochordata) branchial basket revealed by cholinesterase activity. Cell Tissue Res. 257: 285-294.

Arnaudeau S, Kelley WL, Walsh Jr JV, Demaurex N. 2001. Mitochondria recycle Ca^{2+} to the endoplasmic reticulum and prevent the depletion of neighboring endoplasmic reticulum regions. J. Biol. Chem. 276: 29430-29439.

Asai DJ and Brokaw CJ. 1993. Dynein heavy chain isoforms and axonemal motility. TICB 3: 398-402.

Audesirk G, McCaman RE and Willows AOD. 1979. The role of serotonin in the control of pedal ciliary activity by identified neurons in *Tritonia diomedea*. Comp. Biochem. Physiol. 62C: 87-91.

Bannai H, Yoshimura M, Takahashi K and Shingyoji C. 2000. Calcium regulation of microtubule sliding in reactivated sea urchin sperm flagella. J. Cell Sci. 113: 831-839.

Barford D. 1996. Molecular mechanisms of the protein serine/threonine phosphatases. TIBS 21: 407-412.

Beiras R and Widdows J. 1995. Effect of the neurotransmitter dopamine, serotonin and norepinephrine of the ciliary activity of mussel (*Mytilus edulis*) larvae. Marine Biology 122: 597-603.

Bennett DL, Cheek TR, Berridge MJ, De Smedt H, Parys JB, Missiaen L and Bootman MD. 1996. Expression and function of ryanodine receptors in nonexcitable cells. J. Biol. Chem. 271: 6356-6362.

Berridge MJ. 1995. Capacitative calcium entry. Biochem. J. 312: 1-11.

Berridge MJ. 2002. The endoplasmic reticulum: a multifunctional signaling organelle. Cell Calcium 32: 235-249.

Berridge MJ, Bootman MD and Lipp P. 1998. Calcium- a life and death signal. Nature 395: 645-648.

Berridge MJ, Lipp P and Bootman MD. 2000. The versatility and universality of calcium signaling. Nat. Rev. Mol. Cell Biol. 1: 11-21.

Bezprozvanny I, Bezprozvannaya S and Ehrlich BE. 1994. Caffeine-induced inhibition of inositol(1,4,5)-trisphosphate-gated calcium channels from cerebellum. Mol. Biol Cell 5: 97-103.

Bonini NM and Nelson DL. 1988. Differential regulation of *Paramecium* ciliary motility by cAMP and cGMP. J. Cell Biol. 106: 1615-1623.

Bonini NM and Nelson DL. 1990. Phosphoproteins associated with cyclic nucleotide stimulation of ciliary motility in *Paramecium*. J. Cell Sci. 95: 219-230.

Bootman MD, Lipp P and Berridge MJ. 2001. The organisation and functions of local Ca^{2+} signals. J. Cell Sci. 114: 2213-2222.

Bootman MD, Berridge MJ and Roderick HL. 2002. Calcium signalling: more messengers, more channels, more complexity. Curr. Biol. 12: R563-R565.

Bozkurt HH and Woolley DM. 1993. Morphology of nexin links in relation to interdoublet sliding in the sperm flagellum. Cell Motil. Cytoskel. 24: 109-118.

Braiman A, Zagoory O and Priel Z. 1998. PKA induces Ca^{2+} release and enhances ciliary beat frequency in a Ca^{2+}-dependent and –independent manner. Am. J. Physiol. Cell Physiol. 275: C790-C797.

Braiman A, Gold'shtein V and Priel Z. 2000. Feasibility of a sustained steep Ca^{2+} gradient in the cytosol of electrically non-excitable cells. J. Theor. Biol. 206: 115-130.

Braiman A and Priel Z. 2001. Intracellular stores maintain stable cytosolic Ca^{2+} gradients in epithelial cells by active Ca^{2+} redistribution. Cell Calcium 30: 361-371.

Brehm P and Eckert R. 1978. Calcium entry leads to inactivation of calcium channels in *Paramecium*. Science 202: 1203-1206.

Brokaw CJ. 1965. Non sinusoidal bending waves of sperm flagella. J. Exp. Biol. 43: 155-163.

Brokaw CJ. 1989. Direct measurement of sliding between outer doublet microtubules in swimming sperm flagella. Science 243: 1593-1596.

Brokaw CJ. 1999. Bending patterns of ATP-reactivated sea urchin sperm flagella following high salt extraction for removal of outer dynein arms. Cell Motil. Cytoskel. 42: 125-133.

Brose N and Rosenmund C. 2002. Move over protein kinase C, you've got company: alternative cellular effectors of diacylglycerol and phorbol esters. J. Cell Sci. 115: 4399-4411.

Bruce JIE, Giovannucci DR, Blinder G, Shuttleworth TJ and Yule DI. 2004. Modulation of $[Ca^{2+}]_i$ signaling dynamics and metabolism by perinuclear mitochondria in mouse parotid acinar cells. J. Biol. Chem. 279: 12909-12917.

Bugrim AE. 1999. Regulation of Ca^{2+} release by cAMP-dependent protein kinase. A mechanism for agonist-specific calcium signaling? Cell Calcium 25: 219-226.

Burnashev N. 1998. Calcium permeability of ligand-gated channels. Cell Calcium 24: 325-332.

Burnstock G. 1976. Purinergic receptors. J. Theor. Biol. 62: 491-503.

Camello PJ, Petersen OH and Toescu EC. 1996. Simultaneous presence of cAMP and cGMP exert a co-ordinated inhibitory effect on the agonist-evoked Ca^{2+} signal in pancreatic acinar cells. Pflugers Arch. 432: 775-781.

Casey DM, Toshiki Y, Kamiya R and Witman GB. 2003. DC3, the smallest subunit of the *Chlamydomonas* flagellar outer dynein arm-docking complex, is a redox-sensitive calcium-binding protein. J. Biol. Chem. 278: 42652-42659.

Castrodad FA, Renaud FL, Ortiz J and Phillips DM. 1988. Biogenic amines stimulate regeneration of cilia in *Tetrahymena thermophila*. J. Protozool. 35: 260-264.

Catapane EJ. 1983. Comparative study of the control of lateral ciliary activity in marine bivalves. Comp. Biochem. Physiol. 75C: 403-405.

Chameau P, Van de Vrede Y, Fossier P and Baux G. 2001. Ryanodine-, IP_3- and NAADP-dependent calcium stores control acetylcholine release. Pflugers Arch. 443: 289-296.

Chia FS, Buckland-Nicks J and Young CM. 1984. Locomotion of marine invertebrate larvae: a review. Can. J. Zool. 62: 1205-1222.

Chin D and Means AR. 2000. Calmodulin: a prototypical calcium sensor. TICB 10: 322-328.

Chini EN, Beers KW, Dousa TP. 1995. Nicotinic adenine dinucleotide phosphate (NAADP) triggers a specific calcium release system in sea urchin eggs. J. Biol. Chem. 270: 3216-3223.

Chiyotani A, Tamaoki J, Sakai N, Isono K, Kondo M and Kondo K. 1992. Thromboxane A_2 mimetic U46619 stimulates ciliary motility of rabbit tracheal epithelial cells. Prostaglandins 43: 111-120.

Christensen ST, Guerra C, Wada Y, Valentin T, Angeletti RH, Satir P and Hamasaki T. 2001. A regulatory light chain of ciliary outer arm dynein in Tetrahymena thermophila. J Biol Chem. 276: 20048-54.

Christopher KJ. 1997. Stimulation of ciliary activity by serotonin in isolated ciliated cells from *Helisoma trivolvis* embryos: involvement of cyclic AMP, Ca^{2+}, and protein kinase C. MSc. thesis. University of Alberta, Edmonton.

Christopher K, Chang JP and Goldberg JI. 1996. Stimulation of cilia beat frequency by serotonin is mediated by a Ca2+ influx in ciliated cells of Helisoma trivolvis embryos. J. Exp. Biol.199: 1105-1113.

Christopher KJ, Young KG, Chang JP and Goldberg JI. 1999. Involvement of protein kinase C in serotonin-stimulated ciliary activity in Helisoma trivolvis embryos. J. Physiol. 515: 511-522.

Chu S and Kennedy JR. 1994. Intra-epithelial palatine nerve endings and their regulation of ciliary activity of frog palate epithelium. J. Comp. Physiol. A 175: 505-518.

Cibert C. 2001. Elastic extension and jump of the flagellar nexin links: a theoretical mechanical model. Cell Motil. Cytoskel. 49: 161-175.

Clapman DE. 1995. Calcium signaling. Cell: 80: 259-268.

Cole AG, Mashikournia A, Parries SC and Goldberg JI. 2002. Regulation of early embryonic behavior by nitric oxide in the pond snail, *Helisoma trivolvis*. J. Exp. Biol. 205: 3143-3152.

Collins TJ, Lipp P, Berridge MJ and Bootman MD. 2001. Mitochondrial Ca^{2+} uptake depends on the spatial and temporal profile of cytosolic Ca^{2+} signals. J. Biol. Chem. 276: 26411-26420.

Collins TJ, Berridge MJ, Lipp P and Bootman MD. 2002. Mitochondria are morphologically and functionally heterogeneous within cells. EMBO J. 21: 1616-1627.

Cooper DMF. 2003. Regulation and organization of adenylyl cyclase. Biochem. J. 375: 517-529.

Cosson J. 1992. The covalent oscillator: a paradigm accounting for the sliding/bending mechanism and wave propagation in cilia and flagella. Biol. Cell 76: 319-327.

Croll RP and Voronezhskaya EE. 1996. Early elements in gastropod neurogenesis. Dev. Biol. 173: 344-377.

Csukai M and Mochly-Rosen D. 1999. Pharmacologic modulation of protein kinase C isozymes: the role of racks and subcellular localisation. Pharmacol. Res. 39: 253-259.

Delmas P, Crest M, and Brown DA. 2004. Functional organization of PLC signaling microdomains in neurons. TINS 27: 41-47.

Dempsey EC, Newton AC, Mochly-Rosen D, Fields AP, Reyland ME, Insel PA and Messing RO. 2000. Protein kinase C isozymes and the regulation of diverse cell responses. Am. J. Physiol. Lung Cell Mol. Physiol. 279: L429-L438.

Dentler WL. 1990. Linkages between microtubules and membranes in cilia and flagella. In: Bloodgood RA., editor, Ciliary and Flagellar Membranes. New York: Plenum Press.

Di Benedetto G, Magnus CJ, Gray PTA and Mehta A. 1991. Calcium regulation of ciliary beat frequency in human respiratory epithelium *in vitro*. J. Physiol. 439: 103-113.

Diefenbach TJ, Koehncke NK and Goldberg JI. 1991. Characterization and development of rotational behavior in Helisoma embryos: role of endogenous serotonin. J. Neurobiol. 22: 922-934.

Diefenbach TJ, Sloley BD and Goldberg JI. 1995. Neurite branch development of an identified serotonergic neuron from embryonic *Helisoma*: evidence for autoregulation by serotonin. Dev. Biol. 167: 282-293.

Diefenbach TJ, Koss R and Goldberg JI. 1998. Early development of an identified serotonergic neuron is *Helisoma trivolvis* embryos: serotonin expression, de-expression and uptake. J. Neurobiol. 34: 361-376.

Diener DR, Ang LH and Rosenbaum JL. 1993. Assembly of flagellar radial spoke proteins in *Chlamydomonas*: identification of the axoneme binding domain of radial spoke protein 3. J. Cell Biol. 123: 183-190.

Dillon RH and Fauci LJ. 2000. An integrative model of internal axoneme mechanics and external fluid dynamics in ciliary beating. J. Theor. Biol. 207: 415-430.

Doran SA, Tran N, Eskicioglu C, Stachniak T, Ahn KC and Goldberg JI. 2003. Constitutive and permissive roles of nitric oxide activity in embryonic ciliary cells. Am.J.Physiol. Regul. Integr. Comp. Physiol. 285: R348-355.

Doran SA, Koss R, Tran CH, Christopher KJ, Gallin WJ and Goldberg JI. 2004. Effect of serotonin on ciliary beating and intracellular calcium concentration in identified populations of embryonic ciliary cells. J. Exp. Biol. 207: 1415-1429.

Dremier S, Kopperud R, Doskeland SO, Dumont JE and Maenhaut C. 2003. Search for new cyclic AMP-binding proteins. FEBS Letters 546: 103-107.

Duchen MR. 1999. Contributions of mitochondria to animal physiology: from homeostatic sensor to calcium signaling and cell death. J. Physiol. 516: 1-17.

Dutcher SK, Huang B and Luck DJL. 1984. Genetic dissection of the central pair microtubules of the flagella of *Chlamydomonas reinhardtii*. J. Cell Biol. 98: 229-236.

Dutcher SK. 1995. Flagellar assembly in two hundred and fifty east-to-follow steps. TIG 11: 398-404.

Eckert R. 1972. Bioelectric control of ciliary activity. Science 176: 473-481.

Ehrlich BE, Kaftan E, Bezprozvannaya S and Bezprozvanny I. 1994. The pharmacology of intracellular Ca^{2+}-release channels. Trends Pharmacol. Sci. 15: 145-149.

Essner J J, Vogan K J, Wagner MK, Tabin CJ, Yost HJ and Brueckner M. 2002. Conserved function for embryonic nodal cilia. Nature 418: 37-38.

Evans JH and Sanderson MJ. 1999. Intracellular calcium oscillations regulate ciliary beat frequency of airway epithelial cells. Cell Calcium 26: 103-110.

Filippin L, Magalhaes PJ, Di Benedetto G, Colella M and Pozzan T. 2003. Stable interactions between mitochondria and endoplasmic reticulum allow rapid accumulation of calcium in a subpopulation of mitochondria. J. Biol. Chem. 278: 39224-39234.

Friebe A and Koesling D. 2003. Regulation of nitric oxide sensitive guanylyl cyclase. Circ. Res. 93: 96-105.

Gafni J, Munsch JA, Lam TH, Catlin MC, Costa LG, Molinski TF and Pessah IN. 1997. Xestospongins: potent membrane permeable blockers of the inositol 1,4,5-triphosphate receptor. Neuron 19: 723-733.

Gaillard AR, Diener DR, Rosenbaum JL and Sale WS. 2001. Flagellar radial spoke protein 3 in an A-kinase anchoring protein (AKAP). J. Cell Biol. 153: 443-448.

Ganitkevich VY. 2003. The role of mitochondria in cytoplasmic Ca^{2+} cycling. Exp. Physiol. 88.1: 91-97.

Gardner LC, O'Toole E, Perrone CA, Giddings T and Porter ME. 1994. Components of a "dynein regulatory complex" are located at the junction between the radial spokes and the dynein arms in *Chlamydomonas* flagella. J. Cell Biol. 127: 1311-1325.

Genazzani AA and Galione A. 1997. A Ca^{2+} release mechanism gated by the novel pyridine nucleotide, NAADP. Trends Pharmacol. Sci. 18: 108-110.

Genazzani AA, Mezna M, Dickey DM, Michelangeli F, Walseth TF and Galione A. 1997. Pharmacological properties of the Ca^{2+}-release mechanism sensitive to NAADP in the sea urchin egg. Br. J. Pharm. 121: 1489-1495.

Gertsberg I, Hellman V, Fainhstein M, Weil S, Silberberg SD, Danilenko M and Priel Z. 2004. Intracellular Ca^{2+} regulates the phosphorylation and the dephosphorylation of ciliary proteins via the NO pathway. J. Gen. Physiol. 124: 527-540.

Gheber L and Priel Z. 1989. Synchronization between beating cilia. Biophys. J. 55: 183-191.

Gibbons IR. 1995. Dynein family of motor proteins: present status and future questions. Cell Motil. Cytoskel. 32: 136-144.

Gibbons BH and Gibbons IR. 1973. The effect of partial extraction of dynein arms on the movement of reactivated sea-urchin sperm flagella. J. Cell Sci. 13: 337-357.

Goldberg JI. 1995. Neuronal development in embryos of the mollusk, *Helisoma trivolvis*: multiple roles of serotonin. Adv. Neural Sci.: 2: 67-87.

Goldberg JI and Kater SB. 1989. Expression and function of the neurotransmitter serotonin during development of the *Helisoma* nervous system. Dev. Biol. 131: 483-495.

Goldberg JI. 1998. Serotonin regulation of neurite outgrowth in identified neurons from mature and embryonic *Helisoma trivolvis*. Persp. Dev. Neurobiol. 5: 373-387.

Gray J and Hancock GJ. 1955. The propulsion of sea-urchin spermatozoa. J. Exp. Biol. 32: 802-814.

Green A, Smallman LA, Logan AC and Drake-Lee AB. 1995. The effect of temperature on nasal ciliary beat frequency. Clin. Otolaryngol. 20: 178-180.

Griffiths EJ. 2000. Use of ruthenium red as an inhibitor of mitochondrial Ca^{2+} uptake in single rat cardiomyocytes. FEBS Letters 486: 257-260.

Grynkiewicz G, Poenie M and Tsein RY. 1985. A new generation of Ca^{2+} indicators with greatly improved fluorescence properties. J. Biol. Chem. 260: 3440-3450.

Gueron S and Levit-Gurevich K. 1999. Energetic considerations of ciliary beating and the advantage of metachronal coordination. PNAS 96: 12240-12245.

Gueron S and Levit-Gurevich K. 2001. A three-dimensional model for ciliary motion based on the internal 9 + 2 structure. Proc. R. Soc. Lond. 268: 599-607.

Habermacher G and Sale WS. 1995. Regulation of dynein-driven microtubule sliding by an axonemal kinase and phosphatase in *Chlamydomonas*. Cell Motil. Cytolskel. 32: 106-109.

Habermarcher G and Sale WS. 1996. Regulation of flagellar dynein by an axonemal type-1 phosphatase in *Chlamydomonas*. J. Cell Sci. 109: 1899-1907.

Hajnoczky G, Csodas G, Madesh M and Pacher P. The machinery of local Ca^{2+} signalling between sarco-endoplasmic reticulum and mitochondria. J. Physiol. 529.1: 69-81.

Hamasaki T, Murtaugh TJ, Satir BH and Satir P. 1989. *In vitro* phosphorylation of *Paramecium* axonemes and permeabilized cells. Cell Motil. Cytoskel. 12: 1-11.

Hamasaki T, Barkalow K, Richmond J and Satir P. 1991. cAMP-stimulated phosphorylation of an axonemal polypeptide that copurifies with the 22S dynein arm regulates microtubule translocation velocity and swimming speed in *Paramecium*. Proc. Natl. Acad. Sci. USA 88: 7918-7922.

Hamasaki T, Barkalow K and Satir P. 1995. Regulation of ciliary beat frequency by a dynein light chain. Cell Motil. Cytoskel. 32: 121-124.

Hanafy KA, Krumenacker JS and Murad F. 2001. NO, nitrotyrosine, and cyclic GMP in signal transduction. Med. Sci. Monit. 7: 801-819.

Hansen M, Boitano S, Dirksen ER and Sanderson MJ. 1995. A role for phospholipase C activity but not ryanodine receptors in the initiation and propagation of intercellular calcium waves. J. Cell Sci. 108: 2583-2590.

Hinrichsen RD and Blackshear PJ. 1993. Regulation of peptide-calmodulin complexes by protein kinase C *in vivo*. Proc. Natl. Acad. Sci. 90: 1585-1589.

Holwill MEJ and Satir P. 1994. Physical model of axonemal splitting. Cell Motil. Cytoskel. 27: 287-298.

Holwill MEJ, Foster GF, Hamasaki T and Satir P. 1995. Biophysical aspects and modeling of ciliary motility. Cell Motil. Cytoskel. 32: 114-120.

Huang B, Ramanis Z and Luck DJL. 1982. Supressor mutants in *Chlamydomonas* reveal a regulatory mechanism for flagellar function. Cell 28: 115-124.

Hubbard MJ and Cohen P.. 1993. On target with a new mechanism for the regulation of protein phosphorylation. TIBS 18: 172-177.

Hug H and Sarre TF. 1993. Protein kinase C isoenzymes: divergence in signal transduction? Biochem. J. 291: 329-343.

Hunter T and Vogel S. 1985. Spinning embryos enhance diffusion through gelatinous egg masses. J. Exp. Mar. Biol. Ecol. 96: 303-308.

Iwadate Y. 2003. Photolysis of caged calcium in cilia induces ciliary reversal in *Paramecium caudatum*. J. Exp. Biol. 206: 1163-1170.

Iwadate Y and Suzaki T. 2004. Ciliary reorientation is evoked by a rise in calcium level over the entire cilium. Cell Motil. Cytoskel. 57: 197-206.

Jacobson J and Duchen MR. 2004. Interplay between mitochondria and cellular calcium signalling. Mol. Cell. Biochem. 256.257: 209-218.

Jain B, Rubinstein I, Robbins RA, Leise KL and Sisson JH. 1993. Modulation of airway epithelial cell ciliary beat frequency by nitric oxide. Biochem. Biophys. Res. Comm. 191: 83-88.

Jin I and Hawkins RD. 2003. Presynaptic and postsynaptic mechanisms of a novel form of homosynaptic potentiation at *Aplysia* sensory-motor neuron synapses. J. Neurosci. 23: 7288-7297.

Johnson JD and Chang JP. 2000. Function- and agonist-specific Ca^{2+} signaling: the requirement from and mechanism of spatial and temporal complexity in Ca^{2+} signals. Biochem. Cell Biol. 78: 217-240.

Kamiya R. 1995. Exploring the function of inner and outer dynein arms with *Chlamydomonas* mutants. Cell Motil. Cytoskel. 32: 98-102.

Kargacin GJ, Ali Z and Kargacin ME. 1998. Ruthenium red reduces the Ca^{2+} sensitivity of Ca^{2+} uptake into cardiac sarcoplasmic reticulum. Pflugers Arch. 436: 338-342.

Kikushima K, Yagi T and Kamiya R. 2004. Slow ADP-dependent acceleration of microtubule translocation produced by an axonemal dynein. FEBS Letters 563: 119-122.

Kimura Y, Yoshida M and Morisawa M. 2003. Interaction between noradrenaline or adrenaline and the beta 1-adrenergic receptor in the nervous system triggers early metamorphosis of larvae in the ascidian, *Ciona savignyi.* Dev. Biol. 258: 129-140.

King SM. 2000. The dynein microtubule motor. Biochimica et Biophysica Acta. 1496: 60-75.

King SM. 2003. Organization and regulation of the dynein microtubule motor. Cell Biol. Int. 27: 213-215.

King SM and Witman GB. 1988. Structure of the alpha and beta heavy chains of the outer arm dynein from *Chlamydomonas* flagella. Location of epitopes and protease-sensitive sites. J. Biol. Chem. 263: 9244-9255.

Kits KS and Mansvelder HD. 1996. Voltage gated calcium channels in molluscs: classification, Ca^{2+}-dependent inactivation, modulation and functional roles. Inverte. Neurosci. 2: 9-34.

Kobayashi K, Tamaoki J, Sakai N, Chiyotani A and Takizawa T. 1988. Inhibition of ciliary activity by phorbol esters in rabbit tracheal epithelial cell. Lung 167: 277-284.

Konishi M and Watanabe M. 1995. Resting cytoplasmic free Ca^{2+} concentration in frog skeletal muscle measured with fura 2 conjugated to high molecular weight dextran. J. Gen. Physiol. 106: 1123-1150.

Kopperud R, Krakstad C, Selheim F and Doskeland SO. 2003. cAMP effector mechanisms. Novel twists for an 'old' signaling system. FEBS Letters 546: 121-126.

Korngreen A and Priel Z. 1996. Purinergic stimulation of rabbit ciliated airway epithelia: control by multiple calcium sources. J. Physiol. 497.1: 53-66.

Koshtoyants KS, Buznikov GA and Manukhin BN. 1961. The possible role of 5-hydroxytryptamine in the motor activity of embryos of some marine gastropods. Comp. Biochem. Physiol. 3: 20-26.

Koss R, Diefenbach TJ, Kuang S, Doran SA and Goldberg JI. 2003. Coordinated development of identified serotonergic neurons and their target ciliary cells in *Helisoma trivolvis* embryos. J. Comp. Neurol. 457: 313-325.

Krumenacker JS, Hanafy KA and Murad F. 2004. Regulation of nitric oxide and soluble guanylyl cyclase. Brain Res. Bull. 62: 505-515.

Kuang S. 2002. Dual function sensorimotor neurons mediate a behavioral response to hypoxia in embryos of *Helisoma trivolvis*. Ph.D. thesis. University of Alberta, Edmonton.

Kuang S and Goldberg JI. 2001. Laser ablation reveals regulation of ciliary activity by serotonergic neurons in molluscan embryos. J. Neurobiol. 47: 1-15.

Kuang S, Doran SA, Wilson RJA, Goss GG and Goldberg JI. 2002. Serotonergic sensory-motor neurons mediate a behavioral response to hypoxia in pond snail embryos. J. Neurobiol. 52: 73-83.

Kultgen PL, Byrd SK, Ostrowski LE and Milgram SL. 2002. Characterization of an A-kinase anchoring protein in human ciliary axonemes. Molec. Biol. Cell 13: 4156-4166.

Lansley AB, Sanderson MJ and Dirksen ER. 1992. Control of the beat cycle of respiratory tract cilia by Ca^{2+} and cAMP. Am. J. Physiol. 263: L232-L242.

Lansley AB and Sanderson MJ. 1999. Regulation of airway ciliary activity by Ca^{2+}: simultaneous measurement of beat frequency and intracellular Ca^{2+}. Biophys. J. 77: 629-638.

LeDizet M and Piperno G. 1995. The light chain p28 associates with a subset of inner dynein arm heavy chains in *Chlamydomonas* axonemes. Mol. Biol. Cell 6: 697-711.

Levin R, Braiman A and Priel Z. 1997. Protein kinase C induced calcium influx and sustained enhancement of ciliary beating by extracellular ATP. Cell Calcium 21: 103-113.

Li D, Shirakami G, Zhan X and Johns RA. 2000. Regulation of ciliary beat frequency by the nitric oxide-cyclic guanosine monophosphate signaling pathway in rat airway epithelial cells. Am. J. Respir. Cell Mol. Biol. 23: 175-181.

Lieb T, Frei CW, Frohock JI, Bookman RJ and Salathe M. 2002. Prolonged increase in ciliary beat frequency after short-term purinergic stimulation in human airway epithelial cells. J. Physiol. 538.2: 633-646.

Lindemann CB. 1994. A model of flagellar and ciliary functioning which uses the forces transverse to the axoneme as the regulator of dynein activity. Cell Motil Cytoskel. 29: 141-154.

Lindemann CB and Kanous KS. 1995. "Geometric Clutch" hypothesis of axonemal function: key issues and testable predictions. Cell Motil. Cytoskel. 31: 1-8.

Linder JU and Schultz JE. 2003. The class III adenylyl cyclases: multipurpose modules. Cell. Signalling 15: 1081-1089.

Luck DJL. 1984. Genetic and biochemical dissection of the eukaryotic flagellum. J. Cell Biol. 98: 789-794.

Lytton J, Westlin M and Hanley MR. 1991. Thapsigargin inhibits the sarcoplasmic or endoplasmic reticulum Ca-ATPase family of calcium pumps. J. Biol. Chem. 277: 17067-17071.

Ma W, Silberberg SD and Priel Z. 2002. Distinct axonemal processes underlie spontaneous airway ciliary activity. J. Gen. Physiol. 120: 875-885.

Machemer H. 1972. Ciliary activity and the origin of metachronism in *Paramecium*: effects of increased viscosity. J. Exp. Biol. 57: 239-259.

Mapara S, Goldberg JI and Gallin WJ. 2001. Cloning, phylogenetic analysis and localization of two serotonin receptors from the pond snail *Helisoma trivolvis*. Soc. Neurosci. Abs. 786.4

Marois R and Carew TJ. 1997. Projection patterns and target tissues of the serotonergic cells in larval *Aplysia californica*. J. Comp. Neurol. 386: 491-506.

Marsden JR and Hassessian H. 1986. Effects of Ca^{2+} and catecholamine on swimming cilia of the trochophore larva of the polychaete *Spirobranchus giganteus* (Pallas). J. Exp. Mar. Biol. Ecol. 95: 245-255.

Maruyama I. 1984. Conflicting effects of noradrenalin on ciliary movement of frog palatine mucosa. Eur. J. Pharmacol. 97: 239-245.

Maruyama I, Yamamoto T, Ochi J, Nakai Y and Yamada S. 1983. Dopaminergic innervation and inhibition of ciliary movement in the epithelium of frog palatine mucosa. Eur. J. Pharmacol. 90: 325-331.

Maruyama I, Inagaki M and Momose K. 1984. The role of serotonin in mucociliary transport system in the ciliated epithelium of frog palatine mucosa. Eur. J. Pharmacol. 106: 499-506.

Matlib MA, Zhou Z, Knight S, Ahmed S, Choi KM, Krause-Bauer J, Phillips R, Altschuld R, Katsube Y, Sperelakis N and Bers DM. 1998. Oxygen-bridged dinuclear ruthenium amine complex specifically inhibits Ca^{2+} uptake into mitochondria *in Vitro* and *in Situ* in single cardiac myocytes. J. Biol. Chem. 273: 10223-10231.

Maurer DR and Liebman J. 1988. Effects of ethanol on *in vitro* ciliary motility. J. Appl. Physiol. 65: 1617-1620.

Matsuyama H, Takahashi H, Watanabe K, Fujimaki Y and Aoki Y. 2004. The involvement of cyclic adenosine monophosphate in the control of schistosome miracidium cilia. J. Parasitol. 90: 8-14.

Mellor H and Parker PJ. 1998. The extended protein kinase superfamily. Biochem. J. 332: 281-292.

Miglietta LAP and Nelson DL. A novel cGMP-dependent protein kinase from *Paramecium*. J. Biol. Chem. 263: 16096-16105.

Minoura I, Yagi T and Kamiya R. 1999. Direct measurement of inter-doublet elasticity in flagellar axonemes. Cell Struct. Func. 24: 27-33.

Mogami Y, Watanbe K, Ooshima C, Kawano A and Baba SA. 1992. Regulation of ciliary movement in sea urchin embryos: dopamine and 5-HT change the swimming behavior. Comp. Biochem. Physiol. 101C: 251-254.

Momayezi M, Kissmehl R and Plattner H. 2000. Quantitative immunogold localization of protein phosphatase 2B (calcineurin) in *Paramecium* cells. J. Histochem. Cytochem. 48: 1269-1281.

Morales B, Barrera N, Uribe P, Mora C and Villalon M. 2000. Functional cross talk after activation of P2 and P1 receptors in oviductal ciliated cells. Am. J. Physiol. Cell Physiol. 279: C658-C669.

Morse DM, Smullen JL and Davis CW. 2001. Differential effects of UTP, ATP and adenosine on ciliary activity of human nasal epithelial cells. Am. J. Physiol. Cell Physiol. 280: C1485-C1497.

Murakami A. 1983. Control of ciliary beat frequency in *Mytilus*. J. Submicrosc. Cytol. 15: 313-316.

Murakami A. 1987. Control of ciliary beat frequency in the gill of *Mytilus* – I. Activation of the lateral cilia by cyclic AMP. Comp. Biochem. Physiol. 86C: 273-279.

Murakami A and Eckert R. 1972. Cilia: activation coupled to mechanical stimulation by calcium influx. Science 175: 1375-1377.

Murakami A and Takahashi K. 1975. Correlation of electrical and mechanical responses in nervous control of cilia. Nature 257: 48-49.

Murakami A and Machemer H. 1982. Mechanoreception and signal transmission in the lateral ciliated cells on the gill of *Mytilus*. J Comp. Physiol. 145: 351-362.

Muto E, Kamiya R and Tsukita S. 1991. Double rowed organization of inner arms in *Chlamydomonas* flagella revealed by tilt series, thin-section electron microscopy. J. Cell Sci. 99:57-66.

Mwimbi XKMS, Muimo R, Treharne KJ, Sijumbila G, Green M and Mehta A. 2002. 4α-phorbol negates the inhibitory effects of phorbol-12-myristate-13-acetate on human cilia and alters the phosphorylation of PKC. FEBS Letters 530: 31-36.

Mwimbi XK, Muimo R, Green MW and Mehta A. 2003. Making human nasal cilia beat in the cold: a real time assay for cell signalling. Cell Signal. 15: 395-402.

Naitoh Y and Eckert R. 1969. Ionic mechanisms controlling behavioral responses of *Paramecium* to mechanical stimulation. Science 164: 963-965.

Naitoh Y and Eckert R. 1972. The control of ciliary activity in protozoa. In: Sleigh MA, editor, Cilia and flagella. New York: Academic Press.

Nakamura S and Tamm SL. 1985. Calcium control of ciliary reversal in ionophore-treated and ATP-reactivated comb plates of ctenophores. J. Cell Biol. 100: 1447-1454.

Nakano I, Kobayashi T, Yoshimura M and Shingyoji C. 2002. Central-pair-linked regulation of microtubule sliding by calcium in flagellar axonemes. J. Cell Sci. 116: 1627-1636.

Nakaoka Y, Tanaka H and Oosawa F. 1984. Ca^{2+}-dependent regulation of beat frequency of cilia in *Paramecium*. J. Cell Sci. 65: 223-231.

Nakaoka Y, Tokioka R, Shinozawa T, Fujita J and Usukura J. 1991. Photoreception of *Paramecium* cilia: localization of photosensitivity and binding with anti-frog rhodopsin IgG. J. Cell Sci. 99: 67-72.

Nakaoka Y and Iwatsuki K. 1992. Hyperpolarization-activated inward current associated with the frequency increase in ciliary beating of *Paramecium*. J. Comp. Physiol. A 170: 723-727.

Nguyen T, Chin WC, O'Brien JA, Verdugo P and Berger AJ. 2001. Intracellular pathways regulating ciliary beating of rat brain ependymal cells. J. Physiol. 531.1: 131-140.

Nlend MC, Bookman RJ, Conner GE and Salathe M. 2002. Regulator of G-protein 2 modulates purinergic calcium and ciliary beat frequency responses in airway epithelia. Am. J. Respir. Cell Mol. Biol. 27: 436-445.

Noguchi M, Sasaki JY, Kamachi H and Inoue H. 2003. Protein phosphatase 2C is involved in the cAMP-dependent ciliary control in *Paramecium caudatum*. Cell Motil. Cytoskel. 54: 95-104.

Omoto CK and Kung C. 1979. The pair of central tubules rotates during ciliary beat of *Paramecium*. Nature 279: 532-534.

Omoto CK and Witman GB. 1981. Functionally significant central-pair rotation in a primitive eukaryotic flagellum. Nature 290: 708-710.

Omoto CK, Yagi T, Kurimoto E and Kamiya R. 1996. Ability of paralyzed flagella mutants of *Chlamydomonas* to move. Cell Motil. Cytoskel. 33: 88-94.

Omoto CK, Gibbons IR, Kamiya R, Shingyoji C, Takahashi K and Witman GB. 1999. Rotation of the central pair microtubules in eukaryotic flagella. Mol. Biol. Cell 10: 1-4.

Ovadyahu D, Eshel D and Priel Z. 1988. Intensification of ciliary motility by extracellular ATP. Biorheology 25: 489-501.

Paparo AA and Murphy JA. 1975a. The effect of Ca on the rate of beating of lateral cilia in *Mytilus edulis* – I. A response to perfusion with 5-HT, DA, BOL and PBZ. Comp. Biochem. Physiol. 50C: 9-14.

Paparo AA and Murphy JA. 1975b. The effect of Ca on the rate of beating of lateral cilia in *Mytilus edilus* – II. A response to electrical stimulation of the branchial nerve. Comp. Biochem. Physiol. 50C: 15-19.

Paparo AA and Murphy JA. 1978. Cilioexcitatory and cilioinhibitory processes initiated by light on two identifiable neuronal pigments in *Mytilus edilus*. J. Exp. Biol. 76: 47-61.

Paradiso AM, Mason SJ, Lazarowski ER and Boucher RC. 1995. Membrane-restricted regulation of Ca^{2+} release and influx in polarized epithelia. Nature 377: 643-646.

Parekh AB. 2003a. Mitochondrial regulation of intracellular Ca^{2+} signaling: more than just simple Ca^{2+} buffers. News Physiol. Sci. 18: 252-256.

Parekh AB. 2003b. Store-operated Ca^{2+} entry: dynamic interplay between endoplasmic reticulum, mitochondria and plasma membrane. J. Physiol. 547.2: 333-348.

Park MK, Ashby MC, Erdemli G, Petersen OH, Tepikin AV. 2001. Perinuclear, perigranular and sub-plasmalemmal mitochondria have distinct functions in the regulation of cellular calcium transport. EMBO J. 20: 1863-1874.

Patel-King RS, Benashki SE, Harrison A and King SM. 1996. Two functional thioredoxins containing redox-sensitive vicinal dithiols from the *Chlamydomonas* outer dynein arms. J. Biol. Chem. 271: 6283-6291.

Patel-King RS, Gorbatyuk O, Takebe S and King SM. 2004. Flagellar radial spokes contain a Ca^{2+}-stimulated nucleotide diphosphate kinase. Molec. Biol. Cell 15: 3891-3902.

Pavlova GA, Willows AO and Gaston MR. 1999. Serotonin inhibits ciliary transport in esophagus of the nudibranch mollusk *Tritonia diomedea*. Acta. Biol. Hung. 50: 175-184.

Pazour GJ and Witman GB. 2003. The vertebrate primary cilium is a sensory organelle. Curr. Opin. Cell Biol. 15: 105-110.

Pires A, Coon SL and Hadfield MG. 1997. Catecholamines and dihydroxyphenylalanine in metamorphosing larvae of the nudibranch *Phestilla sibogae Bergh* (Gastropoda: Opisthobranchia). J. Comp. Physiol. (A) 181: 187-194.

Piperno G, Huang B, Ramanis Z and Luck DJ. 1981. Radial spokes of *Chlamydomonas* flagella: polypeptide composition and phosphorylation of stalk components. J. Cell Biol. 88: 73-79.

Piperno G, Mead K, LeDizet M and Moscatelli A. 1994. Mutations in the "dynein regulatory complex" alter the ATP-insensitive binding sites for inner dynein arms in *Chlamydomonas* axonemes. J. Cell Biol. 125: 1109-1117.

Pizzo P, Fasolato C and Pozzan T. 1997. Dynamic properties of an inositol 1,4,5-triphosphate- and thapsigargin-insensitive calcium pool in mammalian cell lines. J. Cell. Biol. 136: 355-366.

Plattner H and Klauke N. 2001. Calcium in ciliated protozoa: sources, regulation, and calcium-regulated cell functions. Int. Rev. Cytol. 201: 115-208.

Porter ME. 1996. Axonemal dyneins: assembly, organization and regulation. Curr. Opin. Cell Biol. 8: 10-17.

Pozzan T, Rizzuto R, Volpe P and Meldolesi J. 1994. Molecular and cellular physiology of intracellular calcium stores. Physiol. Rev. 74: 595-636.

Preston RR and Saimi Y. 1990. Calcium ions and the regulation of motility in *Paramecium*. In: Bloodgood RA., editor, Ciliary and Flagellar Membranes. New York: Plenum Press.

Rebecchi MJ and Pentyala SN. 2000. Structure, function, and control of phosphoinositide-specific phospholipase C. Physiol. Reviews 80: 1292-1335.

Reed W and Satir P. 1980. Calmodulin in mussel gill epithelial cells: role in ciliary arrest. Annu. N.Y. Acad. Sci. 356: 423-426.

Rivera JA. 1962. Volume 15: Cilia, ciliated epithelium, and ciliary activity. In: Alexander P and Bacg ZM, general editors, International Series of Monographs on Pure and Applied Biology. New York: Pergamon Press Inc.

Rizo J and Sudhof TC. 1998. C_2-domains, structure and function of a universal Ca^{2+}-binding domain. J. Biol. Chem. 273: 15879-15882.

Rizzuto R, Bernardi P and Pozzan T. 2000. Mitochondria as all-round players in the calcium game. J. Physiol. 529.1: 37-47.

Ruvolo PR. Intracellular signal transduction pathways activated by ceramide and its metabolites. Pharmacol. Research 47: 383-392.

Sakato M and King SM. 2003. Calcium regulates ATP-sensitive microtubule binding by *Chlamydomonas* outer arm dynein. J. Biol. Chem. 278: 43571-43579.

Salathe M, Pratt MM and Wanner A. 1993a. Cyclic AMP-dependent phosphorylation of a 26 kD axonemal protein in ovine cilia isolated from small tissue pieces. Am. J. Respir. Cell Mol. Biol. 9: 306-314.

Salathe M, Pratt MM and Wanner A. 1993b. Protein kinase C phosphorylation of a ciliary membrane protein and inhibition of ciliary beating. J. Cell Sci. 106: 1211-1220.

Salathe M and Bookman RJ. 1995. Coupling of [Ca2+]i and ciliary beating in cultured tracheal epithelial cells. J. Cell Sci. 108: 431-440.

Salathe M, Lipson EJ, Ivonnet PI and Bookman RJ. 1997. Muscarinic signaling in ciliated tracheal epithelial cells: dual effects of Ca^{2+} and ciliary beating. Am. J. Physiol. Lung Cell. Mol. Physiol. 272: L301-L310.

Salathe M and Bookman RJ. 1999. Mode of Ca^{2+} action on ciliary beat frequency in single ovine airway epithelial cells. J. Physiol. 520.3: 851-865.

Salathe M, Lieb T and Bookman RJ. 2000. Lack of nitric oxide involvement in cholinergic modulation of ovine ciliary beat frequency. J. Aerosol Med. 13: 219-229.

Salathe M, Ivonnet PI, Lieb T and Bookman RJ. 2001. Agonist-stimulated calcium decreases in ovine ciliated airway epithelial cells: role of mitochondria. J. Physiol. 531.1: 13-26.

Sale WS and Satir P. 1977. Direction of active sliding of microtubules in *Tetrahymena* cilia. Proc. Natl. Acad. Sci. USA 74: 2045-2049.

Sanders MA and Salisbury JL. 1989. Centrin-mediated microtubule severing during flagellar excision in *Chlamydomonas reinhardtii*. J. Cell Biol. 105: 1799-1805.

Sanderson MJ and Dirksen ER. 1986. Mechanosensitivity of cultured ciliated cells from mammalian respiratory tract: implications for the regulation of mucociliary transport. Proc. Natl. Acad. Sci. USA: 83: 7302-7306.

Saraste M, Sibbald PR and Wittinghofer A. 1990. The P-loop – a common motif in ATP and GTP-binding proteins. TIBS 15: 430-434.

Satir P. 1968. Studies on cilia: III. Further studies on the cilium tip and a "sliding filament" model of ciliary motility. J. Cell Biol. 26: 345-365.

Satir P. 1995. Landmarks in cilia research from Leeuwenhoek to us. Cell. Motil. Cytoskel. 32: 90-94.

Satir P, Wais-Steder J, Ledbuska S, Nasr A and Avolio J. 1981. The mechanochemical cycle of the dynein arm. Cell Motility 1: 303-327.

Satir P and Matsuoka T. 1989. Splitting the axoneme: implications for a "switch-point" model of dynein activity in ciliary motion. Cell Motil. Cytoskel. 14: 345-358.

Satir P and Sleigh MA. 1990. The physiology of cilia and mucociliary interactions. Annu. Rev. Physiol. 52: 137-155.

Satir P, Baralow K and Hamasaki T. 1993. The control of ciliary beat frequency. TICB 3: 409-412.

Sawisky GR. 2004. A study of the intracellular signalling mechanisms in PACAP-stimulated GH and GTH-II secretion in goldfish pituitary cells. MSc. thesis. University of Alberta, Edmonton.

Schoppe J, Hochstrate P and Schule WR. 1997. Caffeine mediates cation influx and intracellular Ca^{2+} release in leech P neurons. Cell Calcium 22: 385-397.

Schultz JE, Grunemund R, Hirschhausen RV and Schonefeld U. 1984. Ionic regulation of cyclic AMP levels in *Paramecium tetraurelia*. FEBS Letters 167: 113-116.

Schultz JE, Klumpp S, Benz R, Schurhoff-Goeters WJ and Schmid A. 1992. Regulation of adenylyl cyclase from *Paramecium* by an intrinsic potassium conductance. Science 255: 600-603.

Silvester NR. 1988. Hydrodynamics of flow in *Mytilus* gills. J. Exp. Mar. Biol. Ecol. 120: 171-182.

Sim ATR and Scott JD. 1999. Targeting of PKA, PKC and protein phosphatases to cellular microdomains. Cell Calcium 26: 209-217.

Sisson JH. 1995. Ethanol stimulates apparent nitric oxide-dependent ciliary beat frequency in bovine airway epithelial cells. Am. J. Physiol. 268: L596-L600.

Sitsapesan R, McGarry SJ and Williams AJ. 1995. Cyclic ADP-ribose, the ryanodine receptor and Ca^{2+} release. TIPS 16: 386-391.

Sleigh MA. 1966. The co-ordination and control of cilia. Symp. Soc. Exp. Biol. 20: 11-31.

Smith EF. 2002a. Regulation of flagellar dynein by the axonemal central apparatus. Cell Motil. Cytoskel. 52: 33-42.

Smith EF. 2002b. Regulation of flagellar dynein by calcium and a role for an axonemal calmodulin and calmodulin-dependent kinase. Mole. Biol. Cell 13: 3303-3313.

Smith EF and Sale WS. 1992. Regulation of dynein-driven microtubule sliding by the radial spokes in flagella. Science 257: 1557-1559.

Smith EF and Lefebvre PA. 1997. The role of central apparatus components in flagellar motility and microtubule assembly. Cell Motil. Cytoskel. 38: 1-8.

Smith JR. 1982. A survey of endogenous dopamine and serotonin in ciliated and nervous tissue of five marine bivalves, with evidence for specific, high-affinity dopamine receptors in ciliated tissue of *Mytilus californianus*. Comp. Biochem. Physiol. 71C: 57-61.

Soliman S. 1983. Pharmacological control of ciliary activity in the young sea urchin larva. Effects of monoaminergic agents. Comp. Biochem. Physiol. 760: 181-191.

Soliman S. 1984. Pharmacological control of ciliary activity in the young sea urchin larva. Studies on the role of Ca2+ and cyclic nucleotides. Comp Biochem Physiol C. 178: 183-91.

Springett GM, Kawasaki H and Spriggs DR. 2004. Non-kinase second-messenger signaling: new pathways with new promise. BioEssays 26: 730-738.

Stefano GB, Catapane EJ and Stefano JM. 1977. Temperature dependent ciliary rhythmicity in *Mytilus edilus* and the effects of monoaminergic agents on its manifestation. Biol. Bull. 153: 618-629.

Stephens RE and Prior G. 1992. Dynein from serotonin-activated cilia and flagella: extraction characteristics and distinct sites for cAMP-dependent protein phosphorylation. J. Cell Sci. 103: 999-1012.

Strommel EW. 1984a. Calcium regenerative potentials in *Mytilus edulis* gill abfrontal epithelial cells. J. Comp. Physiol. A 155: 445-456.

Strommel EW. 1984b. Calcium activation of mussel gill abfrontal cilia. J. Comp. Physiol. A 155: 457-469.

Strommel EW. 1986. Mechanical stimulation activates beating in calcium-arrested lateral cilia of *Mytilus edulis* gill. J. Muscle Res. Cell Motil. 7: 237-244.

Strommel EW and Stephens RE. 1985. Cyclic AMP and calcium in the differential control of *Mytilus* gill cilia. J. Comp. Physiol. A. 157: 451-459.

Summers KE and Gibbons IR. 1971. Adenosine triphosphate induced sliding of tubules in trypsin-treated flagella of sea urchin sperm. Proc. Natl. Acad. Sci. USA 68: 3092-3096.

Sutto Z, Conner GE and Salathe M. 2004. Regulation of human airway ciliary beat frequency by intracellular pH. J. Physiol. 560.2: 519-532.

Syed NI and Winlow W. 1989. Morphology and electrophysiology of neurons innervating the ciliated locomotor epithelium in *Lymnaea stagnalis* (L). Comp. Biochem. Physiol. 93A: 633-644.

Tamaoki J, Kondo M and Takizawa T. 1989. Effect of cAMP on ciliary function in rabbit tracheal epithelial cell. J. Appl. Physiol. 66: 1035-1039.

Tamaoki J, Chiyotani A, Sakai N and Konno K. 1993. Stimulation of ciliary motility mediated by atypical beta-adrenoreceptor in canine bronchial epithelium. Life Sci. 53: 1509-1515.

Tamaoki J, Kondo M, Takeuchi S, Takemura H and Nagai A. 1998. Vasopressin stimulates ciliary motility of rabbit tracheal epithelium: role of V_{1b} receptor-mediated Ca^{2+} mobilization. Am. J. Respir. Cell Mol. Biol. 19: 293-299.

Tamm SL. 1988. Calcium activation of macrocilia in the ctenophore *Beroe*. J. Comp. Physiol. A 163: 23-31.

Tamm S. 1994. Ca^{2+} channels and signalling in cilia and flagella. TICB 4: 305-310.

Tamm SL and Terasaki M. 1994. Visualization of calcium transients controlling orientation of ciliary beat. J. Cell. Biol. 125: 1127-1135.

Tang YG and Zucker RS. 1997. Mitochondrial involvement in post-tetanic potentiation of synaptic transmission. Neuron 18: 483-491.

Tarasiuk A, Bar-Shimon M, Gheber L, Korngreen A, Grossman Y and Priel Z. 1995. Extracellular ATP induces hyperpolarization and motility stimulation of ciliary cells. Biophys. J. 68: 1163-1169.

Tarran R, Argent BE and Gray MA. 2000. Regulation of a hyperpolarization-activated chloride current in murine respiratory ciliated cells. J. Physiol. 524.2: 353-364.

Tasken K and Aandahl EM. 2004. Localized effects of cAMP mediated by distinct routes of protein kinase A. Physiol. Rev. 84: 137-167.

Taylor HC, Satir P and Holwill MEJ. 1999. Assessment of inner dynein arm structure and possible function in ciliary and flagellar axonemes. Cell Motil. Cytoskel. 43: 167-177.

Thastrup O, Cullen PJ, Drobak BK, Hanley MR and Dawson AP. 1990. Thapsigargin, a tumor promoter, discharges intracellular Ca2+ stores by specific inhibition of the endoplasmic reticulum Ca2(+)-ATPase. PNAS 87: 2466-2470.

Tombal B, Denmeade SR and Isaacs JT. 1999. Assessment and validation of a microinjection method for kinetic analysis of $[Ca^{2+}]_i$ in individual cells undergoing apoptosis. Cell Calcium 25: 19-28.

Tsein RW and Tsien RY. 1990. Calcium channels, stores and oscillations. Annu. Rev. Cell Biol. 6: 715-760.

Uhler GC, Huminski PT, Les FT and Fong PP. 2000. Cilia-driven rotational behavior in gastropod (*Physa elliptica*) embryos induced by serotonin and putative serotonin reuptake inhibitors (SSRIs). J. Exp. Zool. 286: 414-421.

Uzlaner N and Priel Z. 1999. Interplay between the NO pathway and elevated $[Ca^{2+}]_i$ enhances ciliary activity in rabbit trachea. J Physiol. 516.6: 179-190.

Varhaus EF and Deyup IJ. 1953. The effect of ATP on cilia of the pharyngeal mucus of the frog. Science 6: 553-554.

Verdugo P. 1980. Ca^{2+}-dependent hormonal stimulation of ciliary activity. Nature 283: 764-765.

Voronezhskaya EE, Hiripi L, Elekes K and Croll RP. 1999. Development of catecholaminergic neurons in the pond snail, *Lymnaea stagnalis*: I. Embryonic development of dopamine-containing neurons and dopamine-dependent behaviors. J. Comp. Neurol. 404: 285-296.

Wada Y, Mogaml Y and Baba SA. 1997. Modification of ciliary beating in sea urchin larvae induced by neurotransmitters: beat-plane rotation and control of frequency fluctuations. J. Exp. Biol. 200: 9-18.

Walczak CE and Nelson DL. 1993. *In vitro* phosphorylation of ciliary dyneins by protein kinases from *Paramecium*. J. Cell Sci. 106: 1369-1376.

Wargo MJ and Smith EF. 2003. Asymmetry of the central apparatus defines the location of active microtubule sliding in *Chlamydomonas* flagella. PNAS 100: 137-142.

Wargo MJ, McPeek MA and Smith EF. 2004. Analysis of microtubule sliding patterns in *Chlamydomonas* flagellar axonemes reveals dynein activity on specific doublet microtubules. J. Cell Sci. 117: 2533-2544.

Warner FD. 1976. Ciliary inter-microtubule bridges. J. Cell Sci. 20: 101-114.

Weisman Z, Fink A, Alon A, Poliak Z, Tabachnik E, Priscu L and Bentwich Z. 1990. Leukotriene C4 decreases the activity of respiratory cilia *in vitro*. Clin. Exp. Allergy 20: 389-393.

Weiss T, Gheber L, Shoshan-Barnatz V and Priel Z. 1992. Possible mechanism of ciliary stimulation by extracellular ATP: involvement of calcium-dependent potassium channels and exogenous Ca^{2+}. J. Membrane Biol. 127: 185-193.

Willows AOD, Pavlova GA and Philips NE. 1997. Modulation of ciliary beat frequency by neuropeptides from identified molluscan neurons. J. Exp. Biol. 200: 1433-1439.

Wirschell M, Pazour G, Yoda A, Hirono M, Kamiya R and Witman GB. 2004. Oda5p, a novel axonemal protein required for the assembly of the outer dynein arm and an associated adenylate kinase. Mol. Biol. Cell 15: 2729-2741.

Witman GB. 1990. Introduction to cilia and flagella. In: Bloodgood RA., editor, Ciliary and Flagellar Membranes. New York: Plenum Press.

Wong LB, Park CL and Yeates DB. 1998. Neuropeptide Y inhibits ciliary beat frequency in human ciliated cells via nPKC, independently of PKA. Am. J. Physiol. Cell Physiol. 275: C440-C448.

Wood RL and Luft JH. 1965. The influence of buffer systems on fixation with osmium tetroxide. J. Ultrastruct. Res. 12: 22-45.

Woodward OM, Cain SD, Pavlova GA and Willows AOD. 2002. CNS modulation of Cl^- currents in ciliated foot epithelial cells controls locomotion in *Tritonia diomedea*. Soc. Neurosci. Abstr. 465.14.

Woodward OM and Willows AOD. 2003. CNS modulation of calcium activated chloride current in pedal epithelial cells controls ciliary locomotion in the nudibranch mollusk *Tritonia diomedea*. Soc. Neurosci. Abstr. 403.5.

Woolley DM. 1997. Studies on eel sperm flagellum. I. The structure of the inner dynein complex. J. Cell Sci. 110: 85-94.

Wyatt TA, Spurzem JR, May K and Sisson JH. 1998. Regulation of ciliary beat frequency by both PKA and PKG in bovine airway epithelial cells. Am. J. Physiol. Lung Cell. Mol. Physiol. 275: L827-L835.

Wyatt TA, Forget MA and Sisson JH. 2003. Ethanol stimulates ciliary beating by dual cyclic nucleotide kinase activation in bovine bronchial epithelial cells. Am. J. Pathol. 163: 1157-1166.

Yang B, Schlosser RJ, and McCaffrey TV. 1996. Dual signal transduction mechanisms modulate ciliary beat frequency in upper airway epithelium. Am. J. Physiol. Lung Cell. Mol. Physiol. 270: L745-L751.

Yang J, McBride S, Mak DOD, Vardi N, Palczewski K, Haeseleer F and Foskett JK. 2002. Identification of a family of calcium sensors as protein ligands of inositol trisphosphate receptor Ca(2+) release channels. Proc. Natl. Acad. Sci. USA 99: 7711-7716.

Yang P, Diener DR, Rosenbaum JL and Sale WS. 2001. Localization of calmodulin and dynein light chain LC8 in flagellar radial spokes. J. Cell Biol. 153: 1315-1325.

Yang P, Yang C and Sale WS. 2004. Flagellar radial spoke protein 2 is a calmodulin binding protein required for motility in *Chlamydomonas reinhardtii*. Eukaryotic Cell 3: 72-81.

Yeromin AV, Roos J, Stauderman KA and Cahalan MD. 2004. A store-operated calcium channel in *Drosophila* S2 cells. J. Gen. Physiol. 123: 167-182.

Zagoory O, Braiman A, Gheber L and Priel Z. 2001. Role of calcium and calmodulin in ciliary stimulation induced by acetylcholine. Am. J. Physiol. Cell Physiol. 280: C100-C109.

Zagoory O, Braiman A and Priel Z. 2002. The mechanism of ciliary stimulation by acetylcholine: roles of calcium, PKA and PKG. J. Gen. Physiol. 119: 329-339.

Zhan X, Li D and Johns RA. 2003. Expression of endothelial nitric oxide synthase in ciliated epithelia of rats. J. Histochem. Cytochem. 51: 81-87.

Zhang L and Sanderson MJ. 2003. The role of cGMP in the regulation of rabbit airway ciliary beat frequency. J. Physiol. 551.3: 765-776.

Zhou Z and Bers DM. 2002. Time course of action of antagonists of mitochondrial Ca uptake in intact ventricular myocytes. Pflugers Arch. 445:132-138.

APPENDIX- *IN VIVO* Ca^{2+} IMAGING IN ENC1

Ca^{2+} has been proposed to organize early cellular development based on the pattern of signals generated and is a critical trigger for gene transcription (Spitzer, 1994). Spontaneous Ca^{2+} signaling has been observed in several different development models (for review see Jaffe, 1999). Limited study, however, has been conducted on developmental Ca^{2+} signals *in vivo*. Thus, it is unknown how endogenous influences, such as growth factors, affect these signals during development. The objective of this original project was to determine a protocol to image changes in $[Ca^{2+}]_i$ in ENC1 *in vivo* and to examine spontaneous and 5-HT-stimulated Ca^{2+} signals during neuronal development. As many cell types exhibit spontaneous changes in $[Ca^{2+}]_i$ during the course of development, it was anticipated that ENC1 would exhibit such Ca^{2+} signals and that these signals would change over the course of development. Furthermore, as ENC1 regulates its own development through autocrine secretion of 5-HT (Diefenbach *et al.*, 1995) and since pulsatile secretions of 5-HT stimulate rotational surges for the embryo, it was hypothesized that these secretions would also stimulate fluctuations in $[Ca^{2+}]_i$.

To image $[Ca^{2+}]_i$ within ENC1, the embryos were loaded with a fluorescent calcium indicator with an excitation wavelength of 488 nm to allow use with the argon laser of confocal laser scanning microscopes (CLSM). The enhanced spatial control of the CLSM was necessary to isolate the fluorescent signal from ENC1 from background fluorescence of the surrounding tissue. Additionally, the computer control of the laser enabled msec resolution, which was advantageous in capturing rapid changes in calcium signals.

Loading trials with the AM-ester form of various Ca^{2+} indicators were performed. Of the dyes tested (Fura 2, calcium green, Fluo-3 and Fluo-4), Fluo-4 produced the most reliable results with a sufficient signal within the embryo. Fluo-4 was dissolved in DMSO with 20% (v/v) Pluronic-127 and loaded at a concentration of 100 μM in HS. The prepared dye was added to isolated embryos in HS at room temperature. Previous studies (Christopher, unpublished, Weins, unpublished) and preliminary trials indicated that extended loading times were required. However, imaging of ENC1 revealed that the dye was compartmentalized intacellularly as a result of longer incubation times. The conditions of 100 μM Fluo-4 AM loaded for three hours at 28 °C was the protocol used for loading whole *Helisoma* embryos.

ENC1 imaging revealed that the neurons preferentially accumulated the dye with respect to most of the embryo (App. Figure 1). The strongest fluorescent signal appeared within the apical granular layer. This is not altogether unexpected since ENC1 has a large nucleus that does not appear to load with the dye. The large yolk cells and various ciliated bands of the embryo also appeared to consistently load the dye (App. Figure 1). The ciliated cells, however, displayed a "patchy" appearance. It is unknown if this is due to compartmentalization of the indicator or the result of how ciliary cells' uptake membrane-permeable indicators. Initial results showed that ENC1 did exhibit spontaneous changes in $[Ca^{2+}]_i$ (App. Figure 2).

To verify that changes in fluorescence were representing changes in $[Ca^{2+}]_i$ and to allow for quantifiable estimates of $[Ca^{2+}]_i$,, trials were preformed where the embryos were loaded with two indicators to enable ratiometric imaging. Fluo-4 AM was co-loaded with fura red AM using the same protocol as for one dye (App. Figure 3). Lipp and Niggli (1993) outlined this method for ratiometric Ca^{2+} imaging with confocal microscopes. The ratio of fluorescence produced from these two indicators, which are excited at the same wavelength (488 nm) and collected at separate wavelengths (fluo-4: 520nm; fura red: 660 nm), are compared to ratio values which have been calibrated to known $[Ca^{2+}]_i$. Fura red fluorescent signal decreases upon binding to Ca^{2+} and thus, the ratio of fluo-4/fura red should increase with increases in $[Ca^{2+}]_i$. Although initial results seemed promising (App. Figure 4), most of the trials with the two dyes indicated that in many instances the dyes were paralleling each other (App. Figure 5). These results indicated that changes in fluorescence were probably not due to fluctuations in $[Ca^{2+}]_i$ but possibly due to movement of the cell. This suspicion was supported by evidence from an E30 embryo where movement of the cell was evident due to gut contractions (App. Figure 6).

To confirm that ENC1 was moving, a non Ca^{2+}-sensitive fluorescent indicator was used. Carboxy SNARF-1 (Molecular Probes, Eugene, Oregon) is a fluorescent intracellular pH dye also excited at 488 nm but with a longer emission wavelength (650 nm) than fluo-4. Therefore, changes in $[Ca^{2+}]_i$ would only be detected from the fluo-4 signal, assuming intracellular pH remains relatively stable. Coincident changes in fluorescence did indicate movement of ENC1. This was also confirmed by observing animated series of images collected over a given time course, where ENC1 was observed to move away from the specified region of interest.

Although embryos were immobilized between the coverslip and the slide during imaging, ENC1 was observed to move in all three planes. Due to this movement it was not possible to accurately determine changes in fluorescence within a specific region of interest. It was unknown if changes in the fluorescent signal were due to changes in Ca^{2+} or whether these changes were due to movement of ENC1 within the embryo. Additionally, no obvious pharmacological agent, which would immobilize the embryo without disrupting the physiology of ENC1, was identified. For these reasons this project was discontinued in favor of further examining the embryonic ciliary cells.

References

Diefenbach TJ, Sloley BD and Goldberg JI. 1995. Neurite branch development of an identified serotonergic neuron from embryonic *Helisoma*: evidence for autoregulation of by serotonin. Developmental Biology 167: 282-293.

Jaffe LF. 1999. Organization of early development by calcium patterns. BioEssays 21: 657-667.

Lipp P and Niggli E. 1993. Ratiometric confocal Ca^{2+}-measurements with visible wavelength indicators in isolated cardiac myocytes. Cell Calcium 14: 359-372.

Spitzer NC. 1994. Spontaneous Ca^{2+} spikes and waves in embryonic neurons: signaling systems for differentiation. TINS 17: 115-118.

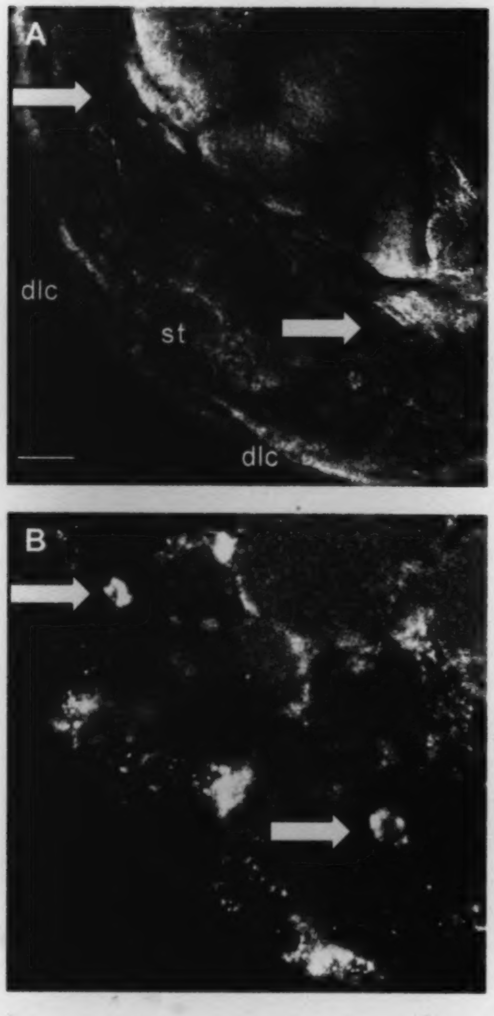

Appendix Figure 1- ENC1 loads with fluo-4 AM. A. A DIC micrograph indicating the location of both ENC1s in an E25 embryo. B. A confocal fluorescence micrograph showing a fluo-4 signal within both ENC1s, excited at 488 nm. Also evident is a fluorescence signal within the dorsal-lateral ciliary bands and the cilia lining the dorsal surface of the stomadeum. Arrows indicate the location of ENC1. Scale bar is 10 μM. st- stomadeum, dlc- dorsal-lateral cilia

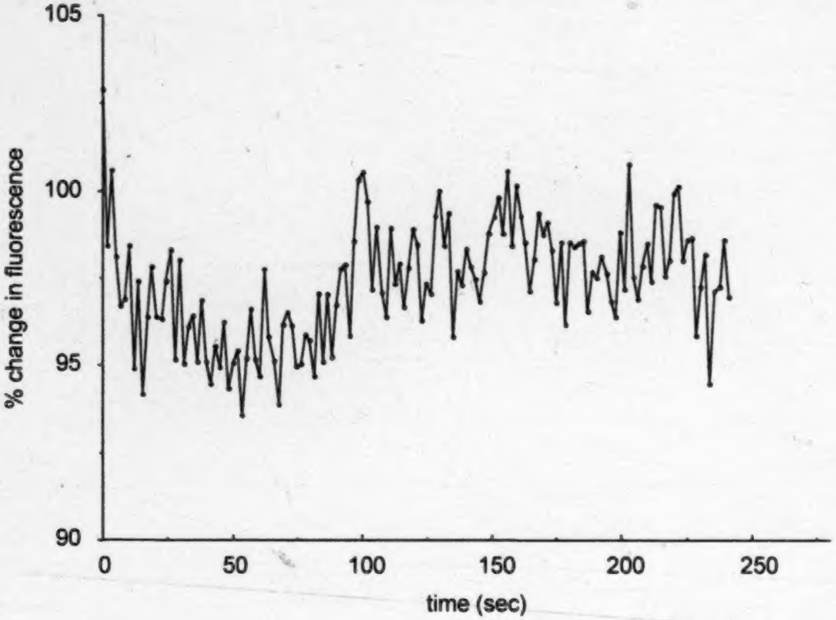

Appendix Figure 2. A representative graph of the percent change in fluorescence within ENC1 over time. E25 embryos were loaded with the Ca^{2+} indicator Fluo-4 and the percent change in fluorescence was determined from ENC1. Data is normalized to the averaged fluorescence value for the first five time points.

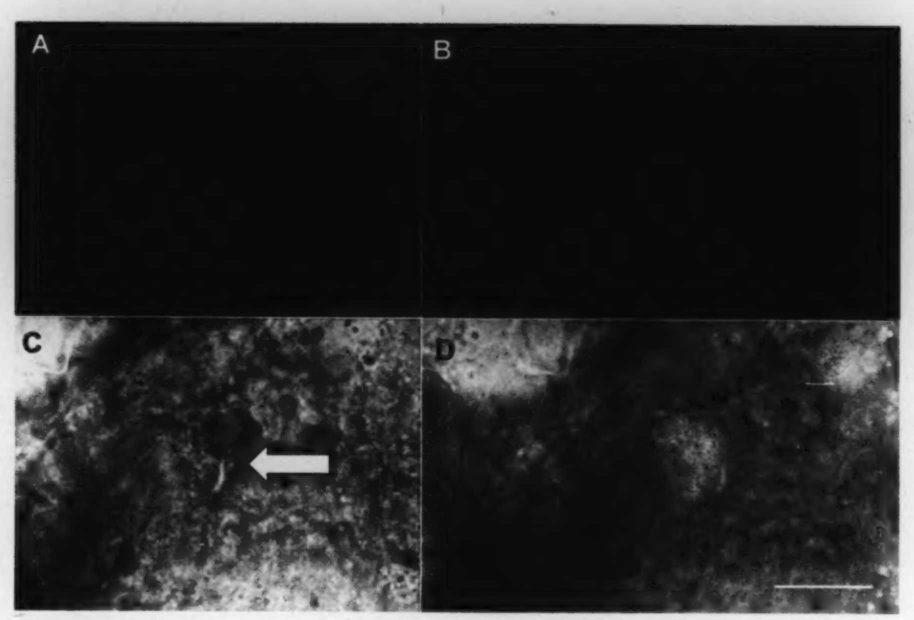

Appendix Figure 3. ENC1 loaded with both fluo-4 and fura red. **A** ENC1 loaded with fura red AM. **B** ENC1 loaded with fluo-4 AM. **C** A DIC micrograph of ENC1. The nucleus and nucleolus are evident in the left of the cell body and the remainder of the cell body has a granular appearance. It is this granular region that is loaded with dye as evident in A and B. **D** An overlay of both fluorescent signals over the DIC image. Scale bar is 10 μm.

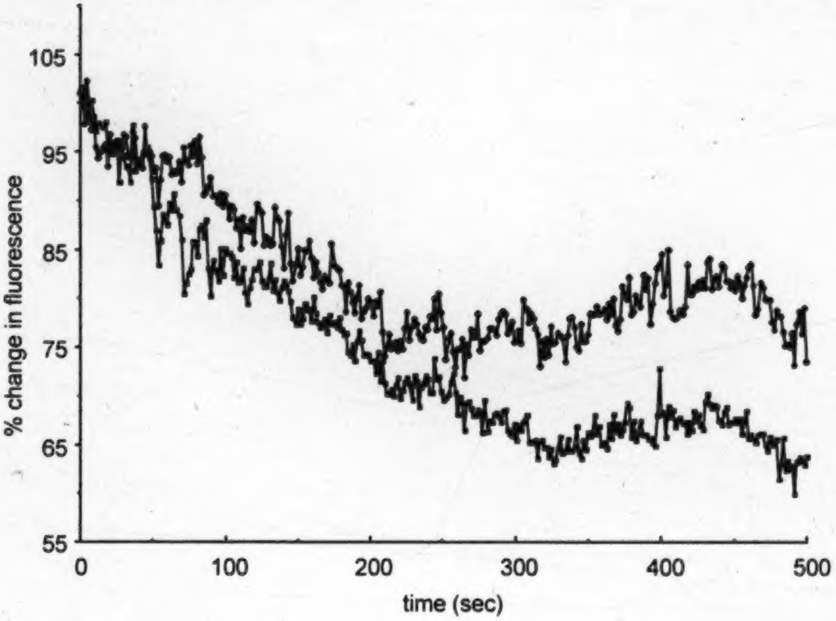

Appendix Figure 4. Changes in fluorescent signal within ENC1, as indicated by the two indicators: Fluo-4 (open squares) and Fura Red (filled diamonds). This is representative data. At some points differing indicator responses are evident. All values are normalized to the average of the initial 10 values collected.

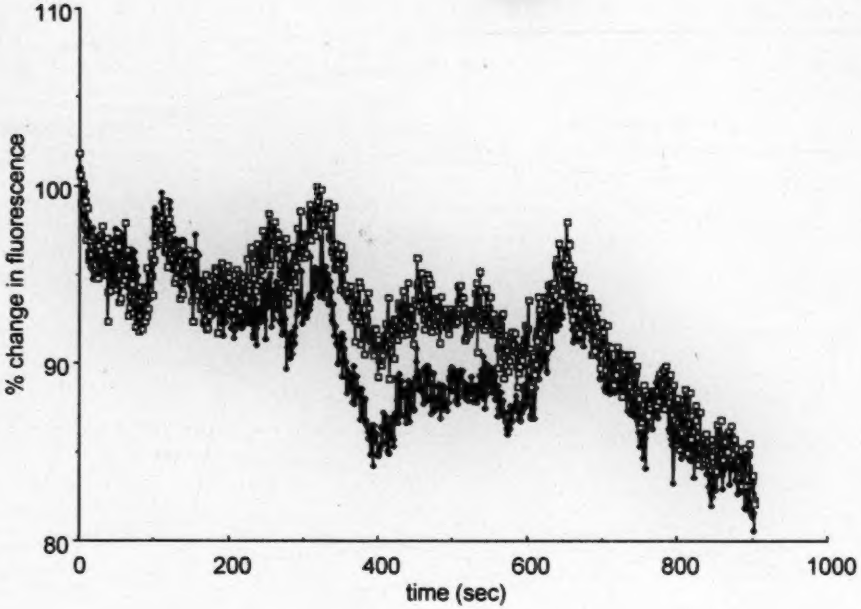

Appendix Figure 5. Parallel changes in fluorescence between both indicators in ENC1. Fura Red is denoted by the filled diamonds and Fluo-4 by the open squares. This is representative data, normalized to the average of the first 10 values recorded.

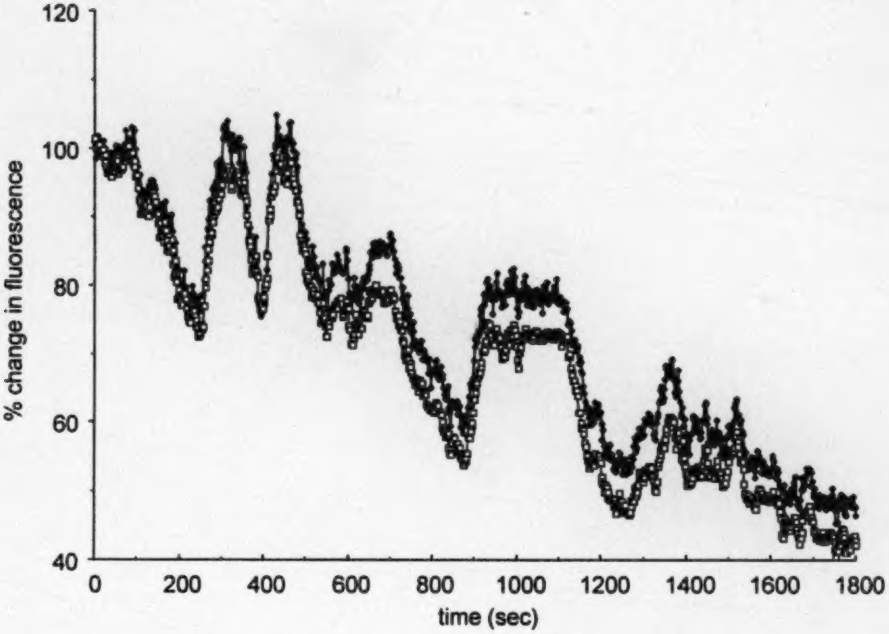

Appendix Figure 6. Changes in fluorescence due to gut contraction within an E30 embryo. Coordinated changes in Fura Red (filled diamonds) fluorescence and Fluo-4 fluorescence (open squares) indicated movement artifacts associated with gut contraction events (not shown). This is representative data, normalized to the average of the first 10 values.